# Unravelling the main physiological processes driving drought-induced tree mortality

Marylou Mantova

UNIVERSITÉ CLERMONT AUVERGNE

ÉCOLE DOCTORALE DES SCIENCES DE LA VIE - SANTÉ – AGRONOMIE – ENVIRONNEMENT

# THÈSE

Présentée par

**Marylou MANTOVA**

Pour l'obtention du grade de

**Docteur d'Université**

Spécialité : **Biologie Végétale**

---

# UNRAVELLING THE MAIN PHYSIOLOGICAL PROCESSES DRIVING DROUGHT-INDUCED TREE MORTALITY

---

*Soutenue publiquement le 20 octobre 2022*

**Président du jury :**

**Jean-Louis JULIEN**, Professeur, Université Clermont-Auvergne

**Rapporteurs :**

**Charlotte GROSSIORD**, Professeur, EPFL, Lausanne (Suisse)

**Gregory GAMBETTA**, Professeur, Bordeaux Sciences Agro, Université de Bordeaux

**Examinatrice :**

**Celia M. RODRIGUEZ-DOMINGUEZ**, Chercheur, IRNAS-CSIC, Séville (Espagne)

**Directeur de thèse :**

**Hervé COCHARD**, Directeur de Recherche, INRAe, Clermont-Ferrand

**Co-Encadrant de thèse :**

**José M. TORRES-RUIZ**, Chercheur, INRAe, Clermont-Ferrand

*… A ma grand-mère qui n'aura malheureusement pas eu le temps de voir ce travail achevé mais qui aura fait en sorte que je ne meure pas de faim en me donnant un paquet de gâteaux « pour Clermont » tous les 15 jours pendant les deux premières années de cette thèse…*

# Remerciements

Premièrement, je tiens à remercier mes encadrants, **José M. Torres-Ruiz** et **Hervé Cochard**.

Merci tout d'abord à **Torres** d'avoir eu confiance en moi lorsque je changeais de direction à la fin de mon Master 1. Merci de m'avoir fait découvrir le monde de l'hydraulique des plantes et de m'avoir permis d'en tuer plein lors de mon stage de Master 2. Qui aurait cru qu'une anomalie sur un LVDT (comment ça un arbre presque complètement embolisé pourrait réussir à mobiliser de l'eau ???), qui finalement n'en était pas une, ouvrirait les portes de ce travail de thèse ? Merci pour la confiance que tu m'as accordée tout au long de cette thèse, en me laissant, d'un côté, gérer à mon rythme ce travail, mais aussi, en me motivant tous les jours. Merci pour ton encadrement, ton accompagnement, tes conseils et ta patience durant ces trois, presque quatre, dernières années. Merci aussi de m'avoir permis de devenir bilingue en Espagnol, *sí*, *sí*, je connais maintenant une multitude d'insultes ainsi que des phrases essentielles pour survivre dans n'importe quel labo telles que *¿Vamos a comer?*

Un grand merci aussi à **Hervé**. Tout d'abord, merci de m'avoir laissé ton bureau, très inspirant et surtout beaucoup plus lumineux que le mien, pendant la fameuse « période COVID ». Merci pour ta bonne humeur constante, tes conseils précieux, ton soutien en mathématiques (et surtout ta patience indéfectible à me réexpliquer 50 fois comment calculer le point d'intersection de l'axe x de la tangente d'une fonction logistique à quatre paramètres, c'est pourtant simple non ?) et enfin merci pour les nombreuses opportunités que tu as pu me créer au cours de ces trois dernières années. Je suis très fière d'être ~~probablement~~ ta première doctorante à soutenir~~, mais n'allons pas trop vite, il peut se passer plein de choses d'ici la soutenance~~.

Je tenais aussi à remercier les membres de mon jury de thèse : **Charlotte Grossiord**, **Gregory Gambetta**, **Celia Rodriguez-Dominguez** et **Jean-Louis Julien** qui ont accepté d'évaluer ce travail mais aussi les membres de mon comité de thèse : **Sylvain Delzon**, **Régis Burtlett** et **Florence Volaire** qui ont amené de précieux conseils tout au long de la thèse.

A big thank you to **Noel. M. (Missy) Holbrook** who welcomed me as a visiting student, thanks to the *Fulbright* program, in her lab for four months between the end of 2021 and the beginning of 2022. Staying in your lab was a real life-changing experiment. I grew as a scientist and as a person by staying there. So, again, thank you Missy. Also, thank you to everyone at the **Holbrook lab** at Harvard for amazing discussions and extraordinary science. A special thanks to **Sophie Everbach**, my office colleague there, for all the amazing discussions we had during those four months. Also, a big thank you to **Yakir Preisler** for challenging me scientifically with fascinating debates and for saving my European/French-self with incredible Mediterranean food throughout those four months and by giving me wonderful addresses in the Boston area. Thanks also to **Lani, Joe** and **Mateo** who became a second family to me during my stay in Boston. I had an amazing time living with you.

Cette thèse, et particulièrement le dernier chapitre, n'aurait pas été possible sans le soutien et le travail des équipes de microscopie. Tout d'abord, thank you to **Adam Graham** and **Nicky Watson** at the *Harvard Center for Nanoscale Study* who trained me on the cryo-SEM

and helped me transfer my knowledge to our microscopy platform in Clermont. Un grand merci à **Claire Szczepaniak**, **Lorraine Novais Gameiro** et **Christelle Blavignac** pour avoir accepté de travailler sur du matériel végétal, d'avoir brillamment mené la préparation des coupes de mes échantillons et surtout pour la superbe ambiance qui règne au CICS de Clermont. Un grand merci aussi à **Nicole Brunel** pour son aide dans l'élaboration des protocoles de microscopie et dans l'observation des cellules cambiales au cours de cette dernière année de thèse. Enfin, un grand merci à **Steven Jansen** qui m'a accueillie dans son laboratoire de l'Université de Ulm en Allemagne et avec qui les échanges ont été plus que bénéfiques.

Cette thèse s'étant déroulée en grande partie au sein de **l'UMR PIAF**, je tiens donc à remercier toutes les personnes avec qui j'ai pu partager ces dernières années. Merci pour votre bonne humeur et les nombreux échanges intéressants que nous avons pu avoir au cours de la fameuse « Pause-Café » de 10h30, pause que j'ai bien évidemment respectée presque religieusement pendant ces 3 années de thèse. Un grand merci donc à toutes les personnes qui m'ont aidé au cours de cette thèse, que ce soit au niveau informatique, pour l'entretien des plantes ou pour la mise en place des expérimentations. Ainsi, merci à **Norbert Frizot** pour avoir réglé mes dizaines de problèmes informatiques et surtout pour sa gentillesse depuis mon arrivée au PIAF. Un grand merci aussi à **Aline Faure** et **Patrice Chaleil** ainsi qu'à toute l'équipe de **Végépole** pour avoir parfaitement veillé sur mes plantes jusqu'à ce que je ne les tue par sécheresse. Un énorme merci à **Julien Cartailler** pour son soutien technique incroyable tout au long de cette thèse. Merci d'avoir préparé et paramétré les centrales de LVDT, d'avoir écrit un protocole d'utilisation des cavicams et surtout d'avoir toujours été disponible dans les moments de galère (« Oui Julien ? J'ai un problème… »). Merci à **Pierre Conchon** d'avoir réalisé les scans tomo nécessaires aux résultats de cette thèse, pour son soutien moral et pour avoir été bien souvent la seule personne présente au labo à 7h30 ! Merci à **Sylvie Vayssié**, **Dominique Tiziani** et **Béatrice Meteix** d'avoir géré mes (nombreux) déplacements. Mention spéciale à **Dominique** pour avoir répondu à mon appel de détresse un jeudi soir à 19h pour un départ à Paris le lendemain à 8h, merci d'avoir, en quelque sorte, sauvé le chapitre 3 de cette thèse. Enfin, merci à **Nicolas Donès**, ma copine. Un grand merci pour toutes nos conversations et surtout merci d'avoir toujours été à l'écoute. Je suis toujours un peu déçue ne pas avoir dépassé Benjamin dans ton classement de tes doctorants préférés mais j'accepterai quand même la deuxième place 😉 Enfin, merci à tous les membres de l'équipe **Sureau** pour vos précieux conseils au cours de ces années de recherche et pour le fameux « esprit Sureau » qui règne dans l'équipe.

Je tenais aussi à remercier tous mes collègues **stagiaires-doctorants-non-titulaires-post-docs-et-Ludo** (je continue la tradition) pour les bons moments passés ensemble au cours de cette thèse. Tout d'abord merci à mes stagiaires **Romane Ducaroix**, **Mathilde Scheuber** et **Alexandre Gonzalez** pour le travail qu'ils ont accompli pendant leurs stages respectifs. Leur bonne humeur et leur envie d'apprendre ont été très motivantes. Un énorme merci à **Alex** qui a été un peu le stagiaire idéal et l'homme parfait, probablement l'homme de ma vie (ah oui mince… c'est vrai… quel dommage !!!). Merci d'avoir été mon taxi en m'amenant régulièrement à la gare de (très) bonne heure ou à l'aéroport. Je suis contente et fière de voir que ton travail acharné en master, bien que présentant une incertitude de mesure, comment

dire ? certaine, aura su payer. Je te souhaite bon courage pour ta thèse et te laisse ainsi la garde du *LabEau* (bon courage pour le tenir propre, ne deviens pas trop fou) et bientôt de mon bureau. Un grand merci à tous les doctorants avec qui j'ai pu passer quelques bons moments et sans qui cette thèse n'aurait certainement pas été la même : **Alexandre**, avec qui nous nous serons suivis de la licence 2 jusqu'au doctorat, **Arnold**, **Arnoul, Erwan, Mahaut, Marianne** et surtout **Tsiky**.

Merci **Tsiky** d'avoir partagé le bureau pendant ces deux dernières années. Merci pour tous les moments de rire, parfois de pleurs (on a quand même failli renommer le bureau « le saule pleureur » à un certain moment), de commérages et pour tous les moments absurdes que nous avons pu vivre ensemble. On ne se sera quasiment jamais entendu sur la température du bureau (ce n'est pas Madagascar ici !!) mais on aura quand même passé de bons moments ! Merci pour tous ces moments d'échanges, de fou-rires en principes de la relaxation (l'astre solaire) et de défis scientifiques (hâte d'écrire ce fameux papier Mantova & Andriantelomanana, parce que, il faut l'avouer, dans l'autre ordre c'est imprononçable). Désolée d'avoir autant squatté le tableau du bureau, j'espère que tu ne m'en veux pas…

Merci aussi à **Maurin** pour tous les moments extraordinaires passés ensemble. J'ai adoré gravir le PDD avec toi dans la neige et sans équipements, si ce n'est le fameux bâton mystick. Heureusement que nous étions mieux équipés pour gravir le Sancy ! Merci pour tous les moments thérapie sur ton ballon de gym au bureau et merci pour nos virées BK avec ton bolide décapotable.

Merci à **Cyril** (ou peut-être Cédric je ne sais plus 😄) pour toutes nos discussions scientifiques mais aussi pour les moments de pause et de soutien lors de la rédaction de cette thèse.

Enfin, un grand merci à **Ludo**, monsieur météo du labo. Merci pour tes alertes grêles (souvent fausses) et orages mais aussi merci pour ton célèbre « *ça va bien se passer* ». Un grand merci pour ton aide et surtout pour ton dévouement à m'assister pour la réalisation des fameuses *P-V curves*, sache qu'en plus de savoir peser des feuilles à la perfection, tu fais aussi un secrétaire idéal. Merci aussi pour tes (très) nombreux « moments beaufs » qui ont certainement constitué l'une des études les plus longues et acharnées de cette thèse. C'est ainsi, qu'après deux ans et demi de travail, je vais enfin pouvoir confirmer au monde entier (je m'emballe peut-être un peu) que tes moments beaufs suivent bien une distribution normale centrée sur midi ($r^2$=0.8) (*voir Figure exceptionnelle*).

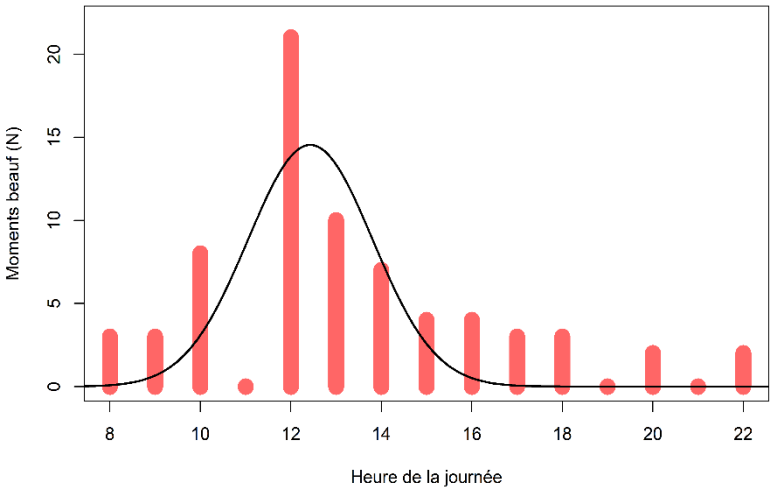


**Figure exceptionnelle.**
**Les « moments beauf » de Ludo.** Les barres représentent le nombre de « moments beauf » relevés sur la période de Septembre 2019 à Juin 2022 en fonction de l'heure de la journée. Une régression suivant une courbe Gaussienne à 4 paramètres est représentée par la ligne noire ($R^2$=0.8) et démontre que le pic d'activité est situé aux alentours de 12h.

Puis finalement, merci d'avoir fait croire à tout le labo que j'étais de nationalité russe avec pour seules bases une rencontre estivale avec des cheveux un peu trop blonds, un anglais un peu trop bon et un nom de famille se terminant par « ova ». Il est bien connu que mes frères se nomment « Mantov ». спасибо Людо !

Un immense merci aux **Zouz'in (rat)** pour leur soutien incroyable tout au long de ces trois, presque quatre dernières années. Merci pour vos permanences au bureau des plaintes que ce soit le lundi à 7h ou le vendredi à 23h. **Lia**, merci d'avoir été ma première collègue de bureau en tant que doctorante, merci pour nos fou-rires, nos analyses sur le tableau, la truffade au mois de juin et surtout pour toutes les expressions que nous avons régulièrement pu échanger (les bons comptes font les bons amis, c'est une affaire qui roule…). **Lise-Marie**, châtelaine attitrée, merci pour cette nuit de folie passée avec toi lors du xylem meeting en 2019 et qui a littéralement changé ma vie. Merci pour tous tes câlins forcés qui ont peut-être un peu changé ma personne. Bien que tu n'aies passé que très peu de temps dans le bureau du bas, merci de l'avoir renommé le « Bureau des Châtelaines ». **Lucie**, merci d'avoir été la meilleure co-stagiaire de master et d'avoir partagé tes brownies et autres savanes avec moi. Sache que certaines de nos créations hantent encore et toujours le bureau des stagiaires. Merci pour tes mille-et-unes histoires de vie, toutes aussi surprenantes que passionnantes les unes que les autres. J'ai adoré nos virées en voiture en ville agrémentées d'une boule disco et de cet incroyable son qu'est *Ibiza*. Enfin je pense que je dois mon intégration au laboratoire à **Marine**, ma mère INRA, qui m'a littéralement adoptée alors que je restais assise dans mon coin en salle de pause. Merci de m'avoir renseigné environ un million de fois sur toutes les démarches administratives à effectuer et surtout merci pour tous nos échanges musicaux en cyto, aussi variés que surprenants, (Francis, PNL, Taylor Swift *isn't it ?*…). Finalement, n'oublie pas que *blue is the color of the planet from the view above* (quelle observatrice cette Lana !).

Cette thèse et surtout mon séjour aux Etats-Unis n'auraient certainement pas été aussi funs sans la rencontre, au détour d'un repas *Fulbright* dans les jardins de l'ambassadeur des Etats-Unis en France, de ce qui fût un coup de cœur amical : **Marie**, saltimbanque de mon séjour *Fulbright*. Merci de m'avoir accueillie et fait visiter Boston avec ton fameux *Marie's tour* et ton légendaire sens de l'orientation. Merci d'avoir partagé ma passion *road trips* qui nous a mené à Cape Cod (« *comment ça les photos devant chez les Kennedy sont interdites ?* ») mais aussi plus d'une fois dans le Rhode Island (« *Ah mais c'est pas gratuit de visiter les mansions de Newport ?* ») et enfin dans le Vermont. Merci pour toutes les expériences culinaires que nous avons pu vivre ensemble, nos brunchs un weekend sur deux, *The cooked goose* et le homard de Noël. Finalement, merci de m'avoir légué ta recette du houmous.

Merci aussi à la **Dream Team**, Julie et Marion de m'avoir permis de décompresser et de voyager ces dernières années. Merci, **Julie** pour ton soutien moral tout au long de mes années fac, de nos skypes en licence jusqu'à ta visite à Boston. **Marion**, merci pour ton soutien indéfectible depuis la 4ème, merci d'être « le tonton beauf de la famille », et enfin merci pour tes centaines de phrases absurdes (« *ça n'a pas duré longtemps mais ça a quand même duré un petit moment* ») qui ont donné lieu à des dizaines de post-it, qui je te le promets, trouveront leur place dans un carnet très prochainement.

Enfin, merci à **ma famille**, **mes frères** et surtout ma **mère**. Merci pour votre soutien et votre motivation tout au long de ces (nombreuses) années d'études. Un grand merci à ma mère d'avoir supporté l'immense coût de ces années de fac et d'avoir su toujours me conseiller, m'écouter et m'accompagner dans mes choix lorsque j'avais des doutes. Merci pour ton fameux « il faut toujours aller jusqu'au bout, tu verras après ».

*"The drought was the very worst, when the flowers that we'd grown together died of thirst"*

*- Taylor Swift, Clean, 1989, (2014) -*

# Valorisation

**Articles académiques en préparation**

Mantova Marylou, Steven Jansen, Cochard Hervé, Szczepaniak Claire, Brunel Nicole, Delzon Sylvain, King Andrew, Torres-Ruiz José M. *From cellular death to tree death: when meristems matter.*

**Article académique soumis**

Mantova Marylou, Cochard Hervé, Burlett Régis, Delzon Sylvain, King Andrew, Rodriguez-Dominguez Celia M., Ahmed Mutez A., Trueba Santiago, Torres-Ruiz José M. *On the path from xylem hydraulic failure to downstream cell death.* [New phytologist]

**Articles académiques publiés**

Mantova Marylou, Menezes-Silva Paulo E., Badel Eric, Cochard Hervé, Torres-Ruiz José M. *The interplay of hydraulic failure and tree mortality explains tree capacity to recover from drought.* [Physiologia Plantarum, 2021]

Mantova Marylou, Herbette Stéphane, Cochard Hervé, Torres-Ruiz José M. *Hydraulic failure and tree mortality: from correlation to causation.* [Trends in Plant Science, 2022]

**Article académique en co-auteur**

McDowell Nate G., Sapes Gerard, Pivovaroff Alexandria, Adams Henry D., Allen Craig D., Anderegg, William R. L., Arend Matthias, Breshears David D., Brodribb Tim, Choat Brendan, Cochard Hervé, De Cáceres Miquel, De Kauwe Martin G., Grossiord Charlotte, Hammond William M., Hartmann Henrik, Hoch Günter, Kahmen Ansgar, Klein Tamir, Mackay D. Scott., Mantova Marylou, Martínez-Vilalta Jordi, Medlyn Belinda E., Mencuccini Maurizio, Nardini Andrea, Oliveira Rafael S., Sala Anna, Tissue David T., Torres-Ruiz José. M., Trowbridge Amy M., Trugman Anna T., Wiley Erin, Xu Chonggang. *Mechanisms of woody-plant mortality under rising drought, CO2 and vapour pressure deficit.* [Nature Reviews Earth & Environment, 2022]

**Poster**

Mantova Marylou, King Andrew, Delzon Sylvain, Cochard Hervé, Torres-Ruiz José M. On the path from xylem hydraulic failure to downstream cell death. Assessing Plant Vascular Function Through Optical Approaches - Gordon Research Conference. 5-10 juin 2022

**Communications orales**

Mantova Marylou. Cochard Hervé, King Andrew, Delzon Sylvain, Holbrook Noel Michele, Torres-Ruiz José M. On the path from xylem hydraulic failure to leaf cell death. Multiscale Plant Vascular Biology - Challenges for Plant Vascular Function in the Anthropocene - Gordon Research Seminar. 4 juin 2022

Mantova Marylou. Menezes-Silva Paulo Eduardo, King Andrew, Delzon Sylvain, Badel Eric, Cochard Hervé, Torres-Ruiz José M. Linking the main physiological mechanisms driving drought-induced tree mortality: a focus on leaves cells. 24èmes Journées de l'Ecole Doctorale SVSAE. 27 mai 2021

Mantova Marylou. Menezes-Silva Paulo Eduardo, Badel Eric, Cochard Hervé, Torres-Ruiz José M. The interplay of hydraulic failure and cell vitality explains tree capacity to recover from drought. 1st event of the Connecting Plants and People Webinar Series. 20 mai 2021

**Communiqué de presse**
Sécheresse : mieux comprendre les mécanismes de mortalité des plantes. 17 novembre 2021

**Exercice de vulgarisation scientifique**
Mantova Marylou. Understanding tree mortality under drought conditions. Birches School (Lincoln, MA, USA). 10 février 2022

# Contents

# List of Acronyms

| | |
|---|---|
| **BLC** | Bark Living Cells |
| **BRW** | Before Re-Watering |
| **C1** | Initial conductivity of the effusate |
| **C2** | Maximal conductivity of the effusate |
| **CWC** | Canopy Water Content |
| **Dim-1** | Dimension 1 of Principal Component Analysis |
| **Dim-2** | Dimension 2 of Principal Component Analysis |
| **DW** | Dry Weight |
| **EL** | Electrolyte leakage – cell lysis |
| **$EL_{50}$** | Relative Water Content at which 50% of cellular damages is observed |
| **$EL_{max}$** | Relative Water Content at which the maximum level of cellular damages if observed |
| **FAO** | Food and Agricultural Organisation |
| **FDA** | Fluorescein Diacetate |
| **FW** | Fresh Weight |
| **GDP** | Gross Domestic Product |
| **GHG** | GreeHouse Gas |
| **GOE** | Great Oxydation Event |
| **$K_i$** | Initial Conductance |
| **$K_{max}$** | Maximal Conductance |
| **KMO** | Kaiser-Meyer-Olkin test |
| **$LD_{50}$** | Lethal threshold for hydraulic failure at which 50% of trees die |
| **$LD_{50}$-EL** | Lethal threshold for cellular damages at which 50% of trees die |
| **$LD_{50}$-RC** | Lethal threshold for stem diameter recovery at which 50% of trees die |
| **$LD_{50}$-RWC** | Lethal threshold in Relative Water Content at which 50% of the trees die |
| **$LD_{50}$-PLD** | Lethal threshold in Percentage Loss of stem Diameter at which 50% of the trees die |
| **LVDT** | Linear Variable Differential Transformer |
| **NLS** | Non-Linear Regression; four-parameters logistic regression |
| **ONF** | Franch National Forest Office |
| **$P_{12}$** | Xylem tension inducing 12% loss of hydraulic conductance |
| **$P_{50}$** | Xylem tension inducing 50% loss of hydraulic conductance |
| **$P_{88}$** | Xylem tension inducing 88% loss of hydraulic conductance |
| **PCA** | Principal Component Analysis |
| **PEP** | Percentage of Embolised Pixels |
| **PLC** | Percentage Loss of hydraulic Conductance |
| **PLD** | Percentage Loss of Stem Diameter |
| **PV** | Pressure-Volume |
| **RC** | Stem diameter Recovery Capacity |

| | |
|---|---|
| **ROS** | Reactive Oxygen Species |
| **RWC** | Relative Water Content |
| **$RWC_{12}$** | Relative Water Content at which 12% of xylem cavitation is observed |
| **$RWC_{50}$** | Relative Water Content at which 50% of xylem cavitation is observed |
| **$RWC_{88}$** | Relative Water Content at which 88% of xylem cavitation is observed |
| **$RWC_{crit}$** | Critical Relative Water Content below which cell integrity is compromised |
| **$RWC_{Leaf}$** | Leaf Relative Water Content |
| **$RWC_{Stem}$** | Stem Relative Water Content |
| **SEM** | Scanning Electron Microscopy |
| **SSP** | Share Socioeconomic Pathways |
| **TEM** | Transmission Electron Microscopy |
| **TLP** | Turgor Loss Point |
| **TW** | Turgid Weight |
| **VPD** | Vapor Pressure Deficit |
| **WUE** | Water Use Efficiency |
| **$\varepsilon$** | Cell modulus of elasticity |
| **$\Psi$** | Water Potential |
| **$\Psi_g$** | Gravitational Potential |
| **$\Psi_{Leaf}$** | Leaf Water Potential |
| **$\Psi_m$** | Matrix Potential |
| **$\Psi_p$** | Hydrostatic Potential |
| **$\Psi_s$** | Osmotic Potential |
| **$\Psi_{Stem}$** | Stem Water Potential |
| **$\Psi_{Xylem}$** | Xylem Water Potential |

# List of Figures

# List of Tables

# List of Supplementary Figures

# List of Supplementary Tables

# *Bibliography Synthesis*

# Part 1. From the bacterial life to forest ecosystems

## 1. From cyanobacteria to vascular plants: The « tree » of life

### *1.1.Living underwater*

Plants, from the Latin *vegetus* meaning "lively", are defined as living organisms with a thallus or a set of roots, stems, leaves, flowers, formed by cells with a cellulose wall, capable of elaborating its organic matter (notably by photosynthesis) from the mineral and gaseous elements of the environment or living in symbiosis or parasitism with other species. They are characterised by a relatively low mobility and sensitivity, reproducing sexually or vegetatively (CNRTL, 2012). Their precursors, cyanobacteria, some oxyphototrophic eubacteria, were identified for the first time in Precambrian fossils around 3.8 billion years ago (Figure 1). These cyanobacteria, present in water, would have played a major role in the production of oxygen in the atmosphere and would have been responsible for the Great Oxidation Event (GOE) of the Earth's atmosphere that took place in the oceans *via* oxygenic photosynthesis (Van Kranendonk *et al.*, 2012). By producing their organic matter from mineral matter and $CO_2$ *via* photosynthesis, the primitive organisms generated a large production of $O_2$ that originally reacted with iron compounds in the ocean, resulting in the precipitation of hematite and magnetite. However, 2.4 billion years ago, the ocean experienced a depletion of ferrous iron which caused an accumulation of $O_2$ first in the ocean and then in the atmosphere. As a result, 2.1 billion years ago, the GOE lead to an atmosphere that presented an oxygen concentration close to 4%, which allowed the emergence of aerobic cell life (Barley *et al.*, 2005; Kump & Barley, 2007; Scott *et al.*, 2008).

### *1.2.Terrestrialization*

Land plants evolved from chlorophytic algae (i.e., green algae) that appeared during the Cambrian period, 510 million years ago (Figure 1). These green algae were the result of an endosymbiosis of a cyanobacteria and are defined as photosynthetic eukaryotes that present a double-membrane plastids containing chlorophyll a and b and accessory pigments (beta-carotenes and xanthophyll) (Lewis & McCourt, 2004), i.e., presenting a structure very close to present-day photosynthetic organisms. However, it was not until the Upper Ordovician, 460 million years ago (Figure 1), that plants conquered the land and gave rise to the first land plants, which were then mainly represented by the bryophyte group (Kenrick & Crane, 1997).

With the terrestrialization of individuals, land plants have been confronted with an aerial environment that brings new constraints. In comparison with the aquatic environment, the aerial environment has a low availability of water and is desiccating. Therefore, to survive and develop in such an environment, plants must be able to draw water and nutrients from where they are available, i.e., from the soil, and thus develop an efficient system for drawing these elements. In addition to this low water availability, the desiccating atmosphere and high luminosity associated with lead to greater evaporation. Thus, structures regulating the water loss of plants appear necessary for survival. Therefore, the presence of a cuticle, limiting water loss, and of stomata, regulating the evapotranspiration, appear to be an evolutionary advantage in this hostile environment. But the hostility of the aerial environment does not stop

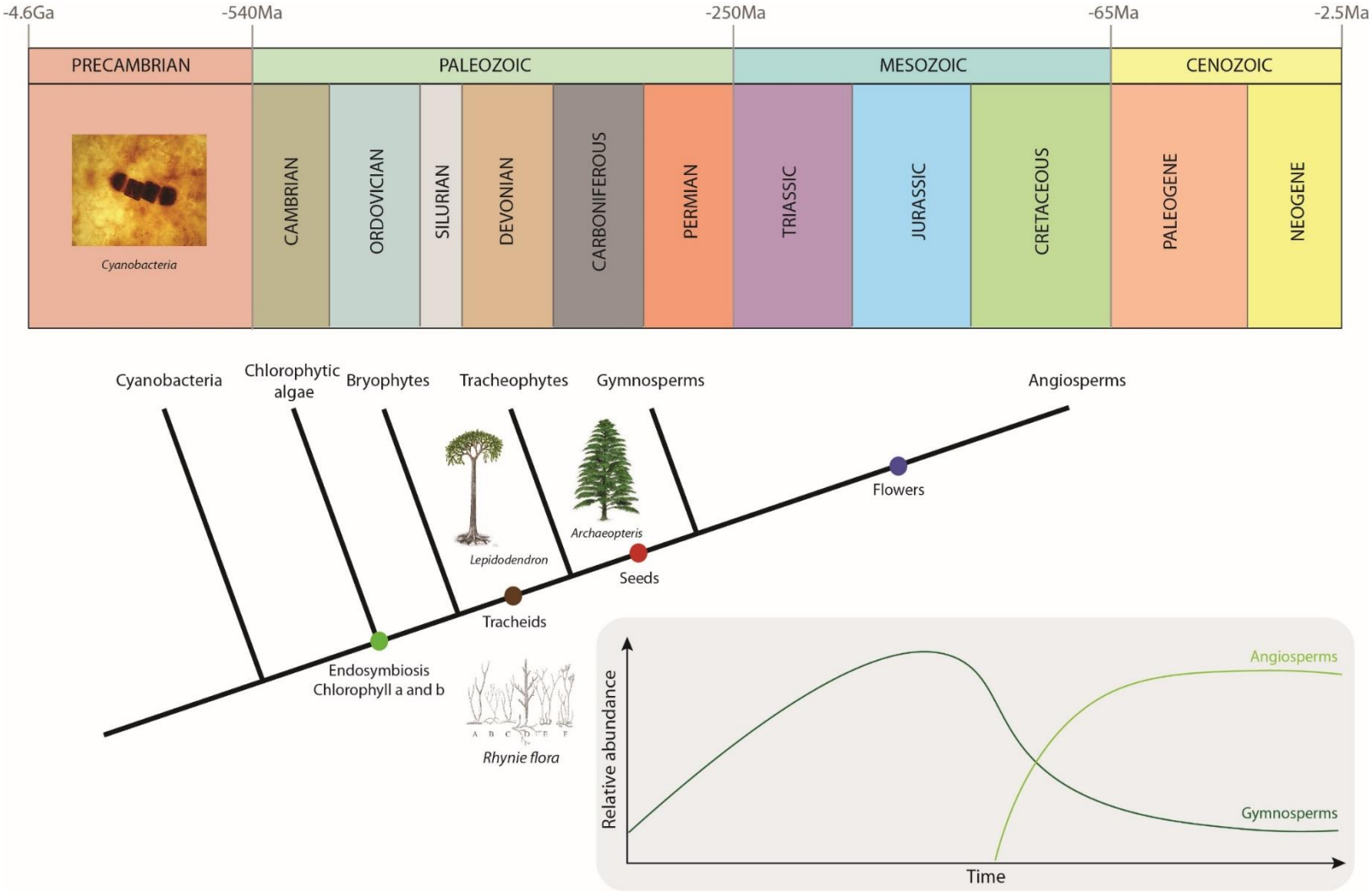


**Figure 1.** Simplified geologic time scale showing plants apparition and diversification through time. ©Marylou Mantova

there, indeed, unlike the aquatic environment, this one is not buoyant, the buoyancy being zero in this environment. Thus, this is how the diversification of terrestrial flora began, at the end of the Silurian period, about 420 million years ago, giving rise, at the beginning of the Lower Devonian (-410 Ma) (Figure 1), to a predominantly herbaceous flora such as the Rhynie flora, characterised within a fossiliferous layer located near the village of Rhynie, in Scotland. This Rhynie flora, consisted of seven monospecific genera, had plants less than 50cm tall, spreading horizontally over large areas (Edwards, 2004). The Rhynie environment was open and humid with a high availability of resources, be it light, water or mineral elements. The plants in this flora reproduced by vegetative propagation, which allowed rapid occupation of the available space. Thus, the plants were able to colonise drier ground than before (Edwards, 2004).

However, the low availability of water and minerals required the presence of conductive tissues to transport these elements to the different parts of the plant. Thus, considering the constraints of this new environment, it was also within this Rhynie flora that the first vascular plants were characterised. Indeed, five out of seven genera had a xylem containing tracheids allowing the transport of water in cells with rigid walls (Edwards, 2004). This characteristic, which is inseparable from growth in height (Speck & Vogellehner, 1988; Niklas, 1994; Raven, 2018), enabled the plants to reach a height of about 50 cm. The Rhynie flora also showed that plants shared space and resources and distributed themselves according to the conditions of the environment and interspecific competition. Thus, the plants of the Rhynie flora ultimately modified the environment in which they grew, generating new environments with different constraints.

## 2. Catching the light: when the first trees appear

### *2.1.Historical apparition of trees in the biosphere*

Rapidly during the Devonian (-419.2Ma to -358.9Ma) (Figure 1), the diversification of terrestrial plants, both in terms of major taxa and within taxa, led to significant competition for resources, including light (Meyer-Berthaud & Decombeix, 2009). This competition then seemed to select, in different groups, adaptive characters that build the characteristic morphology of the tree: a high height, allowing it to outstrip other plants and to be the first to receive solar radiation; the presence of a true leaf, or megaphyll, facilitating photosynthesis; and a root apparatus with secondary structures allowing the vegetative apparatus to be anchored in the soil. This arborescent form was then acquired, in the course of evolution, in different taxa within a limited period of time, making the tree an evolutionary convergence due to common environmental constraints (Meyer-Berthaud & Decombeix, 2009).

The first traces of trees were observed in fossils dating from the end of the Middle Devonian (-393.3Ma to -382.7Ma) (Meyer-Berthaud & Decombeix, 2009) (Figure 1). These tree traces, discovered in the famous sedimentary deposits of the Lake Erie shoreline (New York State, USA), that also contained the first known forest: the Gilboa forest (Stein *et al.*, 2012), were identified as belonging to the genus *Lepidosigillaria* (Lycophyte). One of the most spectacular pieces of evidence of this lycophyte is represented by the "Naples tree", a fossilised tree that presented a 3.40m long and 38cm wide trunk that was covered by leaf cushion (Meyer-

Berthaud & Decombeix, 2009). Thus, in Gilboa, about 390Ma years ago, plants reaching multi meters height were already existing.

However, it was not until the Upper Devonian (-382.6 Ma to -358.9 Ma) (Figure 1) that the first tree with a form similar to present-day forms was characterised (Meyer-Berthaud *et al.*, 1999). Cosmopolitan, it was found in South Africa, Germany, Russia, and the United States. This pregymnosperm spermatophyte, named *Archaeopteris*, is considered to be the closest tree to the present-day forms both in morphology and internal anatomy (Meyer-Berthaud *et al.*, 1999) (Figure 2). Indeed, it is reconstructed as a tree that can reach 30 to 40 metres in height, with a trunk up to 1.50 metres in diameter and capable of producing lateral branches (Figure 2A). Unlike *Lepidosigillaria*, which presented microphylls, *Archeopteris* developped megaphylls, i.e., modern leaves that allowed it to capture a lot of light energy (Meyer-Berthaud *et al.*, 2000). Its trunk, made up of wood, was produced by a bifacial cambium reminiscent of that of modern conifers with tracheids and rays. This bifacial cribrovascular cambium produced both internal secondary xylem and external secondary phloem, which improved upright growth and height, and ameliorated the exchange of nutrients within the tree (Figure 2B). Thus, it is this improved nutrition, as well as its root system (very similar to that of current conifers with secondary structures), that helped explaining the significant development of a crown with a very high production of leaves and branches, leading *Archeopteris* to have a long-life span (around 30 years).

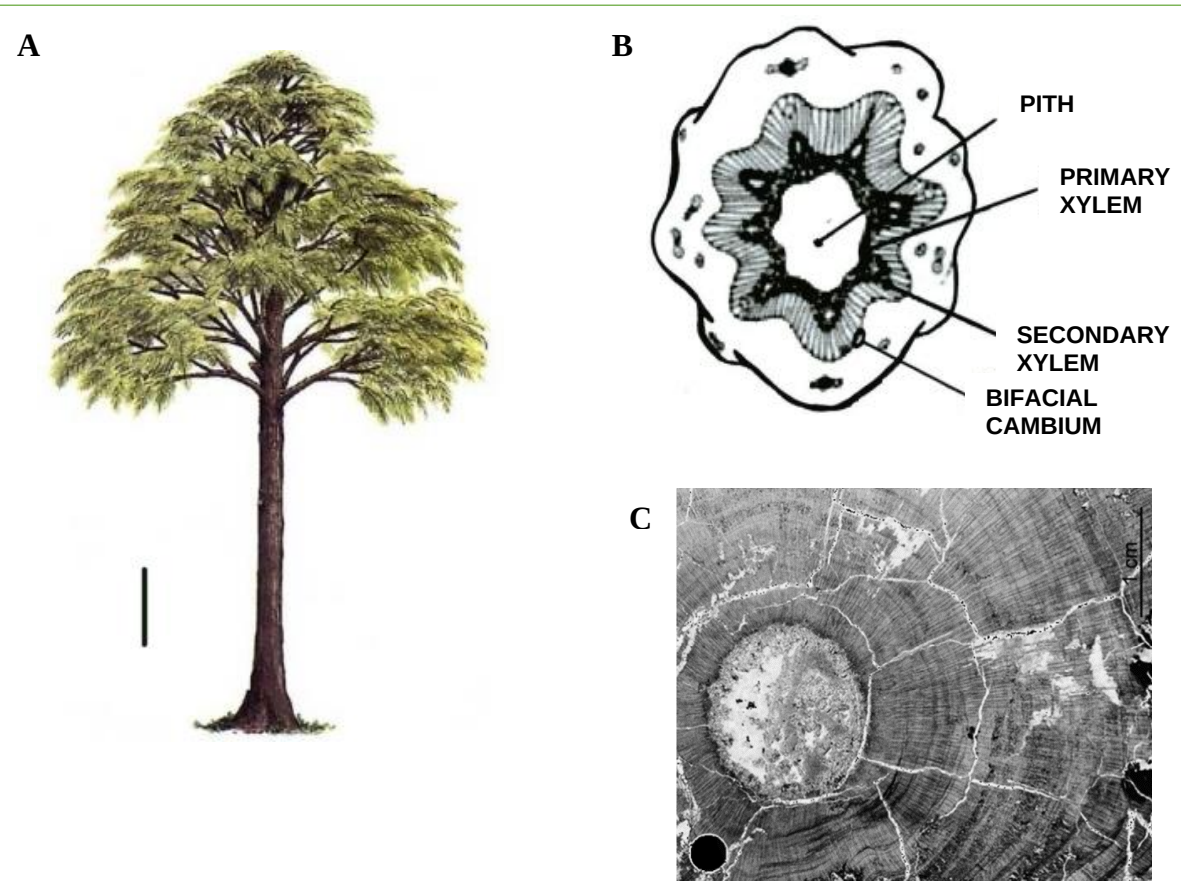


**Figure 2. A.** Representation of an *Archaeopteris* tree. Scale bar on the left represents one meter. (Willis & McElwain, 2014)
**B.** Reconstitution of a transversal cut of an *Archaeopteris* tree. The cambium is bifacial and produces on the inside xylem and on the outside phloem. (Willis & McElwain, 2014)
**C.** Transverse section of the stem of *Archaeopteris*, note the thickness of the wood around the primary vascular part, in the centre. (Meyer-Berthaud & Decombeix, 2009)

*2.2.What do you mean? A tree*

The tree, as we know it today, is defined by the Food and Agricultural Organisation (FAO) as a plant species capable, under non-limiting environmental conditions, of growing to at least 5m in height as an adult (FAO 2015). This general definition includes both woody and non-woody plants. However, a definition proposed by the Centre National de Ressources Textuelles et Lexicales (CNRTL) specifies the FAO one by proposing to define a tree as a woody plant of variable size, whose trunk is granulated with branches from a certain height, thus highlighting the importance of lignification and branching and, therefore, of secondary growth to describe a tree (CNRTL 2012).

## 3. From trees to forests

It was during the Upper Devonian (-382.6 Ma to -358.9 Ma) (Figure 1) that plant formations comprising tree-like plants developed. Forests were then composed of species of the genus *Archeopteris* and spread throughout the world. By modifying the edaphic conditions of the environment by providing shade with the help of their canopy, the forests created, on the ground, conditions of temperature, humidity and sunlight that were very different from those that have prevailed until now outside these plant formations (Algeo *et al.*, 2016). Thus, the variations in temperature and light parameters were greatly attenuated, both during the day and within a dry season. The environment that was thus created on the ground benefited from relatively stable conditions. Moreover, the regular renewal of the *Archeopteris* crown caused a consequent production of plant matter which would first generate litter and then humus leading to a modification of the nature of the substrate itself resulting in a chemical evolution of the soil (Algeo *et al.*, 2016). But the impact of the appearance of forests on the environment was not limited to the modification of soil properties. Indeed, by fixing a large quantity of $CO_2$ regularly fossilised in the lithosphere, forests participated in the modification of the climate and have most certainly contributed to the important cooling that marked the end of the Devonian and the beginning of the Carboniferous (-358.9Ma) (Algeo *et al.*, 2016).

The Carboniferous period (-358.9Ma to -298.9Ma) (Figure 1), although colder than the Devonian period, saw the development of luxuriant forests constituting the *coal flora*. These were marked by the presence of numerous Pteridophytes such as the arborescent Lycophytes (*Lepidodendron*) and other ferns, but also the first archaic Gymnosperms (*Cordaitales*) which made up 10 to 20% of this flora (Biswas & Johri, 1997). The gymnosperms reached their abundance and diversification peak from the Jurassic era to the early Cretaceous period (between 200 and 150 million years ago), when up to 50 000 fossil species were counted (compared with c.a. 1000 species today), before slowly declining and giving way to angiosperms, whose first pollens appeared at the beginning of the Cretaceous period (130 million years ago) and which became dominant at the end of the period (66 million years ago) (Roland *et al.*, 2008) (Figure 3).

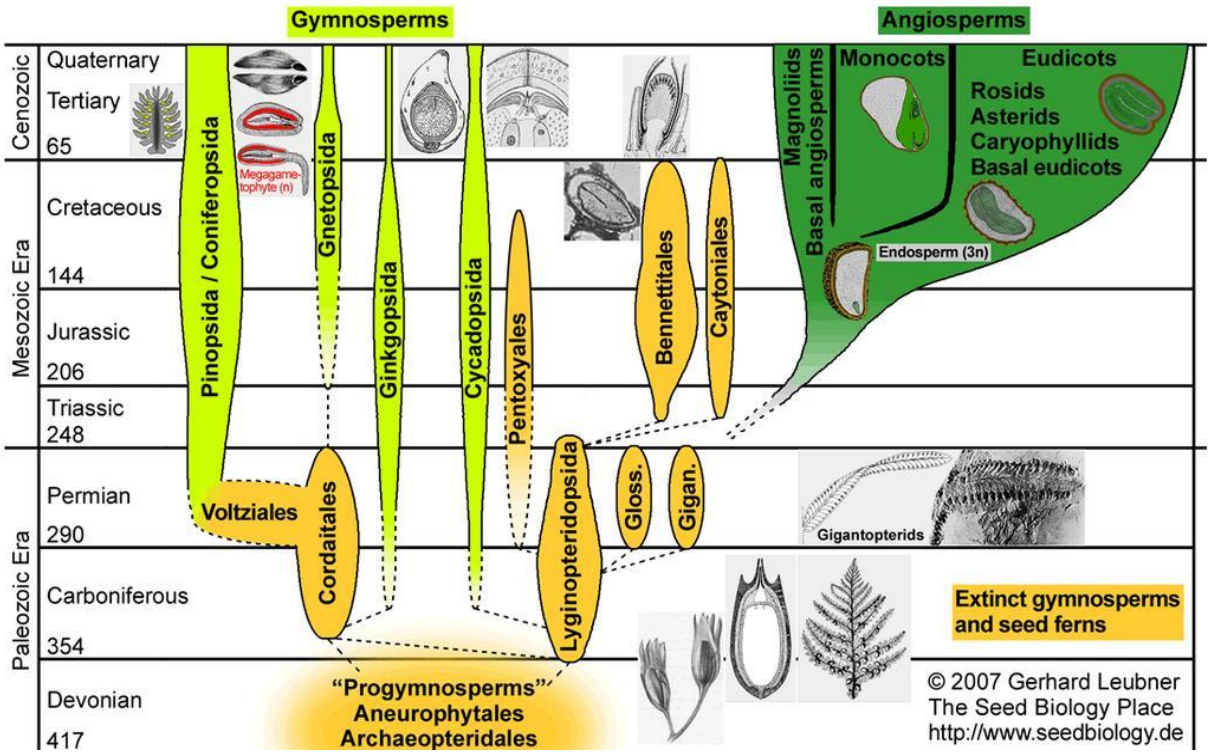


**Figure 3.** Representation of the relative abundance of Gymnosperms and Angiosperms through the geologic timescale. Gymnosperms, although abundant during the Carboniferous and Permian eras became less and less predominant as the Angiosperms appeared and developed.

Unlike their sister group the gymnosperms (from the Greek words *gymno* 'naked' and *sperma* 'seeds'), the angiosperms represented an evolutionary leap forward as plants enclosed their ovules (and then their seeds) in an ovary, which protected them from their environment. In addition, their evolutionary success was also largely attributed to their leaves. Indeed, as the climate warmed up in the Middle Cretaceous and the sea level rose, angiosperms would have had an advantage because their leaves had a high stomatal density and numerous veins that facilitated their rate of transpiration and the achievement of photosynthesis, thus allowing them to grow more (Simonin & Roddy, 2018). Therefore, angiosperms would have rapidly diversified to include, today, about 300,000 species (Figure 3). Thus, the forest ecosystem, built from the Devonian to the Cretaceous, with its biological diversity and its essential place in the matter and energy cycles of the terrestrial biosphere, although disrupted by the Cretaceous-Tertiary biological crisis, had hardly change in its organisation or in its mode of functioning and had given rise to the current forest ecosystems.

## 4. From forests to forest economy

The current forest ecosystem is defined by the FAO as land occupying an area of more than 0.5 hectares with trees reaching a height of more than 5 metres and a tree crown covering more than 10% of the land surface, or with trees capable of reaching these thresholds in situ (FAO, 2020). This forest ecosystem represents, at the global level, 4.06 billion hectares which corresponds to 31% of the total land area (FAO, 2020) and is distributed for more than half in five countries: Russia, Brazil, Canada, USA, and China (Figure 4). However, this area is constantly decreasing at the rate of deforestation, corresponding to the conversion of forest to other land uses, affecting 10 million hectares per year over the period 2015-2020 (FAO, 2020).

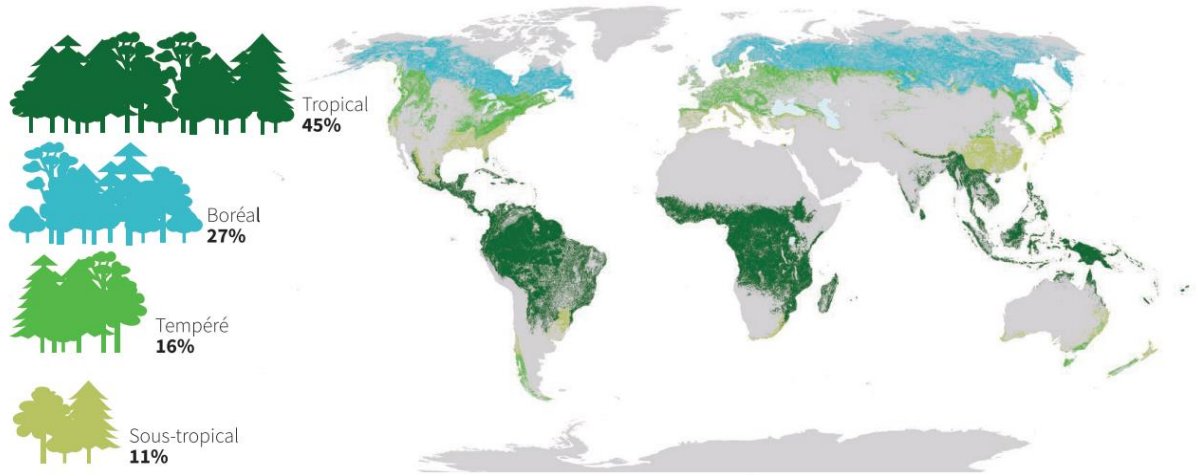


**Figure 4.** Distribution of the different forest ecosystems around the world. (FAO, 2020)

Yet, although in danger of deforestation, forests are of great economic importance to humanity. For example, in China, the forestry industry employs more than 60 million people in 2020 and generates a wood production of 88.11 million $m^3$ and an income of nearly 1.081 trillion US dollars (United Nations Department of Economic and Social Affairs, 2021). In the United States, forest products provide employment for 955,400 people generating an income of $11 billion per year (United Nations Department of Economic and Social Affairs, 2021). On another level, France is the 4th most forested country in Europe as there are approximately 16.7 million hectares of forest in mainland France (Antoni *et al.*, 2020). Economically, the forestry and wood industry generate 38.8 million $m^3$ of wood and 26 billion euros each year, which in 2018 corresponded to 1.1% of gross domestic product (GDP). This same sector has a significant social importance as it directly employs 392,700 people and indirectly employs 62,000 others. In total, 454,700 jobs in France, i.e., 1.4% of the working population, are directly dependent on the health of our forests (https://fibois-france.fr/chiffres-cles/). Thus, approximately 30% of the world's forests are used for wood production.

In addition to its strong economic impact, forests also provide humanity with numerous social and ecosystem services (Ayres & Lombardero, 2000). Indeed, 180 million hectares of forest are used globally for social services such as recreation, tourism, education, research and conservation of sites of cultural or spiritual importance (Allen *et al.*, 2010; FAO, 2020). It also provides many ecosystem services such as watershed protection, air purification and soil

protection against erosion (Allen *et al.*, 2010). The forest also has the advantage of being a reservoir for the biodiversity of fauna and flora. For example, in metropolitan France, 138 species of trees, 73 species of mammals, 120 species of birds, 30,000 species of fungi and as many insects are found in the forest (https://www.onf.fr/onf/forets-et-espaces-naturels/) . Finally, forests are essential for the global climate balance through their roles as carbon sinks, biomass production, soil maintenance and climate regulation (Reichstein *et al.*, 2013). In particular, it is estimated that 8 billion tons of $CO_2$ are absorbed each year worldwide, making forests the second largest carbon sink on the planet after the oceans.

Although forests play a crucial role in sustaining life on the planet, providing economic and ecosystem services, they are prey to numerous destructive events, whether anthropogenic and/or climatic, which regularly lead, in addition to deforestation, to tree death and forest dieback.

# Part 2. Trees in a changing environment: from climate change to forest dieback

## 1. A changing climate

### *1.1.Climate change: definition, causes and consequences on temperatures*

Climate change is defined by the United Nations Framework Convention on Climate Change as "a change of climate which is attributed directly or indirectly to human activity that alters the composition of the global atmosphere and which is, in addition to natural climate variability, observed over comparable time periods.". In general, climate change is assimilated to global warming which is defined as "the estimated increase in global mean surface temperature averaged over a 30-year period, or the 30-year period centred on a particular year or decade, expressed relative to pre-industrial levels." (IPCC, 2018).

Global warming, as of today, is mainly caused by the accumulation of greenhouse gases (GHGs) in the atmosphere. Since the pre-industrial era, increasing anthropogenic GHGs emission were noticed mainly driven by the economic and population growth (IPCC, 2021). Due to anthropogenic activities, the concentration of GHGs (mainly $CO_2$) grows at an important rate and get to levels that were never reached in the last 800,000 years (IPCC, 2014). Thus, even if it exists natural sinks, such as forests (Pan *et al.*, 2011) and oceans, and natural carbon reservoirs such as rock and sediments, the IPCC demonstrated that 40% of the $CO_2$ emissions remained in the atmosphere since 1750 and the beginning of the industrial revolution which saw the improvement of the steam engine, the mechanisation of processes and the development of factories (IPCC, 2014) (Figure 5).

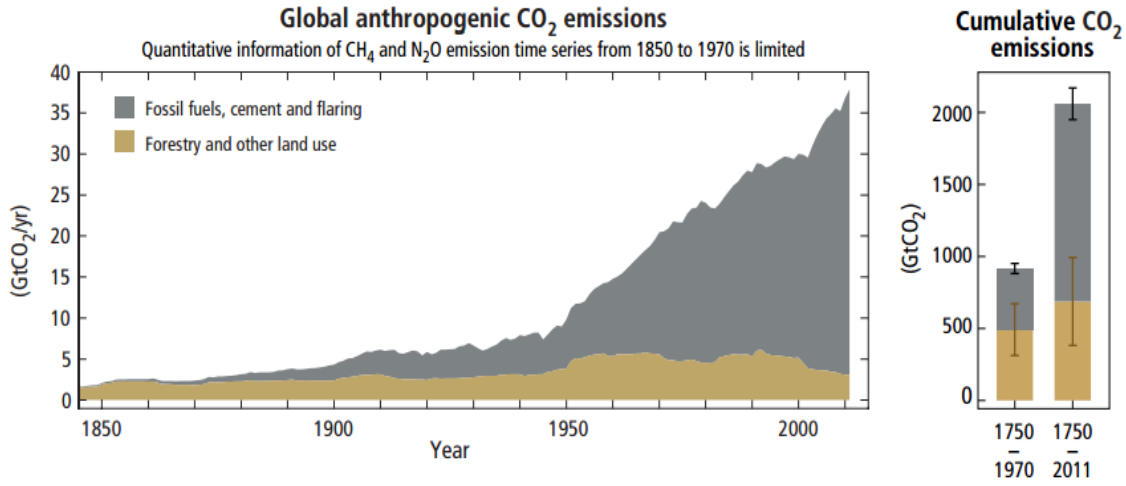


**Figure 5.** Annual global anthropogenic $CO_2$ emissions. Half of the cumulative anthropogenic $CO_2$ emissions between 1750-2011 were emitted in the last 40 years mainly due to fossil fuel combustion linked with economic development. (IPCC, 2014)

This accumulation of $CO_2$ in the atmosphere is positively correlated with temperature changes as the global mean peak surface temperature increases in a range of 0.8°c to 2.5°c per trillion tons of carbon emitted as $CO_2$. Thus, according to the SSP5-8.5 scenario, worst-case scenario, simulating an Earth surface temperature warming of 4.5°c relative to 1850-1900, the temperature elevation could reach between 1.5°C at the south of Latin America and +11°C at the North Pole by 2100 leading to an atmosphere composition and a global surface temperature by 2300 comparable to the one of the early Eocene period, i.e., 60 million years ago (Arias *et al.*, 2021; IPCC, 2022) (Figure 6).

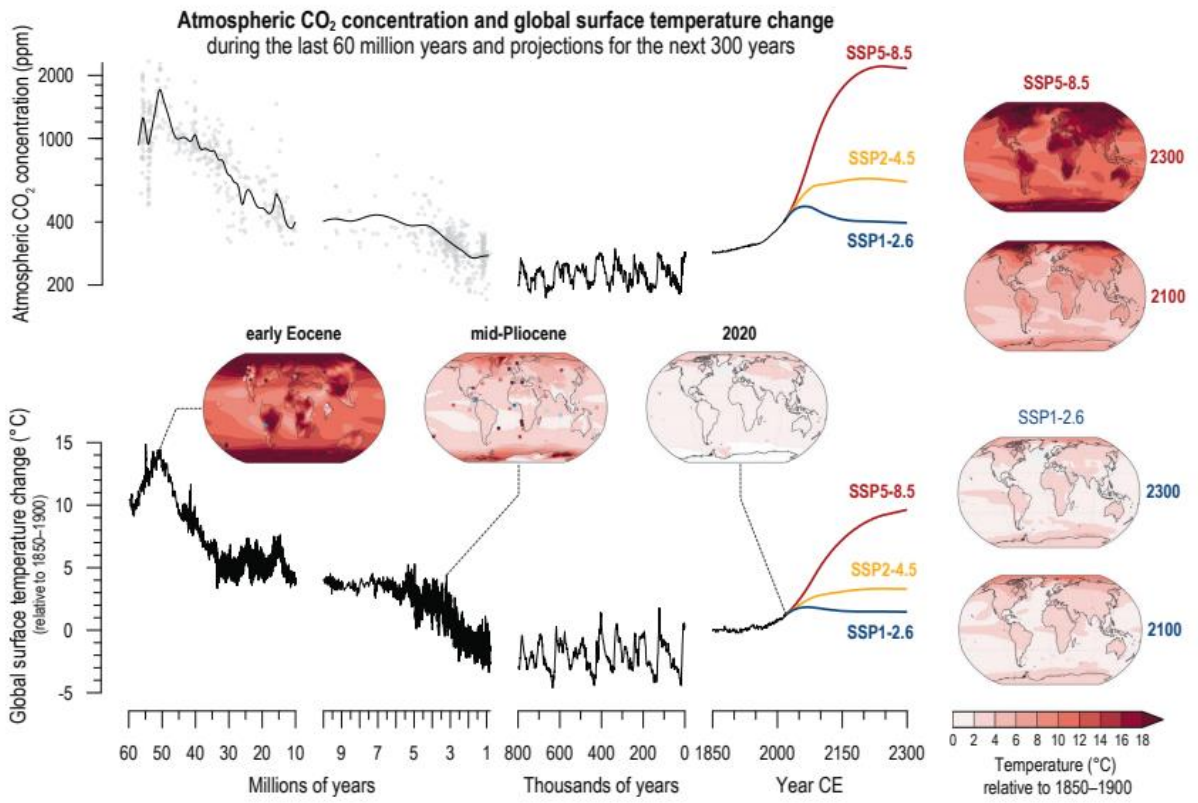


**Figure 6.** Changes in atmospheric $CO_2$ and global surface temperature (relative to 1850-1900) from the deep past to the next 300 years. (Arias *et al.*, 2021)

### *1.2.Effects of global warming on water availability*

Changes in water cycle are likely to occur with global warming. Thus, the IPCC reports that changes in precipitation will not be uniform worldwide. Indeed, wet regions are expected to become wetter while dry regions are likely to get drier (Trenberth *et al.*, 2014; IPCC, 2022) (Figure 7). For example, under the moderated climate change scenario SSP2-4.5, it is to be expected that Southern Europe will experiment precipitations reduced by 20% compared to present days (Figure 7). More importantly, model predictions show that changes in precipitation patterns will not only increase the frequency of drought events but also their intensity and duration (Trenberth *et al.*, 2014; IPCC, 2022).

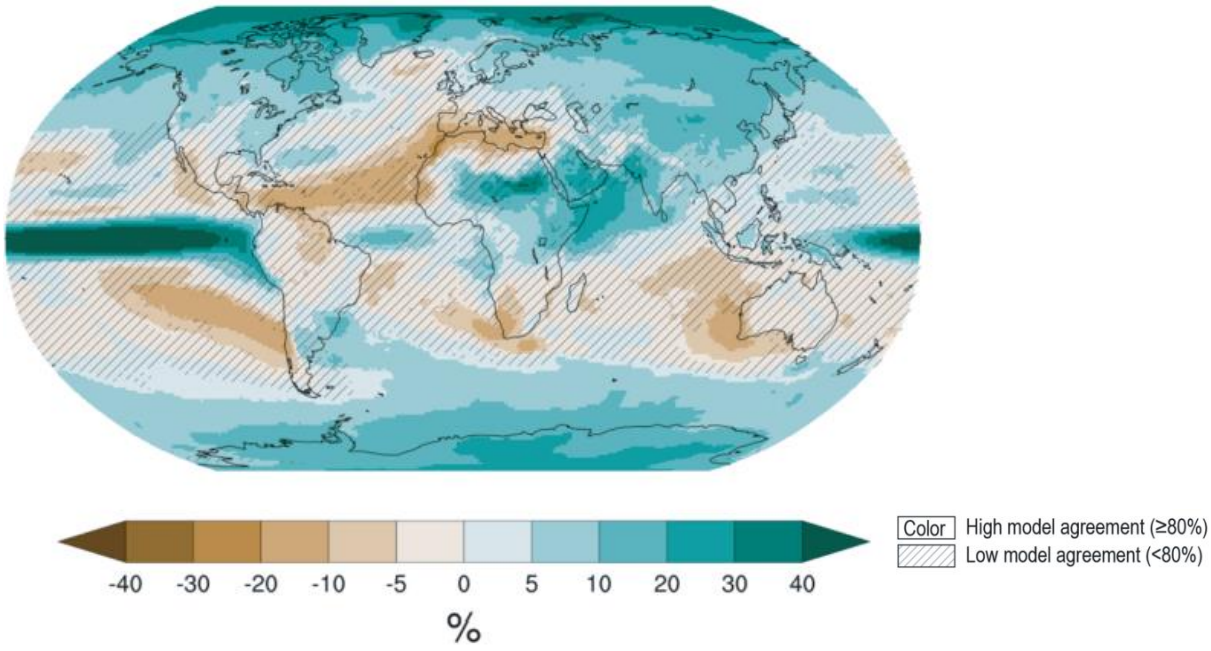


**Figure 7.** Long-term (2081–2100) projected annual mean changes (%) relative to present-day (1995–2014) in the SSP2-4.5 emissions scenario for precipitation. (Arias *et al.*, 2021)

### *1.2.1. Lower precipitations consequences: What is drought?*

Droughts are complex phenomenon, and their definition can include water stress as well as elevation in temperatures. However, even though it exists four different definitions for drought, meteorological drought seems to be the more common one and the one that is the most related to tree physiology (Wilhite & Glantz, 1987). Indeed, meteorological drought is defined as "a meteorological anomaly characterized by a prolonged and abnormal moisture deficiency" (Palmer, 1965) or a as "prolonged absence or marked deficiency of precipitation" or as "a deficiency of precipitation that results in water shortage for some activity or some group" or, finally, as "a period of abnormally dry weather sufficiently prolonged for the lack of precipitation to cause a serious hydrological imbalance" (IPCC, 2022). Thus, in all definitions, meteorological drought relies on a shortage in precipitations leading to a water imbalance and will be the one used for the remaining of this PhD report.

### *1.2.2. Examples of drought-induced forest die-off*

Vegetation mortality can be induced by multiple factors including the recurrence of climate stress, insects pests and diseases (Franklin *et al.*, 1987; Miao *et al.*, 2009; McDowell *et al.*, 2022). However, studies in plant mortality frequently agree in that water limitation is one of the main causes of plants death (McDowell *et al.*, 2022). In fact, it has been shown that when plants undergo recurrent exposure to drought, their growth decreases significantly and their risk to die increases (Pederson, 1998; Suarez & Ghermandi, 2004). Numerous episodes of drought-induced forest mortality have been observed in the last decades (Allen *et al.*, 2010, 2015; Hartmann *et al.*, 2018) with evidences of the consequences of hotter-droughts (Hammond *et al.*, 2022) (Figure 8). For example, important widespread drought-induced tree mortality events were reported in Africa such as in the tropical moist forest of Uganda (Lwanga, 2003), in New-Zealand with the mortality of *Nothofagus* forests (Hosking & Hutcheson, 1988) and in

France during the heat wave and drought during the summer 2003 (Landmann & Dreyer, 2006).

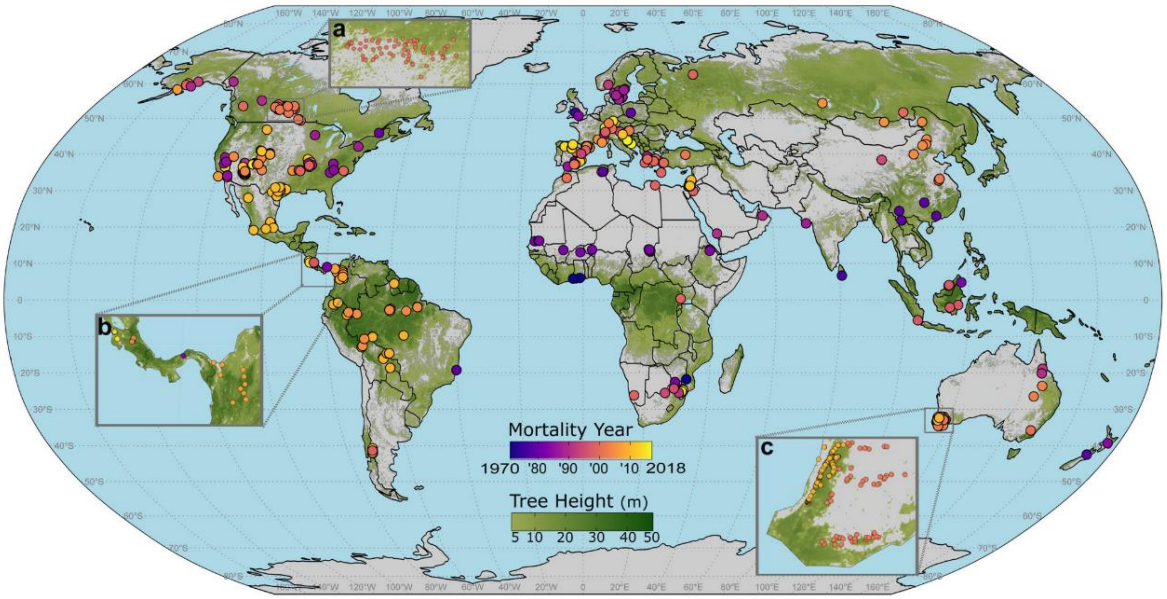


**Figure 8.** Location of substantial drought and heat-induced tree mortality around the globe since 1970. (Hammond *et al.*, 2022)

As those drought events are likely to get more frequent and more intense in a near future (Trenberth *et al.*, 2014) (Figure 9), it is important to highlight the role of drought in determining the composition and structure of forests globally (Allen *et al.*, 2010, 2015).

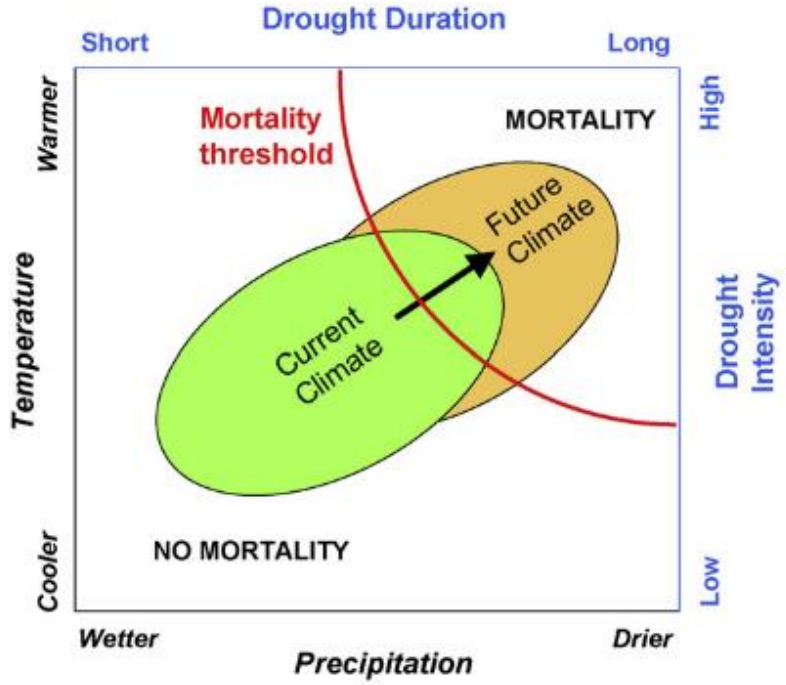


**Figure 9.** Conceptual diagram showing range of variability of "Current Climate" parameters for precipitation and temperature, or for drought duration and intensity. "Future Climate" shows increases in extreme drought and temperature events associated with projected global climate change, indicating heightened risks of drought-induced die-off for current tree populations. (Allen *et al.*, 2010)

Indeed, an important number of forests worldwide are located in areas where the risk for drought is expected to increase in the next decades. Thus, e.g., the progressive water loss during the California drought (2012-2015) led to the loss of 102 million trees (Asner *et al.*, 2016). Contrary to California, which can be considered as a water-limited region, some non-water-limited areas experienced similar consequences induced by drought. This was the case for the tropical northern area of Australia, where 6% of the mangrove vegetation died from drought event combining high temperatures and low precipitations back in late 2015, early 2016 (Duke *et al.*, 2017). In France, in 2019, many areas experienced below average precipitation patterns, which had strong impact on both forest ecosystems and forests productivity. It was reported that each year over the period from 2011 to 2019 in France, 10 $Mm^3$ of wood died due to the consequences of climate change (less precipitations and higher temperatures) which corresponds to approximately 0.6 $m^3$ of wood per hectare per year (IGN, 2021) (Figure 10). In 2019, for example, the French National Forest Office (ONF) registered in the Auvergne-Rhône-Alpes region many drought-induced tree mortality events that affected some of the key tree species of the region, such as spruce, beech, fir, and Scots pine.

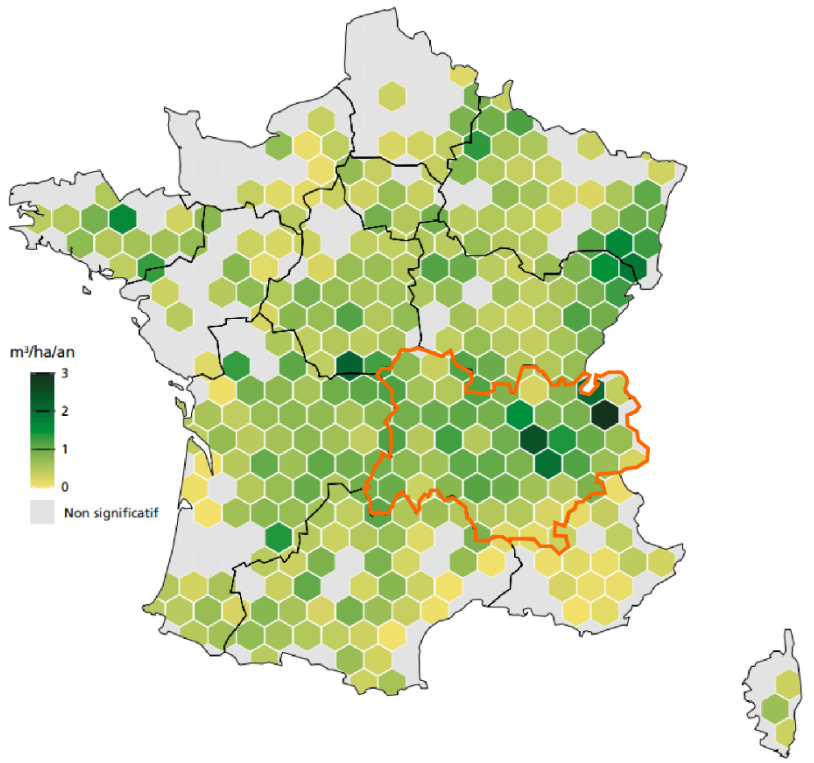


**Figure 10.** Distribution of forest mortality in France over the period 2011-2019.
The orange line surrounds the Auvergne-Rhône-Alpes region. (Adapted from IGN, 2021)

Although, in theory, an increase in atmospheric $CO_2$ could be correlated with improved photosynthetic efficiency and therefore better tree growth (Wertin *et al.*, 2010; Lewis *et al.*, 2013), it has been shown that this increase in $CO_2$ does not ameliorate the negative effects of high temperatures on drought-induced tree mortality (Duan *et al.*, 2014). In fact, rising $CO_2$ and warming could provide conditions for structural overshoot, where forests rapidly gain biomass and leaf area to levels not hydraulically sustainable during the eventual hotter droughts which could promote increasing mortality (Hammond *et al.*, 2022; McDowell *et al.*,

2022). Thus, forests are sensitive to climate change and because they play an important role in the carbon balance (Pan *et al.*, 2011) that, at the same time, helps regulating the climate (Reichstein *et al.*, 2013), it is crucial to prevent and predict the occurrence of drought-induced tree mortality event. For this, it is necessary to understand the mechanisms driving drought-induced tree mortality as well as identifying physiological traits that could be used as proxies for identifying when the decaying process in a tree has started.

## 2. Drought-induced tree mortality

### *2.1.Death in tree physiology*

In tree physiology, tree death has originally been defined as "[a] thermodynamic equilibrium between the organism and the environment, in which plants no longer have energy gradients to drive metabolism or regenerate."(McDowell, 2011). However, it was pointed out that tree death from drought was poorly define and that the definition given by McDowell in 2011 remained limited in utility as it did not provide proxies that can help to identify clearly if a tree is dead or not (Anderegg *et al.,* 2012b). Thus, Anderegg *et al.* (2012b), proposed that tree death can be considered as "a complete system failure due to lack of water resources" highlighting the central role of water in its definition. However, despite these definitions of tree death, in practice, it is difficult to determine if a tree is dead or not. Indeed, even if Anderegg *et al.*, settled a definition for tree's death, they pointed out that their definition was based on the ability of the tree to recover or not from drought events. They also highlighted that studies needed to clearly define what tree mortality was and provide with criteria that could permit the irrevocable identification of dead trees. Considering this, Mantova *et al.* (2022) proposed as a new definition for tree death and defined it as the irreversible cessation of the metabolism in a tree. More precise, they explained how from a plant–water relation point of view, tree death occurs when a tree is no longer able to maintain its key physiological functions (e.g., growth and/or reproduction). This definition thus focuses on the key roles of meristematic tissues for maintaining a tree alive.

### *2.2.Causes of tree death under drought conditions*

Tree mortality under stressing conditions has originally been described as occurring induced by multiple factors such as **predisposing factors** (e.g., genetic potential, climate change …), **inciting factors** (e.g., insects attacks, drought …) and **contributing factors** (e.g., viruses …) (Manion, 1981) (Figure 11). Predisposing factors are long-term stresses that weaken a tree and increase its susceptibility to subsequent incitants or inciting stresses. Inciting factors are described as relatively short-duration stresses that significantly impacts the physiological functioning of a tree that may or may not recover to its prior state. The contributing factors occur after a tree experienced the inciting factors and contribute to further reduce the vigour of the tree until death occur (Manion, 1981). More recently, it has been shown that tree mortality can be induced by multiple factors such as the recurrence of climate stress, insects pest and diseases (Franklin *et al.*, 1987; Miao *et al.*, 2009; McDowell *et al.*, 2022).

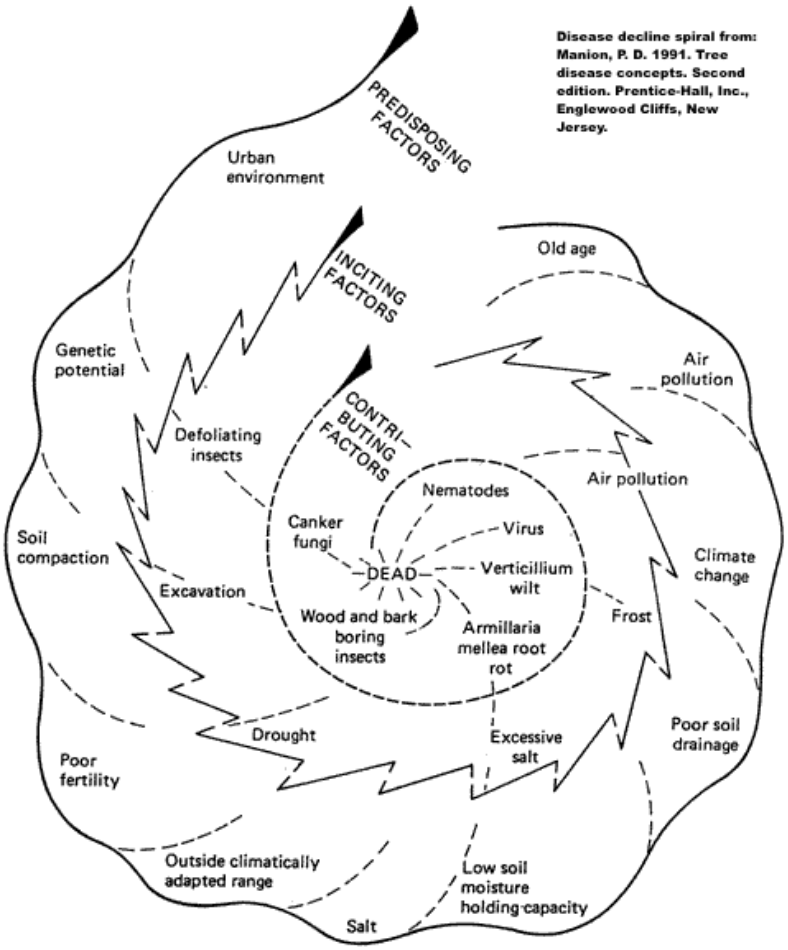


**Figure 11.** Manion spiral representing how predisposing factors, inciting factors and contributing factors can lead to tree death. (Manion, 1981)

However, studies in tree mortality frequently agree in that water limitation is one of the main causes of tree death. Indeed, as trees undergo a recurrent exposure to drought, their growth decline significantly and their risk to die increases (Pederson, 1998; Suarez & Ghermandi, 2004). In addition, it seems that trees are likely to die when exposed to prolonged drought periods with high air temperatures and vapor pressure deficit (VPD) (see Part 3, 1.3.3) conditions causing an exacerbated need for an already limited water (Swetnam & Betancourt, 1998; Breashears *et al.*, 2005; Bigler *et al.*, 2006). Thus, when trees are exposed to water-stress conditions, trees, in the first place, close their stomata in order to limit water losses (Hogg & Hurdle, 1997; Buckley, 2005; Berry *et al.*, 2010). While protecting against the water losses, stomata closure constraints the $CO_2$ diffusion that could result in a significant reduction of the photosynthetic carbon uptake. Under these conditions, trees continue to maintain their metabolism and has thus a continuous demand for carbohydrates. Therefore, under prolonged or recurrent period of mild drought, trees could suffer, as a last resort, from **carbon starvation** and succumb to it (McDowell *et al.*, 2008). However, carbon starvation occurs when the duration of the water-stress is very long (i.e., last for years). Thus, it has been demonstrated that **drought-induced tree mortality is related to drought intensity and drought duration** (McDowell *et al.*, 2008) (Figure 12).

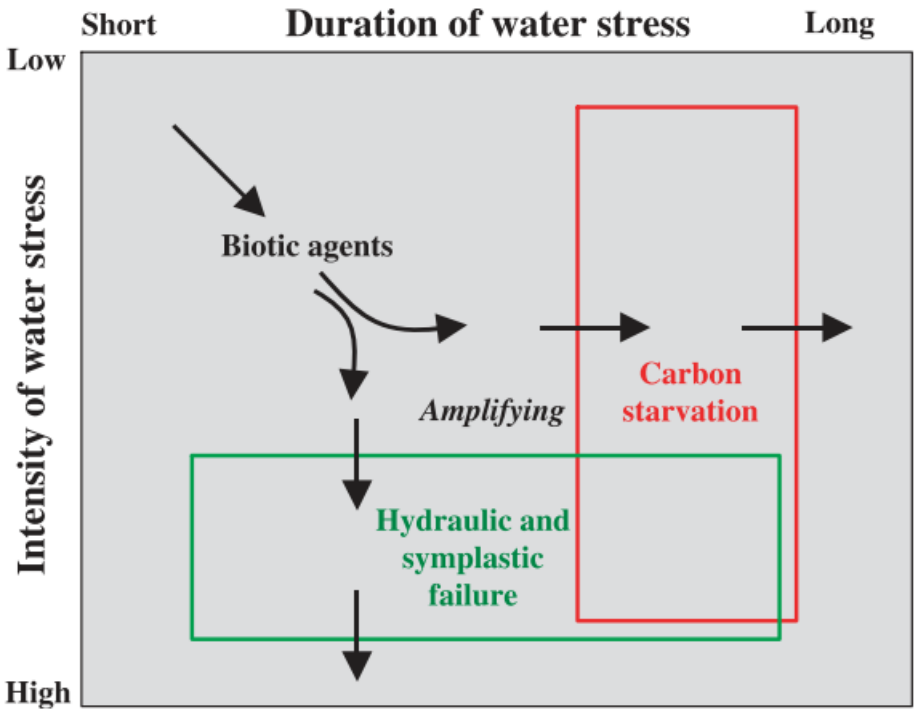


**Figure 12.** Theoretical relationship, based on the hydraulic framework, between the temporal length of drought (duration), the relative decrease in water availability (intensity), and the three hypothesized mechanisms underlying mortality. (McDowell *et al.*, 2008)

If the water stress conditions are intense, i.e., have a high intensity and short to long duration, trees will likely die from **hydraulic failure**. Indeed, despite their efforts to reduce water loss by closing their stomata (Jones & Sutherland, 1991; Bartlett *et al.*, 2016; Martin-StPaul *et al.*, 2017), plants still suffer from water-stress as their water potential decrease due to water loss through the cuticle (Kerstiens, 1996; Billon *et al.*, 2020) and stomatal leakiness (Oren & Pataki, 2001). Even though stomatal closure occurs rapidly when trees desiccate (Hochberg *et al.*, 2017), carbon starvation is a state that need several years to be reached. Therefore, in a context of climate change where drought have already an higher intensity compared to the ones occurring years ago (IPCC, 2022), several studies evaluating the physiological response of trees to drought have shown that trees were more likely to die from hydraulic failure than from carbon starvation (Hartmann *et al.*, 2013; Urli *et al.*, 2013; Delzon & Cochard, 2014). Thus, McDowell *et al.* (2022) **have proposed a renewed and adapted to drought version of the Manion spiral** showing that trees can die because of predisposing factors, both external (e.g., rising temperature or competition) or internal (e.g., low growth or structural damages), drought stress factors (e.g., turgor loss or soil-to-root conductivity loss) and dying factors (meristem death or hydraulic failure) putting the dying factor as the most important ones for provoking death under drought conditions (Figure 13). Thus, on this spiral, defence failure, runaway cavitation, hydraulic failure, meristem death, cell membrane damage and irreversible dehydration all appear as the key physiological mechanisms to explain and predict tree mortality from drought. Therefore, it seems crucial to understand the not only the physiological processes happening during drought, but also the ones occurring before and at the point of xylem hydraulic failure in order to understand how tree survival is being affected

by drought. For this, a better understanding of the tree water functioning is required to comprehend how trees die from being exposed to water-shortage conditions.

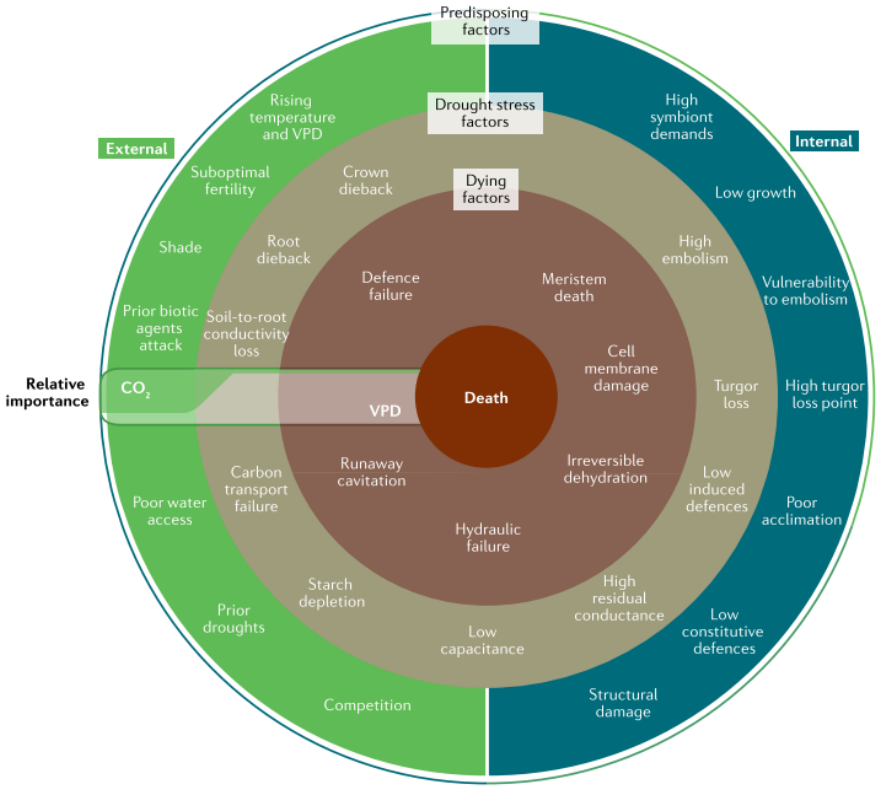


**Figure 13.** Interconnection of mortality processes. The death of the tree results from the interaction of external drivers, processes of hydraulic failure and carbon starvation and their interdependent mechanisms. (McDowell *et al.*, 2022)

# Part 3. Tree water functioning and dysfunctioning

## 1. Water circulation in trees

### *1.1.Water in plants: the basis of life*

Water plays a crucial role in the life of plants. It has a biochemical and mechanical role. Firstly, its biochemical role is mainly in the synthesis of organic matter *via* photosynthesis. In fact, to carry out these processes, plants must absorb $CO_2$ from the atmosphere. This absorption of $CO_2$ requires water, in order to open plants' stomata, and defines the Water Use Efficiency (WUE). WUE is a measure of the quantity of biomass produced per unit of water used by the plant. It is a concept introduced by Briggs and Shantz just over 100 years ago (Briggs & Shantz, 1913), which depends on both the saturated vapor pressure (itself varying with temperature) and the $CO_2$ diffusion gradient (Sperry, 2003). Thus, even though plants can control their WUE by adjustments in leaf temperature and photosynthetic capacity, WUE is mainly dictated by atmospheric $CO_2$ concentration (Sperry, 2003). Thus, over time, the WUE varied greatly as the $CO_2$ diffusion gradient varied from 0.5KPa in the Silurian/Devonian that presented a $CO_2$ concentration of about 2200 ppm and a mean temperature of 20°c (Brugger *et al.*, 2019) to 0.05KPa in the Carboniferous which presented a $CO_2$ concentration of about 450 ppm and a mean temperature of about 25°c (Franks *et al.*, 2013) (Figure 14). Thus, while the Silurian WUE was equivalent to 22 molecules of water used per molecule of $CO_2$ absorbed, it was of 390 molecules of water per molecule of $CO_2$ absorbed in the Carboniferous (Berner & Kothavala, 2001; Sperry, 2003).

Therefore, $CO_2$ uptake, which takes place *via* the stomata, exposes plants to significant water losses and thus threatens them with dehydration if water transport is not efficient.

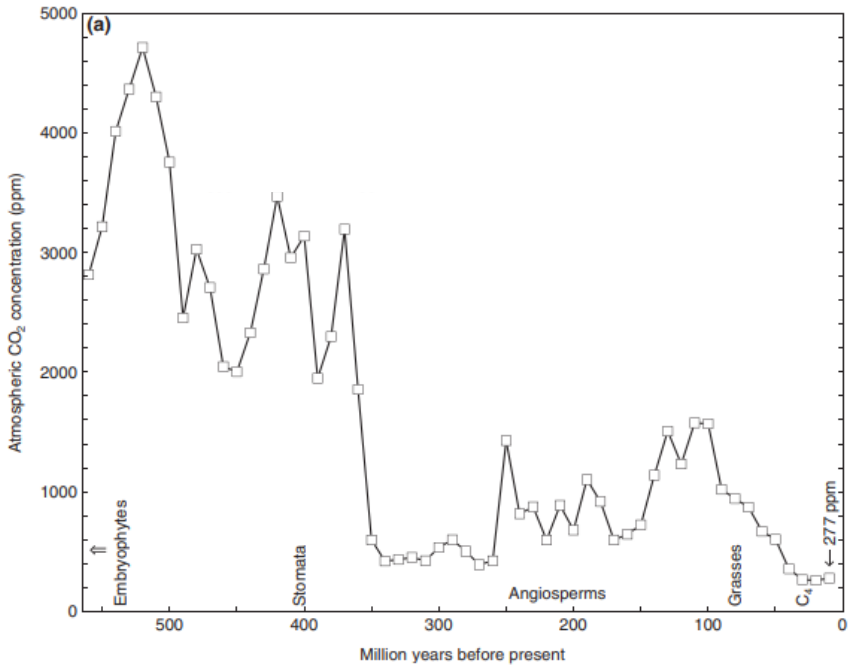


**Figure 14.** Atmospheric $CO_2$ concentration through time from 560 to 10 million years ago simulated by the GEOCARBSULF model. (Adapted from Franks *et al.*, 2013)

Considering nowadays $CO_2$ concentration (about 420 ppm) and mean temperature (15°c), it is estimated that for every gram of organic matter synthesised, 500g of water is absorbed by the roots, transported through the plant, and evaporated into the atmosphere (Taiz & Zeiger, 2006).

Secondly, water also plays a mechanical role in the life of plants, as it allows the plant to obtain a certain rigidity. Indeed, plant cells have a cell wall that allows them to support an internal hydrostatic pressure called the turgor pressure (Taiz & Zeiger, 2006). This turgor pressure is essential for many physiological processes such as the opening and closing of stomata or for growth by providing the force required for cell elongation. It also plays a role in mechanical processes such as the rigidity and stability of non-lignified tissues. Therefore, although water is the most abundant of all the resources that plants need to grow and function, it is also the most limiting. Indeed, the slightest imbalance in the water uptake/transpiration balance can lead to a lack of water and a malfunction of many cellular processes (Taiz & Zeiger, 2006). Thus, in a desiccating aerial environment, being able to balance water uptakes and losses is a challenge for terrestrial plants.

### *1.2.Water transport in trees*

#### *1.2.1. Two different type of sap, two different pathways*

Water in plants circulates through two vascular tissues: the xylem and the phloem, which transport raw and elaborated sap respectively. Raw sap is composed of inorganic nutrients taken from the soil and transported in the acropetal direction, i.e., from the roots to the leaves. Elaborated sap, on the other hand, is enriched with organic molecules. It is produced in the leaves during photosynthesis and circulates in the basipetal direction, i.e., from the leaves to the so-called "sink" organs and provides carbon nutrition. Thus, photosynthesis requires that the leaves have easy access to water (Taiz & Zeiger, 2006).

#### *1.2.2. The xylem, an efficient mode of water transport*

Plant's development in height since the Devonian period added constraints of water transport (Meyer-Berthaud & Decombeix, 2009). In fact, as water was only present in the substrate, water-conducting tissues had to be put in place in order to allow its transport from the roots to the various parts of the trees. Thus, the development of a secondary xylem, also called wood, was observed for the first time in the fossil trees of the sediments of Lake Erie and improved the conductivity of the tissues by a factor of 6 (Sperry, 2003) and consequently ensured a better synthesis of organic matter. While today sap flow occurs *via* the secondary xylem that is composed of both living cells (reserve parenchyma, vessel-associated cells, sometimes secretory cells) and dead cells providing sap transport (tracheids and vessels) and mechanical support (fibre) (Taiz & Zeiger, 2006), this was not the case when wood appeared during the Devonian. Indeed, tracheids were the only type of xylem (Sperry, 2003) and it was not until 140 million years later, during the Permian (-298.9Ma to -251.9Ma), that vessels appeared in five different groups (Baas & Wheeler, 1996). This evolution, linked to the decrease in $CO_2$ concentration at the end of the Cretaceous and a decrease in WUE requiring more water to fix the same amount of $CO_2$, favoured plants with vessels whose hydraulic

conductivity is twice that of tracheids (Sperry, 2003), thus enabling them to bring water to the leaves more efficiently.

As of today, tracheids are found mainly in gymnosperms, which have homoxylated wood (Figure 15A), whereas vessels, which are an association of dead cells, are present in angiosperms, that present heteroxylated wood (Figure 15B) (Evert, 2006).

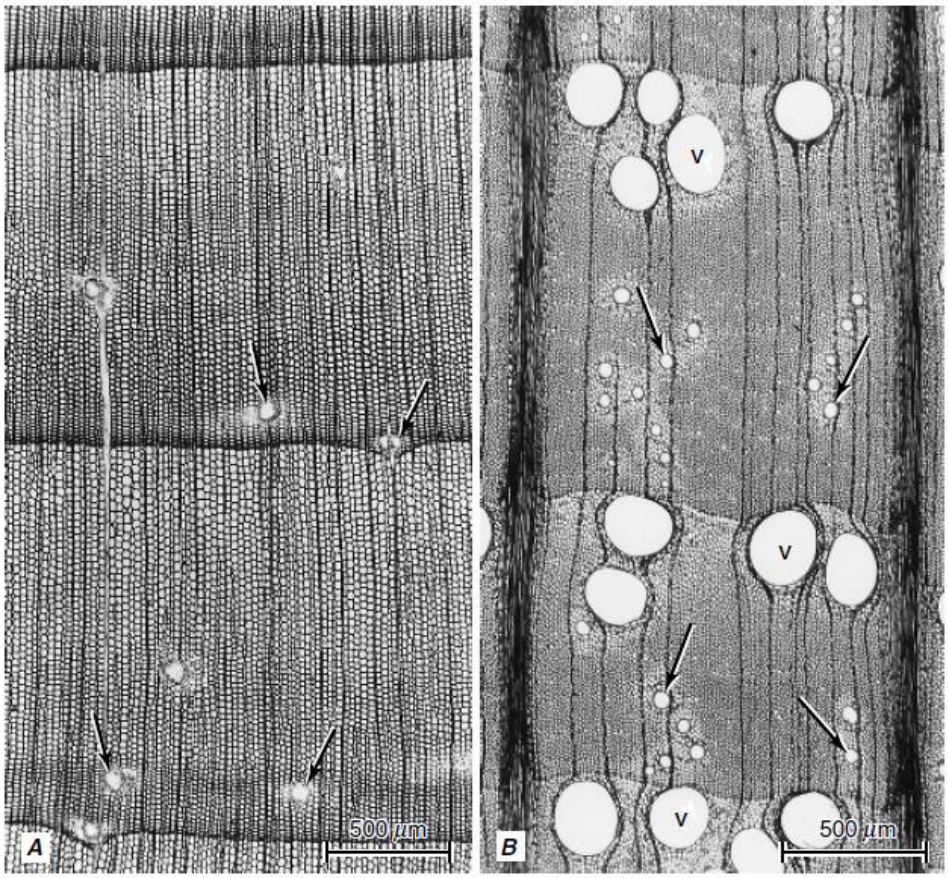


**Figure 15.** **A.** Wood of white pine (*Pinus strobus*), a conifer, in transverse section. The wood is homoxylated. **B.** Wood of red oak (*Quercus rubra*), an angiosperm, in transverse section. The wood is heteroxylated. (Evert, 2006).

The maturation of tracheids and vessels involves the production of a secondary cell wall and cell death. This cell death results in the loss of the cytoplasm and all its contents. As a result, xylem cells are devoid of membranes and organelles. They then appear under microscopy as empty with thick lignified walls. The tracheids, formed by a single cell, are elongated in the shape of a spindle and are organised in vertical rows that overlap. Water flows from tracheid to tracheid *via* pits in the side walls (Figure 16). These pits are microscopic regions where the secondary wall is absent and the primary wall is thin and porous allowing water to pass through (Taiz & Zeiger, 2006). In conifers, these pits have a torus in the centre that acts as a valve that will close the pit in case of water stress (Figure 16).

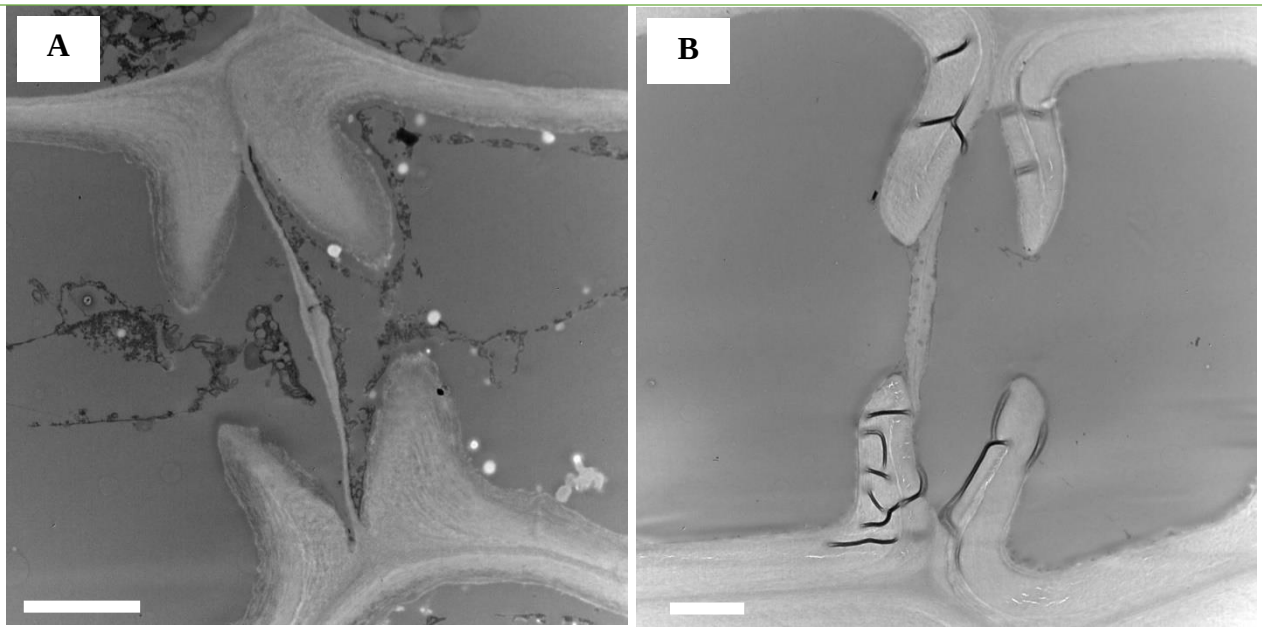


**Figure 16.** Transversal cuts of *Abies concolor* tracheids observed with Transmission Electron Microscopy at the 'Centre d'Imagerie Cellulaire Santé' in Clermont-Ferrand.
**A.** Close-up of the pit membrane with the torus in the centre.
**B.** Close-up of the pit membrane with the torus pressed to the cell wall showing reaction to water stress. Scale bars represents 2microns.

The vessel elements are generally shorter and wider than tracheids and have a perforated plate at each end (Figure 17). The presence of this perforated plate at each end allows the vessel elements to stack up to form a longer duct called a vessel. Thus, the vessels, which are multicellular, can reach lengths ranging from a few centimetres to several metres (Zimmermann, 1983). Due to their open ends, vessels elements provide an efficient pathway for water circulation (Figure 17) (Taiz & Zeiger, 2006).

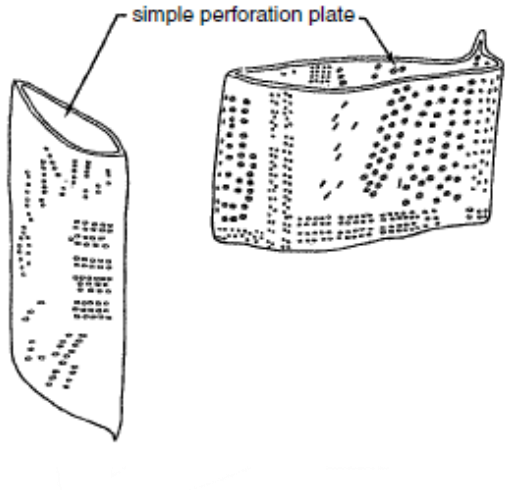


**Figure 17.** Illustration of a vessel element and perforation plate. (Evert, 2006)

## *1.3.Mechanisms of water circulation in trees*

### *1.3.1. Soil-plant-atmosphere continuum*

Water is absorbed at the root level by osmosis and transpiration. It circulates between the cells (**apoplasmic** pathway) or through the cell walls (**symplasmic** pathway) to the Caspary band where the symplasmic pathway is forced to the xylem (Figure 18) (Taiz & Zeiger, 2010).

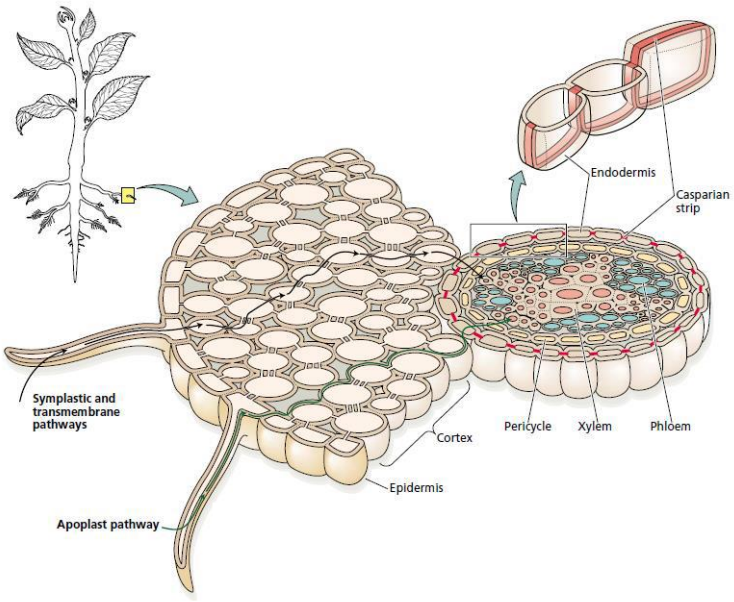


**Figure 18.** Water absorption at the root level. The apoplasmic pathway is represented in green and the symplasmic pathway in black. (Taiz & Zeiger, 2010)

The xylem then provides a low-resistivity pathway for water to ascend to the leaves (Kirkham, 2005; McElrone *et al.*, 2013). Indeed, for a xylem transport velocity estimated, in the case of a perfect tube (without asperity) at 4mm.s-1 when the radius is equal to 40µm, the pressure gradient required to move water within it is equivalent to 0.02MPa.m$^{-1}$. In comparison, to move water from cell to cell at a velocity of 4mm.s-1, it is necessary to generate a pressure gradient equivalent to 2*10$^{8}$ MPa.m$^{-1}$, i.e., ten orders of magnitude greater than during transport within the xylem. Thus, if water has to be forced upwards over a distance of 100 metres, which corresponds to the height of the tallest trees in the world, i.e., Sequoia (*Sequoia sempervirens*) in the USA and Eucalyptus (*Eucalyptus regnans*) in Australia, a pressure gradient of 2MPa would be required to reach the top of the tree. However, this would not take into account the effect of gravity and a pressure difference of 3MPa would be required between the base of the tree and the tip of the branches to bring water to the top of the trees (Taiz & Zeiger, 2006).

Therefore, it is necessary to generate a pressure gradient for the water to rise inside the plant. In theory, this pressure gradient could be caused by a positive pressure at the base of the plant or a negative pressure (tension) at the top of the plant. Although positive pressure may exist at the roots, it rarely exceeds 0.1MPa. Thus, it does not appear to be sufficient to allow the movement of the water column in the plant. Therefore, a mechanism explaining the ascent of water in the plant was proposed by Dixon and Joly in 1894: the *Cohesion-Tension*

*Theory of sap ascent*. This mechanism owes its name to the fact that the cohesive properties of water are required in order to support the important tensions undergone by the water columns in the xylem. In the cohesion-tension theory, the source of negative pressure (tension) develops at the surface of the leaf cell walls. Thus, the cell walls act as fine capillary networks that retain water. As these cells are in direct contact with the drying atmosphere, the water retained on the surface of the cell walls gradually evaporates, while some is still retained in the interstice of the walls. An air-water meniscus is formed which, due to the high surface tension of the water, generates a tension (negative pressure). The more water is removed from the walls by evapotranspiration, the more the curvature of the meniscus increases, and the more negative pressure is generated (Taiz & Zeiger, 2006). Thus, water is continuously drawn towards the leaves, *via* evaporation from the leaf surface, which generates the movement of the water column from the roots to the leaves (Meinzer *et al.*, 2001; Brown, 2013) (Figure 19). This movement is the result of purely physical forces and therefore does not require energy expenses as the energy required for this movement comes solely from the solar energy that reaches the leaf and causes an increase in the temperature of the leaf and the surrounding air, leading to the evaporation of water. A tension gradient is then generated from the atmosphere to the ground forming the **soil-plant-atmosphere continuum** (Taiz & Zeiger, 2006) (Figure 19).

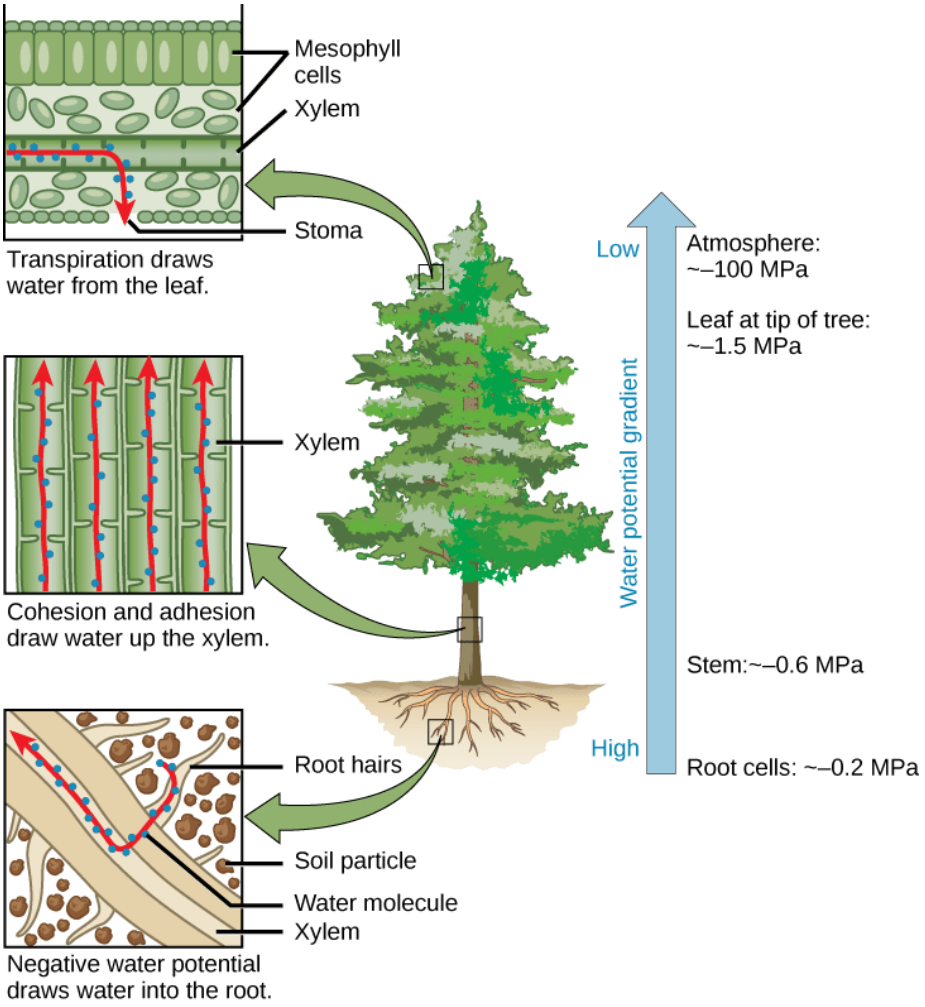


**Figure 19.** Representation of water transport through the soil-plant-atmosphere continuum (*extracted from* https://openstax.org/books/biology-2e/pages/30-5-transport-of-water-and-solutes-in-plants).

### *1.3.2. Long distance water transport: Pressure-driven bulk flow*

In plants, as transpiration generates a negative pressure throughout the plant and the resistance to water flow through the soil-plant-atmosphere continuum generates a negative pressure gradient, **pressure-driven bulk flow** of water is responsible for long-distance transport of water in the xylem. Bulk flow represents the concerted movement of groups of molecules en mass, most often in response to a pressure gradient. In contrast to diffusion, pressure-driven bulk flow is independent of solute concentration gradients, as long as viscosity changes are negligible (Taiz & Zeiger, 2006).

Thus, the tension difference between two points is explained by the equation (1):

$$(1)\ \Delta\Psi = F * R$$

Where ΔΨ is the pressure difference between two points, F the water flow and R the resistance of the conductive elements to the passage of water between two points. The **water potential** (Ψ) represents a measure of free energy per volume unit, expressed in J.m-3, equivalent to a measure of pressure whose international unit is the Pascal (Pa). The water potential therefore represents the avidity of a compartment to water. Thus, if the water potential is negative, energy will be required to separate the water from its initial compartment. If it is positive, the water will give up energy to return to its initial state.

### *1.3.3. Water potential, composition and variations*

Plant water potential (Ψ) is a parameter that varies according to the time of day or during the seasons or even according to precipitations (Klepper, 1968; Ameglio & Cruiziat, 1992). It represents the resultant energy of osmotic (Ψs), pressure (Ψp), gravity (Ψg) and matrix (Ψm) forces. It is expressed by the following equation (2) (Taiz & Zeiger, 2006) :

$$(2)\ \Psi = \Psi_s + \Psi_p + \Psi_g + \Psi_m$$

The reference state is the water potential of pure water at room temperature and pressure.

- The *osmotic potential* (Ψs) represents the effect of dissolved solutes on the water potential. Solutes reduce the free energy of water by diluting it and causing the disorganisation of the system and consequently reduces the free energy. Pure water thus has an osmotic potential equal to 0.
- The term (Ψp) corresponds to *the hydrostatic pressure of the solution*, for a plant cell this term corresponds to the turgor pressure. Thus, if a cell is turgid (full of water), the hydrostatic potential will be positive. Therefore, positive pressures increase the water potential while tensions decrease it.
- The term (Ψg) is *the effect of gravity* on water. It depends on the height (h) of the water column, the density of the water (ρw) and the acceleration due to gravity. Thus, a height of 10m translates into a change in water potential of 0.1MPa.
- Ψm correspond to the *matrix potential* and is only used in the case of a soil. It represents the forces exerted by the capillary forces of the soil. Thus, its value depends on the type of soil, size of its particles and abundance and diameter of colloids.

Therefore, for expressing the water potential of trees that are less than 10 meters in height, the Ψg and Ψm components are often neglected and the water potential is simplified as follows (3) (Taiz & Zeiger, 2006):

$$(3)\ \Psi = \Psi_s + \Psi_p$$

The sap in the plant always moves from the most positive to the most negative water potential (Nobel, 2009). Thus, the bulk flow causes the ascent of the sap within the soil-plant-atmosphere continuum from the roots, in the soil which has a water potential of about -0.01MPa for a soil under field capacity conditions, to the atmosphere whose water potential is extremely negative, about -100MPa.

At the level of a plant, variations in water potential are determined by the amount of water available in the soil, the evaporative demand of the air and the hydraulic resistance of the plant. An essential parameter, the VPD, expressed in PSI or Kilopascal, allows to express how a plant responds to the evaporative demand of its environment. This VPD is the difference between the amount of moisture in the air and the amount of moisture that the air can potentially hold when saturated and is a curvilinear function of temperature (Lawrence, 2005). When VPD increases, meaning that the air is dry, i.e., has a more negative water potential, plant transpiration increases resulting in a need to pump more water from the roots. Therefore, in order to avoid excessive water loss due to a VPD increase, plants close their stomata which will avoid a too critical increase in the tension in the xylem vessels. However, an increase in plant transpiration caused by a high VPD will result in both soil dehydration, which, combined with the effect of the VPD itself, will present a more negative water potential, resulting in an abrupt decrease in plant water potential (Dai, 2013). Conversely, if the VPD of the plant's environment decreases, i.e., the air becomes loaded with moisture, then transpiration will decrease until it ceases completely. Thus, the VPD has a linear relationship with the level of evapotranspiration and its modification causes a variation of the Ψ of the plant.

Within plants, cell growth, photosynthesis and productivity are strongly influenced by Ψ and Ψ thus appears a good indicator of plant health. For example, when the soil dehydrates, during a drought for example, $\Psi_{soil}$ becomes more negative, and $\Psi_{plant}$ also decreases and can reach lethal level. Thus, very high VPD levels can lead to water stress in the plant which will increase their mortality risk. Therefore, increases in background mortality may be related to higher VPD conditions due to global warming. Indeed, regional trends of increasing background mortality are observed in North America, the Amazon Basin and Europe, and suggest that a common factor underlies changes in woody plant mortality (Hartmann *et al.*, 2018; McDowell *et al.*, 2022).

## 2. Water circulation in a drying environment

### *2.1.Xylem hydraulic failure, definition, and mechanism*

During a drought event, as the air of the atmosphere get drier and VPD increases, the leaf cuticular conductance increases (Riederer, 2006; Hasanuzzaman *et al.*, 2018) and the soil water availability decreases. As this happens, $\Psi_{xylem}$ decreases (Dai, 2013) resulting in an increment of the xylem tension, after the plants have closed their stomata (Jones & Sutherland, 1991;

Bartlett *et al.*, 2016; Martin-StPaul *et al.*, 2017), which can induce the occurrence of cavitation events in the xylem conduits (McDowell *et al.*, 2008, 2022) as water moves in trees under metastable conditions. Cavitation is the change from liquid water to water vapour under increased tension. This change in water phase results in the formation of gas bubbles termed *emboli* (Figure 20) in xylem conduits (Dixon & Joly, 1894; Tyree & Sperry, 1989) which can accumulate within a vessel, generates a gas-filled void referred as *embolism*, and provoke the hydraulic dysfunction of the xylem, thus reducing plant water transport capacity. This is especially the case during intense drought, where the embolism can spread throughout the entire xylem and cause a systemic failure of the system (Choat *et al.*, 2016b). As the percentage of embolised vessels increases, the hydraulic conductance of the xylem decreases until de flow of water stops and provokes the desiccation of the tree tissues, the cell death, and as a last resort, the death of the tree (McDowell *et al.*, 2008, 2022; Mantova *et al.*, 2022).

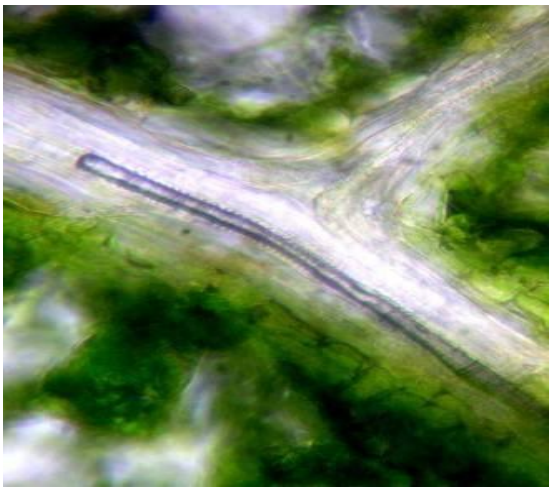

**Figure 20.** Photograph of an emboli within a xylem vessel of a *Juglans nigra* leaf. (Cochard & Delzon, 2013)

### *2.2.Cavitation formation: air-seeding theory*

A large number of observations have shown that cavitation of xylem vessels is induced by **air-seeding theory** (Tyree, 1997; Choat *et al.*, 2016b) and this hypothesis has been tested experimentally (Cochard *et al.*, 1992). The study of the air-seeding process showed that the cavitation phenomenon occurred at the pit-membranes (Zimmermann, 1984; Sperry *et al.*, 1988) (Figure 21).

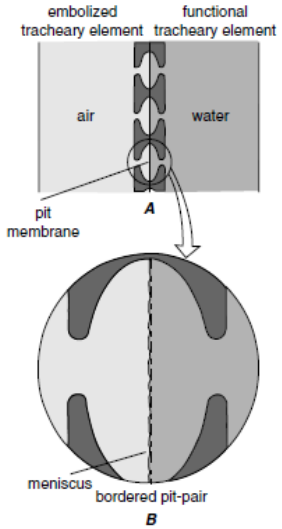


**Figure 21.** **A.** Diagram showing bordered pit-pair between tracheary elements, one is embolized and non-functional. **B.** Detail of a pit membrane. If a tracheary element is embolized, air cannot spread to the adjacent functional tracheary element because of the surface tension of the air-water meniscus spanning the pores in the pit membrane. (Evert, 2006)

Indeed, the punctations that serve as hydraulic connections between the vessels allow the passage of water while preventing the passage of air. However, when among two adjacent vessels, one is functional (filled with water, under tension) and the other is embolized (filled with air), the pressure difference between the two creates the risk that an air bubble will pass through the wall of the pit-membrane, which then provides a site for cavitation nucleation in the functional vessel (Ponomarenko *et al.*, 2014). Thus, when at the pit-membrane, the tension exceeds the pressure required to pull air from an empty vessel to a filled vessel, air-seeding occurs. This air-seeding represents the appearance of a vacuum inside the water column. However, because of the tension present in the vessels (*see also 1.3. Mechanisms of water circulation in trees*), as soon as a small bubble formed by air-seeing succeeds in entering a vessel through the pores of the pit-membrane, it expands immediately until the tension forces on the walls are released.

## *2.3. Vulnerability to cavitation*

### *2.3.1. Measuring xylem vulnerability to cavitation: currents methods and vulnerability overview*

Xylem vulnerability to cavitation is usually evaluated by constructing **vulnerability curves to cavitation** that represent how the percentage loss of hydraulic conductance (PLC) induced by cavitation varies with the xylem tension, i.e., the xylem water potential (Ψ) (Figure 22). These vulnerability curves can be constructed with various methods going from, historically, the acoustic method (Milburn & Johnson, 1966) that detected the sound of a cavitation events or, to the Sperry method that measured the loss of hydraulic conductance caused by embolism by estimating the rate of embolism within a sample (Sperry *et al.*, 1988). Most of the vulnerability curves are constructed nowadays by using the Cavitron method which use centrifugal forces to increase the xylem sap tension and generate cavitation events reducing the hydraulic conductance of the sample (Cochard, 2002a). However, new methods arise such as the optical method that detect the changes in light transmittance between air-filled vessels and water-filled vessels (Ponomarenko *et al.*, 2014; Brodribb *et al.*, 2016), or the use of X-ray microtomography (micro-CT) that proposes a direct visualization of xylem embolism using high resolution (Brodersen *et al.*, 2010; Cochard *et al.*, 2015).

These vulnerability curves provide useful information about the kinetics of cavitation for different species (Figure 22). The xylem tension inducing 50% loss of hydraulic conductance ($P_{50}$ value) is commonly used when comparing the resistance to cavitation between species (Cochard *et al.*, 2008; Brodribb, 2017) (Figure 22). Indeed, vulnerability to cavitation is extremely variable across species and biomes (Delzon *et al.,* 2010 ; Choat *et al.,* 2012) (Figure 23). For example, a meta-analysis of 167 species from different biomes showed $P_{50}$ ranging from -0.18 to -14.1 MPa (Figure 23) (Maherali *et al.*, 2004) and it was even measured in *C. tuberculata* a $P_{50}$ equal to -18.8MPa (Larter *et al.*, 2015).

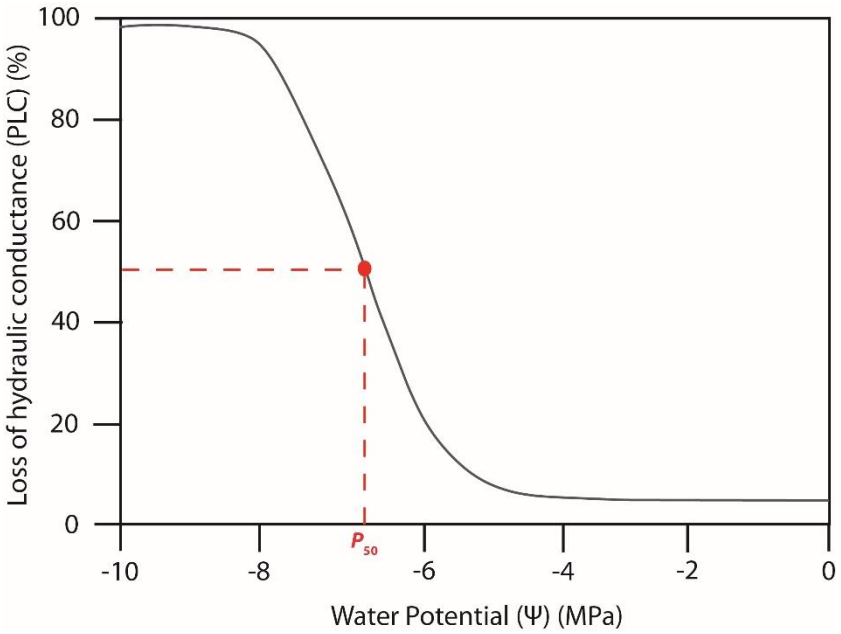


**Figure 22.** Theoretical vulnerability curve to cavitation representing the loss in hydraulic conductance (PLC) regarding a decrease in water potential (Ψ). $P_{50}$, the water potential value inducing 50% loss of xylem hydraulic conductance, is represented in red. ©Marylou Mantova

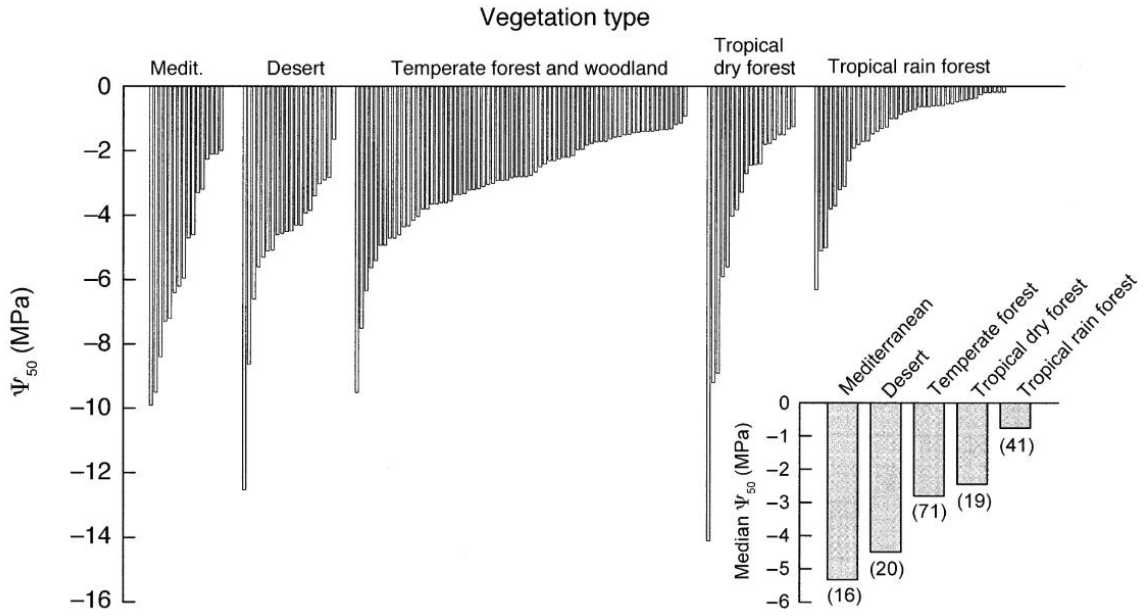


**Figure 23.** Distribution of vulnerability to water-stress-induced cavitation ranked by magnitude within five vegetation types. (Maherali *et al.*, 2004)

### 2.3.2. *Variability of the vulnerability to cavitation across/within species and within a same plant*

Across species, different strategies have been developed throughout evolution to preserve the integrity of the plant vascular system and they are all defined by two different constraints: the ability to maintain relatively high plant Ψ values by limiting water losses under drought conditions (Blackman *et al.*, 2016 ; Martin-StPaul *et al.*, 2017); and the physical limits of the xylem vessels (Lens *et al.*, 2011). From the anatomical point of view, it has been

reported that the cavitation resistance for angiosperms is linked with the thickness of the intervessel pit membrane. Thus, the resistance to embolism seems to increases along with the thickness of the intervessel pit membrane (*Li et al.,* 2016). For gymnosperm, the water passes from one tracheid to another through bordered pits. Thus, cavitation vulnerability is linked with the ratio between the torus diameter and the pit aperture i.e., torus overlap (Delzon *et al.*, 2010; Bouche *et al.*, 2014).

When we look at xylem vulnerability to cavitation within the same species, some studies have shown that there are few or no differences within core populations (Wortemann *et al.*, 2011; Torres-Ruiz *et al.*, 2013). However, other studies have shown that marginal populations have developed ways to protect their xylem either based on evolutionary phenomena or plasticity. For example, in a study of 15 European populations of *Fagus sylvatica*, small but significant differences in stem $P_{50}$ were found (Stojnić *et al.*, 2018). Indeed, the stem $P_{50}$ varied from -2.84 to -3.55MPa depending on the location of the sampling and an increase in cavitation resistance was observed in conjunction with an increase in temperature and aridity of the sampling location. Indeed, southern beech populations that had grown in a drier climate showed a higher resistance to cavitation than northern European populations that had grown in more favourable conditions and these differences could be explained by changes in pit membrane properties (Stojnić *et al.*, 2018).

Apart from the variation in vulnerability to cavitation across and within species, it has been reported that resistance to cavitation can also vary significantly within a plant when we compare the cavitation resistance of its different organs (leaves, stems and roots) generating a hydraulic segmentation. In general, more distal organs, such as leaves, are at greater risk of embolism than basal organs such as trunk (Tyree & Zimmermann, 2002; Choat *et al.*, 2005). This hydraulic segmentation could be explained in two ways. First, during transpiration the xylem water potential ($\Psi_{xylem}$) will always be more negative in the distal part than in the core parts and would therefore translates in a greater probability of cavitation in the distal organs. Secondly, the organs may differ in their vulnerability to cavitation. For example, a study conducted on *Vitis vinifera* showed how the petiole $P_{50}$ was higher than the stem $P_{50}$ making the petioles more vulnerable to cavitation than the stems (Charrier *et al.*, 2016).

Finally, it has been shown how ontogeny has a significant effect in leaf residual transpiration with higher residual conductance in older leaves than in the younger ones and could provoke different timing of hydraulic failure in a same organ (Hasanuzzaman *et al.*, 2017; Charrier *et al.*, 2018). Indeed, despite presenting the same vulnerability to cavitation (i.e., the same $P_{50}$), because of their lower residual conductance, younger leaves could be less exposed to hydraulic failure than older leaves that, on the contrary, would enhance the risk of hydraulic failure of the tree.

# Part 4. Hydraulic failure and tree mortality: from correlation to causation

PUBLISHED IN *TRENDS IN PLANT SCIENCE* ON APRIL 2022

*Authors:*
*Mantova Marylou, Herbette Stéphane, Cochard Hervé, Torres-Ruiz José M.*

**Abstract**

Xylem hydraulic failure has been recognized as a pervasive factor for triggering drought-induced tree mortality. However, foundational evidence of the mechanistic link connecting hydraulic failure with living cell damages and tree death has not been identified yet, compromising our ability to predict mortality events. Meristematic cells are involved in the recovery of trees from drought and focusing on their vitality and functionality after a drought event could provide novel information on the mechanistic link between hydraulic failure and drought-induced tree mortality. This opinion piece focuses on the cell critical hydration status for tree recovering from drought and how it links with the membrane integrity of the meristems.

**Highlights**

- Xylem hydraulic failure has been shown to be a ubiquitous factor for tree death from drought, but the mechanistic link between the two processes remains unclear.
- As meristematic cells are involved in the recovery of trees from drought, determining the damage they suffer during their progressive dehydration under water stress and its relationship to the loss of hydraulic function will provide new information on the mechanistic link between hydraulic failure and drought-induced mortality.
- The RWC, altered redox status and physical constraints that meristematic cells can support more accurately define meristem membrane integrity, and consequently meristems survival and so tree recovery, than the $P_{50}$ and $P_{88}$ values used hitherto as thresholds for drought-induced tree mortality in mechanistic models.
- The capacity of trees to relocate stored water between tissues is crucial for buffering the variation in the RWC and redox status of meristematic cells, determining the cell mortality timeline and therefore the resistance of different species to drought.

## 1. Dying of thirst

Ongoing climate change is modifying surface temperature and precipitation patterns in many areas worldwide (IPCC, 2014). As a consequence, drought episodes are more frequent, longer, and more intense (Trenberth *et al.*, 2014), having already a marked impact on tree survival and forest dieback (Allen *et al.*, 2010; Anderegg *et al.*, 2012b). There is therefore an urgent need to predict what species will succumb to drought and where and when this will occur (Trumbore *et al.*, 2015) in order to anticipate the degree to which the expected future climatic changes will affect forests structure and function.

Physiologically, **tree death** (see Glossary) is usually assessed by evaluating a tree's ability to recover its key physiological functions, such as exchanges of matter and energy with its environment, or resprout, that is to say produce or regenerate new organs or tissues in the following vegetative season (Brodribb & Cochard, 2009; Anderegg *et al.*, 2012b; Barigah *et al.*, 2013b). A tree is considered to have died as a result of a drought episode when, once exposed to more favourable conditions, it is unable to perform these key physiological functions. The ability of a tree to survive a drought episode is therefore linked to its ability to ensure the survival of the key meristematic cells, both **primary** and **secondary**, such as undifferentiated meristematic apical cells responsible for the development of new organs, cambium cells involved in the development of vascular tissues and the subero-phelloderm cells responsible for the development of bark tissues, as well as root and shoot apical meristems responsible for the primary growth of the plant. If a drought episode is intense enough to affect the vitality of one or more of these key meristematic tissues, it may hinder the tree's ability to maintain its metabolism and ultimately to survive.

In the past decades, much effort has been made to understand tree hydraulic functioning and especially the link between **xylem embolism** and drought-induced tree mortality (Choat *et al.*, 2018). Embolism occurs when excessive tensions in the xylem tissue cause cavitation events in the xylem conduits that block water transport from the roots to the leaves. Cavitation occurs under severe drought conditions and has been identified as a ubiquitous factor for tree death from drought (Box 1) (McDowell *et al.*, 2008). Several studies have shown that the water potential inducing a loss of hydraulic functioning of ca. 50% or ca. 88% ($P_{50}$ for conifers and $P_{88}$ for angiosperms, respectively) (Brodribb & Cochard, 2009; Barigah *et al.*, 2013b), can be considered as an indicator for drought-induced tree mortality or lack of full recovery in some species (Urli *et al.*, 2013; Salmon *et al.*, 2015; Adams *et al.*, 2017). These threshold levels of embolism thus define the point of **hydraulic failure** of the xylem tissue that correspond to the point where the conductance capacity of the sap pathway is unable to avert the runaway cavitation of the xylem leading to the progressive dehydration of the distal organs. The process of cavitation has been widely studied, and the critical $P_{50}$ and $P_{88}$ values have been determined for different species (Delzon *et al.*, 2010; Choat *et al.*, 2012) and used as thresholds for modelling tree mortality under drought conditions (Brodribb *et al.*, 2020; Lemaire *et al.*, 2021). However, although $P_{50}$ and $P_{88}$ have been strongly correlated to tree resistance to drought in many cases, recent studies have shown that $P_{50}$ and $P_{88}$ values are not always correlated with mortality. It has been reported that conifers showing a percentage loss of conductance (PLC) of 80% (i.e., higher than 50%) and angiosperms with a PLC close to 100%

(i.e., higher than 88%) are still able to recover from drought once irrigated (Li *et al.*, 2015; Hammond *et al.*, 2019; Mantova *et al.*, 2021). These findings thus question the reliability of the $P_{50}$ and $P_{88}$ indicators for predicting tree death and, more importantly, it highlights the importance of determining the mechanistic link between xylem embolism and mortality in order to determine how hydraulic failure affects the capacity of trees to recover from drought. To explain the variation in PLC thresholds across individuals or species we argue that besides the level of embolism, the level of cell damage in the meristematic tissues should also be taken into account when evaluating a tree's capacity to recover from drought. Indeed, even though the cellular desiccation that results from hydraulic failure has been part of the framework proposed by McDowell *et al.* (McDowell *et al.*, 2008, 2011), **studies focused on demonstrating explicitly this link are virtually inexistent** (Kursar *et al.*, 2009; Brodribb *et al.*, 2021) **and none have worked at the meristematic level**. Thus, there are two fundamental aspects that have so far been considered independently but which must be brought together to properly identify, explain and understand the causes of drought dieback: **(i) tree mortality is physiologically determined by meristematic cells vitality, and (ii) hydraulic failure is a strong determinant of drought-induced tree mortality**. Only by considering both aspects together we will be able to elucidate the mechanistic links between hydraulic functioning, **cell death** and finally tree mortality. This opinion piece aims to shed the light on the mechanistic links between hydraulic failure and drought-induced tree mortality by providing a new approach on tree mortality that assumes that saving key meristematic cells from dehydration and allowing their rehydration are the two critical points for tree survival. This approach thus encourages new studies focused on cell water status, in particular at the meristems level to set new thresholds for predicting tree mortality with mechanistic models (Blackman *et al.*, 2016; Martin-StPaul *et al.*, 2017).

**Box 1. Drought-induced mortality: Dying of thirst** ***(see also. Water circulation in a drying environment)***

Drought-induced tree mortality is related to drought intensity, duration and frequency (McDowell *et al.*, 2008). Under extreme drought conditions (i.e., long intense droughts), tree mortality mostly arises from xylem hydraulic failure (Choat *et al.*, 2012; Urli *et al.*, 2013).

During a severe drought event, soil water availability decreases while evaporative demand and cuticle conductance increase, resulting in an increment of the xylem tension that induces the occurrence of cavitation events in the xylem. Cavitation is the change from liquid water to water vapour under increased tension. This change in water phase results in the formation of gas bubbles termed 'emboli' in xylem conduits (Dixon & Joly, 1894; Tyree & Sperry, 1989). The cavitation of one xylem element can spread throughout the xylem vessel (Choat *et al.*, 2016b) when xylem tension increases owing to an increased vapour pressure deficit. As the percentage of cavitated vessels increases, the hydraulic conductance of the xylem decreases until the flow of water stops and causes the dehydration of the tree tissues, cell death, and the death of the tree.

Vulnerability to cavitation is extremely variable across species and biomes (Delzon *et al.*, 2010; Choat *et al.*, 2012) and is usually evaluated by constructing vulnerability curves representing the percentage loss of hydraulic conductance (PLC) induced by cavitation with regard to

xylem tension (i.e., xylem water potential). From these curves are extracted the xylem tension inducing 50% loss of hydraulic conductance ($P_{50}$) and that inducing 88% loss of hydraulic conductance ($P_{88}$). $P_{50}$ is generally used as an indicator of tree resistance to cavitation. When modelling tree survival from drought, $P_{50}$ and $P_{88}$ have been used, so far, as lethal thresholds for conifers and angiosperms respectively (Brodribb *et al.*, 2020; Lemaire *et al.*, 2021). However, recent experimental results do not always support both of these numbers and particularly $P_{50}$ (Hammond *et al.*, 2019; Mantova *et al.*, 2021) which emphasize the need to consider other physiological traits when trying to define a mortality threshold.

## 2. Looking at cell death to predict tree death

### *2.1.Cell mortality under drought conditions: Membrane integrity matters*

One of the main causes of drought-induced tree mortality is the direct cellular consequences of dehydration ending in cell death (McDowell *et al.*, 2008; Blum & Tuberosa, 2018). Cell death in plants occurs by two different mechanisms: programmed cell death and necrotic cell death. **Necrosis** is the main process induced by a range of abiotic stresses (e.g., drought) (Van Doorn *et al.*, 2011). While undergoing necrosis, cells usually present various anatomical features, such as swelling of the mitochondria (Scott & Logan, 2008), early rupture of the plasma membrane and/or shrinkage of the protoplast (Van Doorn & Woltering, 2005; Van Doorn *et al.*, 2011). The loss of integrity of the membrane structure in necrotic cells and thus the early rupture of the plasma membrane have already been reported in plants exposed to frost due to dehydration preceding cell death (Pearce, 2001). Under fast dehydration, the cell's membrane changes from a liquid crystalline phase to a gel phase that can lead to a lateral phase separation of membrane constituents and cause membrane leakage (Crowe *et al.*, 1992; Koster *et al.*, 2010; Cruz de Carvalho *et al.*, 2017). Guadagno *et al.* (2017) showed how the stability of the cellular membrane and thus its rupture was closely linked to a plant's water status. They proposed a theoretical mechanism of plant mortality based on membrane disruption as the most proximal cause of plant mortality under drought conditions (Figure 24).

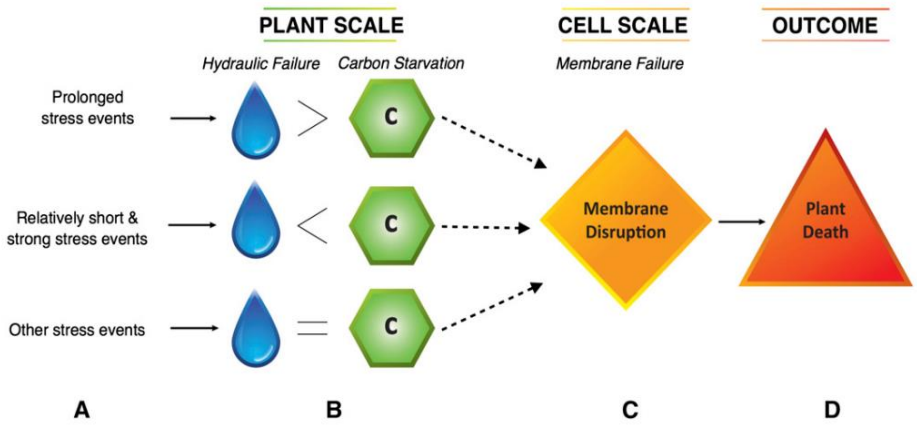


**Figure 24.** Theoretical framework of plant mortality. (Guadagno *et al.*, 2017)

Recent observations of Mantova *et al.* have lent this theoretical mechanism some experimental support by showing how cell membrane integrity can work as an indicator for evaluating capacity to recover from drought in conifers (Mantova *et al.*, 2021). To work towards elucidating the causes of drought-induced tree mortality and improve our capacity to predict it, **it is thus crucial to focus future research on the mechanisms and sequence of events associated with cell mortality and, especially with cell membrane failure**.

### *2.2.What fails? Focus on cell membrane failure*

Under drought conditions, membrane failure usually occurs by either structural changes related to the loss of solvation of the polar groupings of amphiphilic lipids (Cruz de Carvalho *et al.*, 2017) or to the biochemical modifications induced by the lipid peroxidation that results from the accumulation of **reactive oxygen species** (ROS) (Suzuki *et al.*, 2012; Petrov *et al.*, 2015). Abiotic stress such as drought increases the production and accumulation of ROS, leading to an oxidative stress [30, 31]. This ROS accumulation damages a broad variety of organic substances including the membrane components (Suzuki *et al.*, 2012; Petrov *et al.*, 2015), in which it causes a modification of protein and lipid peroxidation leading to membrane leakage and consequently to cell lysis and cell death (Suzuki *et al.*, 2012; Petrov *et al.*, 2015; Guadagno *et al.*, 2017). Looking at the survival strategy of plants able to support extreme dehydration levels, i.e., able to survive with low water content in their tissues (e.g., resurrection plants), ROS accumulation is counteracted by an increase in ROS-scavenging enzymes and antioxidant compounds (Beck *et al.*, 2007; Singh *et al.*, 2015), which prevent cell membrane disruption and maintain cell integrity (Ingle *et al.*, 2007). ROS accumulation, and the altered cell redox status, is therefore a ubiquitous factor for cell mortality during water stress owing to its effects on cell membrane integrity, whence the importance of focusing future research on the relationship between drought-induced ROS accumulation, or more generally cell redox status, and cell membrane stability in perennial organs. **Our hypothesis is therefore that cell ROS accumulation or the altered cell redox status are good candidates for identifying a threshold for cell mortality during drought**, excluding the possible effects of pathogens and insects attacks, and to some extent for tissue vitality and more generally for organ and whole tree death (Figure 25, Key Figure), especially when evaluating meristematic tissues. There is thus an urgent need to consider both cell death and ROS accumulation or redox status of living cells crucial for recovery when seeking an indicator for tree mortality or lack of recovery capacity.

Although altered redox status of the cells has been demonstrated as one of the causes of membrane failure under drought conditions, not only biochemical processes but also various physical constraints could be also involved in the processes provoking **cellular death**. Indeed, **cellular cavitation** and **cell cytorrhysis** have been speculated as potential mechanisms driving cell mortality under water stress (Oertli, 1986; Rajashekar & Lafta, 1996) (Figure 26). On the one hand, cellular cavitation (Sakes *et al.*, 2016) could provoke lethal cellular injury by the rupture of the protoplasm when cell are exposed to important negatives pressures under frost conditions (Rajashekar & Lafta, 1996). Similarly, when trees are exposed to drought conditions and the water potential decreases progressively, cellular cavitation events could probably occur in various cell types including the meristematic ones. On the other hand, cytorrhysis and collapse of the cell (Taiz & Zeiger, 2006; Beck *et al.*, 2007) has also been describe

in previous studies in cells undergoing water stress (Rajashekar & Lafta, 1996; Yang *et al.*, 2017) and could represent a major form of cell injury and, consequently, meristems damage in trees under severe drought conditions. However, whether cellular cavitation and cytorrhysis provoke cellular death by membrane disruption is, to date, unknown and would require experimental studies including microscopy techniques, such as cryo-scanning electron microscopy (cryo-SEM), to visualize both the cell shape and plasma membrane integrity. Whether those physical constraints occur at the meristems level and could work as an indicator for tree mortality or capacity of recovery is still unresolved and would require further studies targeting especially those key tissues for tree survival (Figure 25). Therefore, whether these physical processes are mutually exclusive of the oxidative stress remains still unknown.

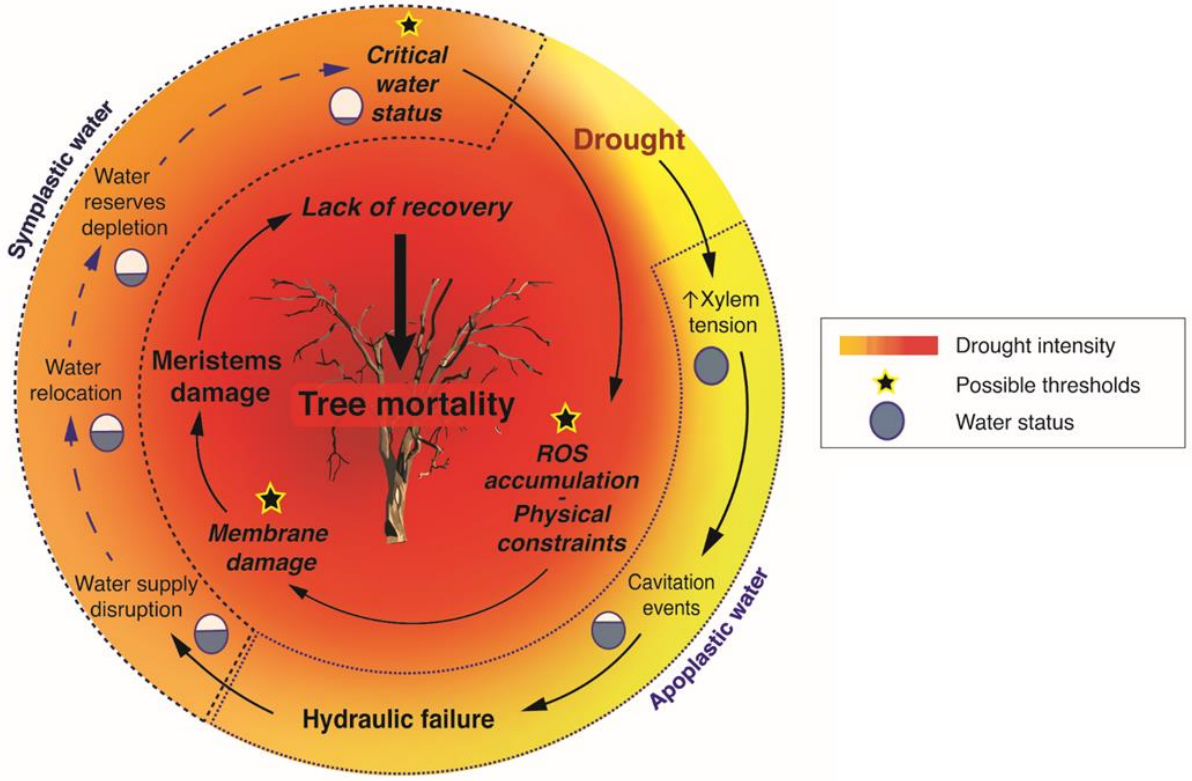


**Figure 25. Key Figure. Integrative framework representing the main processes explaining the correlation between hydraulic failure and tree mortality.**
Drought-induced tree mortality is currently predicted with mechanistic models using thresholds that mark a point of no return from drought. Although there is a strong correlation between a high loss of conductance in trees ($P_{50}$ for conifers and $P_{88}$ for angiosperms) and their mortality, some trees can still survive drought after high losses in their hydraulic capacity. This new approach emphasises the importance of studying the link between the disruption of cell water supply due to xylem hydraulic failure and a change of water status in the meristematic cells. It also shows the consequences of a critical water status on the production of reactive oxygen species (ROS) as well as changes in the physical constraints on the cells, which can cause severe membrane damage in the meristematic cells and eventually induce their death. This framework thus presents the new possible thresholds that, according to the different hypotheses presented in the text, could be used to implement mechanistic models for predicting tree mortality in the context of climate change. In this figure, the arrows represent the sequence of events leading to tree mortality. The broken blue arrows represent the hypothetical sequence of events requiring further studies.

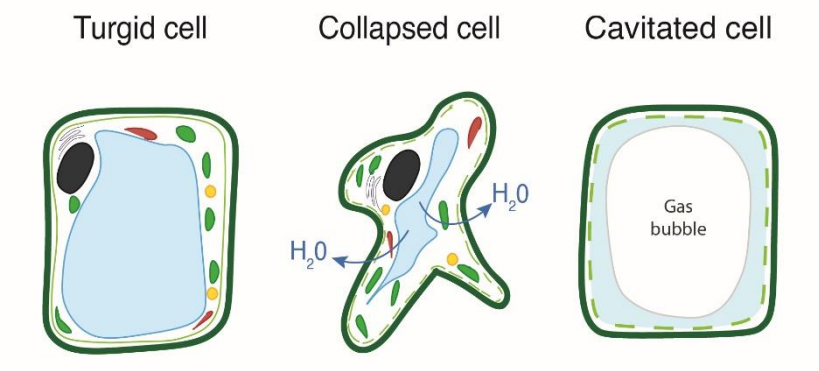


**Figure 26.** Illustrations representing the different shapes of cells before (turgid cell) and after a water stress (collapsed cell or cavitated cell). As the water stress progresses, theoretically, cells can either reach a state of cytorrhysis or cavitation. Cytorrhysis occurs when the cytoplasm and cell wall shrink as a unit resulting in the cell wall being mechanically deformed as the cell loses volume. Cavitation occurs when a critical pressure is reached causing the cytoplasm fractures and the formation of a gas bubble.
(*Adapted from* Mantova *et al.*, 2022)

### 3. Tree water relations and meristematic tissues mortality

In the meristematic approach proposed for assessing drought-induced dieback, meristematic elements (e.g., primary and secondary meristems) are the key elements for evaluating a tree's capacity to survive intense drought episodes (Chaffey, 1999; Gričar *et al.*, 2014; Li & Jansen, 2017). During drought, it has been shown how roots undergo progressive contraction and rupture of cambial cells leading to their disintegration in severely water-stressed and non-recovering seedlings (Li & Jansen, 2017) highlighting the relevance of these meristematic cells (Thomas, 2013; Klimešová *et al.*, 2015) when evaluating tree senescence and death. Besides the meristematic tissues, it is also important to consider the relevance of other cell types such as cortical parenchyma, that may dedifferentiate to produce 'adventitious' meristems once the meristematic cells have lost their capacity to differentiate and develop into other tree tissues and organs (Malamy & Benfey, 1997; Laux, 2004). However, how the capacity of the meristematic cells to differentiate and to the other cell type (e.g., parenchyma cells) to dedifferentiate is affected by the progressive reduction in plant hydraulic functioning and the dehydration of the tissues, is largely unknown and deserves further attention from both physiological and ecological points of view.

In plants undergoing a drought resulting in rapid extreme dehydration, cells also undergo water stress by reduced **relative water content** (RWC) (Box 2), which can eventually induce cell death (Tardieu, 1996). Meristematic cells will thus also start to dehydrate and enter the cell death phase (Singh *et al.*, 2015), displaying evidence of necrosis as they approach their critical water status. **It is therefore to be expected that there will be a threshold in RWC below which these cells will show evidence of dehydration-induced necrosis**. However, previous studies on the critical water status allowing cell survival under water stress conditions have highlighted that the critical water status for survival varies among cell types, organs and species. This is the case for some seed types able to keep their capacity to germinate up to RWC values of ca. 22% (Finch-Savage, 1992), whereas the critical RWC for leaf survival ranges between 7.0% and 58.5% depending on the species (Kursar *et al.*, 2009). Like leaves,

most mesophytic plants cannot withstand an RWC below 50% (Verslues *et al.*, 2006). **Reaching critical RWC in meristematic tissues will therefore affect the capacity of a whole tree to recover from drought.** This RWC threshold, however, may vary across species according to their resistance to drought and to their mechanisms to protect cells from dehydration (e.g., production of late embryogenesis abundant proteins in seeds (Beck *et al.*, 2007)). Using RWC, that has been recently presented as a more mechanistically relevant metric of plant lethal water stress (Martinez-Vilalta *et al.*, 2019; Sapes & Sala, 2021), as a threshold for meristematic cells mortality and thus tree recovery capacity would greatly improve mechanistic models aimed to predict and anticipate the resilience of trees after drought events, a crucial step in forecasting catastrophic forest dieback (Blackman *et al.*, 2016; Martin-StPaul *et al.*, 2017) (Figure 25). As membrane integrity seems a good indicator of cell vitality and is related to cell water content (Pearce, 2001; Wang *et al.*, 2008; Chaturvedi *et al.*, 2014; Guadagno *et al.*, 2017), **a focus on the sequence of events taking meristematic cells into necrosis with regard to RWC could set a physiological threshold for meristematic cells death and thus tree survival** (Figure 25). Also, as RWC, oxidative stress and physical constraints are interrelated, the ascertainment of which threshold is prominent would help to precisely determine the physiological threshold for meristematic cells beyond which they lose their ability to differentiate. The time at which different species reach these threshold levels will therefore depend on both their dehydration rates during drought (Pammenter & Berjak, 2014) and on their resistance to drought according to their mechanisms to avoid oxidative stress (Beck *et al.*, 2007). **Describing the main processes taking meristematic cells to critical dehydration levels during drought, how it varies across organs (bole, branch tips, roots) and species and how they all interact with each other – including hydraulic functioning, residual conductance, and capacitance of the different tissues and organs – is a promising future research direction towards the identification of the mechanistic processes underlying drought-induced tree mortality**.

**Box 2. Relative Water Content (RWC): a useful indicator when trying to understand and anticipate drought-induced tree mortality.**

Martinez-Vilalta *et al.* (2019) has recently stated that a good predictor of drought-induced tree mortality should have a mechanistic basis, should be integrative, threshold-prone, scalable, and easy to measure and monitor. Thus, RWC that is a direct measure of the dehydration state of plant organs and is tightly linked with cell volume and turgor should be a good candidate for assessing cell mortality. Indeed, RWC is expressed relative to the maximum water a tissue can hold at saturation. Therefore, it should be less prone to variation across organ and species than water potential. For example, it has been shown that, if the water potential at turgor loss point greatly varies across species, the leaf RWC at turgor loss point is however relatively constant (Bartlett *et al.*, 2012). Therefore, because this measure is maintained constant under mild drought, it should show, under severe water-stress, substantial change preceding death (Martinez-Vilalta *et al.*, 2019) and that would imply a threshold-like behavior. Moreover, as its decrease has been consistently linked with membrane dysfunction (Guadagno *et al.*, 2017), monitoring the decrease in RWC could help identifying the point of no return for cell integrity. Indeed, it seems reasonable to hypothesize that large variation in $\Psi$ over time and among species aim to maintain as constant an RWC as possible, or, at least, above some critical threshold below which irreversible turgor loss and dehydration occurs (Martinez-Vilalta *et al.*,

2019). More importantly, despite methodological concerns about the correct determination of RWC (i.e., the 'over-saturation' effect) (Arndt *et al.*, 2015), RWC appears as easy to measure as the Ψ but presents the advantage to being able to be monitored down to very low water status (i.e., to water potential <-10MPa) which is impossible using the classical 'gold standard' pressure chamber method. Finally, the greatest advantage of water content is that it can be assessed directly at large spatial scales through remote-sensing techniques and could be estimated from organs to ecosystems *via* remote sensing making it scalable (Ullah *et al.*, 2012; Wang & Li, 2012; Mirzaie *et al.*, 2014; Rao *et al.*, 2019; Marusig *et al.*, 2020).

### *3.1. Hydraulic functioning and dysfunctioning*

The water content of any organ or tissue of a tree is determined by the balance between water loss and absorption. Water losses are mainly due to stomatal or residual transpiration (Cochard, 2019; Billon *et al.*, 2020) and are therefore imposed by microclimatic conditions. Water absorption depends mainly on the ability of trees to extract water from the soil and transport it upwards to the meristematic cells (Figure 27). Thus, under drought conditions, the increasing environmental evaporative demand causes an increasing tension in the xylem, inducing cavitation events and finally the hydraulic failure of the water transport system when it undergoes a runaway effect leading to complete loss of its conductance (Tyree & Zimmermann, 2002). This dysfunction of the water transport system causes a significant reduction in the amount of water supplied to the tree's living tissues, which will accordingly decrease their RWC, increase the percentage of water-stressed cells and finally trigger cell necrosis processes (Figure 27) (Kursar *et al.*, 2009). While McDowell *et al.* (2008) has already mentioned that hydraulic failure leads to cellular death, little is known on the desiccation of the actual meristems, probably because of the difficulty to access those elements. **However, the desiccation of the meristems could provide us with the mechanical link between hydraulic failure and tree mortality** (Hammond *et al.*, 2019; Mantova *et al.*, 2021). Thus, as significant correlations between high levels of PLC and tree mortality have been reported for several species (Brodribb & Cochard, 2009; Barigah *et al.*, 2013b; Urli *et al.*, 2013), **the central hypothesis we advance here is that the hydraulic failure of the xylem is the triggering factor in the irreversible dehydration of meristematic cells, severely impairing their water absorption capacity and thus their water content, so leading to their death.** A reduced RWC resulting from hydraulic failure should therefore be ubiquitous to all tree tissues independently of their function (Kursar *et al.*, 2009; Martinez-Vilalta *et al.*, 2019; Sapes *et al.*, 2019; Sapes & Sala, 2021) and would certainly be found at meristematic tissues level causing cells death and ultimately the inability of the tree to recover from drought (McDowell *et al.*, 2008; Blum & Tuberosa, 2018) (Figure 27, Figure 28). However, accessing the meristematic tissues might be challenging in practice. Therefore, as a first step, the sampling of buds would allow to efficiently link the hydraulic failure of the xylem with meristems mortality. Then, once this link is evaluated, accessing cambial cells using e.g., transmission electron microscopy would allow to make a significant step forward in the understanding of tree death from drought (Li & Jansen, 2017). As RWC thresholds have the potential to be use for remote sensing tree mortality (Rao *et al.*, 2019; Marusig *et al.*, 2020) another step forward would be to observe how meristems RWC might relate to canopy moisture content (Saatchi *et al.*, 2013; Asner *et al.*,

2016) to be able to predict more accurately the consequences of drought on trees' survival at the population and the landscape level.

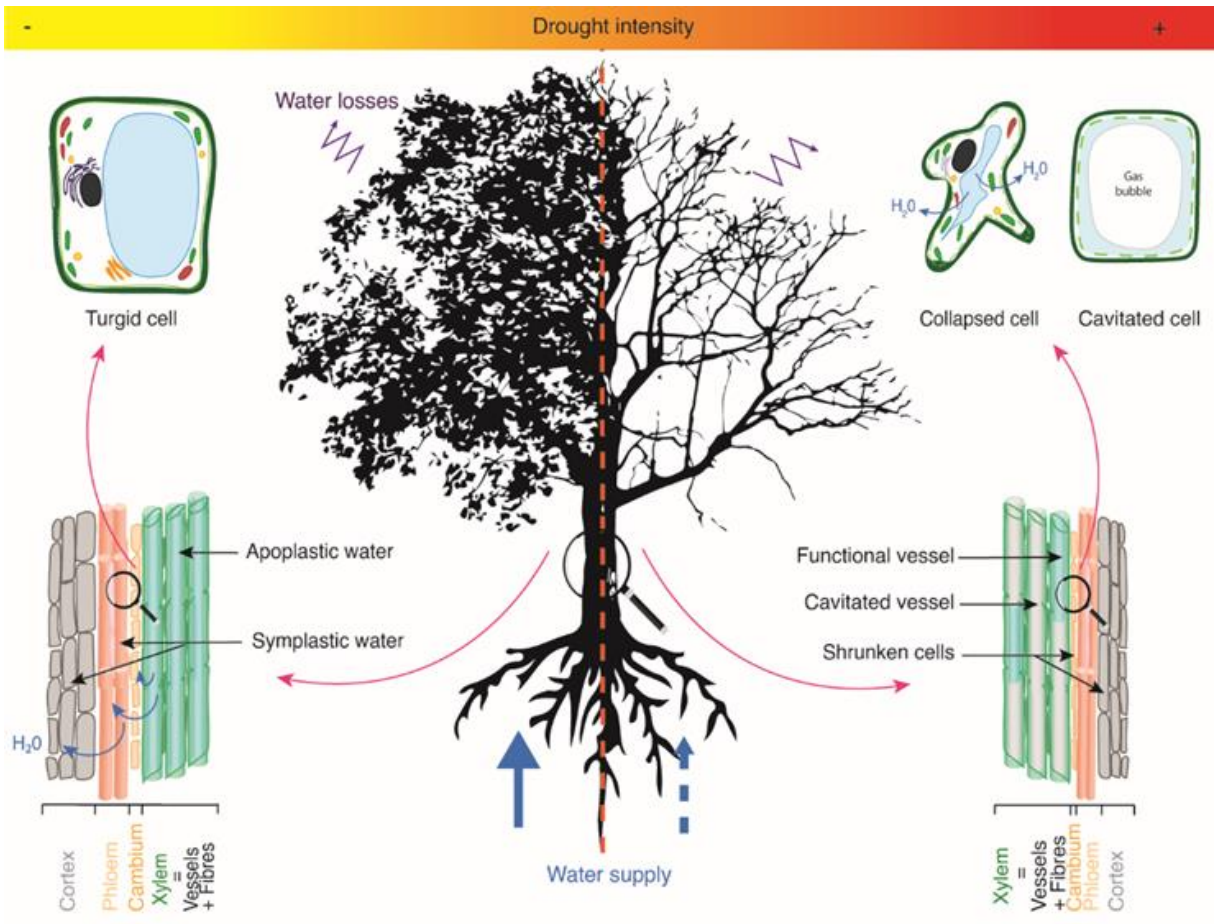


**Figure 27.** Consequences of water stress on tree water transport and tree cells.
Under mild water stress conditions, trees are able to keep their hydraulic system almost fully functional, and water is continuously transferred from the xylem (apoplastic water) to the cells in the living reservoir (symplastic water) maintaining the turgidity and integrity of the cells. As water stress is exacerbated, the loss of hydraulic conductance in the xylem pathway (PLC) increases until it causes xylem hydraulic failure, when the water supply cannot meet the tree's water requirements. Concomitantly to the loss of xylem conductance, water transport from the xylem to the living tissues (e.g., cortex and cambium) is disrupted and the metabolism of cells relies first on water supply and finally on their own water reserves. Consequently, cells start to dehydrate, shrink, collapse or cavitate and finally die from necrosis when they lose their membrane integrity.

Recent studies have reported tree mortality events when the losses in stem xylem conductance were higher than the proposed PLC thresholds of 50% and 88% for conifers and angiosperms, respectively and that the PLC value provoking tree death is likely to vary across individuals and species (Vilagrosa *et al.*, 2003; Hammond *et al.*, 2019; Mantova *et al.*, 2021). **This has thus highlighted the importance of (i) revisiting the $P_{88}$ and $P_{50}$ thresholds; and (ii) the need to determine more accurately the PLC leading to the runaway dehydration of meristematic cells**. Under hydraulic failure conditions, the water lost through transpiration will lead to the dehydration of the meristematic tissues that will ultimately desiccate and die

(Figure 28). As suggested by Hammond *et al.* (2019), there should thus be a sequence of events occurring when significant losses in hydraulic functioning are reached, leading to meristems and tree death (Figure 25; Figure 28). Along this sequence, we hypothesize that the cell metabolism would depend first on the tree's water reserves at the **apoplastic** level, and once this water is depleted, on their own water content (**symplastic**). As this is in turn exhausted, meristematic cells will undergo dehydration and death by necrosis (McDowell *et al.*, 2008) (Figure 25). Thus, to validate our hypothesis, evidence of meristematic cell necrosis should appear after high losses in plant hydraulic functioning that would alter the water status of the meristems (Figure 28). As meristem water content depends to a large extent on tree water supply related to tree hydraulic functioning, a better understanding is needed of the minimal tree hydraulic conductance required to keep the meristematic tissues hydrated and so allow the tree's recovery from drought. What matters is (i) whether meristematic cell dehydration can be delayed through the radial relocation of water within the stem during drought (Holbrook, 1995; Pfautsch *et al.*, 2015; Preisler *et al.*, 2021) and (ii) under what conditions the cell can rehydrate once re-supplied with water.

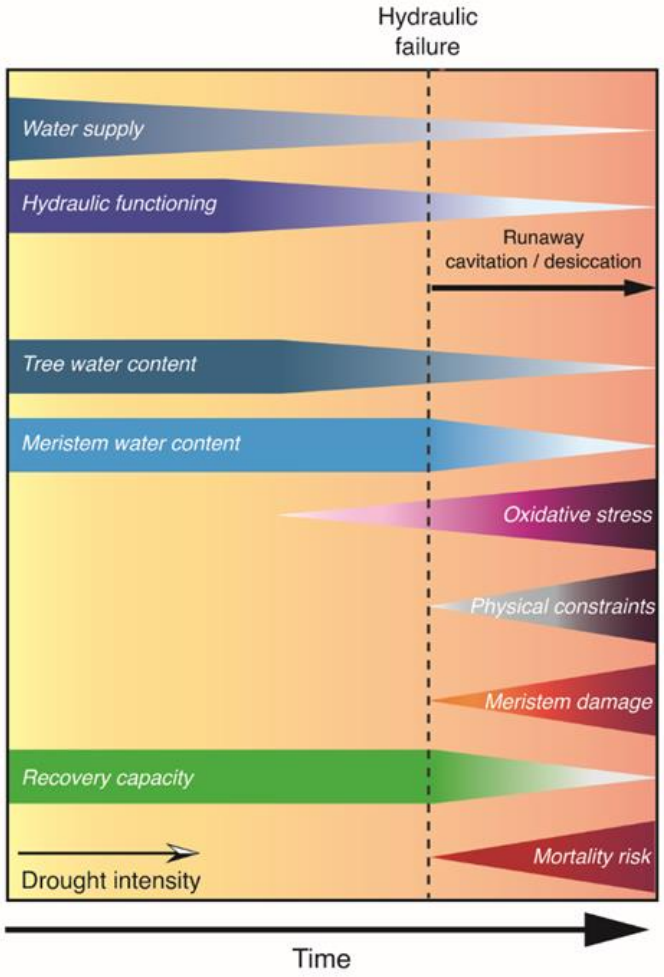


**Figure 28.** Drought consequences on tree water transport and content.

As drought intensity is exacerbated (from yellow to orange) and water supply decreases, xylem hydraulic functioning decreases until it reaches hydraulic failure, when water supply no longer meets water demand. Concomitantly to the loss of hydraulic functioning, tree water content diminishes and causes the dehydration of the meristems and an increase in oxidative stress. After reaching xylem hydraulic failure, meristematic cells enter the phase of irreversible dehydration and finally incur damage, particularly at membrane level. Consequently, the recovery capacity of the tree diminishes, and the mortality risk increases. Quantifying meristematic cell water content at the time of increasing cell damage (i.e., evidence of meristems damage) (black broken line) could identify thresholds below which the tree will be unable to recover from drought and will ultimately die.

### *3.2. Avoiding meristematic cells mortality*

As already described, xylem hydraulic failure disrupts the water supply to a tree's living tissues (Choat *et al.*, 2016b) and forces downstream organs to rely on their own water reserves (symplastic) (Epila *et al.*, 2017). Although plant water storage has been widely studied in terms of localisation (Tyree & Yang, 1990; Holbrook, 1995), the link between water release and hydraulic failure, mobilisation to maintain the metabolism of meristematic cells, and possible refilling of the reserves after a drought event have been poorly evaluated (Preisler *et al.*, 2021). In general, there are two main types of water storage reservoirs in plants: symplastic reservoirs (i.e., inside the living cells) and apoplastic reservoirs (Figure 25) (Tyree & Yang, 1990; Holbrook, 1995). The water stored in these two reservoirs can be mobilised during drought as tree's water potential decreases (Tyree & Yang, 1990; Lamacque *et al.*, 2020). In general, there is a bidirectional transport of water between inner bark and xylem in angiosperms through the symplasmic space of ray parenchyma cells. Thus, water moves from phloem to the mature xylem *via* the parenchyma cells and the cambial zone (Pfautsch *et al.*, 2015). As the formation of emboli in the xylem is initiated, the apoplastic water pools seems to be mobilised to preserve living tissue (i.e., symplastic compartments) hydration state rather than to buffer xylem cavitation (Tyree & Yang, 1990; Knipfer *et al.*, 2019). As demonstrated with X-ray micro-CT, the water contained in the xylem matrix embedding xylem vessels (i.e., mainly fibres) is released to the adjacent tissues concomitant with stem shrinkage and the formation of embolism (Tyree & Yang, 1990; Knipfer *et al.*, 2019). As the xylem tension increases, more cavitation events are observed in those xylem vessels located close to the vascular cambium, along with more air-filled cells within the xylem matrix (Knipfer *et al.*, 2019). This suggests that the mobilisation of these water reserves could partially buffer the water depletion in the symplastic reservoirs that could include key living tissues for tree survival (Figure 25) (Knipfer *et al.*, 2019; Preisler *et al.*, 2021). By bringing together all of these recent results, it can be hypothesized that water released from the xylem matrix (apoplastic compartment) is moved to the adjacent tissues and consequently to meristematic tissues (symplastic compartment) to keep their cells metabolically active. Once all of the water stored in both the apoplastic and the symplastic compartments has been released, tree living tissues and cells will ultimately dry out, and meristematic cells will suffer from mainly oxidative stress, cavitation and cytorrhysis and finally die (Figure 25). However, there remain significant open questions about the possible role of the water supplied from the bark in protecting the cambial cells from dehydration. The testing of this hypothesis will require new experimental studies focused specifically on describing the processes of water release and water relocation, their mechanistic link with hydraulic functioning, and the sequence and timing of the events and processes occurring in the apoplastic and symplastic compartments to protect the meristematic cells during drought (Holbrook, 1995; Körner, 2019).

## 4. Concluding remarks and future perspectives

Tree mortality is physiologically determined by meristematic cells vitality. However, the consequences of drought on these cells and the subsequent recovery of the trees are still under-researched (see *outstanding questions*). As various recent studies have identified a significant correlation between losses in hydraulic functioning and drought-induced tree mortality, it is now crucial to determine the mechanistic link between these two processes by evaluating the effect of hydraulic failure on the water content of the different tree organs and tissues, and especially on the meristematic cells. In addition, the evaluation of meristematic cell integrity with regard to RWC, redox status, and physical constraints would provide novel and valuable information about the physiological thresholds determining cell mortality, which would be most useful when implementing mechanistic models aimed at the prediction of tree mortality and thus forest dieback under drought conditions (Figure 25). Following the dynamic of dehydration of the meristematic cells from the beginning of tree dehydration and especially once the tree has reached xylem hydraulic failure at stem level is central to addressing key physiological questions related to drought-induced mortality, such as:

(i) Whether there is a mechanistic link between xylem cavitation, meristems water content, ROS accumulation and membrane stability.

(ii) Whether there is any critical threshold in RWC and/or oxidative stress and/or physical constraints from which the meristematic cells begin to show significant damage, and whether they are influenced by the duration and intensity of the drought.

(iii) Whether trees have evolved a water relocation strategy to protect key plant tissues from dehydration to maintain their capacity to recover from drought.

## Acknowledgements

This research was supported by La Région Auvergne-Rhône-Alpes "*Pack Ambition International 2020*" through the project *'ThirsTree'20-006175-01, 20-006175-02*, and the Agence Nationale de la Recherche, Grant/Award Number ANR-18-CE20-0005, '*Hydrauleaks'*.

**Outstanding questions**

- What is the sequence of events ending in meristematic cell death?
- Is the hydraulic failure of the tree water transport system the triggering factor in the irreversible dehydration of meristematic cells?
- What level of hydraulic dysfunction is necessary to cause a reduction in RWC that induces significant damage to meristematic tissues?
- Does this hydraulic dysfunction level vary among species with different drought resistance strategies?
- Are ROS accumulation and RWC level critical for meristematic cell survival?
- How do critical ROS and RWC vary with drought intensity and among species?
- What level of cell damage can trees withstand before they lose their ability to recover and so die from drought?
- Can meristematic cell dehydration be delayed through radial relocation of water in the stem during drought?

## Glossary

**Apoplastic water:** water stored outside cell plasmalemma (e.g., cell wall, intercellular spaces) or in dead cells (e.g., vessels, fibres, tracheids).

**Cellular cavitation:** occurs when the evaporation of water from the cell causes the radial walls to come closer and the lateral wall to cave inwards. When a critical pressure is reached, the cytoplasm fractures and a gas bubble form inside the cell.

**Cellular death:** a cell is considered dead when: (i) the cell has lost plasma membrane integrity; (ii) the cell, including its nucleus, has undergone complete fragmentation into apoptotic bodies; or (iii) cell fragments have been engulfed by an adjacent cell *in vivo*.

**Cytorrhysis:** the permanent and irreparable shrinkage of the cell resulting in the cell wall being mechanically deformed as the cell loses volume due to the loss of internal positive pressure.

**Hydraulic failure:** a physiological status in which the loss of hydraulic conductance of the xylem undergoes a runaway effect leading to the irreversible dehydration of the distal organs.

**Necrotic plant cell death or necrosis:** cell injury leading to premature cell death typically observed in cells undergoing abiotic stress. Necrosis is an acute cell death response that develops rapidly in several minutes to one day.

**Primary meristems:** type of meristematic tissues responsible for the primary growth of the plant (e.g., apical meristems) – that is, growth in height or length. Primary meristems are directly derived from embryonic cells.

**Reactive Oxygen Species (ROS):** oxygenated chemical species such as free radicals, oxygen ions and peroxides that are made chemically highly reactive by the presence of unpaired valence electrons.

**Relative water content (RWC):** indicator of the water status of a tree organ or tissue. Calculated relative to the water status at saturation.

**Secondary meristems:** type of meristematic tissues responsible for the secondary growth of the plant (e.g., cambium, phellem) – that is, growth in girth or thickness. Secondary meristems are derived from the permanent tissues.

**Symplastic water:** refers to the water stored in the cell plasmalemma, corresponding to the intracellular

# *Context and Objectives of the Thesis*

# Context and Objectives of the thesis

As previously described, the ongoing climate change is modifying surface temperature and precipitation patterns in many areas worldwide and provokes drought episodes that will become more frequent, longer, and intense in the next few years. As a consequence, forests diebacks, that have already been reported around the world, are likely to become more and more recurrent in a near future. As the trend of high temperatures and heatwaves looks set to continue, there is therefore an urgent need to better understand the physiological processes for drought-induced tree mortality to accurately predict the risk of future forest dieback and their effect on forests composition. Indeed, drought and its associated high temperatures are now widely considered as key drivers for tree mortality globally.

In general, drought-induced tree mortality is linked to two non-mutually exclusive processes: carbon starvation and hydraulic failure. However, recent work has provided strong evidence that drought-induced mortality is mainly associated with the failure of the water transport in the xylem tissue of plants. This xylem hydraulic failure occurs when, under drought conditions, the evaporative demand and tree transpiration rate increase xylem sap tension and, consequently, the risk of embolism formation in the xylem conduits. As the percentage of embolised conduits increases (PLC), the hydraulic functioning of the xylem diminishes until the flow of water stops, provoking the desiccation of the tree tissues and, eventually, the death of a tree.

Although the link between tree mortality and xylem hydraulic failure is clear and has been extensively evaluated, the physiological causes behind the correlation between drought-induced tree mortality and xylem hydraulic failure that would explain the capacity of recovery after drought remain poorly understood although this capacity of recovery could be related with the integrity of the meristematic tissues. Therefore, from a tree ecophysiological and a physiological point of view, this thesis aims to:

(i) Identify the key physiological traits that determine the tree capacity to recover from drought.

(ii) Evaluate the mechanistic link between xylem hydraulic failure and downstream cell mortality.

(iii) Determine the main changes occurring at the plant tissue level and, particularly at the cambium level, explaining the lack of recovery after drought.

To reach these objectives, the thesis work was divided in three different experiments. In the first one, working at the stem level, we aimed to determine the key physiological traits that could explain trees' capacity to recover from drought. For this, taking into consideration the theoretical framework for plant mortality proposed by Guadagno *et al.* (2017), we decided to work mainly on the combination of two physiological traits: RWC and cell membrane damage (Figure 29).

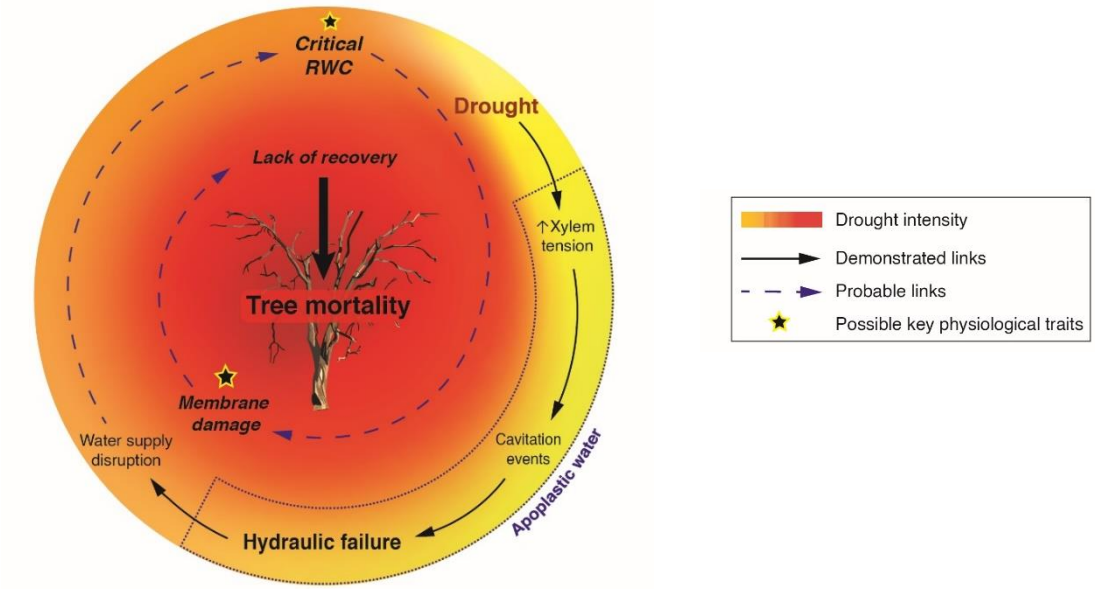


**Figure 29.** Partial framework presenting the possible key physiological traits explaining the correlation between hydraulic failure and tree mortality. (*Adapted from* Mantova *et al.*, 2022)

After elucidating that the interplay of RWC and cell vitality could explain tree capacity to recover from drought, we went on the path from xylem hydraulic failure to cell mortality in an easily accessible organ: the leaf, and thus assessed the mechanistic link connecting both processes (Figure 30).

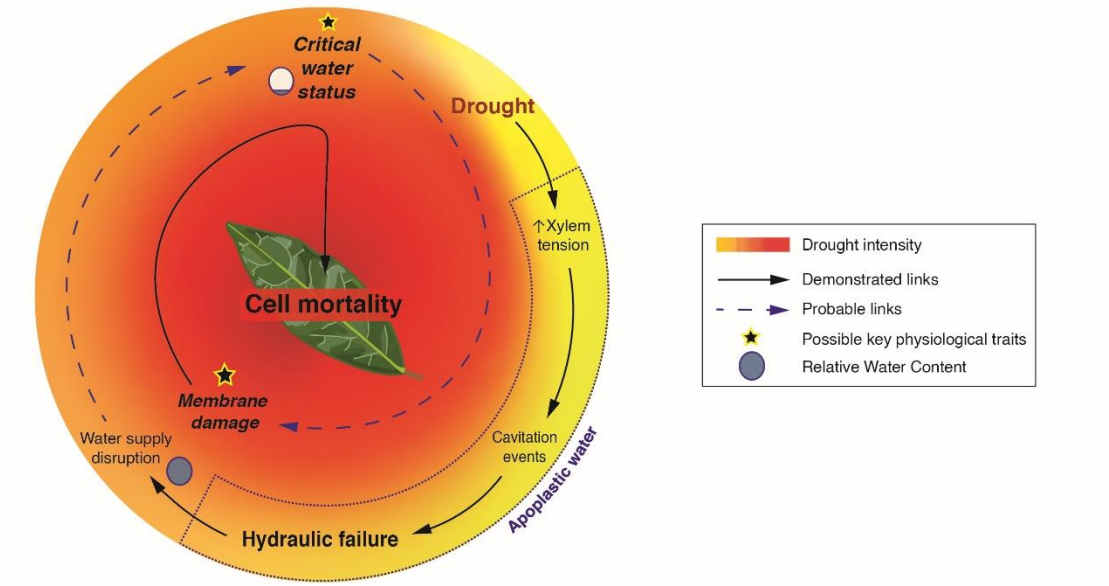


**Figure 30.** Partial framework presenting the probable links connecting xylem hydraulic failure and cell mortality. (*Adapted from* Mantova *et al.*, 2022)

Finally, extrapolating our findings at the leaf level, we evaluated how the water impairment caused by cavitation could refrain trees to recover from drought. For this, we took into consideration the findings of the Chapter 1 and 2 of this thesis, re-applied the same methods to a larger experiment and tried to explain how trees can or cannot recover from drought by focusing our work on evaluating the integrity of specific meristematic cells: the cambium ones (Figure 31).

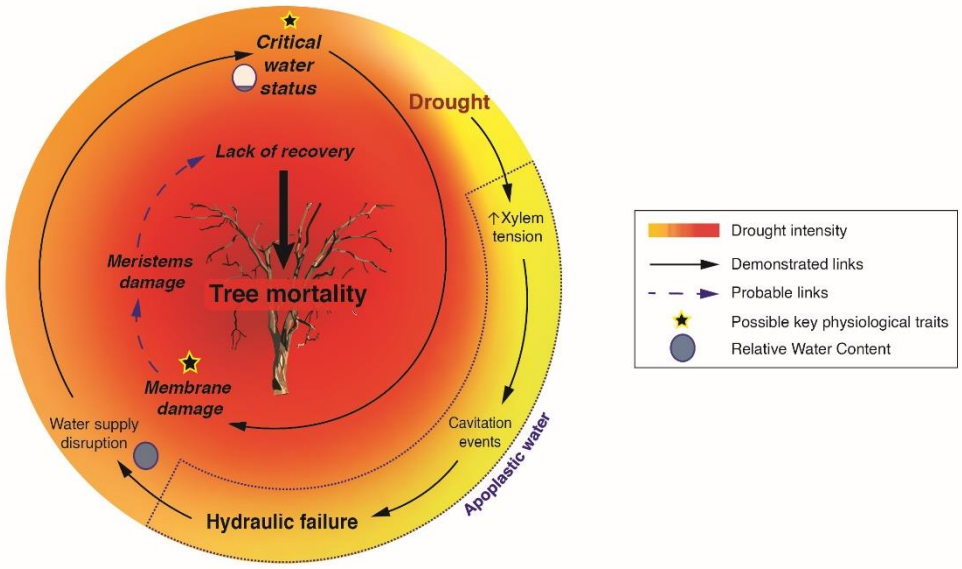


**Figure 31.** Partial framework presenting how meristems damages could matter when trying to explain tree mortality under drought conditions. (*Adapted from* Mantova *et al.*, 2022)

# 1

# *The interplay of hydraulic failure and cell vitality explains tree capacity to recover from drought*

This chapter aimed to identify new key physiological traits that could determine the ability of trees to recover from a drought event. Although $P_{50}$ and $P_{88}$ have long been associated with failure to recover from a drought event, the physiological causes of tree mortality remained unclear. Furthermore, a study by Hammond *et al.* (2019) showed that $P_{50}$ was not appropriate to use as a mortality threshold since some Loblolly pines with PLCs of ~80% could survive the drought event, regrowth and resprout the following year. Thus, given that a tree's capacity to survive from drought appears to be intimately related to its ability to produce new xylem in its perennial organs, we hypothesized here that, this capacity must be associated with the ability to keep key tissues alive in order to re-grow and resprout the following year. Thus, since McDowell *et al.* (2008) hypothesis was based on the fact that hydraulic failure causes tree death by decreasing the water supply to the tree and thus decreasing the water content of its tissues, we chose to focus on the water status of our trees in an attempt to determine new key physiological thresholds for determining survival. As the literature has shown that a decrease in RWC is linked to a dysfunction of the cell metabolism and ultimately a rupture of their membranes (Guadagno *et al.*, 2017), the aim of this study was to combine both water content and membrane dysfunction measurements (also known as an indicator of cellular integrity) in order to determine new physiological thresholds that can be used to implement mechanistic models for predicting tree mortality such as the SurEau model (Cochard *et al.*, 2021).

# Chapter 1. The interplay of hydraulic failure and cell mortality explains tree capacity to recover from drought

PUBLISHED IN *PHYSIOLOGIA PLANTARUM* ON JANUARY 2021

*Authors:*
*Mantova Marylou, Menezes-Silva Paulo E., Badel Eric, Cochard Hervé, Torres-Ruiz José M.*

**Abstract**

Global climatic models predict an increment in the frequency and intensity of drought events, which have important consequences on forest dieback. However, the mechanisms leading to tree mortality under drought conditions and the physiological thresholds for recovery are not totally understood yet. This study aimed to identify what are the key physiological traits that determine the tree capacity to recover from drought. Individuals of a conifer (*Pseudotsuga menziesii* M.) and an angiosperm (*Prunus lusitanica* L.) species were exposed to drought and their ability to recover after rehydration monitored. Results showed that the actual thresholds used for recovery from drought based on percentage loss of conductance (PLC) (i.e., 50% for conifers, 88% for angiosperms) do not provide accurate insights about the tree capacity for surviving extreme drought events. On the contrary, differences in stem relative water content ($RWC_{Stem}$) and the level of electrolytes leakage (EL) were directly related to the capacity of the trees to recover from drought. This was the case for the conifer species, *P. menziesii,* for which higher $RWC_{Stem}$ and lower EL values were related to the recovery capacity. Even if results showed a similar trend for the angiosperm, *P. lusitanica*, as for the conifers, the differences between the two traits were much more subtle and did not allow an accurate differentiation between trees able to recover from drought and those that were not. $RWC_{Stem}$ and EL could work as indicators of tree capacity to recover from drought although more studies are required, especially in angiosperms, to confirm this observation.

## 1. Introduction

Forests represent approximately 30% of the global continental surface (Food and Agriculture Organization, 2006) and provide society with several ecosystem services such as timber production, watershed protection (Allen *et al.*, 2010), hosting biodiversity (Trumbore *et al.*, 2015), and carbon storage and its associated atmospheric feedbacks (Reichstein *et al.*, 2013). Due to the ongoing climate changes and global warming (IPCC 2014), not only the frequency of heatwaves and drought events have increased in many areas worldwide but also their duration and intensity (Allen *et al.*, 2010). A recent data synthesis has suggested that the majority of plant species converge to narrow hydraulic safety margins and thus are very susceptible to changes in rainfall patterns (Choat *et al.*, 2018). Therefore, these higher frequencies and increased severity have exacerbated the occurrence of drought-induced tree mortality events (Keenan *et al.*, 2013; Duan *et al.*, 2014) and, consequently, forests dieback (Hosking and Hutcheson 1988, Lwanga 2003, Landmann and Dreyer 2006).

Although the reduction in water availability can affect virtually all processes associated with plant growth and development, drought-induced tree mortality events are commonly associated with two main processes: carbon starvation and xylem hydraulic failure (McDowell *et al.*, 2008). Under prolonged mild drought conditions, trees partially close their stomata to reduce evapotranspiration and hence the risk of xylem hydraulic failure. However, this stomatal closure constrains $CO_2$ diffusion in leaves and can lead to an important depletion of the carbohydrate pools resulting in carbon starvation (Hogg & Hurdle, 1997; Buckley, 2005; McDowell *et al.*, 2008; Berry *et al.*, 2010; Creek *et al.*, 2020). Even if carbon starvation and xylem hydraulic failure cannot be considered as mutually exclusive processes, recent studies have shown that xylem hydraulic failure is the main cause of tree mortality under severe drought (Urli *et al.*, 2013; Salmon *et al.*, 2015; Adams *et al.*, 2017). Xylem hydraulic failure occurs when the tension in the continuous columns of water that connect the roots with the leaves through the xylem increases and, consequently, exacerbates the risk of cavitation (breakage of the water column) (Tyree & Zimmermann, 2002). This process is widely amplified as soil dries or when the evaporative demand increases. Thus, under extreme drought conditions, as the percentage of cavitated conduits increases, the hydraulic conductance of the xylem decreases until the flow of water stops and provokes the desiccation of the plant tissues, cells death and, finally, the death of the tree (McDowell *et al.*, 2008). This makes xylem vulnerability to cavitation one of the main physiological traits when evaluating drought-induced mortality.

Even if the vulnerability to cavitation has been widely evaluated for an important amount of species during the last decades (Delzon *et al.*, 2010; Choat *et al.*, 2012), the relationship between xylem hydraulic failure and tree mortality has not been properly evaluated yet. It is known that $P_{50}$ and $P_{88}$ (i.e., the xylem tension inducing 50 and 88% of loss of hydraulic conductance, respectively) are associated with the capacity of the trees to recover from drought (Brodribb *et al.*, 2010; Delzon & Cochard, 2014; Sperry & Love, 2015; Bolte *et al.*, 2016), but the physiological causes of tree death under extreme drought events remain unclear. Therefore, due to a lack of physiological thresholds to properly define tree mortality both during or after a drought episode, $P_{50}$ and $P_{88}$ values, for conifers and angiosperms respectively (Brodribb and Cochard 2009; Urli *et al.* 2013), are currently used as proxies for mortality when

e.g., modelling the trees' response to drought (Martin-StPaul *et al.*, 2017). However, a recent study by Hammond *et al.* (2019) reported that the appropriateness of $P_{50}$ as an indicator of mortality for conifers should be reconsidered as they defined a lethal threshold at 80% of loss of xylem hydraulic conductivity in loblolly pines (*Pinus taeda* L.). Also, it has recently been reported that branch diameter variations were revealing a point of no recovery in lavender species as plants were not able to recover from drought once their elastic water storage localized in the bark were depleted (Lamacque *et al.*, 2020). These results have raised new questions about the role of xylem hydraulic failure in triggering tree mortality or the minimum hydraulic functioning required for allowing trees to survive and recover from drought.

The ability of the trees to recover after a drought event seems to be tightly related to their ability to grow new xylem (Brodribb *et al.*, 2010) and this ability must be intrinsically linked to their capacity to maintain key living tissues alive in perennial organs, as the stem, that allow them to regrowth and resprout in favourable conditions. Considering the tenet that xylem hydraulic failure should provoke the complete desiccation of the cells and their consequent death leading to whole plant mortality (McDowell *et al.*, 2008), a focus on plant water status and its consequences on cell vitality seems necessary to understand drought-induced mortality (Guadagno *et al.*, 2017; Martinez-Vilalta *et al.*, 2019). This, therefore, highlights the relevance of relative water content (RWC), a direct measure of the plant water status at cell level, as a potential candidate for assessing drought-induced tree mortality (Martinez-Vilalta *et al.*, 2019; Trueba *et al.*, 2019). In addition, and considering that many studies have evinced how low RWC values are linked to membrane dysfunction in plant cells (Wang *et al.*, 2008; Chaturvedi *et al.*, 2014), combining both traits, RWC and membrane dysfunction, would help define physiological thresholds for tree mortality.

The main objective of this study was to identify other physiological traits than the percentage loss of hydraulic conductance (PLC) that could work as an indicator of the tree capacity to recover from drought. For this, a set of plants of *Prunus lusitanica* L. and *Pseudotsuga menziesii* M., i.e., an angiosperm and a conifer species respectively, were exposed to severe drought conditions and allowed to dehydrate until the induction of important losses in hydraulic functioning. At this point, trees were re-watered to check for the capacity to recover from drought. During the dehydration and the recovery phases, we monitored embolism formation and changes in RWC at the stem and the leaf level. We also monitored changes in stem diameter to check whether trees were able to recover from drought after being re-watered, and assessed the vitality of the stem living tissues. Results also provided us with novel information about the causative relationship between PLC and tree mortality and the level of PLC that prevent any recovery from drought in these two species.

## 2. Materials and methods

### *2.1.Plant material and experimental setup*

The experiments were carried out in two species: one angiosperm, *Prunus lusitanica* L. and one conifer, *Pseudotsuga menziesii* M., a shrub and a tree respectively, selected for their contrasted PLC thresholds of drought-induced mortality (i.e., $P_{88}$ and $P_{50}$ respectively). For each species, eight young trees were grown under non-limiting water conditions in 5 and 9.2-L pots, respectively, at the INRAE-PIAF research station of Clermont-Ferrand, France (45877°N, 3814°E). *P. menziesii* individuals were four years old at the time of the experiment while the *P. lusitanica* were two years old. Two weeks before starting the experiment, all trees were moved to a controlled-environment glasshouse cell and kept under natural light and at a mean temperature of 17.7 ± 0.2°C (midday) and 10.9 ± 0.1°C (night). During this period, trees were kept well-irrigated (field capacity) by a drip irrigation system controlled by an electronic timer. After the two weeks of acclimation, a sub-set of trees for each species (from four to six individuals) was exposed to progressive dehydration by withholding the irrigation. In order to determine the critical PLC for recovery and because Hammond *et al.* (2019) reported that conifers were able to recover even beyond $P_{50}$, trees were re-watered to field capacity once reaching water potential values corresponding to significant losses in hydraulic functioning according to their vulnerabilities to cavitation (i.e., PLC > 50% for conifers and PLC> 90% for angiosperms). They were then kept well-irrigated in order to check for recovery from drought.

### *2.2.Vulnerability curves to cavitation*

Prior to the experiment, the vulnerability to cavitation for the two target species was determined to define when trees should be re-watered according to their PLC level. Thus, two different techniques (i.e., one technique per species), reported as highly comparable by Brodribb *et al.* (2017), were used according to the xylem characteristics of each species. Thus, for *P. lusitanica*, xylem vulnerability to cavitation was determined by using the recently developed optical method (Brodribb *et al.*, 2017) to avoid possible biased results related with the open-vessel artefact (Torres-Ruiz *et al.,* 2014, 2015, Choat *et al.,* 2016). Indeed, the use of the Cavitron method in this species was not possible due to the length of the xylem conduits that were longer than the diameter of the rotor available (Sergent *et al.,* 2020). For *P. menziesii,* vulnerability curves were constructed by using the Cavitron technique (Cochard, 2002a) which is highly reliable when used to measure species with short conduits such as conifers (Cochard *et al.,* 2013, Torres-Ruiz *et al.,* 2017). The use of the optical method was not possible for *P. menziesii* because the conduits at the stem level are so short that the cavitation events are not always detectable.

Briefly, for *P. lusitanica*, the entire plant was let to dehydrate under lab conditions while a clamp equipped with a camera was installed in the stem of four trees after removing the bark carefully with a razor blade to expose undamaged xylem. To avoid the over desiccation of the exposed xylem area during the 6.51 ± 0.52 days of dehydration, we applied a thin coat of silicone grease. The camera then captured images every five min during the dehydration process while changes in stem water potential ($\Psi_{stem}$, MPa) were continuously monitored using a psychrometer (PSY1, ICT international, Armidale, Australia) installed centrally on the

main stem of each plant. The Peltier cooling time was adjusted from 10 s (when the plant was well hydrated) to a maximum of 20 s (as the plant dehydrated) to ensure that sufficient water was condensed onto the thermocouple and then evaporated to produce a stable reading of the wet-bulb depression temperature. To ensure the accuracy of the measurements obtained with the psychrometer, regular $\Psi_{stem}$ measurements were carried using a Scholander-type pressure chamber (PMS, Corvallis) in fully developed and healthy leaves previously bagged for at least one hour to prevent transpiration and promote equilibrium with the plant axis (Figure S1). Image sequences were then analysed manually according to Brodribb *et al.* (2016, 2017). The percentage of embolised pixels for each image was calculated as the amount of embolised pixels cumulated and the total embolised area of the scanned area. The vulnerability curve was obtained by plotting $\Psi_{stem}$ against cumulative embolisms (% of total).

For *P. menziesii,* xylem vulnerability to cavitation was assessed with the Cavitron technique (Cochard, 2002a) which uses centrifugal force to increase the water tension in a xylem segment while measuring the decrease in its hydraulic conductance. Thus, five 0.45m-long stem samples from five different well-hydrated trees (i.e., one sample per tree), were debarked to prevent resin contamination and recut under water with a razor blade to a standard length of 0.27m. For constructing the vulnerability curves, the maximum sample conductivity ($K_{max}$) was measured at low speed and relatively high xylem pressure (−0.75 MPa). The xylem pressure was then decreased stepwise by increasing the rotational velocity and the conductivity ($K$) measured at each pressure step. Each pressure was applied on the sample for two minutes. Sample loss of conductivity (PLC, %) was computed at each pressure as follows (4):

$$(4)\ PLC = 100 * \left(1 - \frac{K}{Kmax}\right)$$

The resulting curves were fitted according to Pammenter and Vander Willigen equation (1998) (5) and using the R *'fitPLC'* package (Duursma & Choat, 2017):

$$(5)\ PLC\ or\ Cumulative\ embolism = \frac{100}{\left(1 + e^{(a/25(P-P50))}\right)}$$

where $a$ is the slope of the curve at the inflexion point, $P$ indicates the xylem water potential for the optical method (*P. lusitanica*) or the target pressure reached with the Cavitron (*P. menziesii)*, and $P_{50}$ is the $\Psi_{stem}$ or pressure value at which 50% of the xylem cavitation events had been observed or at which 50% loss of conductivity occurred.

### *2.3.Physiological traits*

During the progressive dehydration imposed to each subset of plants, $\Psi_{stem}$ was continuously assessed by using psychrometers (PSY1, ICT international). Thus, one psychrometer per plant in a total of four plants per species was installed at the stem level and covered with aluminium foil to prevent their direct exposure to the sunlight and minimize any effect of external temperature variations (Vandegehuchte *et al.*, 2014) (Figure 32). Psychrometers recorded the $\Psi_{stem}$ every 30 min. To check the accuracy of the psychrometers, regular $\Psi_{stem}$ measurements were carried using a Scholander-type pressure chamber (PMS,

Corvallis) in two fully developed and healthy leaves per plant, previously bagged for at least one hour to prevent transpiration and promote equilibrium with the plant axis (Figure S1).

**Figure 32.** Stem psychrometer installed on a *Prunus lusitanica* tree, covered in aluminium foil to protect from direct sunlight exposure.

Stem diameter variations were monitored continuously by Linear Variable Differential Transformer (LVDT) sensors (one LVDT per plant in eight plants per species) installed before withholding irrigation (Figure 33). The sensor was applied on the stem with glue and was connected to a data logger (Model CR1000, Campbell Scientific LTD) to collect the stem diameter variations (in µm) every 10 min. By evaluating the dynamics of stem diameter during

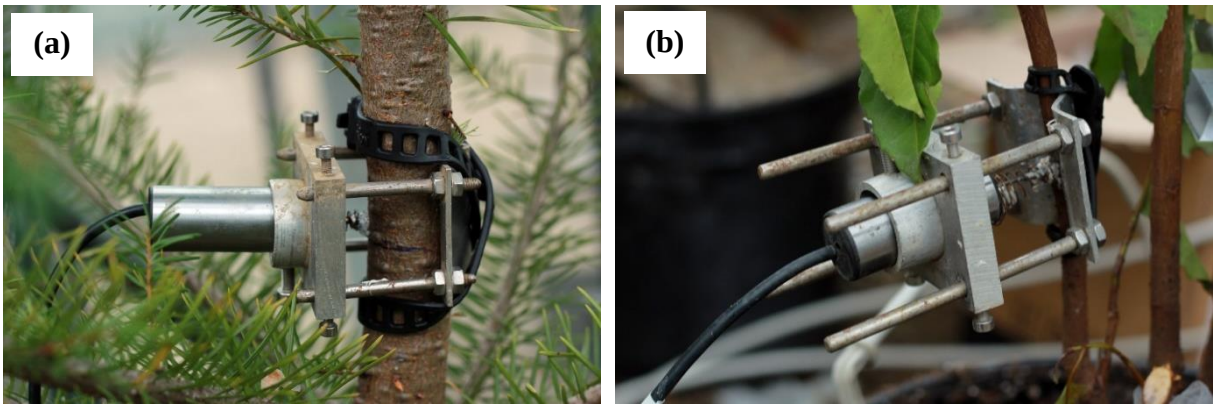


**Figure 33.** LVDT installed on the stem of **(a)** *Pseudostuga menziesii* and **(b)** *Prunus lusitanica*.

the dehydration and recovery phases of the experiment, we were able to evaluate the capacity of the trees to recover from drought (Lamacque *et al.*, 2020).

The RWC was measured at stem ($RWC_{Stem}$) and leaf level ($RWC_{Leaf}$) in all trees before withholding irrigation (Control) and right before re-watering. $RWC_{Stem}$ and $RWC_{Leaf}$ were calculated according to Barrs and Weatherley (1962) (6):

$$(6)\ RWC = \frac{(FW-DW)}{(TW-DW)}\ ,$$

where FW is the fresh weight measured immediately after sampling; TW is the turgid weight measured after immersing the stem in distilled water for 24 h (for $RWC_{Stem}$) or after soaking

the leaf petiole for 24 h in distilled water (for $RWC_{Leaf}$); and DW is the dry weight of the samples after 24 h of drying in an oven at 72°C. All measurements were done using a precision scale (METTLER AE 260, DeltaRange ®) and were performed on three healthy leaves or one to three small stem sections per plant (depending on plant material).

Once the trees reached water potentials corresponding to a PLC of ca. 88% for *P. lusitanica* and 50% for *P. menziesii* according to the vulnerability curves, the PLC was assessed in stems using two different, but comparable, techniques (Cochard, 1992; Torres-Ruiz *et al.*, 2014; Choat *et al.*, 2016a). For *P. lusitanica*, PLC was determined gravimetrically using a xylem embolism meter (XYL'EM, Bronkhorst). For *P. menziesii,* as it was impossible to restore the maximal conductance ($K_{max}$) due to the permanent aspiration of the pit membrane against the cell walls (Cochard *et al.*, 2013), the PLC was assessed by direct observation using X-Ray microtomography (Micro-CT, Nanotom 180 XS; GE) at the PIAF laboratory (INRAE) (Cochard *et al.*, 2015). For both techniques, samples were cut progressively underwater to prevent artefactual increases in the amount of embolism in the samples (Torres-Ruiz *et al.*, 2015).

For the XYL'EM, the PLC was evaluated in three stems (sample length ca. 30mm) per individual in eight individuals per species. The initial $K$ ($K_i$) of each segment was determined using a filtered (0.22 µm) 10 mm KCl and 1 mm CaCl2 perfusion solution made with distilled water (Cochard *et al.*, 2009), and applying a pressure head of 8.5 kPa until a steady-state $K_i$ was attained. In order to determine the maximal conductance ($K_{max}$), samples from *P. lusitanica* were flushed with water at high pressure (200 kPa) for 20 minutes to remove all the embolism. PLC was then calculated using the following equation (7):

$$(7)\ PLC = 100 * \left(1 - \frac{Ki}{Kmax}\right)$$

For Micro-CT, one or two samples per plant were collected, as described for the gravimetric $K$ measurements, and immediately immersed in liquid paraffin wax to prevent dehydration during the scanning. For each 21-min scan, 1000 images were recorded during the 360° rotation of the sample. The X-ray setup was fixed at 70kV and 240µA. At the end of the experiment, samples were cut 3mm above the scanned cross-section, injected with air (0.1MPa) and re-scanned to visualize all the conduits filled with air. The amount of PLC was computed by determining the ratio between the amount of cavitated conduits in the samples before and after cutting the sample.

### *2.4.Cell vitality*

Cell vitality was assessed using two different methods: the electrolytes leakage test (EL) (Zhang & Willison, 1987; Sutinen *et al.*, 1992) and a fluorescein diacetate (FDA) staining process (Widholm 1972). Cell vitality was assessed in both control and drying trees right before rewatering the latter ones. For EL, one to three stem samples per plant (depending on plant material availability) were cut into ten 2-mm thick slices and immersed in test tubes containing 15mL of pure water. Test tubes were shaken at 60 shakes per min during 24h at 5°C to stop enzyme activity. Water conductivity of the effusate (C1) was then measured at room temperature using a conductimeter (3310 SET1, Tetracon® 325, WTW, Weilheim, Germany). Then, all the living cells were killed by autoclaving the samples at 121°C for 30 min (King &

Ludford, 1983), cooled down at room temperature (22°C approx.) for 60 min and the effusate maximal conductivity (C2) measured. The lysis percentage (EL) was then determined as (8):

$$(8)\ EL = \frac{C1}{C2} * 100$$

To stain the cytoplasm of stem living cells and quantify the amount of living cells and their location for each individual, FDA (F7378-10G, SIGMA-ALDRICH) was used. For this, two or three 60 µm-thick stem cross-sections were obtained with a microtome (Leica RM2165) and stained for 20 min in a 1% FDA solution (Widholm 1972). Cross-sections were observed using an inverted fluorescence microscope (Axio Observer Z1, ZEISS; Bright light or YFP filter) within the next hour after staining. An entire cross-section image was obtained by joining images with the same magnification taken from all the cross-section of the sample for both bright light and fluorescence observations. The percentage of bark living cells (BLC) for each cross-section was calculated as follow (9):

$$(9)\ BLC = \frac{FA}{BA} * 100$$

Where FA is the total fluorescent area of the sample and BA is the bark area determined using Fiji software (Schindelin *et al.*, 2012).

### *2.5.Statistical analyses*

Statistical analyses consisted of paired *t*-test (after testing for normality and homogeneity of variances) and Wilcoxon test (for non-normal distribution) and were performed using R programs to compare the set before the drought event (Control) and before re-watering. All tests were performed using a level of significance $\alpha = 0.05$.

## 3. Results

### *3.1.Capacity of recovery from drought*

Vulnerability curves reported $P_{50}$ values of -6.07 and -3.73MPa for *P. lusitanica* and *P. menziesii,* respectively (Figure 34). *P. lusitanica* individuals were thus rehydrated once they reached water potential values of ca. -9.0 to -10.0MPa i.e., above its $P_{88}$ of -8.94MPa. *P. menziesii* were rehydrated once showing water potential of ca. -7.0 to -10.0 MPa ($P_{88}$ = -5.34MPa).

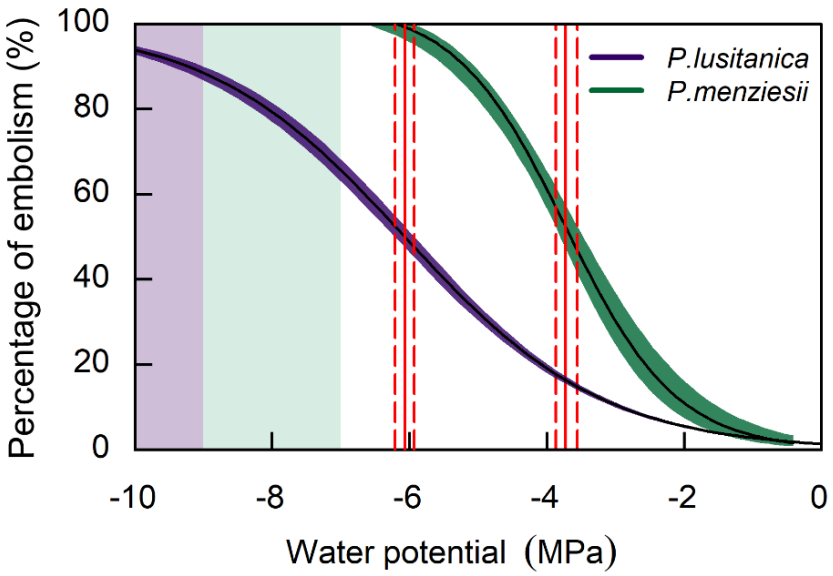


**Figure 34.** Vulnerability curves to cavitation for *Prunus lusitanica* stems and *Pseudotsuga menziesii* stems.
Vulnerability curve for *P. lusitanica* stems obtained on four different samples using the optical method (Brodribb *et al.*, 2017). The $P_{50}$ is evaluated at -6.07MPa while the $P_{88}$ is evaluated at -8.94MPa. Vulnerability curve for *P. menziesii* stems obtained on five different samples using the Cavitron technique developed by Cochard in 2002. The $P_{50}$ is evaluated at -3.73MPa and $P_{88}$ is evaluated at -5.34MPa.
Red solid lines represent the $P_{50}$ while red dashed lines represent the confidence interval around $P_{50}$ at 95%. Violet and green rectangles correspond to the water potential values at which *P. lusitanica* and *P. menziesii* were respectively irrigated.

In control conditions, the mean levels of PLC in the stem for *P. lusitanica* and *P. menziesii* were 6.9 (±3.5 SE) and 7.4 (±2.8 SE) respectively (Figure 35). Right before applying the recovery irrigation, the mean PLC for *P. lusitanica* and *P. menziesii* were 94.4 (±1.98 SE) and 79.5 (±3.7 SE) respectively (Table S1) i.e., above the current point for xylem hydraulic failure for angiosperms (i.e., $P_{88}$) and conifers (i.e., $P_{50}$).

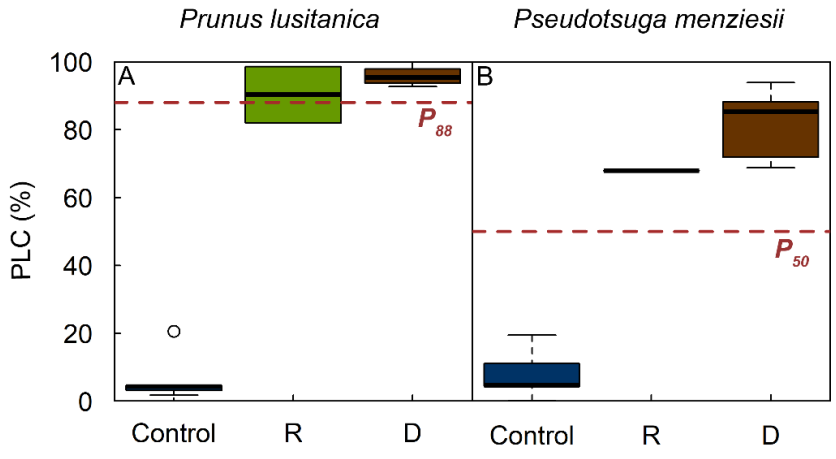


**Figure 35.** Box plots representing the dispersions of percentage loss of conductance (PLC) values for **A.** *Prunus lusitanica* and **B.** *Pseudotsuga menziesii* before water stress (control) and before re-watering for recovering (R) and dead (D) trees measured with the Xyl'EM apparatus for *P. lusitanica* and X-ray micro-CT for *P. menziesii*.

Stems showed a noticeable shrinkage for both species during the time-course of the dehydration for all individuals (Figure 36). After rewatering, two *P. lusitanica* individuals that reached a mean PLC of 90.3 (±8.3 SE) (Figure 35A) showed an increase in stem diameter immediately after being re-hydrated and were considered as recovered trees (Figure 36A). On the contrary, the six individuals that reached PLC of 95.8 (±1.1 SE) showed a continuous decrease in stem diameter after the rehydration and were considered as dead trees (Figure 36C). For *P. menziesii*, only one individual that reached a $\Psi_{stem}$ value of -7.48MPa and a PLC level of 67.9 (Figure 35B) was able to recover in terms of trunk diameter after rewatering

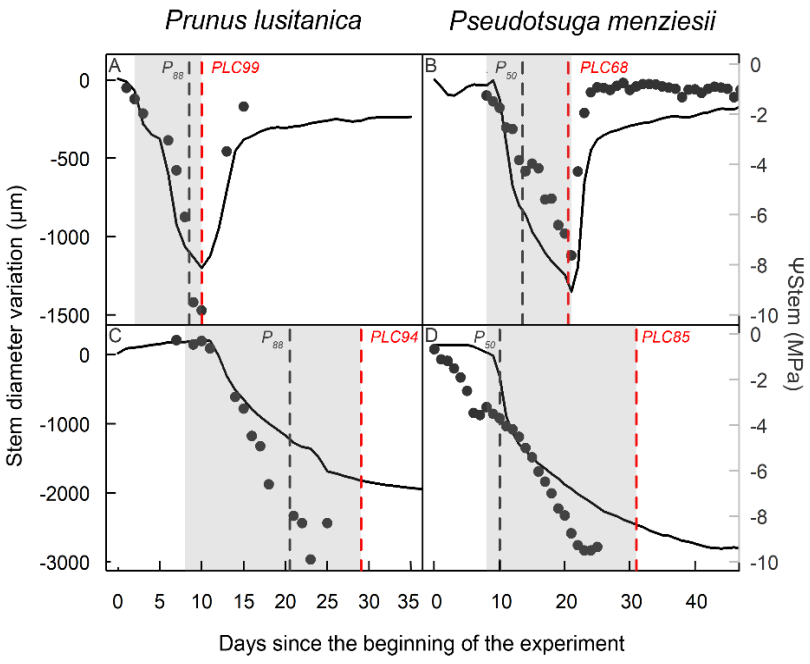


**Figure 36.** Dynamic of the stem diameter (solid line) and evolution of the water potential (dots) during the time-course of the experiment.
The light grey rectangles represent the period where water was withheld to simulate an extreme drought event. The grey dashed line indicates when was reached $P_{88}$ for *Prunus lusitanica* and $P_{50}$ for *Pseudotsuga menziesii*. The red dashed line indicates the day and the percentage loss of conductance (PLC) value at which plant was re-watered.
**A.** and **B.** Recovery of individuals after re-watering in terms of stem diameter.
**C.** and **D.** Dead individuals.

(Figure 36B). All the other individuals continued to show a decrease in stem diameter during the re-watering phase after reaching a mean $\Psi_{stem}$ value of -8.7MPa (±0.5 SE) (Figure 36D) and a mean PLC of 81.1 (±3.8 SE) (Figure 35B).

For both species, individuals that were able to recover from drought showed an increase in $\Psi_{stem}$ concomitantly to the increase in stem diameter (Figure 36A, B) while no recovery in $\Psi_{stem}$ was noticed in trees considered as dead (Figure 36C, D).

A significant decrease in $RWC_{Stem}$ was observed for both species during dehydration as PLC increases (Figure 37A, B; Table S2). In control *P. lusitanica* trees, $RWC_{Stem}$ was of 92.3% (±0.8 SE) whereas it dropped for those exposed to drought to 58.5% (±1.5 SE) for recovered individuals and to 54.7% (±3.6 SE) for dead individuals before re-watering. Differences in $RWC_{Stem}$, however, were not significant when comparing recovered and dead individuals. Similar results were observed for *P. menziesii*, with a significant decrease in $RWC_{Stem}$ noticed for both recovered and dead individuals from drought. Thus, $RWC_{Stem}$ decreased from 83.4% (±1.1 SE) for control trees to 49.8% for recovered and 36.9% (±1.9 SE) for dead trees.

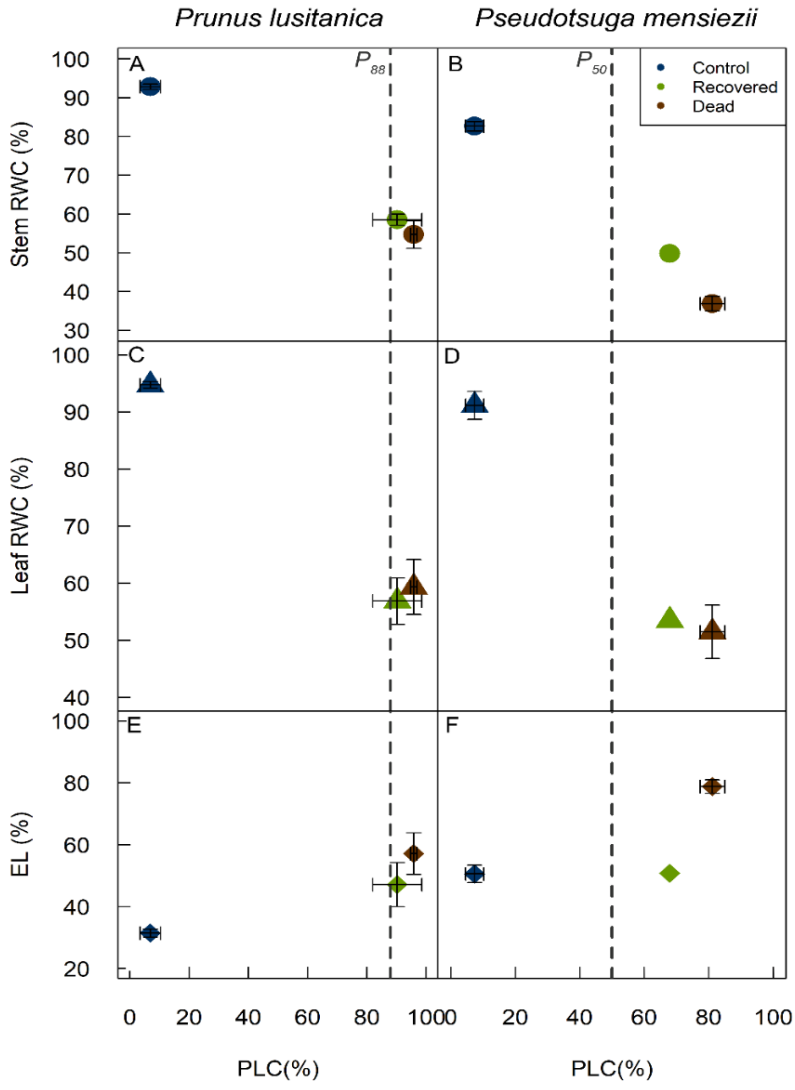


**Figure 37.** Variation of Stem Relative Water Content ($RWC_{Stem}$) (panels **A** and **B**), Leaf Relative Water Content ($RWC_{Leaf}$) (panels **C** and **D**), stem Electrolyte Leakage (EL) (panels **E** and **F**) for *Prunus lusitanica* and *Pseudotsuga menziesii*. Measurements were performed on all individuals in control conditions (Control) and after the drought event (i.e., before applying the recovery irrigation).

Similar to $RWC_{Stem}$, $RWC_{Leaf}$ was significantly impacted in both species during dehydration (Figure 37C, D; Table S2). For *P. lusitanica*, $RWC_{Leaf}$ decreased from 94.8 % (±0.5 SE) (Control) to 56.9% (±4.1 SE) in plants that recovered from drought and to 59.3 % (±4.8 SE) in those that did not recover. For *P. menziesii*, $RWC_{Leaf}$ went from 92.4 % (±2.0 SE) (Control) to 53.5 % in recovered trees or 51.5 % (±4.7 SE) in dead trees. Differences in $RWC_{Leaf}$ were not significant for any of the two species when comparing recovered and dead individuals.

### *3.2.Tissue vitality*

For *P. lusitanica*, all trees showed higher EL values than control ones before re-watering (Figure 37E, F, Table S2) (Control: 29.9% ±1.3 SE; Recovered: 47.12% ± 7.12 SE; Dead: 57.2% ±6.7 SE). However, no differences were noticed when comparing recovered and dead individuals before re-watering (Recovered: 47.1% ±7.1 SE; Dead: 57.2%±6.7 SE). For, *P. menziesii*, only the trees that did not recover showed higher EL values compared to control (Control: 50.6% ±2.2 SE; Dead: 78.8%±2.2 SE). No differences in EL were observed between the recovered individual and control ones (Control: 50.6% ±2.2 SE; Recovered: 50.8%). The recovered individual tends to show lower EL values than the dead ones (Recovered: 50.8%; Dead: 78.8% ±1.2 SE).

In control trees and for both species, the FDA staining showed that living cells were mostly located at the outer bark and phloem level (Figure 38). Before re-watering, the amount of living cells in *P. lusitanica* decreased noticeably in dead trees (Figure 39A; Table S3) (Control: 23.0% ±4.4 SE; Dead: 3.0% ±1.4 SE) but not in trees that recovered (Control: 23.0% ±2.4 SE; Recovered: 15.3%±10.4 SE). For *P. menziesii*, the amount of living cells decreased in trees that did not recover (Control: 10.2% ±2.1 SE; Dead: 0.8% ±0.6 SE) while no noticeable decrease was encountered in trees that recovered (Control: 10.2% ±2.2 SE; R: 7.2%) (Figure 39B; Table S3).

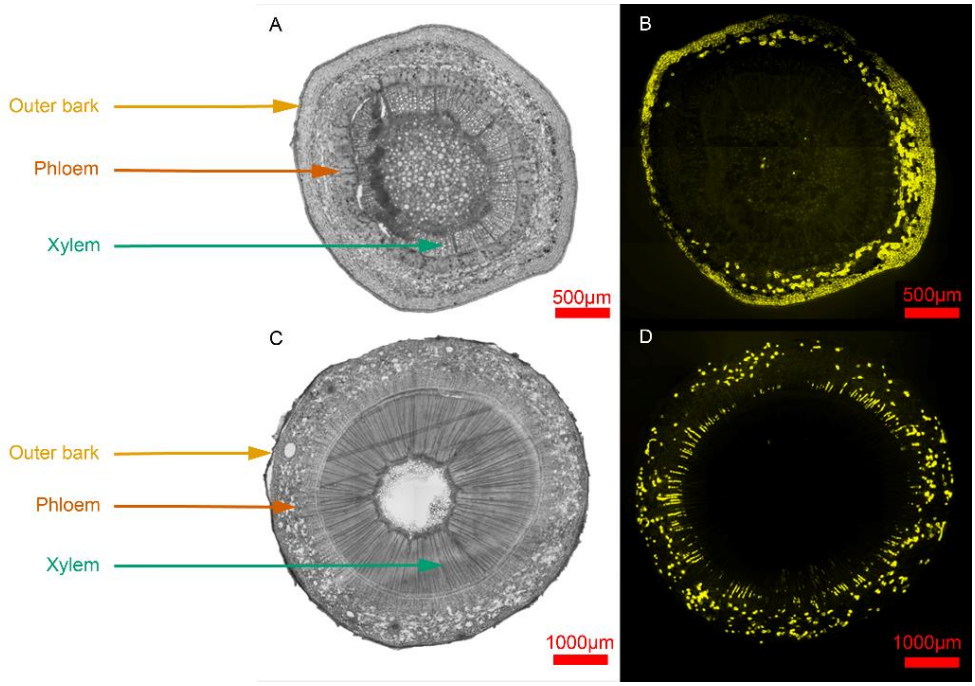


**Figure 38.** Cross-sections of *Prunus lusitanica* (**A** and **B**) and *Pseudotsuga menziesii* (**C** and **D**) stems in control conditions.
Cross-sections were stained using fluorescein diacetate (FDA) (60µm thick cross-section – 1% solution) and microphotographs were taken using a bright light (**A** and **C**) and an inverted fluorescence microscope (YFP filter; **B** and **D**). Fluorescent spots indicate living cells.

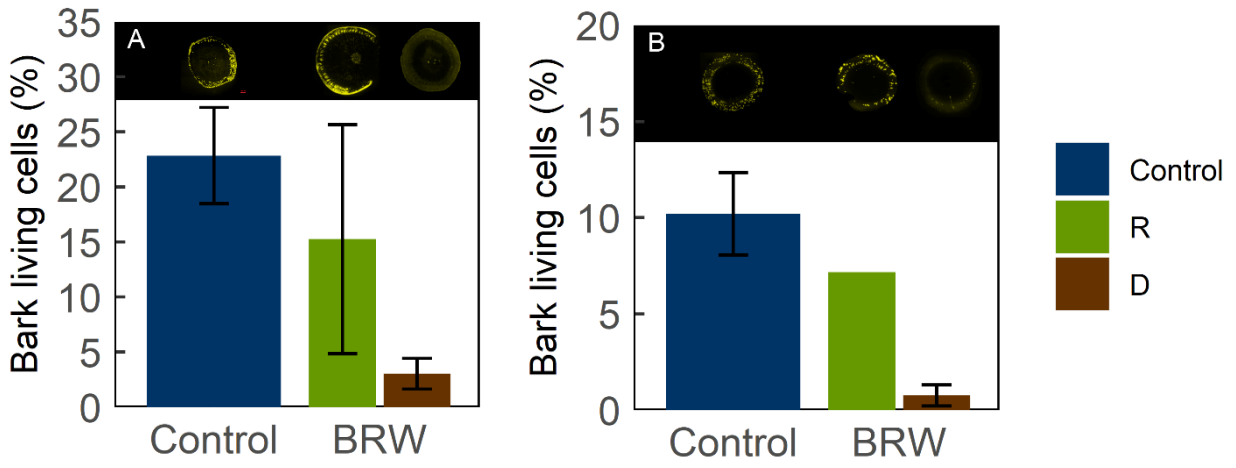


**Figure 39.** Percentage of bark living cells (%BLC) stained with FDA in stem cross-sections in *Prunus lusitanica* (panel **A**) and *Pseudotsuga menziesii* (panel **B**).
"BRW" = before re-watering. "R" refers to recovering trees and "D" refers to dead trees.

## 4. Discussion

Our results provide strong evidence that even when presenting high levels of hydraulic dysfunction, trees were able to recover from an extreme drought event after being re-watered. Indeed, *P. lusitanica* individuals that showed PLC values of 98.6%, i.e., well above the suggested threshold for recovery and point of death for angiosperms ($P_{88}$, Barigah *et al.*, 2013; Urli *et al.*, 2013), recovered from drought according to their stem diameter dynamic (i.e., showed an increase in stem diameter immediately after re-watering) and even flushed new leaves after being re-watered at field capacity (Figure S2). Similarly, *P. menziesii* individuals with PLC values of 67.9%, i.e., above the threshold for recovery for conifers ($P_{50}$, Brodribb and Cochard 2009), were also able to recover once re-watered. These results, therefore, demonstrate how trees are able to recover from drought even when their PLC levels reach higher values than those considered as threshold for recovery for angiosperms and conifers (i.e., $P_{88}$ and $P_{50}$, respectively). These results agree with those provided for loblolly pine (*Pinus taeda* L.) by Hammond *et al.* (2019) which reported a higher chance for trees to die than to survive once reaching PLC levels of 80, i.e., much higher than the $P_{50}$ threshold commonly reported for conifers. In our study, however, no recovery was observed for *P. menziesii* when PLC reached values above 68%, which raises questions on how lethal PLC thresholds vary among tree species. For angiosperms, our results also agree with the ones provided for *Pistacia lentiscus* L. by Vilagrosa *et al.* (2003) that show how drought-induced mortality only occur in plants that reached PLC values of almost 100%. When taken together, all these results highlight the importance of revising the actual recovery and point of death thresholds suggested for angiosperms and conifers. More importantly, these results show that plant mortality occurs when the losses in xylem conductance are important (e.g., >90% of xylem hydraulic dysfunction), suggesting that PLC is not the sole triggering mechanism of plant death under drought conditions.

Unfortunately, any critical thresholds for most of the physiological traits monitored during our experiment were identified as a potential proxy for drought-induced mortality. Thus, it was not possible to evince a clear causal link between stem hydraulic failure and plant

mortality since trees that were not able to recover from drought did not consistently show higher PLC values than those that survived. However, two interesting trends emerged from the $RWC_{Stem}$ and EL results for *P. menziesii*. On one hand, trees recovering from drought tend to show higher $RWC_{Stem}$ than dead ones before re-watering and, on the other hand, trees that recovered tend to show lower EL values than the dead ones. These results agree with Martinez-Vilalta *et al.* (2019) and highlight the importance of plant water content as a potential indicator of mortality risk. However, this was not the case for *P. lusitanica* since similar $RWC_{Stem}$ values were observed in both trees that were able to recover from drought and those that were not. This raises the possibility of using $RWC_{Stem}$ as a proxy for mortality across species, although more confirmatory studies should be carried out especially in angiosperms. At leaf level, $RWC_{Leaf}$ at turgor loss point is relatively high and constant between species (Bartlett *et al.,* 2012), which potentially could make it a useful trait for identifying survival events since noticeable changes in $RWC_{Leaf}$ would occur at high dehydration level preceding death (Martinez-Vilalta *et al.*, 2019). However, no differences in $RWC_{Leaf}$ were detected in our study between recovering and dead trees before re-watering for any of the two species evaluated probably because, at those levels of water stress, leaves were already hydraulically disconnected from the stems in all the individuals. This would favour a faster dehydration of the leaves in comparison with the stems and, therefore, may partially explain the similarly low values for $RWC_{Leaf}$. Therefore, rather than just focusing only on the plant water status, a deeper study on water relocation in trees during drought (Körner 2019) would be required for identifying potential proxies for drought-induced mortality. In fact, a crucial question now is to evaluate if the relocation of water from plant reserves would be enough for keeping key tree tissues hydrated during drought and, therefore, enhancing plant probability of survival after re-watering (Holbrook, 1995).

Regarding cell integrity, recovering trees from drought tend to present lower cell damages than the dead trees before re-watering. *P. menziesii* recovering trees showed seemingly no changes in their percentage of EL even after the drought event. Dead trees, on the contrary, consistently showed higher EL values before re-watering than control trees able to recover in agreement with the results reported by Vilagrosa *et al.* (2010) for *P. lentiscus*. Even if *P. lusitanica* dead and recovering trees did not show any differences in EL, recovering trees were able to resprout and flush new leaves when the stress was alleviated (Figure S2). As higher EL values are the consequences of membrane failure and are associated with cell death (Vilagrosa *et al.*, 2010; Guadagno *et al.*, 2017), these observations suggest that the fatal failure at the cellular scale does not occur homogeneously within the stem and this, as shown by Thomas (2013) and Klimešová *et al.* (2015), allow the resprouting of the plant if the stress is relieved. Therefore, according to our results, the membrane integrity could emerge as a proxy for lack of recovery capacity in conifers since the cell vitality in some of the living tissues at the stem level seems to have a relevant role in drought-induced mortality. However, the link between membrane failure and the loss in stem hydraulic functioning is still unresolved. Indeed, it is still unclear whether the extreme dehydration leads to membrane failure through physical (i.e., cell cavitation, Sakes *et al.,* 2016), collapse and cytorrhysis (Taiz & Zeiger, 2006) or only biochemical processes (Suzuki *et al.*, 2012; Wang *et al.*, 2013; Petrov *et al.*, 2015).

The presence of living cells in stems at the inner bark level was not always related to the survival of the trees after re-watering (i.e., increase in stem diameter). This was the case for *P. lusitanica* where trees showing similar amounts of living cells, differed in their capacity to recover from drought. The presence of living cells in dead trees could be explained by the fact that, under drought conditions, trees can rely on their own water reserves (Epila *et al.*, 2017) which could temporally maintain the metabolism of the cell despite being hydraulically disconnected from the roots. However, once the water reserves are depleted, living tissues would ultimately dry and cells would dehydrate and die. Therefore, not only the presence of living cells is required for allowing the plant to recover from drought but also their hydraulic connection with the other plant tissues and organs upstream. Thus, even at stem PLC values near to 100% for angiosperms or well above 50% for conifers, a minimal hydraulic connection between the soil and the living tissues could be enough to recover from drought if plants have access to water. More studies focused on the link between xylem hydraulic functioning, plant capacitance and cell mortality are therefore required to identify what the thresholds for tree survival to drought are.

## 5. Conclusion

By combining a living-cell staining process with LVDT sensors and PLC measurements, this study showed that the common thresholds for recovery and point of death considered until now, i.e $P_{50}$ for conifers and $P_{88}$ for angiosperms, are not accurate enough for assessing and predicting drought-induced tree mortality. Indeed, our results showed that trees with PLC levels of 98.6% for *P. lusitanica* (angiosperm) and 67.9% for *P. menziesii* (conifer) were still able to recover from drought once re-watered. Thus, even if the link between a high level of stem PLC and tree mortality is clear, there is an urgent need in defining new physiological thresholds for predicting tree mortality with mechanistic models. For conifers, higher $RWC_{Stem}$ and lower EL values were related to a higher capacity to survive drought. However, this was not the case for angiosperms for which no physiological traits were identified as a potential proxy for the capacity of plant to recover although a similar pattern as to the one observed for the conifer species was identified.

## 6. Author contributions

MM and JMTR conceived and designed the experiment. MM and PEMS were responsible for running the measurements and carried out the data analysis. EB supervised the setting up of the micro-CT scans. MM, PEMS, HC and JMTR interpreted the results. MM wrote the first manuscript draft. JMTR, PEMS, HC and EB assisted substantially with manuscript development.

## 7. Acknowledgement

The authors thank Pierre Conchon and Julien Cartailler for their technical assistance, and the PIAF Research Unit staff for their support during this experiment. This research was funded by the project *ANR-18-CE20-0005 Hydrauleaks.*

## 8. Supplementary data

| Species | Timing | Recovering Capacity | N | Mean PLC | sd | se | ci |
|---|---|---|---|---|---|---|---|
| **(a) *Prunus lusitanica*** | **Control** | - | 5 | 6.90 | 7.74 | 3.46 | 9.61 |
| | **BRW** | - | 8 | 94.44 | 5.59 | 1.98 | 4.67 |
| | BRW | Recovered | 2 | 90.30 | 11.74 | 8.30 | 105.46 |
| | BRW | Dead | 6 | 95.82 | 2.65 | 1.08 | 2.78 |
| **(b) *Pseudotsuga mensiezii*** | **Control** | - | 6 | 7.40 | 6.90 | 2.82 | 7.24 |
| | **BRW** | - | 8 | 79.49 | 10.47 | 3.70 | 8.75 |
| | BRW | Recovered | 1 | 67.92 | *NA* | *NA* | *NA* |
| | BRW | Dead | 7 | 81.14 | 10.12 | 3.82 | 9.36 |

**Table S1.** Table summarizing the evolution of the PLC during the time-course of the experiment in **A** *Prunus lusitanica* and **B** *Pseudotsuga menziesii*.
Control values represent the mean value of the measurements performed before the drought event. BRW represents the measurements performed on the individuals the day of the rehydration.

| Species | Measurement | Timing | Recovering Capacity | N | Value | sd | se | ci |
|---|---|---|---|---|---|---|---|---|
| ***(a) Prunus lusitanica*** | $RWC_{Stem}$ | Control | Control | 8 | 92.33 | 2.20 | 0.78 | 1.84 |
| | $RWC_{Stem}$ | BRW | Recovered | 2 | 58.53 | 2.05 | 1.45 | 18.41 |
| | $RWC_{Stem}$ | BRW | Dead | 6 | 54.73 | 8.80 | 3.59 | 9.24 |
| | $RWC_{Leaf}$ | Control | Control | 8 | 94.84 | 1.49 | 0.53 | 1.25 |
| | $RWC_{Leaf}$ | BRW | Recovered | 2 | 56.87 | 5.74 | 4.06 | 51.55 |
| | $RWC_{Leaf}$ | BRW | Dead | 6 | 59.33 | 11.79 | 4.81 | 12.37 |
| | EL | Control | Control | 8 | 29.85 | 3.69 | 1.30 | 3.08 |
| | EL | BRW | Recovered | 2 | 47.12 | 10.06 | 7.12 | 90.42 |
| | EL | BRW | Dead | 6 | 57.16 | 16.40 | 6.70 | 17.21 |
| ***(b) Pseudotsuga menziesii*** | $RWC_{Stem}$ | Control | Control | 8 | 83.40 | 3.08 | 1.09 | 2.57 |
| | $RWC_{Stem}$ | BRW | Recovered | 1 | 49.82 | *NA* | *NA* | *NA* |
| | $RWC_{Stem}$ | BRW | Dead | 7 | 36.86 | 5.14 | 1.94 | 4.75 |
| | $RWC_{Leaf}$ | Control | Control | 8 | 92.44 | 5.65 | 2.00 | 4.72 |
| | $RWC_{Leaf}$ | BRW | Recovered | 1 | 53.47 | *NA* | *NA* | *NA* |
| | $RWC_{Leaf}$ | BRW | Dead | 7 | 51.47 | 12.43 | 4.70 | 11.49 |
| | EL | Control | Control | 8 | 50.55 | 6.28 | 2.22 | 5.25 |
| | EL | BRW | Recovered | 1 | 50.82 | *NA* | *NA* | *NA* |
| | EL | BRW | Dead | 7 | 78.81 | 5.71 | 2.16 | 5.28 |

**Table S2.** Table summarizing the evolution of the stem relative water content ($RWC_{Stem}$), leaf relative water content ($RWC_{Leaf}$) and electrolytes leakage (EL) during the time-course of the experiment in **A** *Prunus lusitanica* and **B** *Pseudotsuga menziesii*.
Control values represent the mean value of the measurements performed before the drought event. BRW represents the measurements performed on the individuals the day of the rehydration.

| Species | Timing | Recovering capacity | N | %BLC | sd | se | ci |
|---|---|---|---|---|---|---|---|
| *(a) Prunus lusitanica* | Control | - | 2 | 22.96 | 3.42 | 2.42 | 30.75 |
| | BRW | Recovered | 2 | 15.26 | 14.70 | 10.39 | 132.05 |
| | BRW | Dead | 6 | 3.04 | 3.40 | 1.39 | 3.57 |
| *(b)Pseudotsuga menziesii* | Control | - | 6 | 10.21 | 5.25 | 2.14 | 5.51 |
| | BRW | Recovered | 1 | 7.17 | *NA* | *NA* | *NA* |
| | BRW | Dead | 7 | 0.77 | 1.45 | 0.55 | 1.34 |

**Table S3.** Table summarizing the evolution of the percentage of bark living cells (%BLC) during the time-course of the experiment in **A** *Prunus lusitanica* and **B** *Pseudotsuga menziesii*. Control values represent the mean value of the measurements performed before the drought event. BRW represents the measurements performed on the individuals the day of the rehydration.

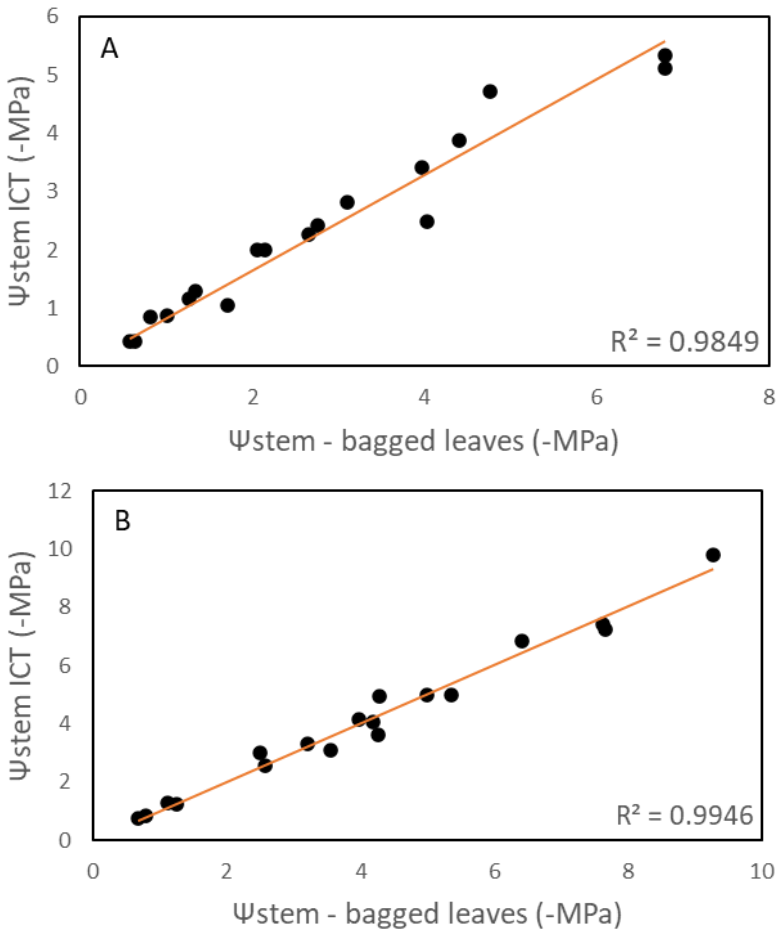


**Figure S1.** Validation of the stem water potential ($\Psi_{stem}$) measurements recorded with psychrometer and compared to the $\Psi_{stem}$ measurements carried out with the Scholander pressure chamber on previously bagged leaves. **A**. for *Prunus lusitanica* and **B.** for *Pseudotsuga menziesii*.

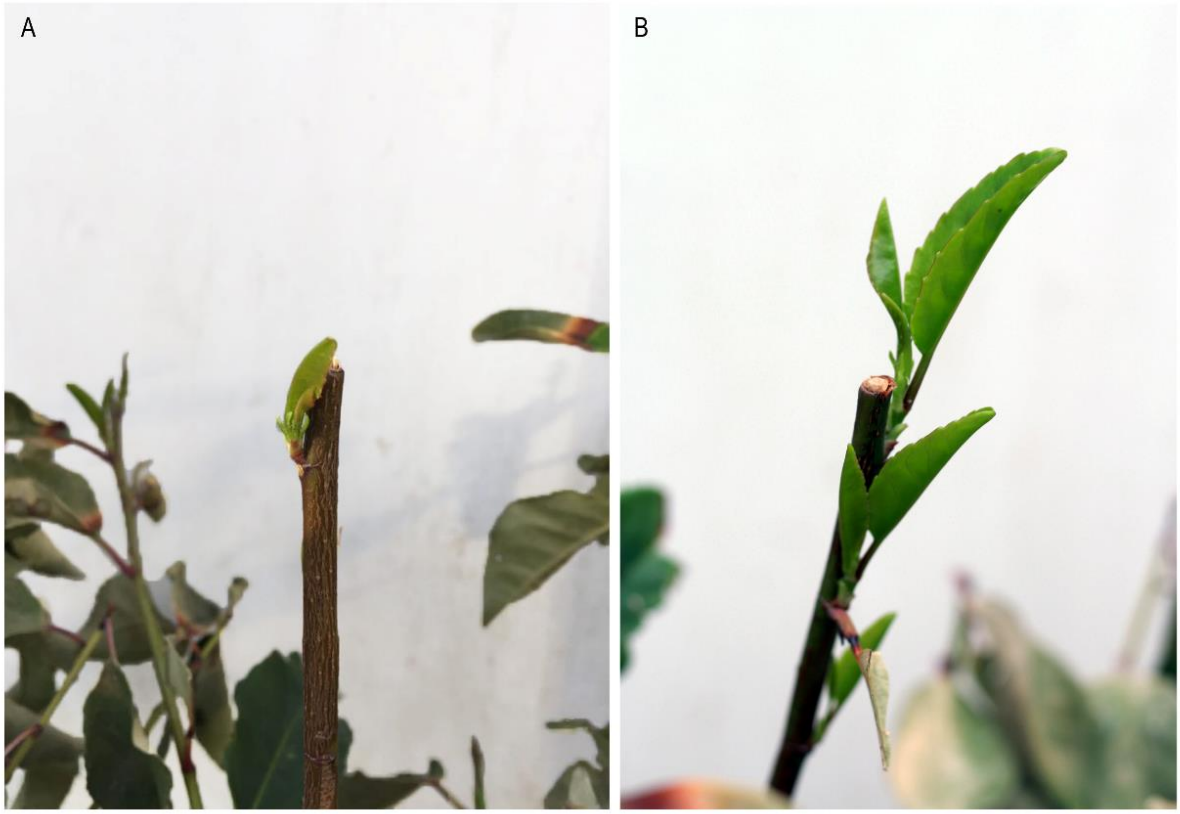


**Figure S2.** Photographs of *Prunus lusitanica* plants flushing new leaves after experimenting a drought event and reaching levels of PLC of 98.6%. **A.** 19 days after re-watering; **B.** 28 days after re-watering.

# 2

# *On the path from xylem hydraulic failure to downstream cell death*

Under many scenarios explaining tree mortality from drought, vascular embolisms are thought to generate water stress by hindering cell water supply, thus provoking their progressive dehydration, altering their metabolism, and finally causing their death by rupture of their plasma membrane. Even though this theoretical trajectory has been largely accepted by the scientific community, its empirical demonstration has almost never been demonstrated. One study from Brodribb *et al.* (2021) has lent this hypothesis some empirical support by focusing on the immediate effect of leaf vein embolism onto cell hydration status and cell photosynthetic activity of tomato mutants. However, they have not directly evaluated the effect of xylem cavitation on cellular integrity and have not demonstrated how the relationship between the loss of xylem conductance and cellular mortality could vary across species.

Therefore, the main objective of this chapter was to elucidate the mechanistic link between xylem hydraulic failure and downstream cell death. Taking into consideration the results from Chapter 1. that demonstrated how the combination of RWC measurements and the evaluation of EL, a measurement of cellular integrity, could be good proxies for plant mortality, we tried to decipher at which level of dehydration cellular integrity would begin to be compromised. Also, we focused on discerning how the loss of hydraulic function due to cavitation and its relationship with cellular death could vary across species with contrasting resistance to cavitation.

# Chapter 2. On the path from xylem hydraulic failure to downstream cell death

SUBMITTED IN *NEW PHYTOLOGIST* ON JULY 5th, 2022

*Authors:*
*Mantova Marylou, Cochard Hervé, Burlett Régis, Delzon Sylvain, King Andrew, Rodriguez-Dominguez Celia M, Ahmed Mutez A., Trueba Santiago, Torres-Ruiz José M.*

**Summary**

***Context and objectives:*** Xylem hydraulic failure has been identified as a ubiquitous factor in triggering drought-induced tree mortality through the damages induced by the progressive dehydration of the plant living cells. However, fundamental evidence of the mechanistic link connecting xylem hydraulic failure to cell death has not been identified yet. The main aim of this study was to evaluate, at the leaf level, the relationship between loss of hydraulic function due to cavitation and cell death under drought conditions and discern how this relationship varied across species with contrasting resistances to cavitation.

***Material and Methods:*** Drought was applied by withholding water on potted seedlings, and their leaves sampled to measure their relative water content (RWC) and cell mortality. Vulnerability curves to cavitation at the leaf level were constructed for each species.

***Results:*** An increment in cavitation events occurrence precedes the onset of cell mortality and more resistant to cavitation species also present a lower critical RWC for cellular death.

***Conclusion:*** Overall, our results indicate that the onset of cellular mortality occurs at lower RWC than the one for cavitation indicating the role of cavitation in triggering cellular death. They also evidenced a critical RWC for cellular death varying with cavitation resistance.

**Key words**

*Drought, cavitation, cell dehydration, membrane leakage, relative water content.*

## 1. Introduction

In the context of the ongoing climate change, the temperature and precipitation patterns are changing in many areas worldwide (IPCC, 2022). Consequently, it has already been reported that the severity of drought episodes is increasing in several areas of the world and is expected to continue to do so in the near future (IPCC, 2022). Climate change which has already shown important consequences on tree survival and forest dieback is therefore expected to dramatically accelerate forest mortality as drought intensity increases (Allen et al., 2010; McDowell et al., 2022).

The mechanisms of tree mortality under drought conditions have been largely evaluated in the last decades and many studies have shown that the impairment of the water transport system leads trees to death through hydraulic failure (Urli et al., 2013; Salmon et al., 2015; Hammond et al., 2019; Mantova et al., 2021). Hydraulic failure occurs under drought conditions when there is an accumulation of emboli within the sapwood past a threshold after which water transport is irrecoverable (McDowell et al., 2022). Even though hydraulic failure has been unequivocally considered as the predominant triggering mechanism for tree death by ecophysiologists and modellers (Anderegg et al., 2015a; Sperry & Love, 2015; Adams et al., 2017; Brodribb et al., 2020; Lemaire et al., 2021), recent studies have shown that the empirically defined percentage loss of conductance (PLC) thresholds, P50 for conifers and P88 for angiosperms, i.e., the water potential value inducing 50% and 88% loss of conductance respectively, were not precise enough when aiming to predict tree response to drought (Hammond et al., 2019; Mantova et al., 2021, 2022). Indeed, trees could recover from water-stress even beyond those PLC thresholds points, i.e., around P80 for conifers (Hammond et al., 2019) and after almost full embolization for angiosperms (Mantova et al., 2021).

Despite McDowell et al. (2008) hypothesizing that hydraulic failure provokes tree mortality by leading to complete desiccation and cellular death, the consequences of hydraulic failure on cellular dehydration per se remain largely unexplored. A single recent study integrating hydraulic failure and cell mortality has shown that vascular network failure in leaves leads to tissues' death (Brodribb et al., 2021). Even though Brodribb et al. (2021) have evinced a strong mechanistic foundation linking xylem network failure and leaf tissue death, the level of PLC at which cellular death occurs and how it varies across species remain unknown. Furthermore, whether cells start to die at the onset of xylem cavitation or whether there is a delay before encountering cell damage remains unclear.

The dysfunction of the water transport system (i.e., the xylem) provoke a significant reduction in the amount of water supplied to trees' living tissues and, consequently, in the water content of all living tissues independently to their function (Kursar et al., 2009). The decrease in relative water content (RWC) at the organ level has been linked with cell membrane disruption and thus cellular death in many studies (Wang et al., 2008; Chaturvedi et al., 2014; Guadagno et al., 2017). These advances at the cellular level have led to a renewed integrative framework linking hydraulic failure and cellular mortality recognizing the relevance of RWC and the level of cell membrane damage as good candidate variables for predicting tree mortality (Mantova et al., 2022). Indeed, RWC presents the advantage of being a metric to which cells respond directly as well as being a direct measurement of the

dehydration state of plant organs. Also, RWC is a valuable water status indicator of cell stress as it represents relative cell volume shrinkage, cell membrane tension and turgor (Zhu, 2016; Sack et al., 2018; Martinez-Vilalta et al., 2019; Sapes et al., 2019). Some empirical evidence has shown that the leaf RWC at turgor loss point (TLP) was relatively high and constant across species compared to the leaf water potential at TLP (Bartlett et al., 2012). Therefore, a relatively constant measure of water status under mild drought conditions should be at risk of significant changes under severe dehydration preceding death (Martinez-Vilalta et al., 2019). Thus, RWC could serve as a potential candidate to define a dehydration threshold (inflection point) below which cells start to suffer from water stress and, as a result, plants may become weakened in their ability to recover from drought (Martinez-Vilalta et al., 2019).

Following initial cavitation, leaves show conjoint changes in leaf colour, and increases in the rate of leaf shrinkage due to the rapid dehydration of the mesophyll downstream (Brodribb et al., 2021). These changes in leaf colour have been attributed to the loss of turgor and the collapse of the palisade cells which decrease the distance between cells, thereby decreasing the light transmittance (Brodribb et al., 2021). However, even though mesophyll dehydration should be associated with structural changes occurring at leaf tissue level and could also be responsible for cellular death (Mantova et al., 2022), it has not been described yet if cells mortality is a consequence of cell cavitation (Rajashekar & Lafta, 1996; Sakes et al., 2016) or collapse and cytorrhysis (Oertli, 1986).

Considering the actual need to understand the underlying processes connecting hydraulic failure and tree mortality (Mantova et al., 2022), the main aims of this study are to (i) evaluate whether the water transport impairment through cavitation is the triggering factor causing cell death under drought conditions, (ii) study whether the relationship between cavitation occurrence and cell death varies across species with contrasted resistances to drought and, (iii) identify a RWC threshold inducing plant cells damage from drought. We worked at the leaf level to elucidate the causal link between a decreasing water supply, caused by xylem cavitation, the decrease in leaf RWC (RWCLeaf) and cell mortality. For this, we investigated three different species having contrasted cavitation resistance: Eucalyptus viminalis, Laurus nobilis and Populus tremula x alba. We exposed individuals of each species to severe drought conditions, and, during the dehydration process, we monitored their water status via the measurement of the leaf water potential (ΨLeaf) and RWCLeaf. During leaf dehydration, we assessed cell vitality using the electrolytes leakage (EL) approach. We also performed synchrotron-based micro-CT to anatomically visualise the consequences of a decreasing water supply on the different leaf tissues and decipher the sequence of events leading to cell death. This approach gave us the opportunity to test the connection between cavitation and cell damages in leaves.

## 2. Material and methods

### *2.1.Plant material and experimental setup*

The experiments were carried out in three tree species: *Eucalyptus viminalis* Labill, *Laurus nobilis* L. and *Populus tremula x alba* (clone INRA 717-1B4), from February to September 2020 (Figure 40). For each species, trees were grown under non-limiting water conditions in 9.2L, 7.5L and 4L pots respectively, at the INRAe PIAF research station of Clermont-Ferrand, France (45877'N, 3814'E) for *E. viminalis* and *P. tremula x alba* and in Les Chères, France (45908'N, 4732'E) for *L. nobilis*. *E. viminalis* trees were three years-old at the time of the experiment while *L. nobilis* individuals were two-years old and *P. tremula x alba* trees were six-months old. For each species, between 6 and 11 plants were exposed to a progressive and total bench dehydration by withholding irrigation.


**Figure 40.** Plant material used for the experiment.
**(a)** *Eucalyptus viminalis,*
**(b)** *Laurus nobilis and*
**(c)** *Populus tremula x alba.*

## 2.2.Leaf physiological traits

### 2.2.1. Pressure volume curves

Pressure-Volume (PV) curves provide information about turgor pressure, osmotic pressure and elastic properties of cells and how these parameters change with cell water content during water stress. PV curves were produced on six leaves per species and the turgor loss point (TLP) (expressed in MPa: $\Psi_{TLP}$ or in percentage of RWC: $RWC_{TLP}$) and modulus of elasticity (ε) were determined according to standard methods for each species (Sack *et al.*, 2010). Briefly, leaves were rehydrated overnight by soaking the leaf petiole in distilled water. $\Psi_{Leaf}$ was measured with a Scholander-type pressure chamber (PMS, Corvallis, Oregon, USA), following precautions and recommendations by Rodriguez-Dominguez *et al.* (2022) while the weight was measured with a balance (METTLER AE 260, DeltaRange ®) along the course of the experiment (13-15 times a day). The leaf dry mass was determined after drying the leaves at 70°C for 3 days.

### 2.2.2. Vulnerability curves to cavitation

Leaf vulnerability to cavitation was assessed using the optical method (Brodribb *et al.*, 2016) in 6 to 8 trees per species. Based on the principle that light interacts differently with xylem that is water filled or air filled, it is possible to compare the quantitative differences in brightness caused by cavitation events between consecutive images and generate vulnerability curves over the decreasing water potential. Briefly, two leaves per individuals and species were installed on a scanner (V800 perfection, Epson, Japan), for *E. viminalis* (Figure 41A), or on clamps equipped with a camera (http://www.opensourceov.org/), for *L. nobilis* and *P. tremula x alba* (Figure 41B, C), and images were taken, using transmitted light to illuminate them, every five minutes during the dehydration process. For both methods, image sequences were then analysed manually according to Brodribb *et al.* (2016, 2017). Briefly, embolism formation can be identified and quantified by subtracting consecutive images as changes in the grey level associated with vascular tissue. Thus, the percentage of embolised area for each image was calculated as the amount of embolism cumulated and the total embolised area of the scanned area.

The vulnerability curves to cavitation were obtained by plotting the leaf water potential ($\Psi_{leaf}$) measured regularly, i.e., once or twice a day depending on the dehydration rate of the tree, in three different neighbour leaves using a Scholander-type pressure chamber (PMS, Corvallis, Oregon, USA), against the percentage of embolized pixels (PEP: % of total). $P_{50}$ (the $\Psi_{leaf}$ value at which 50% of the xylem cavitation events had been observed) was determined by fitting a sigmoid using the equation (10) (Pammenter & Vander Willigen, 1998) where *a* is the slope of the curve at the inflection point:

$$(10)\ PEP = \frac{100}{(1 + e^{(a(\psi leaf - P50))})}$$

$\Psi_{leaf}$ values inducing 50%, 12% and 88% of xylem cavitation (i.e., $P_{50}$, $P_{12}$ and $P_{88}$ respectively) were computed using the R '*fitPLC*' package (Duursma & Choat, 2017).


**Figure 41.** Plant bench dehydration and installation of the optical method. **A.** *Eucalyptus viminalis* tree installed on a scanner. **B.** Clamp with a camera installed on *Laurus nobil*is leaf. **C.** Bench dehydration of a *Populus tremula x alba* sapling equipped with a camera.

### 2.2.3. *Water status, Leaf Relative Water Content and Electrolytes leakage*

Over the progressive bench dehydration of each individual, regular samplings of 3 to 5 leaves (depending on leaf material availability) were carried out for assessing the water status and cellular integrity of each individual. Briefly, $\Psi_{Leaf}$, leaf relative water content ($RWC_{Leaf}$) and leaf cellular integrity through the percentage of electrolytes leakage (EL) were measured on those leaves (Figure 42).

$\Psi_{Leaf}$ was measured using a Scholander-type pressure chamber (PMS, Corvallis, Oregon, USA) while $RWC_{Leaf}$ was measured and calculated according Barrs & Weatherley, (1962). Briefly, for $RWC_{Leaf}$, leaves were cut and immediately placed in a vial to prevent further desiccation. $RWC_{Leaf}$ was then calculated according to (6):

$$(6)\ RWC = \frac{(FW-DW)}{(TW-DW)},$$

where FW is the fresh weight measured immediately after sampling; TW is the turgid weight measured after immersing the leaf in distilled water for 24 hours; and DW is the dry weight of samples after 24 hours of drying in an oven at 70°C. All measurements were done using a precision scale (METTLER ME 204, DeltaRange ®).

EL was measured using an adapted protocol of the original EL protocol of Zhang & Willison, (1987) and Sutinen *et al.* (1992). Each leaf was cut in 1mm slices using a pair of scissors and immersed in test tubes containing 15mL of pure water. Test tubes were shaken at 60 shakes/min overnight at 5°C to stop enzyme activity. Water conductivity of the effusate (C1) was then measured at room temperature (ca. 22°C) using a conductimeter (Seven compact S230, Metter Toledo) and a sensor with a measuring range of 0.001-500µS/cm (Cell Cond InLab 741, Metter Toledo). After C1 measurement, all living cells were killed by autoclaving the samples at 121°C for 30minutes (King & Ludford, 1983). Measurement of the effusate maximal conductivity (C2) was then done at room temperature. The EL was then determined as (8):

$$(8)\ EL = \frac{C1}{C2} * 100$$

EL values were normalised in between 0 and 100 to define a minimum and maximum level of cellular damage by using the mean value of the 10 lowest points and the 10 maximum points.

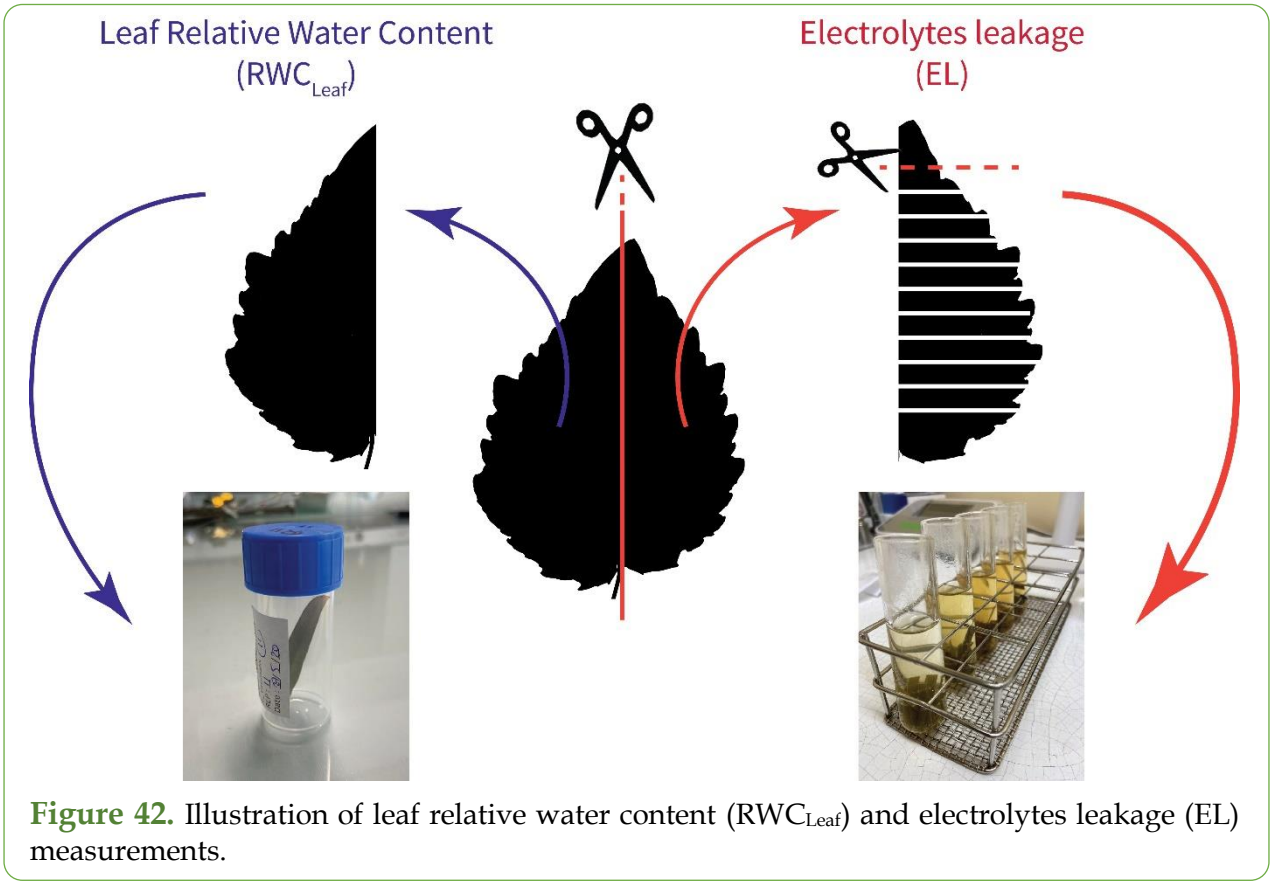


**Figure 42.** Illustration of leaf relative water content ($RWC_{Leaf}$) and electrolytes leakage (EL) measurements.

### 2.2.4. *Cavitation and cellular death dynamics regarding cellular water stress: non-linear regressions and sigmoid parameters*

The images obtained with the optical method for determining the leaf vulnerability curve to cavitation were reused to determine the level of embolism over the decrease in $RWC_{Leaf}$. Using the $RWC_{Leaf}$ data previously collected and a linear regression in phases, we calculated the $RWC_{Leaf}$ for each individual and associated each image to a $RWC_{Leaf}$ value. We then plotted the $RWC_{Leaf}$ against PEP for 6 to 8 individuals per species. The $RWC_{50}$ (the $RWC_{Leaf}$ value at which 50% of the xylem cavitation events had been observed) was determined by fitting a sigmoid using equation (11) (Pammenter & Vander Willigen, 1998) where *a* is the slope of the curve at the inflection point:

$$(11)\ PEP = \frac{100}{(1 + e^{(a(RWCLeaf - RWC50))})}$$

By analogy to the $P_{12}$ and $P_{88}$ points, $RWC_{12}$ and $RWC_{88}$ representing the $RWC_{Leaf}$ value associated with 12% and 88% loss of hydraulic conductance were computed using the '*fitPLC*' R package (Duursma & Choat, 2017) replacing the $\Psi_{Leaf}$ inputs with the $RWC_{Leaf}$ values (Figure 43).

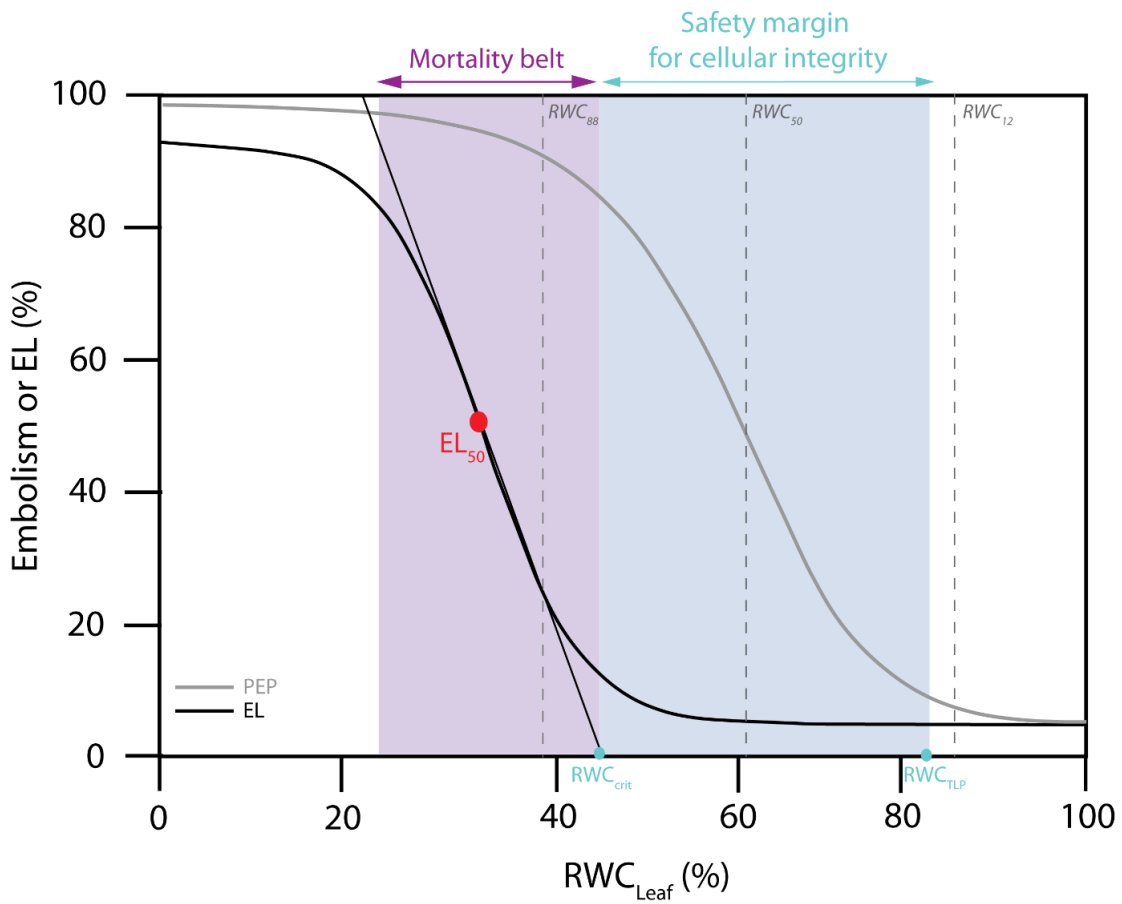


**Figure 43.** Conceptual figure representing, in light blue, the safety margin to cellular integrity in between the leaf relative water content at turgor loss ($RWC_{TLP}$) and the critical leaf RWC ($RWC_{crit}$) and in purple the mortality belt defined through the slope of the tangent of the EL regression at the midpoint ($EL_{50}$). Dashed grey lines represent the RWC values at which 12% ($RWC_{12}$), 50% ($RWC_{50}$) and 88% ($RWC_{88}$) of the vessels are embolized.

In order to visualize the dynamic of cell damage as the $RWC_{Leaf}$ decreased, the percentage of EL was plotted against $RWC_{Leaf}$ for each species. A non-linear regression (NLS), four parameter logistic regression, was fitted using SigmaPlot with the following equation (12):

$$(12)\ NLS = min + \frac{(max-min)}{1+\frac{x}{EL50}^{-Hillslope}}$$

Where $EL_{50}$ represents the $RWC_{Leaf}$ value at which 50% of the cells are dead, *max* and *min* represent the maximum and minimum EL value of the dataset and *Hillslope* the slope of the regression at the inflection point.

From this NLS fitting was extracted the critical level of RWC ($RWC_{crit}$) below which the cells start to incur damages from water stress. By analogy to the air entry pressure defined by Meinzer et al. (2009) and Torres-Ruiz et al. (2017), the $RWC_{crit}$ was determined at the x-intercept of the tangent through the midpoint ($EL_{50}$) of the NLS regression curve and corresponded to 12% of cell damages (Figure 43). The slope of the regression was used to determine the 'Mortality Belt' (Figure 43) i.e., the range in which the decrease in $RWC_{Leaf}$ provokes the maximum cell damage. Combining the EL NLS fitting and the leaf material properties, we calculated, for each species, a safety margin for cellular integrity in between $RWC_{TLP}$ and $RWC_{crit}$ (Figure 43). $RWC_{TLP}$ was used as the starting point of the safety margin for cellular integrity, serving as a proxy for stomatal closure and corresponding to the point where there is a reduction of water losses that prevents an important decrease in RWC.

### *2.3.X-ray micro-CT anatomical analyses*

Synchrotron-based x-ray micro-CT was used to visualize the shape of the cells within the leaf blade of the three studied species at different RWC. 15 leaves sampled from 10 *E. viminalis* individuals, 16 leaves from eight *L. nobilis* individuals and 10 leaves from six *P. tremula x* alba individuals were scanned between September 8 and September 14, 2020, at the French synchrotron facility SOLEIL (Paris, France) using the micro-CT PSICHE beamline (Figure 44). Two weeks before the scans, irrigation was withheld progressively in the different trees in order to generate a wide range of $\Psi_{Leaf}$ and $RWC_{Leaf}$ at the time of scanning.

The leaf of interest was scanned using a high-flux (3.1011 photons $mm^{-2}$) 25-KeV monochromatic X-ray beam. The projections were recorded with a Hamamatsu Orca Flash sCMOS camera equipped with a 250-lm-thick LuAG scintillator and visible light optics providing an effective pixel size of 0.3 µm. The complete tomographic scan included 2048 projections, 50 ms each, for a 180° rotation. Samples were exposed for 75 s to the X-ray beam. Tomographic reconstructions were performed using PyHST2 software (Mirone *et al.*, 2014) employing the method of Paganin (2006). Each leaf scan led to a volume of 2048 images. For each species, three images were extracted from the volumes of five (*E. viminalis*; *L. nobilis*) or six (*P. tremula x alba*) samples and were analysed using *Fiji* software (Schindelin *et al.*, 2012). The different leaf tissues, i.e., epidermis, palisade parenchyma, spongy parenchyma, were outlined in 5 slices per stack using the freehand selection tools and their area determined in $\mu m^2$ using the measuring tool of *Fiji* (Schindelin *et al.*, 2012).

At the same time of the scan, three leaves located next to the scanned leaf were used to measure $\Psi_{Leaf}$ with a Scholander-type pressure chamber (Precis 2000, Gradignan, France). Three other nearby leaves were used to determine the $RWC_{Leaf}$ and three others were used to determine the EL.

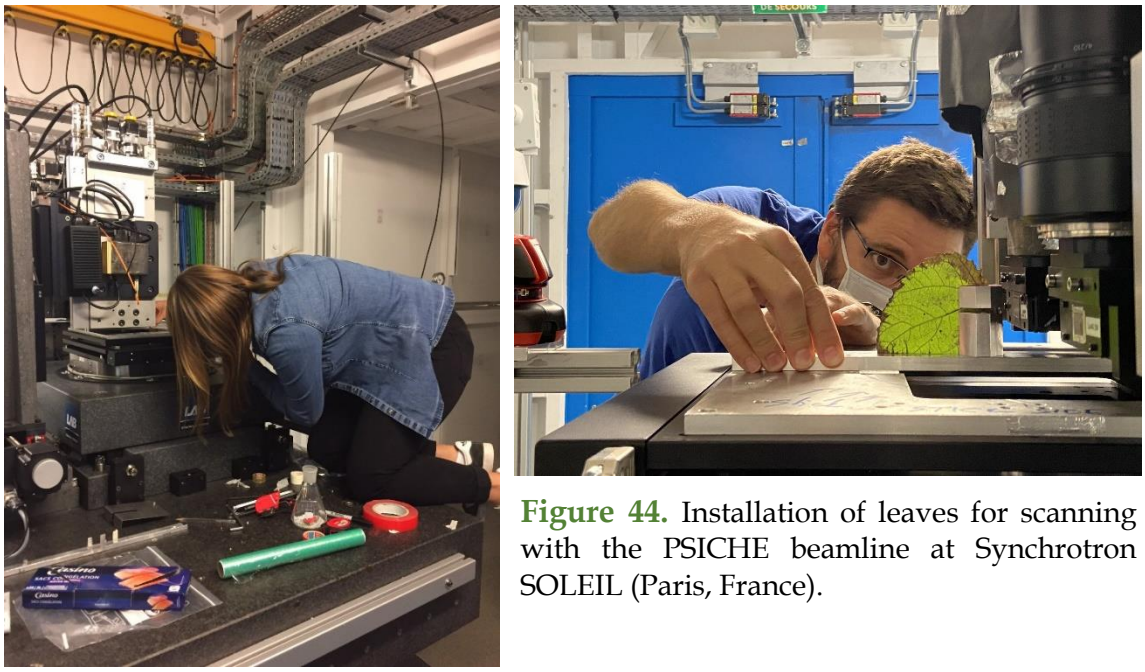

**Figure 44.** Installation of leaves for scanning with the PSICHE beamline at Synchrotron SOLEIL (Paris, France).

### *2.4.Measurements of leaf light transmittance*

During the experiments allowing to generate the vulnerability curves to cavitation, obvious colour changes occurred. In the 8-bit image stacks, these changes could be detected as a darkening of the leaf tissue and thus the stack of images were used to monitor changes in greyscale (Brodribb *et al.*, 2021). For this, using *Fiji* software (Schindelin *et al.*, 2012) and the command "measure stack" from the OSOV toolbox we measured the grey mean value for each image of the stack. The loss in light transmittance was then calculated as the percentage of maximum.

A second noticeable change in leaf colour (i.e., blackening), more intense than the darkening observed along the dehydration was noticed after full embolization of the vessels at very low $RWC_{Leaf}$ and started at the edges of the leaf. Therefore, measurements of the leaf light transmittance were made in the visibly different regions of the leaf. Considering this, synchrotron-based x-ray micro-CT scans were performed on the different regions of the leaf, i.e., in a section with a high light transmittance and in a section with a low light transmittance, allowing distinction of anatomical changes.

## 3. Results

### *3.1.Turgor loss point and leaf resistance to cavitation*

PV curves (Figure S3) allowed determining both TLP and ε for each species. $\Psi_{TLP}$ occurred at -1.31MPa for *P. tremula x alba*, -1.61MPa for *E. viminalis* and -2.46MPa for *L. nobilis* corresponding to $RWC_{TLP}$ values of 89.04%, 88.05% and 90.65%, respectively (Table 1). ε was of 11.39MPa, 10.22MPa and 15.56MPa for *P. tremula x alba*, *E. viminalis* and *L. nobilis* respectively (Table 1). Xylem vulnerability curves (Figure S4) resulted in $P_{50}$ values of -1.96MPa, -3.23MPa and -5.17MPa for *P. tremula x alba*, *E. viminalis* and *L. nobilis* respectively (Table 1).

| Parameter | *P. tremula x alba* | *E. viminalis* | *L. nobilis* |
|---|---|---|---|
| $\Psi_{TLP}$ (MPa) | -1.33 | -1.61 | -2.46 |
| $RWC_{TLP}$ (%) | 89.04 | 88.05 | 90.65 |
| ε (MPa) | 11.39 | 10.22 | 15.56 |
| $P_{12}$ (MPa) | -1.05 | -2.28 | -2.95 |
| $P_{50}$ (MPa) | -1.96 | -3.23 | -5.17 |
| $P_{88}$ (MPa) | -2.88 | -4.17 | -7.39 |
| $RWC_{12}$ (%) | 80.95 | 77.74 | 63.01 |
| $RWC_{50}$ (%) | 61.66 | 60.99 | 51.40 |
| $RWC_{88}$ (%) | 42.38 | 44.24 | 39.80 |
| $\Psi_{crit}$ | -0.97 | -2.81 | -3.27 |
| $RWC_{crit}$ (%) | 70.39 | 58.41 | 55.50 |
| Safety margin (%RWC) | 18.65 | 29.64 | 35.15 |
| $EL_{50}$ (Mpa) | -2.68 | -6.15 | -5.95 |
| $EL_{50}$ (%RWC) | 48.05 | 40.08 | 36.91 |
| $EL_{max}$ (%RWC) | 25.15 | 23.83 | 18.13 |
| Slope NLS | -4.37±0.99 | -5.21±0.60 | -3.79±0.99 |

**Table 1.** Parameters extracted for each species.
$\Psi_{TLP}$ and $RWC_{TLP}$ represent, respectively, the water potential and relative water content (RWC) value at turgor loss point. ε represents the cell modulus of elasticity. $P_{12}$, $P_{50}$ and $P_{88}$ correspond to the water potential value inducing 12%, 50% and 88% of loss of xylem hydraulic conductance respectively. $RWC_{12}$, $RWC_{50}$, $RWC_{88}$ represent the RWC value encountered at 12%, 50% and 88% of loss of xylem hydraulic conductance respectively. $\Psi_{crit}$ and $RWC_{crit}$ symbolize the water potential and RWC values at which cell integrity begins to be compromised by dehydration. The safety margin designates the decrease between the leaf $RWC_{TLP}$ and $RWC_{crit}$. $EL_{50}$ represent the water potential value or RWC value at which 50% of cell damages is encountered. $EL_{max}$ designate the RWC value at which 100% of cell damages is encountered. Slope NLS corresponds to the slope of the regression and represents the rate of cellular mortality.

### 3.2.Dying of thirst?

On the observed sigmoidal opposed dynamics for $RWC_{Leaf}$ and the percentage of embolism during dehydration (Figure 45) three different phases could be distinguished for each species. A first phase between the maximal $RWC_{Leaf}$ at $\Psi_{leaf}$ values of ca. 0MPa and $\Psi_{TLP}$ where $RWC_{Leaf}$ diminished slowly and the amount of embolism remains close to zero; a second phase after reaching the $\Psi_{TLP}$ concomitant to a significant increase in embolism until $P_{88}$ where the $RWC_{Leaf}$ decreased exponentially; and a third phase after hydraulic failure ($P_{88}$) where only residual losses of water occurred and $RWC_{Leaf}$ decreased slightly until reaching a steady state. During the first phase, a decrease in $RWC_{Leaf}$ of ca. 22% for *P. tremula x alba* and of c.a. 10% for *E. viminalis* and *L. nobilis* were observed. Therefore, at $\Psi_{TLP}$, embolism levels of 20.3%, 3.1% and 7.9% were observed for *P. tremula x alba*, *E. viminalis* and *L. nobilis* respectively. During the second phase, as the level of embolism reached 88%, $RWC_{Leaf}$ decreased from 75.8% to 45.6% for *P. tremula x alba*, from 83.2% to 51.1% for *E. viminalis* and from 77.9% to 28.3% for *L. nobilis*. During the third phase, i.e., after reaching $P_{88}$, $RWC_{Leaf}$ continued to decrease until reaching a RWC steady state of ca. 20% for *P. tremula x alba* and *L. nobilis* and of ca. 35% for *E. viminalis*.

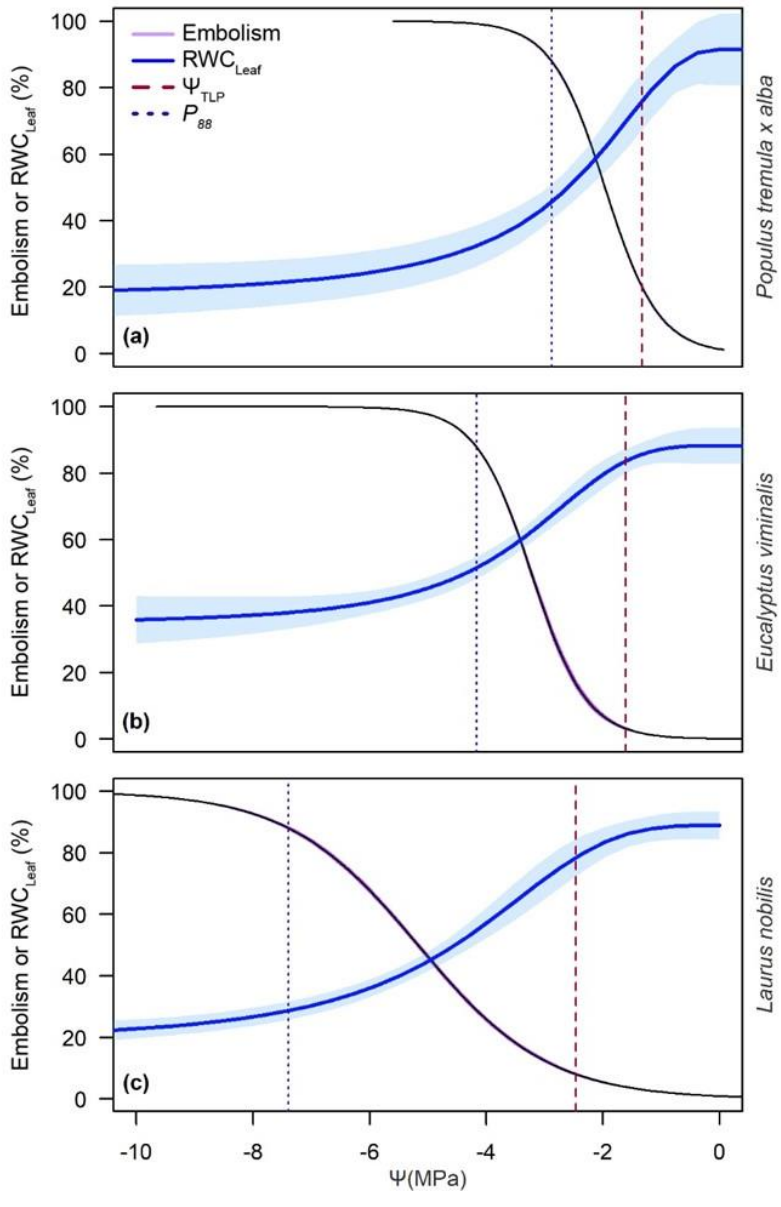


**Figure 45.** Dynamic of embolism and leaf relative water content ($RWC_{Leaf}$) regarding a decrease in water potential (Ψ) for **(a)** *Populus tremula x alba*, **(b)** *Eucalyptus viminalis* and **(c)** *Laurus nobilis*. 95% confidence intervals are represented by shading.

### 3.3. *Cavitate first, die after?*

When combining together leaf physiological traits, embolism and EL versus $RWC_{Leaf}$ (Figure 46), our results clearly showed that cavitation events occurred at higher RWC values than the onset of cell damages. Indeed, $RWC_{12}$ was constantly higher than $RWC_{crit}$ (Table 1, Figure 46). The decreases in RWC between the onset of cavitation and the onset of cell damages were estimated as 10.56% for *P. tremula x alba*, 19.33% for *E. viminalis* and 7.51% for *L. nobilis*.

For the three species, higher embolism levels than EL (Figure 46) were found at any $RWC_{Leaf}$ value. Consequently, for a level of embolism equal to 50%, the levels of EL were of 24.23% for *P. tremula x alba,* 13.52% for *E. viminalis* and 24.24% for *L. nobilis*. Also, at a percentage of embolism equal to 88%, *P. tremula x alba* showed an EL level of 63.89%, *E. viminalis* an EL level of 39.05% and *L. nobilis* an EL level of 43.37%. $EL_{50}$ was observed at varying embolism degrees of 80.15%, 92.14% and 92.12% for *P. tremula x alba*, *E. viminalis* and *L. nobilis* respectively. The maximum level of cell damages ($EL_{max}$) was always subsequent to a 100% amount of embolism for all species.

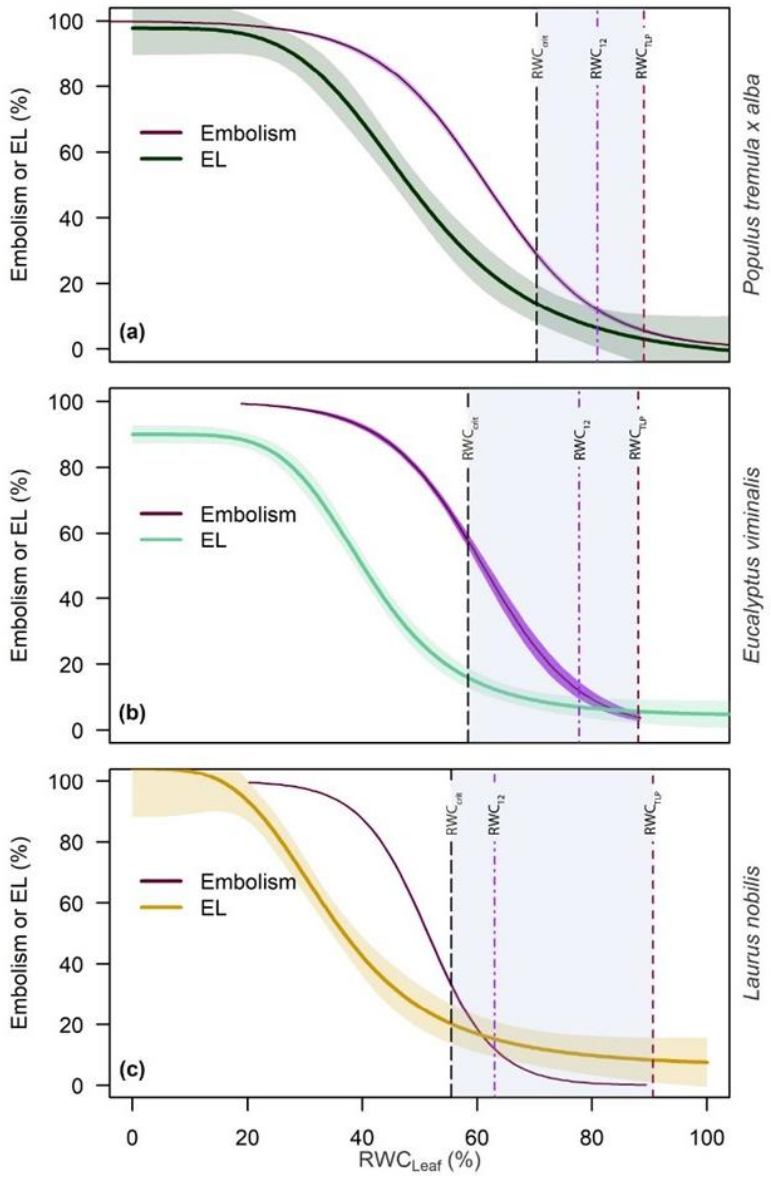


**Figure 46.** Dynamic of embolism and cellular damages (EL) regarding a decrease in leaf relative water content ($RWC_{Leaf}$) for **(a)** *Populus tremula x alba*, **(b)** *Eucalyptus viminalis* and **(c)** *Laurus nobilis*. Blue shaded areas represent the safety margin for cellular integrity calculated between the RWC at turgor loss point ($RWC_{TLP}$) and the critical RWC for cellular integrity ($RWC_{crit}$). 95% confidence intervals are represented by shading.

### 3.4.A more drought-resistant xylem, more resistant cells?

When comparing $RWC_{crit}$ and $P_{50}$, it is observed that more cavitation-resistant species are also able to withstand a higher loss in RWC before suffering cell damages (Figure 47). Thus, *P. tremula x alba* which had reported the lowest resistance to cavitation ($P_{50}$ = -1.96 MPa) also presented the highest $RWC_{crit}$ (70.39%) making its cells the least resistant to dehydration. On the contrary, *L. nobilis* showed the highest resistance to cavitation ($P_{50}$ = -5.17 MPa) and, at the same time the lowest $RWC_{crit}$ (55.50%). *E. viminalis*, which has a $P_{50}$ of -3.24 MPa, presented a $RWC_{crit}$ of 58.41%. However, when calculating a safety margin for cell integrity in between $RWC_{TLP}$ and $RWC_{crit}$, the species' resistance to cavitation and their safety margin to cellular damages were not correlated. *E. viminalis* and *L. nobilis* presented similar safety margins whereas *P. tremula x alba* presented a much narrower one (Figure 46; Table 1).

$EL_{50}$ corresponded to a $RWC_{Leaf}$ value of 48.05%, 40.08% and 36.91% for *P. tremula x alba*, *E. viminalis* and *L. nobilis* respectively. $EL_{50}$ was also consistently found at lower $RWC_{Leaf}$ values in species presenting a higher xylem resistance to cavitation, i.e., lower $P_{50}$.

By looking at the dynamics of cell damages when $RWC_{Leaf}$ went below the $RWC_{crit}$, the rate of cell damages showed no differences between species since there were no differences when comparing the slope of the NLS regressions (Table 1).

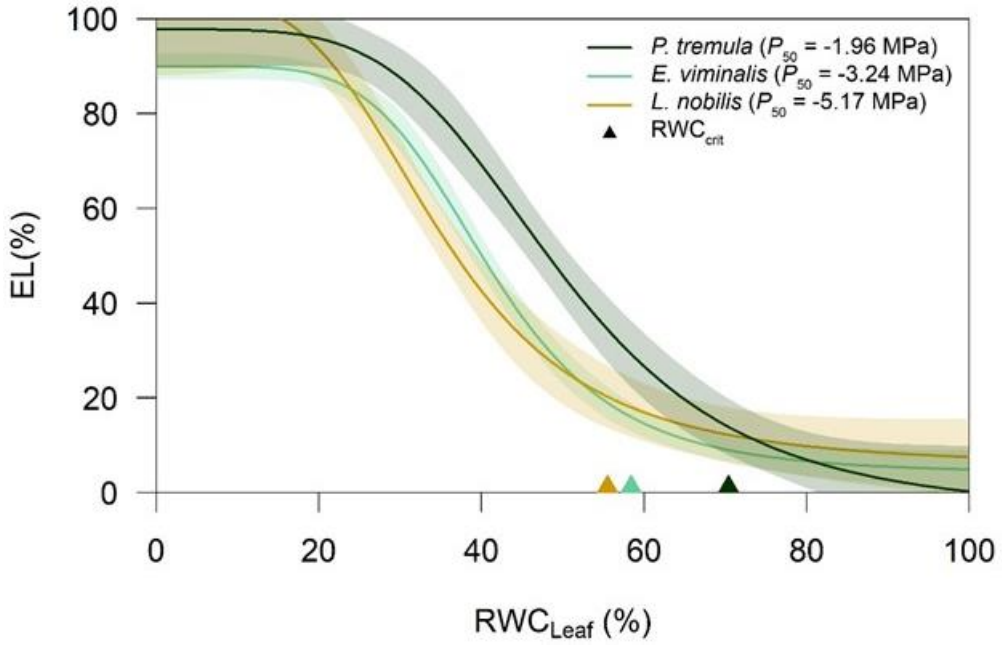


**Figure 47.** Dynamic of cellular damages (EL) regarding leaf relative water content ($RWC_{Leaf}$). Triangles represent the $RWC_{crit}$ identified for each species. 95% confidence intervals are represented by shading.

### 3.5.How to die? X-ray insights

X-ray micro-CT imaging revealed anatomical changes as $RWC_{Leaf}$ decreased and EL increased, with the more evident changes occurring at the mesophyll level (Figure 48). Through the course of dehydration, the mesophyll area was reduced by a factor of 2.95 for *P. tremula x alba*, whereas the reduction in epidermis area was only of 1.70. The same pattern was observed for both *E. viminalis* and *L. nobilis*, which presented a mesophyll area reduction of

2.09 and 1.81 respectively. However, while *E. viminalis* showed a reduction of its epidermis area of 1.47, no changes were observed for *L. nobilis*.

The first mesophyll structural changes under decreasing $RWC_{Leaf}$ occurred at the palisade layer for both *P. tremula x alba* and *L. nobilis* (Figure 48 and Figure 49). However, a different pattern was observed for *E. viminalis* with, first, a conjoint dehydration of the spongy and palisade parenchyma (Figure 48 and Figure 49). In a second time, as the $RWC_{Leaf}$ continued decreasing, main anatomical changes were observed in the spongy parenchyma which showed an important reduction of the cells area for the three species (Figure 48 and Figure 49). Ultimately, and only in the case of *L. nobilis*, a secondary conjoint reduction of the palisade and spongy areas happened.

Leaves of all three species visually became darker as the $RWC_{Leaf}$ decreased. Concomitantly to the decrease in $RWC_{Leaf}$, and after a significant reduction in cell area occurred at the different cells' layers, leaf light transmittance dropped. The start of the loss in leaf light transmittance was synchronized with the start of the increase in EL for all three species. For *P. tremula x alba* and *L. nobilis*, the loss in light transmittance was synchronized with the full dynamic of EL (Figure 48a and c). However, for *E. viminalis*, the maximum loss in light transmittance was attained before reaching the maximum level of EL (Figure 48b).

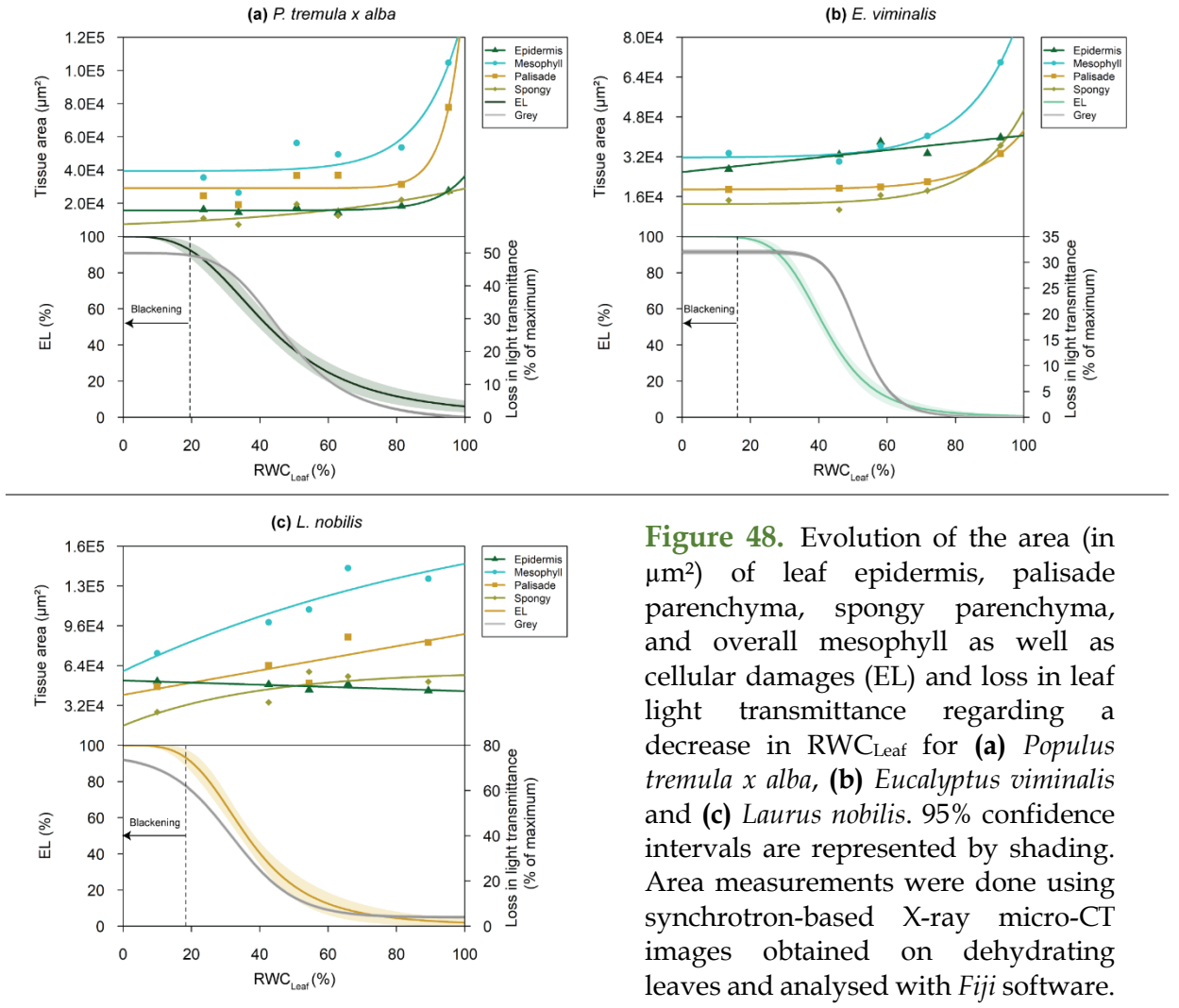


**Figure 48.** Evolution of the area (in µm²) of leaf epidermis, palisade parenchyma, spongy parenchyma, and overall mesophyll as well as cellular damages (EL) and loss in leaf light transmittance regarding a decrease in $RWC_{Leaf}$ for **(a)** *Populus tremula x alba*, **(b)** *Eucalyptus viminalis* and **(c)** *Laurus nobilis*. 95% confidence intervals are represented by shading. Area measurements were done using synchrotron-based X-ray micro-CT images obtained on dehydrating leaves and analysed with *Fiji* software.

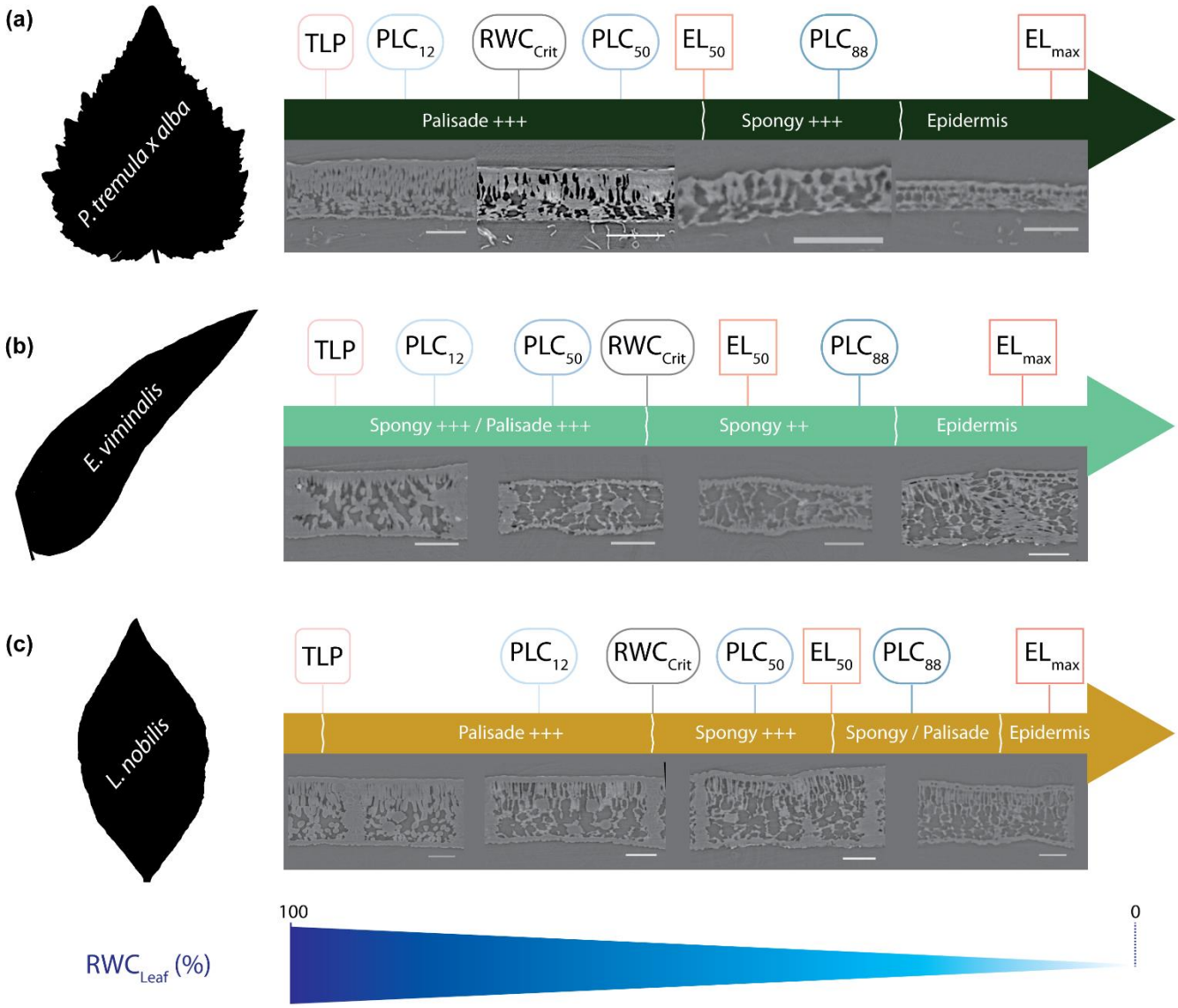


**Figure 49.** Sequence of events, and corresponding synchrotron-based x-ray microCT images, leading to maximal cellular death ($EL_{max}$) regarding a decrease in leaf relative water content ($RWC_{Leaf}$) for **(a)** *Populus tremula x alba*, **(b)** *Eucalyptus viminalis* and **(c)** *Laurus nobilis*.
Scales bars represent 100µm.

After full embolization of the leaf veins, an abrupt blackening easily detectable by the naked eye occurred within the leaf (Figure 50a; Figure S5). Synchrotron-based x-ray micro-CT scans were performed within a single leaf at different locations presenting differences in light transmittance values (Figure 50 a and b**;** Figure S5) and showed that epidermis cells became air-filled (Figure 50c; Figure S5).

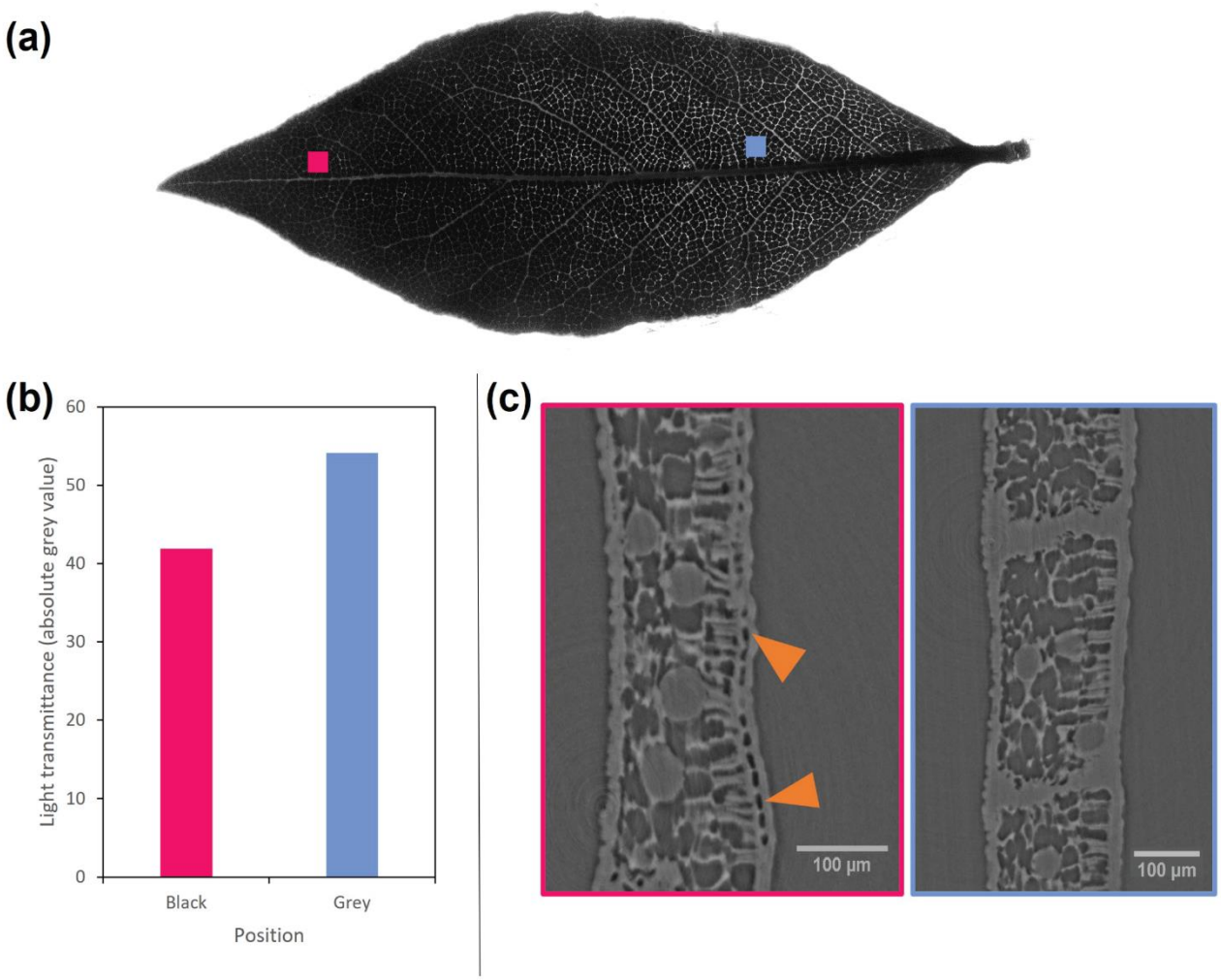


**Figure 50.** Damages at the epidermis level after full embolization of the xylem vessels for *Laurus nobilis*.
**(a)** Scan of a *L. nobilis* leaf ($RWC_{Leaf}$=19.59%, EL=84.49%) obtained in transmitted light. Leaf light transmittance differs within the leaf at the positions marked in red and blue.
**(b)** Measurements of the light transmittance in absolute grey value performed with Fiji software at the respective red and blue positions.
**(c)** Synchrotron-based X-ray micro-CT images obtained on the same *L. nobilis* leaf. The position of each scan is indicated by either the blue or red rectangles on the transmitted light image (a). Orange triangles point at the epidermis cells and indicate the structural changes observed.

## 4. Discussion

### *4.1.Cavitate first, die after!*

Our results evince that, during the progressive dehydration of trees, xylem cavitation precedes the cellular death at the leaf level. Indeed, the onset of cells dehydration-induced damages happens at lower $RWC_{Leaf}$ values than the ones at which the onset of xylem cavitation occurred. In addition, $RWC_{crit}$, the critical water status level inducing cell damage, occurred at varying embolism levels depending on the species (of c.a. 30% for *P. tremula x alba* and *L. nobilis,* and c.a. 58% for *E. viminalis)*. Considering this, our results show that by compromising water delivery to the leaf mesophyll, cavitation provokes a decrease in $RWC_{Leaf}$ that is followed by an increase in cellular damage. These results agree with a recent study on tomato mutants showing that leaf veins cavitation immediately compromised local water supply to the leaf mesophyll enrolling the tissues to death (Brodribb *et al.*, 2021). However, when evaluating such compromise at the whole leaf level, our results suggest that low levels of embolised vessels have no immediate effect on the amount of living cells probably due to higher tolerance to hydraulic disruption provided by the vascular redundancy of the leaves (Sack *et al.*, 2008). Indeed, despite the important variation in cell volume observed at the onset of dehydration when trees still show relatively high values of $RWC_{Leaf}$, no events of cell mortality were encountered.

### *4.2.Different species, different cell death dynamic?*

During dehydration, leaves first showed a significant loss in turgor pressure followed by a progressive cavitation of the leaf veins preceding the appearance of the first cellular structural damages. The $RWC_{Leaf}$ values at which these three processes occur and the differences between them could vary across species according to their resistance to drought. This sequence of events is consistent with the findings of Creek *et al.* (2020) where stomatal closure, which typically occurs at water potential values similar to those for turgor loss points (Brodribb *et al.*, 2003; Bartlett *et al.*, 2016; Trueba *et al.*, 2019), preceded xylem cavitation, and with those of Guadagno *et al.* (2017) where cellular damages occurred after turgor loss. In our study, $RWC_{crit}$ varied with cavitation resistance, with the more resistant species showing more tolerant cells to dehydration, i.e., showing dehydration-induced damages at lower $RWC_{Leaf}$ values. These findings highlight that, despite $RWC_{TLP}$ is relatively constant between species (Bartlett *et al.*, 2012), $RWC_{crit}$ for cell damages might be species dependent and vary with cavitation resistance. This species dependency could be linked to the structure and composition of the cells themselves and their capacity to respond to changes in turgor by either relaxing or tightening cell wall (Moore *et al.*, 2008), thus preventing cells deformation and shrinkage to lethal level (Scoffoni *et al.*, 2014), and death from cytorrhysis, i.e., when the cell shrinks as a unit (Oertli, 1986; Taiz & Zeiger, 2006).

Our results evinced that, despite showing different resistance to cavitation and different $RWC_{crit}$, the slope of the NLS regression determining the mortality belt was similar for the three species studied. This means that as soon as the cells reach their $RWC_{crit}$, cell mortality occurs at the same rate if the $RWC_{Leaf}$ keeps declining at the same pace for the three species. Moreover, it is known that a decreasing RWC due to the dysfunction of the water

transport system should lead to cell dehydration and should consequently provoke cell mortality (McDowell *et al.*, 2022). As a consequence, the mortality of specific key tissues, such as meristems, would certainly lead trees to death by hindering their ability to recover from drought (Mantova *et al.*, 2022). This meristem mortality is therefore expected to occur at similar pace across species once their $RWC_{crit}$ is reached if RWC diminish similarly across species. Thus, this highlights the importance of considering the dehydration rate of the organs and the pace of dehydration during drought and after stomatal closure, e.g., residual transpiration (Billon *et al.*, 2020) when aiming to determine the timing to cell death after turgor loss.

### *4.3.A closer look at the sequence of cell damages*

Changes in leaf light transmittance and leaf colour have been attributed to the collapse of the palisade cells, therefore serving as a proxy for determining leaf cell mortality (Brodribb *et al.*, 2021). By providing a quantification of cellular death through the EL measurements, our results confirm the hypothesis of a correlation between a decrease in $RWC_{Leaf}$, leaf light transmittance and cellular death made by Brodribb *et al.* (2021). However, by performing measurements in different cells layers within the leaf, our study provides a more detailed analysis of the location of the structural changes occurring in leaves during dehydration (Figure 48). Our results suggest a decrease in mesophyll cell volume, that agrees with the results of Momayyezi *et al.* (2022) where *Juglans regia* L. and *Juglans microcarpa* leaves also exhibited drought-induced reductions in mesophyll cell volume, which should be correlated with cellular death (Mantova *et al.*, 2022). Indeed, cell death *via* membrane damage could occur through physical constraints (Mantova *et al.*, 2022) such as cell cavitation, i.e., when a critical pressure in the cell is reached causing the cytoplasm fractures and the formation of a gas bubble (Sakes *et al*, 2016) and/or cytorrhysis, (Oertli, 1986; Taiz & Zeiger, 2006). However, the cell shrinkage observed in our experiment was not always associated with cellular death. In fact, depending on the species, the mesophyll cells could endure a differential reduction in cell volume before showing an increment in EL. Indeed, the mesophyll cells of *P. tremula* and *E. viminalis* were able to support an important volume reduction at the beginning of the dehydration that was not associated with cell mortality. However, for *L. nobilis,* such reduction in mesophyll cell volume was immediately correlated with an increase in cell mortality. Looking closely at the sequence of events, the palisade, spongy and epidermis cells responded differently to dehydration. In the case of *P. tremula x alba* and *L. nobilis*, the palisade cells were the first affected by dehydration whereas there were no differences in the timing of cell volume reduction for the spongy and palisade cells of *E. viminalis*. Ultimately and for all three species, the epidermis cells were the last affected by drought. These differences in response to cell changes in volume could be linked to the size, structure and composition of the cells *per se* as those components might influence the rigidity of the cell wall and thus favour or prevent shrinkage to lethal level (Scoffoni *et al.*, 2014; Joardder *et al.*, 2015).

Our results also highlight that a visual blackening of the leaf occurring at very low RWC, and once the leaf was fully embolised, was provoked by changes happening in the epidermis cells only after strong structural changes were observed in the mesophyll and once most of the leaf living tissues were dead according to the high levels of EL. Epidermis cells were the last prone to structural changes for the three species and somehow became air-filled when reaching very low RWC, provoking a blackening of the leaf that is distinguishable to the

naked eye. However, even though our scans reached a precision of 0.3µm, micro-CT observations were not precise enough to determine which of the two mechanisms (i.e., cell cavitation or cytorrhysis) induced air-filling in epidermis cells at such low RWC values. Other microscopy imaging techniques would be required to further investigate the specific mechanisms inducing mortality at the cellular level under drought conditions.

### *4.4.Die or survive?*

In general, leaves had 50% of cell death once they reached an amount of embolism relatively high (i.e., >80%) for the three species studied. The highest levels of cellular death were observed only after the leaves were almost fully embolised. Therefore, considering the results of Mantova *et al.* (2021) and Vilagrosa *et al.* (2010) showing how the capacity of recovery after drought could be related to the amount of living cells remaining at the time of rewatering, our results raise new questions on the extent to which cell mortality would lead to organ death.

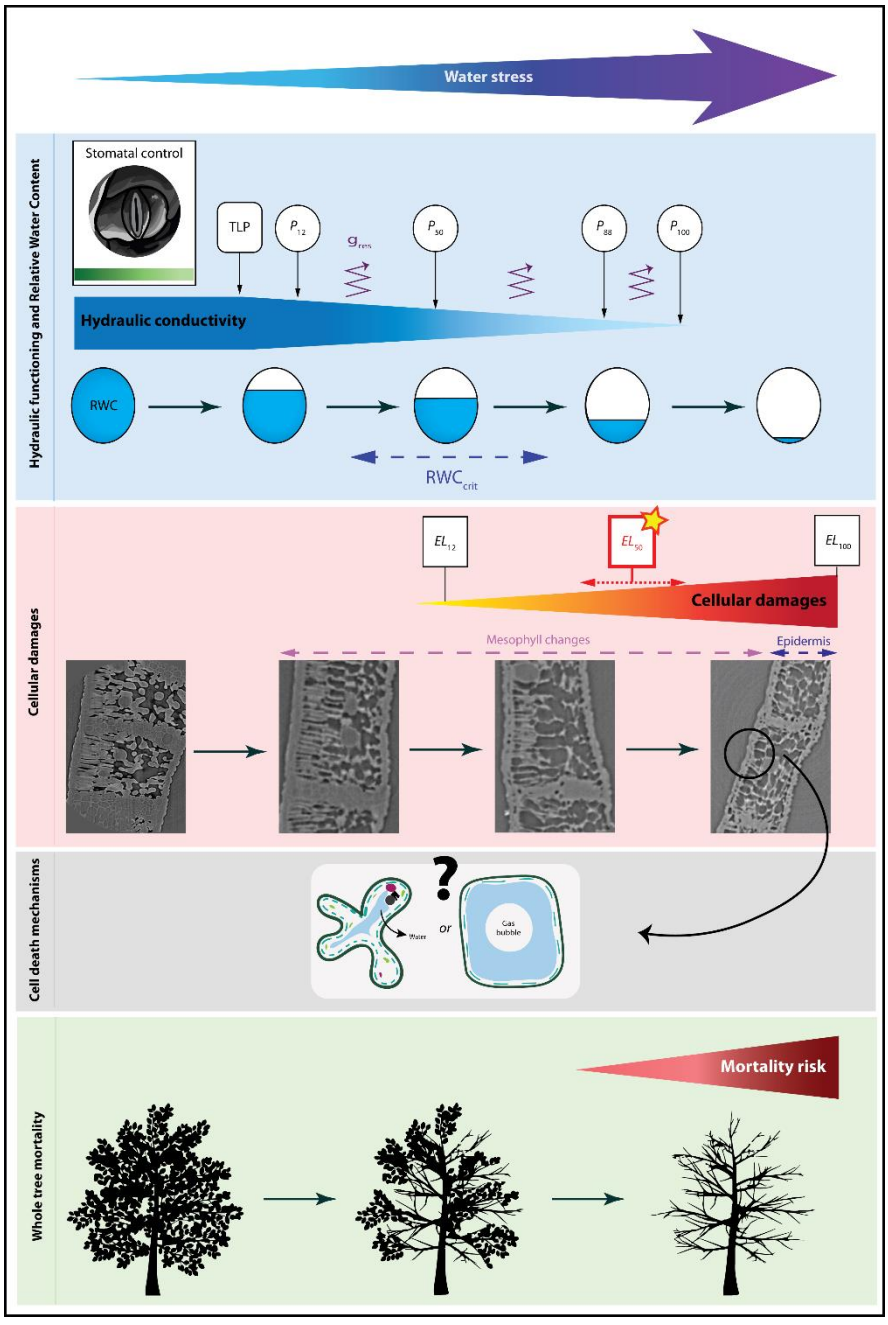


**Figure 51.** Sequence of events leading trees to death. Star highlights $EL_{50}$ as a potential indicator for cellular resistance to drought. Jagged arrows symbolise residual water losses. Black solid arrows represent the sequence of events. Dashed arrows indicate the range where the events can occur.

We hypothesize that, with an estimated 36.11% of living cells at levels of embolism of ca. 90%, it is less likely for *P. tremula x alba* leaves to recover from drought than for *E. viminalis* which leaves showed 60.41% of living cells at a similar embolism level. Determining the critical percentage of cell mortality for organ survival is crucial to precisely elucidate the capacity of an organ and therefore of the tree to recover after being exposed to drought (Figure 51).

## 5. Conclusion and perspectives

By evaluating the variation in $RWC_{Leaf}$, EL and the level of embolism in leaves from trees exposed to a progressive dehydration, our results provide evidence that xylem hydraulic failure precedes the onset of cell mortality. We describe a critical RWC value, an important dehydration threshold, below which living cells start to suffer damages from drought, and that corresponds to a certain degree of embolism occurrence. This critical RWC value varies across species while the rate at which the cellular death progresses after this point seems to be more similar across the species. Although the cell mortality rate seems constant across species, the critical RWC point is lower in more resistant to cavitation species than in the more vulnerable ones. Our results suggest a common evolutionary pathway between cells and xylem resistance to drought which would have made cells from species with a higher resistance to cavitation to withstand higher dehydration levels before showing the first damages. Despite micro-CT analyses showing a clear correlation between cell structural changes and mortality at the mesophyll level along dehydration, it remains unresolved if cells are dying because of cell cavitation or cytorrhysis.

## 6. Author Contribution

Marylou Mantova and José M. Torres-Ruiz conceived and designed the experiment. Marylou Mantova was responsible for running the measurements and carried out the data analysis. Andrew King and Sylvain Delzon supervised the setting up of the micro-CT scans. Marylou Mantova, Régis Burlett, José M. Torres-Ruiz, Santiago Trueba, Mutez A. Ahmed and Celia Rodriguez-Dominguez run the micro-CT scans. Marylou Mantova, José M. Torres-Ruiz, Hervé Cochard and Santiago Trueba interpreted and discussed the results. Marylou Mantova wrote the first manuscript draft. All authors assisted substantially with manuscript development.

## 7. Acknowledgements

This research was supported by La Région Auvergne-Rhône-Alpes "Pack Ambition International 2020" through the project 'ThirsTree'20-006175-01, 20-006175-02, and the Agence Nationale de la Recherche, Grant/Award Number ANR-18-CE20-0005, 'Hydrauleaks'.

## 8. Supplementary data

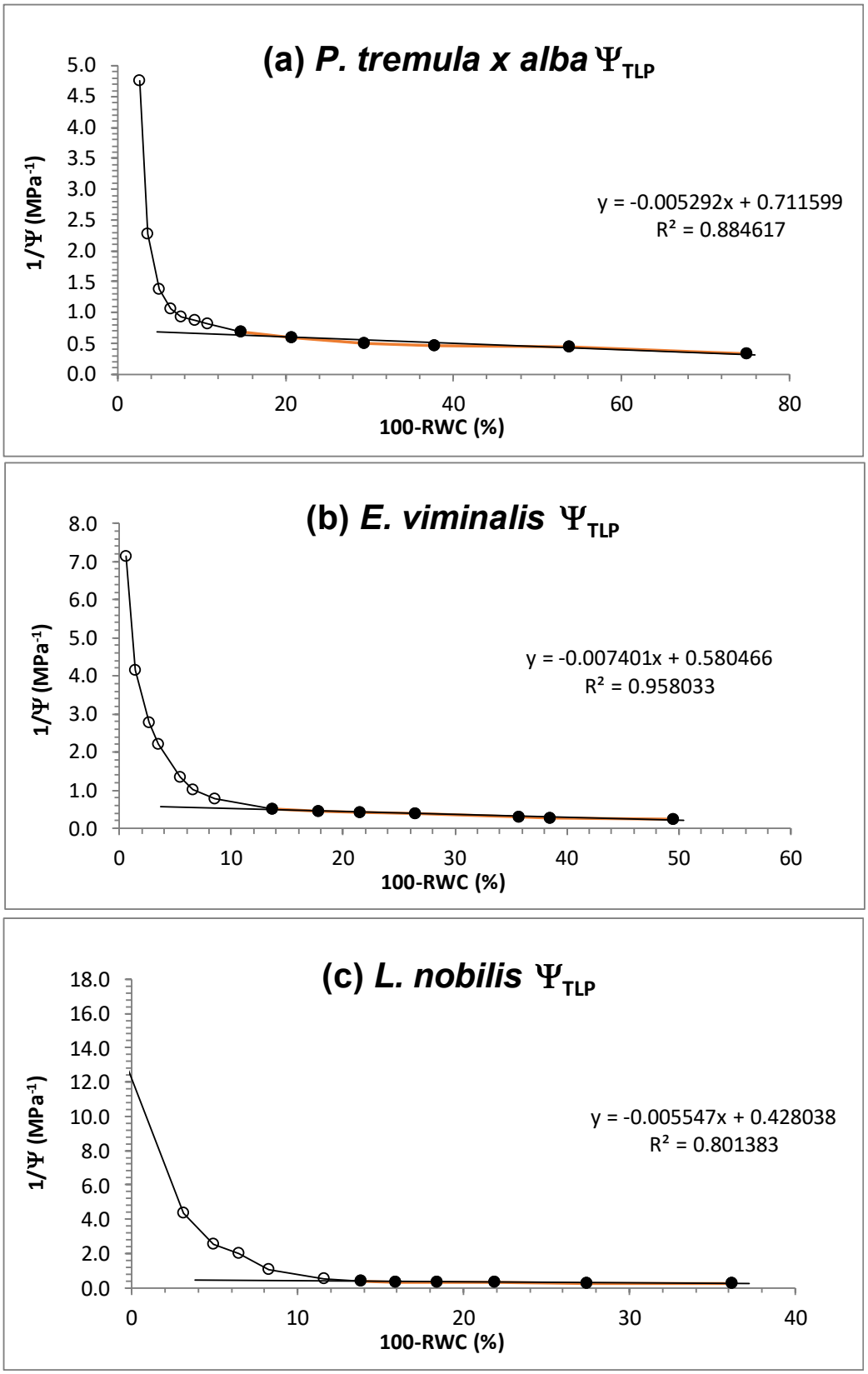


**Figure S3.** Pressure-Volume curves examples for **(a)** *Populus tremula x alba,* **(b)** *Eucalyptus viminalis* and **(c)** *Laurus nobilis.*

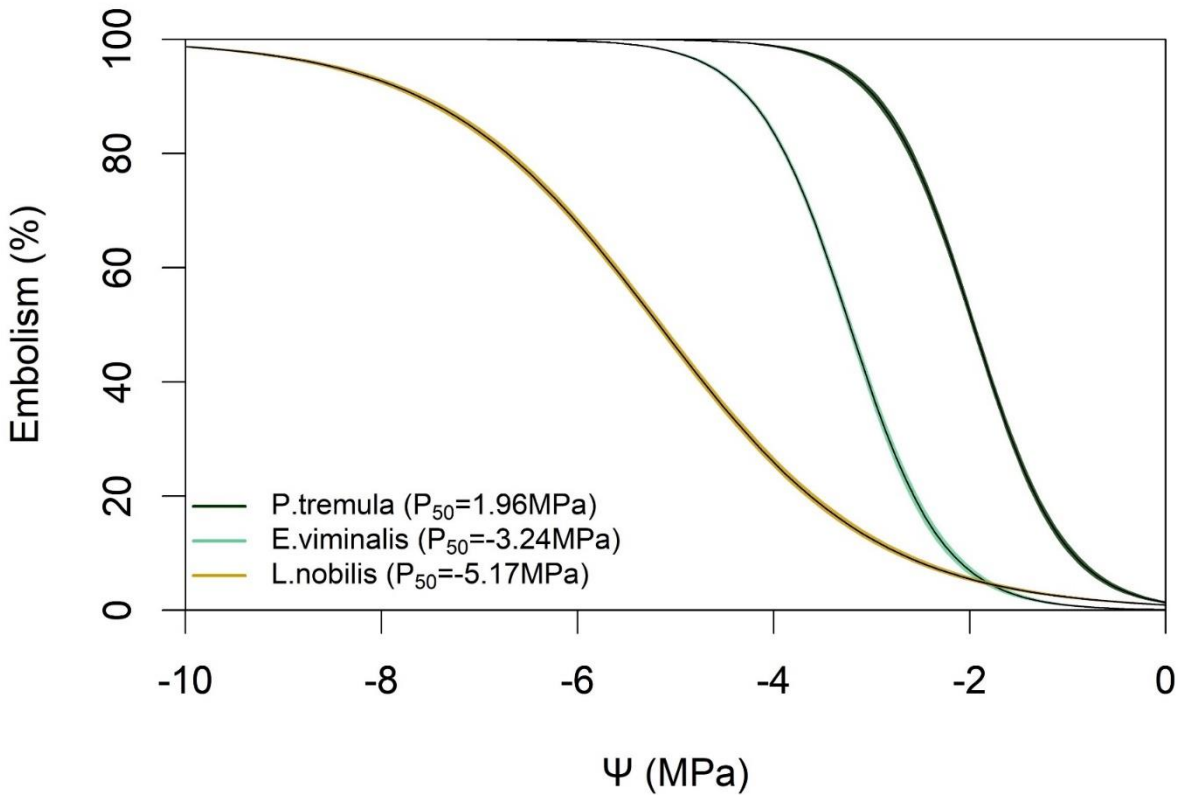


**Figure S4.** Vulnerability curves to cavitation for *Populus tremula x alba*, *Eucalyptus viminalis* and *Laurus nobilis*.

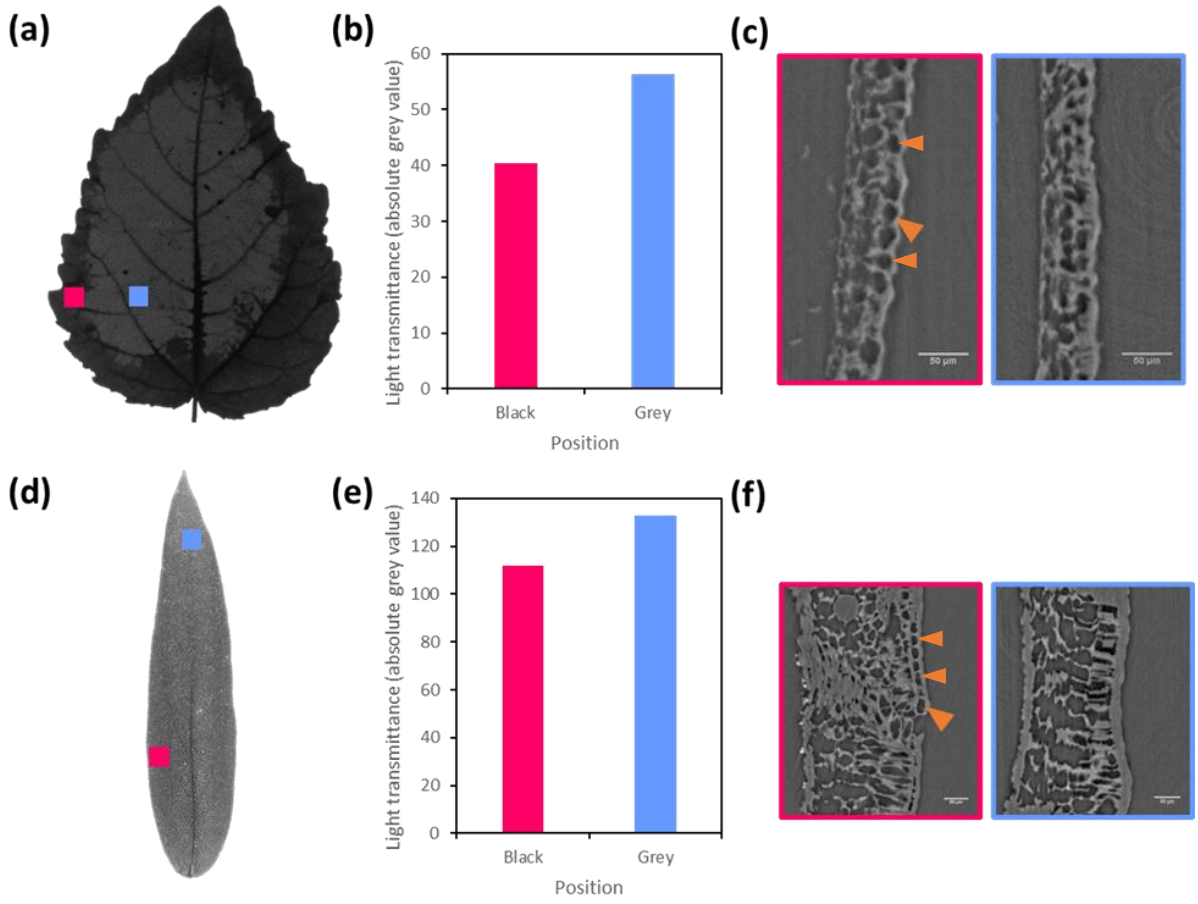


**Figure S5.** Damages at the epidermis level after full embolization of the xylem vessels for *Populus tremula x alba* and *Eucalyptus viminalis* observed with synchrotron-based x-ray microCT.
**(a, d)** Scan of a **(a)** *P. tremula x alba* leaf ($RWC_{Leaf}$=16.01%, EL=67.98%) or **(d)** *E. viminalis* ($RWC_{Leaf}$=5.86%, EL=76.56%) obtained in transmitted light. Leaf light transmittance differs within the leaf at the position marked in red and blue.
**(b, e)** Measurements of the light transmittance in absolute grey value performed with ImageJ at the respective red and blue positions for **(b)** *P. tremula x alba* and **(e)** *E. viminalis*.
**(c, f)** Synchrotron-based X-ray micro-CT images obtained for a leaf of **(c)** *P. tremula x alba* and **(f)** *E. viminalis*. The position of each scan is indicated by either the blue or red rectangles on the transmitted light image **(a, d)**. Orange triangles point at the epidermis cells and indicate the structural changes observed. Scale bars represent 50µm.

# 3

# *From cellular death to tree death: when meristems matter*

For better understanding and predicting the physiological basis of tree mortality under drought conditions, the first two chapters of this thesis work have focused on describing the relationship between a loss of hydraulic conductance and the mortality of the plant or the organ. However, if Chapter 1. has identified some key physiological traits that could work as proxy for identifying tree mortality, it hasn't demonstrated explicitly the link between the loss of hydraulic conductance and mortality. This is the link that has been explicitly studied along Chapter 2. in which we have demonstrated that cellular damages at the leaf level occurred once high levels of embolisms were encountered, and the relative water content of the tissues and cells has declined under a critical value that seemed to vary across species and with trees resistance to cavitation. Taken together, the results from Chapter 1. and Chapter 2. helped us to make progresses towards the elucidation of the physiological bases of mortality under drought conditions. However, they have not explicitly demonstrated the causal link between hydraulic failure and tree mortality. Considering the central hypothesis of our opinion piece presented at the beginning of this thesis, the causal link between xylem cavitation and tree mortality should revolve around meristem integrity. Indeed, from a plant-water relation point of view, tree death should occur when a tree is no longer able to maintain its key physiological functions (e.g., growth and/or reproduction). Thus, if important losses of hydraulic functioning may hinder the integrity of cambial cells, trees would not be able to survive the drought event no matter the amount of cellular death or the level of water remaining in their tissues at the time of re-watering. Therefore, considering this, the principal aim of this chapter was to determine the main changes occurring at plant tissue level, and particularly at the meristem level, explaining the lack of recovery after a drought event.

# Chapter 3. From cellular death to tree death: when meristems matter

*In progress*

*Authors:*
*Mantova Marylou, Jansen Steven, Cochard Hervé, Szczepaniak Claire, Brunel Nicole, Delzon Sylvain, King Andrew, Torres-Ruiz José M.*

**Summary**

***Context and objectives:*** The causal link between xylem hydraulic failure and cellular death has recently been demonstrated empirically at the leaf level and key physiological traits have been identified as potential proxies for predicting tree mortality under drought conditions. However, although the link between hydraulic failure and tree mortality could revolve around the consequences of hydraulic failure on meristems mortality, only a few studies have been specifically evaluating the consequences of a reduced water supply on meristems. Therefore, the main aim of this study was to elucidate the link between a reduced water supply caused by a decrease in hydraulic functioning and cambium mortality.

***Material and Methods:*** Drought was applied by withholding water on two species: *Abies concolor* (Gordon & Glend) Lindl. Ex Hildebr and *Fagus sylvatica* L. (55 potted seedlings for each species) in order to generate different levels of loss of hydraulic functioning and their capacity to recover from drought after a year of re-watering at pot capacity was evaluated. During the time-course of the dehydration, trunk diameter was monitored using stem dendrometers (LVDT). Lateral branches close to the LVDT were sampled the day of the re-hydration to check their water potential, percentage of embolism, relative water content ($RWC_{Stem}$), level of cellular damages and the integrity of the cambial cells.

***Results:*** Trees that survived the drought event generally showed a majority of intact cambial cells before re-watering. In general, a level of $RWC_{Stem}$ superior to 47% for *A. concolor* and 64% for *F. sylvatica* and an ability to recover at least 71% and 46% of stem diameter after re-watering for *A. concolor* and *F. sylvatica* respectively, were associated with better chances to survive from drought.

***Conclusion:*** Overall, our results indicate that maintaining cambium cells integrity could be a key to survive a drought event on a long term.

## 1. Introduction

In 2019, France faced the most intense heatwave registered to date, recording its highest ever temperatures. At the same time, many areas also experienced below average precipitation patterns, which had a strong impact on both forest ecosystems and forest productivity. This was especially the case for the Auvergne-Rhône-Alpes region where, according to the French National Forests Office (ONF), important tree mortality events were registered (Blin *et al.*, 2019). This drought event affected some of the key tree species of the region, such as fir and beech (Blin *et al.*, 2019). As the trend of heatwaves and drought looks set to continue, there is an urgent need to better understand the physiological thresholds for drought-induced tree mortality to accurately predict the risk of future forest dieback and their effect on the forest's composition across the world and particularly in the Auvergne-Rhône-Alpes region.

Drought is now widely considered a key driver for tree mortality globally and earlier work have provided strong evidence that drought-induced mortality is strongly associated with failure of water transport in xylem tissue of plants (Brodribb & Cochard, 2009; Barigah *et al.*, 2013b; Urli *et al.*, 2013; Delzon & Cochard, 2014; Hammond *et al.*, 2019; Mantova *et al.*, 2021; McDowell *et al.*, 2022). Xylem hydraulic failure occurs when xylem sap tension exceeds a certain threshold due to a strong demand for evaporation and transpiration. As the percentage of embolized vessels increases (PLC) with increasing drought stress, the hydraulic functioning of the xylem diminishes until the flow of water stops, provoking the dehydration and ultimate desiccation of the tree tissues and, eventually, the death of the tree (McDowell *et al.*, 2022). Although it is clear that it exists a correlation between tree mortality and hydraulic failure, some recent studies have shown that the usually accepted thresholds in loss of hydraulic conductance ($P_{50}$ for conifers (Brodribb & Cochard, 2009) and $P_{88}$ for angiosperms (Barigah *et al.*, 2013b; Urli *et al.*, 2013)) were not exact as trees could recover from drought once re-watered even when overpassing those points (Hammond *et al.*, 2019; Mantova *et al.*, 2021). In addition, just a few studies, focused on leaves, have tried to demonstrate the causal link between hydraulic failure, a decrease in water content, and tissue mortality (Brodribb *et al.* 2021, see also. Chapter 2.). More importantly, none of them have focused on meristems mortality despite it probably being the key for survival and recovery after a drought-event because of their capacity to generate new tissues and organs under favourable growth conditions (Mantova *et al.*, 2022). It remains unclear, for instance, how the reduction in cell water content and the drought-induced damages in meristematic cells are related to drought-induced tree death. Thus, even though cambium growth and vitality have a significant role on plant survival under drought conditions (Li & Jansen, 2017; Mantova *et al.*, 2022) little is known about the dehydration level of the meristems at the time of hydraulic failure, probably because of the difficulty to access those elements and the expensive and non-immediate techniques needed to assess their integrity, such as transmission electron microscopy (TEM). Therefore, focusing on meristematic cells and determining the level of damage they suffer during the progressive dehydration of the plants under water stress and its relationship to the loss of hydraulic functioning should provide novel information on the mechanistic link between hydraulic failure and drought induced tree mortality.

New possible thresholds for better identifying and predicting tree mortality such as the percentage loss of stem diameter (PLD) (Lamacque *et al.*, 2020), the stem relative water content ($RWC_{Stem}$) and cell membrane damages predicted by the electrolytes leakage method (EL) (Guadagno *et al.*, 2017; Mantova *et al.*, 2021, 2022) have arisen in the recent years. In the study of Lamacque *et al.* (2020), the point of no recovery for lavender species was correlated to the depletion of the elastic water storage localised in the bark of the branches. This inability to move water due to the depletion of the elastic water storage could be correlated with meristem mortality as the capacity of trees to relocate stored water between tissues, and particularly toward the meristematic tissues, could be crucial to buffer the variation in RWC at the meristematic level and thus keep their integrity (Mantova *et al.*, 2022). Therefore, even if the use of the PLD has only been demonstrated for lavender species, where a PLD ~21% corresponded to the point of no recovery, and is yet to be demonstrated for other woody species, a conjoint monitoring of stem diameter, and thus water movement, and of meristem integrity using TEM, as done by Li & Jansen (2017), during a water stress could help deciphering how hydraulic failure could conduct to meristem mortality by provoking a reduced water supply to living tissues (McDowell *et al.*, 2022; Mantova *et al.*, 2022). Mantova *et al.* (2021) have shown that higher values of $RWC_{Stem}$ could help conifers to survive a drought event and this higher $RWC_{Stem}$ values were also associated with lower level of cellular damages. In addition, the relationship between a decrease in RWC and an increase in cellular damages has been recently elucidated at the leaf level and a critical RWC for cellular damages ($RWC_{crit}$) has been identified (see Chapter 2. – *submitted*). However, it remains unknown if this $RWC_{crit}$ values also exist at the stem level, if it helps identifying the onset of meristems mortality, and if it could work as a possible threshold for implementing mechanistic model aiming at predicting tree mortality (Cochard *et al.*, 2021).

Therefore, considering the actual need to understand the underlying processes connecting hydraulic failure and tree mortality, and the urge to identify mechanistic, integrative, scalable and easy to measure and monitor thresholds for predicting tree decaying (Martinez-Vilalta *et al.*, 2019), the main aims of this study are to (i) test the hypothesis that tree mortality is linked to meristem mortality, (ii) evaluate whether the water impairment through cavitation is the triggering factor causing a loss of meristem integrity and (iii) identify new physiological thresholds for predicting tree mortality from drought. For this, a set of plants of *Abies concolor* (Gordon & Glend) Lindl. Ex Hildebr and *Fagus sylvatica* L. were exposed to severe drought conditions and allowed to dehydrate until they reached different levels of water stress. At this point, trees were re-watered to check for their capacity to recover from drought. During the dehydration and the recovery phases, we monitored changes in stem diameter, stem water potential ($\Psi_{Stem}$), embolism formation, changes in stem RWC ($RWC_{Stem}$) and assessed cells vitality at the stem level. We also performed cambium samplings to check its vitality using TEM. This approach gave us the opportunity to test the connection between hydraulic failure and meristem mortality as well as identifying new thresholds for tree mortality.

## 2. Materials and methods

### *2.1.Plant material and experimental setup*

The experiments were carried out in two species: one angiosperm, *Fagus sylvatica* L. and one conifer, *Abies concolor* (Gordon & Glend) Lindl. Ex Hildebr, selected for their contrasted PLC thresholds of drought-induced mortality (i.e., $P_{88}$ and $P_{50}$ respectively). For each species, 55 trees were grown under non-limiting water conditions in 10L and 40L pots, respectively, in Les Chères, France (45.908'N, 4.732'E). *F. sylvatica* individuals were four years old at the time of the experiment while the *A. concolor* were six years old.

The experiments were separated in two phases according to the maximal cambial activity of the trees: *A. concolor* trees were exposed to drought and re-watered in between May 3rd and June 15th, 2021, whereas *F. sylvatica* trees were exposed to drought and re-watered in between June 15th and July 26th, 2021. Two weeks before starting each experiment, all trees were moved to a controlled-environment glasshouse cell and kept under natural light and at a mean temperature of 28.1 ± 2.6 °C (midday) and 21.2 ± 1.5°C (midnight) for *A. concolor* and of 31.0 ± 5.0°C (midday) and 22.6 ± 2.0 °C (midnight) for *F. sylvatica*. During this period, trees were kept well-irrigated (field capacity) by a drip irrigation system controlled by an electronic timer. After the two weeks of acclimation, 5 trees of each species were kept irrigated at field capacity, serving as control trees while 50 trees from each species were exposed to progressive dehydration by withholding the irrigation. In order to determine the critical PLC for recovery and because Hammond *et al.* (2019) reported that conifers were able to recover even beyond $P_{50}$ and Mantova *et al.* (2021) assessed that angiosperms could survive beyond $P_{88}$, trees were re-watered to field capacity once reaching $\Psi_{Stem}$ values corresponding to significant losses in hydraulic functioning according to their vulnerabilities to cavitation (i.e., varying from PLC=30% to 100% for conifers and varying from PLC=70% to 100% for angiosperms) (Figure 52). They were then kept well-irrigated to check for recovery from drought.

### *2.2.Vulnerability curves to cavitation*

Prior to the experiment, the vulnerability to cavitation for the two target species was determined to define when trees should be re-watered according to their PLC level. Thus, for both species, vulnerability curves were constructed by using the Cavitron technique (Cochard, 2002a) which uses centrifugal force to increase the water tension in a xylem segment while measuring the decrease in its hydraulic conductance. Five 0.45m-long stem samples from five different well-hydrated trees (i.e., one sample per tree) were recut under water with a razor blade to a standard length of 0.27m and were debarked on 3 cm at each extremity for *F. sylvatica* and fully debarked for *A. concolor* to prevent resin contamination. For constructing the vulnerability curves, the maximum sample conductivity ($K_{max}$) was measured at low speed and relatively high xylem pressure (−0.75 MPa). The xylem pressure was then decreased stepwise by increasing the rotational velocity and the conductivity ($K$) measured at each pressure step. Each pressure was applied on the sample for two minutes. Sample loss of conductivity (PLC, %) was computed at each pressure as follows (4):

$$(4)\ PLC = 100 * \left(1 - \frac{K}{Kmax}\right)$$

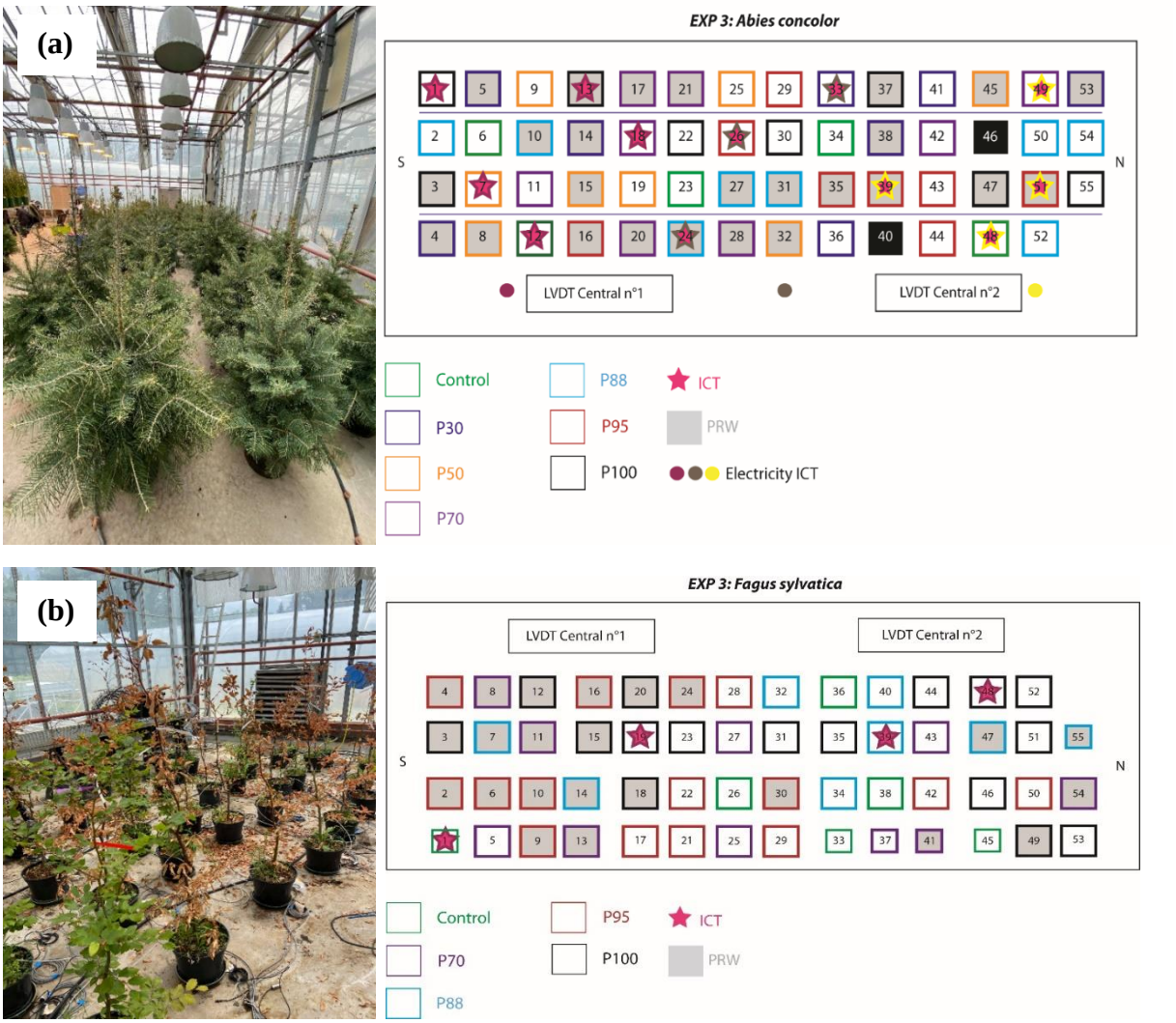


**Figure 52**. Experimental set-up for **(a)** *Abies concolor* trees and **(b)** *Fagus sylvatica* trees and targeted rehydration points as well as trees sampled for post-rewatering (PRW) measurements.

The resulting curves were fitted according to Pammenter and Vander Willigen equation (1998) (5) and using the R *'fitPLC'* package (Duursma & Choat, 2017):

$$(5)\ PLC\ or\ Cumulative\ embolism = \frac{100}{(1+e^{(a/25(P-P50))}}$$

where *a/25* is the slope of the curve at the inflexion point, *P* the target pressure reached with the Cavitron, and $P_{50}$ is the $\Psi_{stem}$ or pressure value at which 50% loss of conductivity occurred.

### 2.3. *Vulnerability to cellular damages under dehydration*

Prior to the experiment, the cellular vulnerability to dehydration was assessed at the stem level for the two targeted species. Briefly, stem relative water content ($RWC_{Stem}$) and the level of cellular damages (EL) were measured as described below on ten *A. concolor* individuals and seven *F. sylvatica* individuals exposed to a progressive bench dehydration by withholding water under lab conditions (T°~25°C).

### 2.3.1. Stem Relative Water Content

Stem relative water content ($RWC_{Stem}$) was calculated according to Barrs and Weatherley (1962) (6):

$$(6)\ RWC_{Stem} = \frac{(FW-DW)}{(TW-DW)}\ ,$$

where FW is the fresh weight measured immediately after sampling; TW is the turgid weight measured after immersing the stem in distilled water for 24 h (for $RWC_{Stem}$); and DW is the dry weight of the samples after 24 h of drying in an oven at 72°C. All measurements were done using a precision scale (METTLER AE 260, DeltaRange ®, Mettler Toledo, Columbus, OH, USA).

### 2.3.2. Stem cell vitality

Cell vitality was assessed using the electrolytes leakage test (EL) (Zhang & Willison, 1987; Sutinen *et al.*, 1992) along dehydration on two to three stem samples sampled (depending on plant material availability). The stem samples were cut into ten 2-mm thick slices and immersed in test tubes containing 15mL of pure water. Test tubes were shaken at 60 shakes per min during 24h at 5°C to stop enzyme activity. Water conductivity of the effusate (C1) was then measured at room temperature using a conductimeter (3310 SET1, Tetracon® 325, WTW, Weilheim, Germany). Then, all the living cells were killed by autoclaving the samples at 121°C for 30 min (King & Ludford, 1983), cooled down at room temperature (22°C approx.) for 60 min and the effusate maximal conductivity (C2) measured. The lysis percentage (EL) was then determined as (8):

$$(8)\ EL = \frac{C1}{C2} * 100$$

### 2.3.3. Cellular death dynamic regarding cellular water stress: non-linear regressions and sigmoid parameters

In order to visualize the dynamic of cell damage as the $RWC_{Stem}$ decreased, the percentage of EL was plotted against $RWC_{Stem}$ for each species. A non-linear regression (NLS), four parameter logistic regression, was fitted using SigmaPlot with the following equation (13):

$$(13)\ \text{NLS}=\min + \frac{(max-min)}{1+\frac{x}{EL50}^{-Hillslope}}$$

Where $EL_{50}$ represents the $RWC_{Stem}$ value at which 50% of the cells are dead, *max* and *min* represent the maximum and minimum EL value of the dataset and *Hillslope* the slope of the regression at the inflection point.

From this NLS fitting was extracted the critical level of RWC ($RWC_{crit}$) below which the cells start to incur damages from water stress. By analogy to the air entry pressure defined by Meinzer *et al.* (2009) and Torres-Ruiz *et al.* (2017), the $RWC_{crit}$ was determined at the x-intercept of the tangent through the midpoint ($EL_{50}$) of the NLS regression curve and corresponded to 12% of cell damages (see Chapter 2. Figure 43). The slope of the regression was used to determine the 'Mortality Belt' (see Chapter 2. Figure 43) i.e., the range in which

the decrease in $RWC_{Stem}$ provokes the maximum cell damage that corresponds to the decrease in $RWC_{Stem}$ between $EL_{12}$ and $EL_{max}$.

### *2.4.Stem diameter variations*

Stem diameter variations were monitored continuously by Linear Variable Differential Transformer (LVDT model DF2.5 and DF5.0; Solartron Metrology, Massy, France) sensors (one LVDT per plant in 55 plants per species) installed before withholding irrigation. The sensor was applied on the stem with glue and was connected to a data logger (Model CR1000, Campbell Scientific LTD) to collect the stem diameter variations (in µm) every 10 min (Figure 53). By evaluating the dynamics of stem diameter during the dehydration and recovery phases of the experiment (Figure 54), we were able to evaluate the stem diameter recovery capacity (RC %) and the percentage loss of diameter (PLD) according Lamacque *et al.* (2020) (Figure 54).

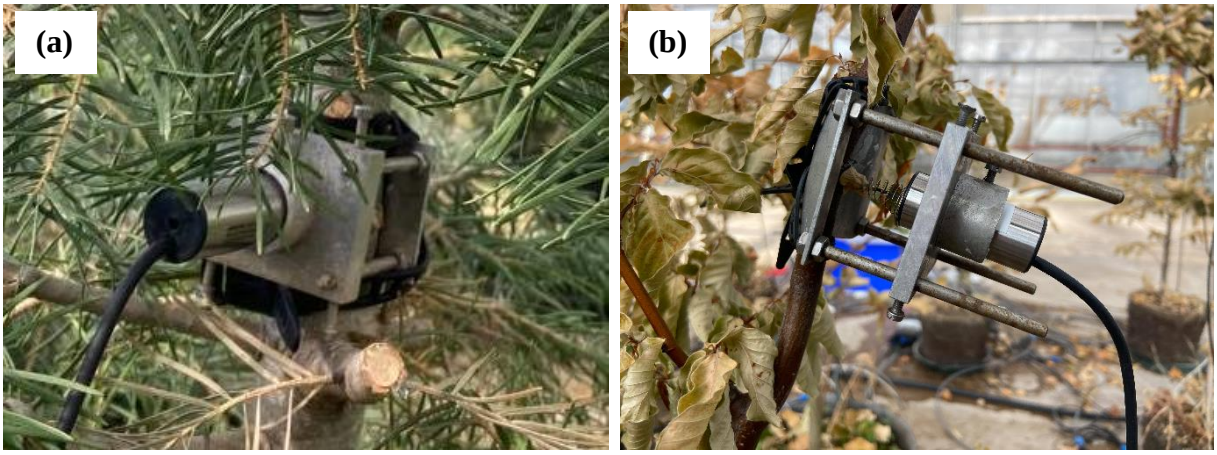


**Figure 53.** LVDT installed on stems of (a) *Abies concolor* and (b) *Fagus sylvatica*.

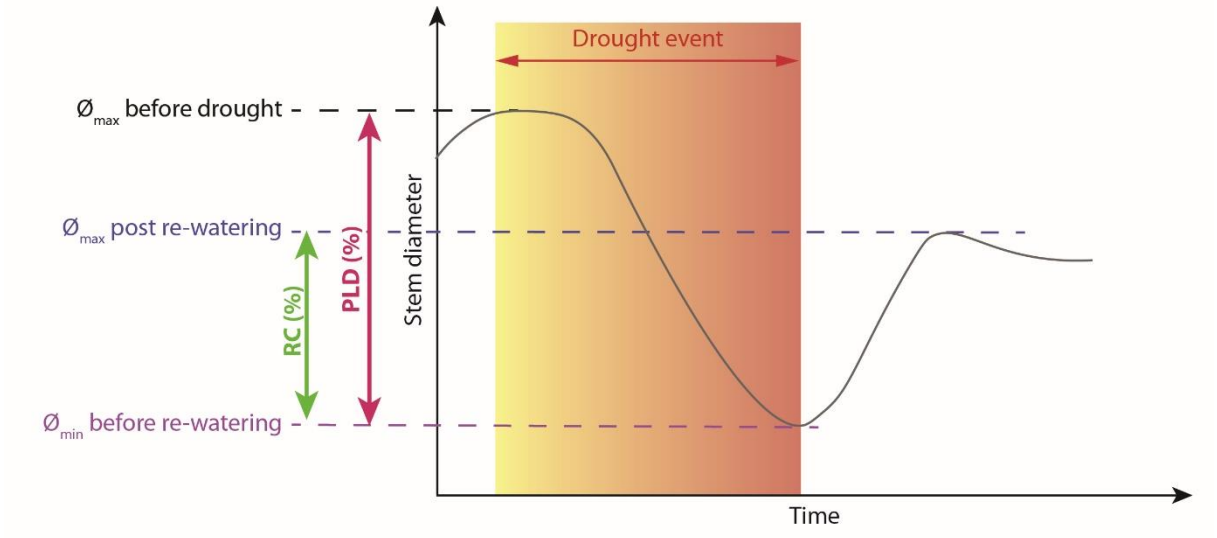


**Figure 54.** Determination of the percentage loss of stem diameter (PLD) during dehydration and stem recovery capacity (RC %) after re-watering according to stem diameter dynamics recorded by LVDT.

### *2.5.Physiological traits*

Five trees were sampled before withholding irrigation (Control) and each tree was sampled right before re-watering (BRW) for evaluating their $\Psi_{stem}$, PLC, $RWC_{Stem}$, EL, and cambial cells vitality on two to three branches (depending on plant material availability) located nearby the LVDT sensor (Figure 55 and Figure 56). $RWC_{Stem}$ and EL were measured in the same manner as presented in the above paragraphs.

**Figure 55.** Sampling of branches nearby the LVDT sensor for physiological measurements. Branches were immediately stored in plastic bag to prevent further dehydration during transport between the glasshouse and the laboratory.

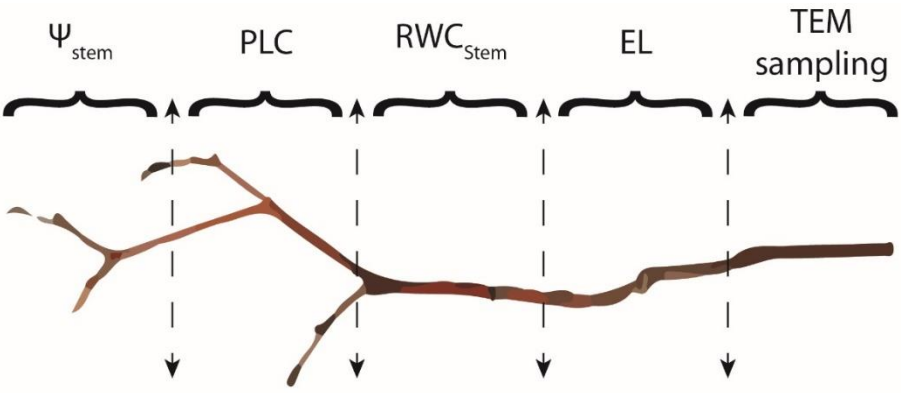


**Figure 56.** Location of the different measurements on a branch taken near the LVDT sensor.

### 2.5.1. *Stem water potential*

During the progressive dehydration imposed to each set of trees, $\Psi_{stem}$ was continuously assessed by using psychrometers (PSY1, ICT international) (Figure 57). Thus, one psychrometer per plant in a total of 12 plants per species was installed at the stem level and covered with aluminium foil to prevent their direct exposure to the sunlight and minimize any effect of external temperature variations (Vandegehuchte *et al.*, 2014). Psychrometers recorded the $\Psi_{stem}$ every hour. To check the accuracy of the psychrometers, midday $\Psi_{stem}$ measurements were carried every day using a Scholander-type pressure chamber (PMS, Corvallis) in 20 plants per species and in one fully developed and healthy leaf per plant, previously bagged for at least one hour to prevent transpiration and promote equilibrium with the plant axis. BRW, $\Psi_{stem}$ was assessed directly at the tip of the three sampled branches to allow other physiological measurements (Figure 56).


**Figure 57.** Installation steps of a stem psychrometer.
**(a)** The stem is locally debarked to expose undamaged xylem. Parafilm is then applied around the stem to create a flat surface on which the psychrometer can be installed. A window, about the size of the psychrometer chamber, is created in the parafilm to allow xylem water potential measurements at the stem level.
**(b)** Installed stem psychrometer on a *Fagus sylvatica* tree. A clamp helps to maintain the psychrometer chamber on the previously debarked area.

### 2.5.2. *PLC determination*

Once the trees reached $\Psi_{Stem}$ values corresponding to a PLC varying from ca. 70% to 100% for *F. sylvatica* and from ca. 30% to 100% for *A. concolor* according to their vulnerability curves, the PLC was assessed in stems using two different, but comparable, techniques (Ganthaler *et al.*, 2022). For *A. concolor,* the PLC was assessed by direct observation using X-Ray microtomography (Micro-CT, Nanotom 180 XS; GE) at the PIAF laboratory (INRAE) (Cochard *et al.*, 2015) and at the French synchrotron facility SOLEIL (Paris, France) using the micro-CT PSICHE beamline. For *F. sylvatica*, PLC was determined by using a staining process involving Safranin (Hietz *et al.*, 2008; Nolf *et al.*, 2016). For both technique, one or two samples per plant were cut progressively underwater to prevent artefactual increases in the amount of embolism in the samples (Torres-Ruiz *et al.*, 2015) and were immediately immersed in liquid paraffin wax to prevent dehydration during the scanning or the coloration.

For *A. concolor*, at the PIAF laboratory, each scan lasted 21 minutes and 1000 images were recorded during the 360° rotation of the sample. The X-ray setup was fixed at 70kV and 240µA. After 3D reconstruction, the spatial resolution of the image was 2.00 × 2.00 × 2.00 µm per voxel. At the SOLEIL synchrotron facility, the stem of interest was scanned using a high-flux (3.1011 photons $mm^{-2}$) 25-KeV monochromatic X-ray beam. The projections were recorded with a Hamamatsu Orca Flash sCMOS camera (Hamamatsu Photonics K.K., Shizuoka, Japan) equipped with a 250-lm-thick LuAG scintillator and visible light optics providing an effective pixel size of 3 µm. The complete tomographic scan included from 2000 to 4000 projections, 50 ms each, for a 180° rotation. Samples were exposed for 75 s to the X-ray beam. The tomographic reconstructions were performed using PyHST2 software (Mirone *et al.*, 2014) employing the method of Paganin (2006). PLC of each section were then calculated similarly to Choat *et al.* (2015), that is, by comparing the area of observed functional and embolized xylem area ($A_f$ and $A_c$, respectively) as (14):

$$(14)\ PLC = (A_c * 100)/(A_c + A_f)$$

For *F. sylvatica*, the conducting xylem elements were stained using segments of 5cm length cut under water. One third of the debarked branch sample was fitted in a silicone tubing and connected under water to a reservoir of 0.1% solution (w/v) of safranin, mounted 40 cm above the outflow end of the sample (Mayr & Cochard, 2003). When dye solution appeared at the outflow end of the sample, which happened after an hour of perfusion, the reservoir was disconnected, and the dye was washed from the sample for an hour with ultrapure water. Cross sections (c. 20µm thick) were obtained using a microtome (Leica RM2165, Wetzlar, Germany), mounted in Eukitt (Electron Microscopy Science, Hatfield, PA, USA) and observed using a light microscope (Axio Observer Z1, ZEISS, Jena, Germany). An entire cross-section image was obtained by joining images with the same magnification taken from all the cross-section of the sample using a camera (Axiocam MRc, ZEISS, Jena, Germany). The amount of PLC was computed by determining the ratio between the amount of unstained conduits and stained conduits using the *Fiji* software (Schindelin *et al.*, 2012).

### *2.5.3. Cambium cells vitality: Transmission electron microscopy (TEM)*

One cambium sample per seedling was used for TEM observations. About 3 to 5 slivers of stem cambium (1 to 2 $mm^3$) were cut from a sample (Figure 58) and immediately stored in a standard TEM fixative solution (3% glutaraldehyde, 4% paraformaldehyde, 0.1 M Phosphate buffer, PH 7.4) in a fridge (at 5°c) until post-fixation and sectioning. Electron microscopy preparations were all performed by the "*Centre d'Imagerie Cellulaire Santé*" (Clermont-Ferrand, France). All chemical products were from Electron Microscopy Science and distributed in France by Delta Microscopies. The cambium samples were washed in 0.1 M phosphate buffer, postfixed with 1% buffered osmium tetroxide for 4 h, rinsed 3 times in 0.1M phosphate buffer for 10min, dehydrated with a gradual ethanol series (30%, 50%, 70%, 95%), and embedded with Epon resin. Semi-thin sections (c. 700 nm thick) were subsequently cut from embedded samples with an UC7 ultramicrotome (Leica, Wetzlar, Germany), stained with 0.5% toluidine blue in sodium tetraborate, and mounted on slides with Eukitt. Ultrathin sections (70 nm) were cut using a UC7 ultramicrotome (Leica, Wetzlar, Germany), stained with uranyl acetate and lead citrate and were mounted on 150mesh copper grids (EMS FCF-150-Cu). The ultra-thin

transverse sections were observed with a Hitachi H-7650 TEM (Hitachi Ltd., Tokyo, Japan) at 80 kV accelerating voltage. Photos were taken with a Hamamatsu AMT40 camera (Hamamatsu Photonics K.K, Shizuoka, Tokyo, Japan).

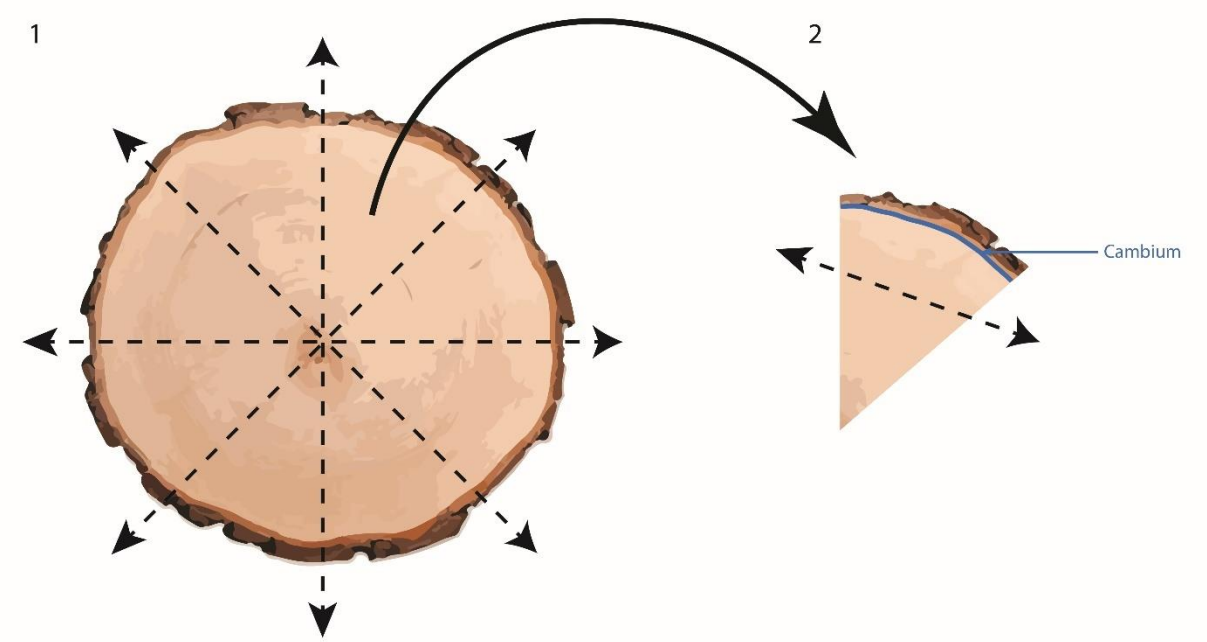


**Figure 58.** Cutting of the branch sample with a razor blade **(1)** to retrieve the cambial zone **(2)**. Dashed lines represent the different cuts operated on the sample.

### *2.6.Survival determination*

Monitoring for survival or mortality occurred during the following growing season (from April to June 2022) and allowed to determine if a tree had survived from the drought event if new growth were observed after rewatering.

### *2.7.Logistic regressions and statistical analyses*

We analysed the effect of PLC, $RWC_{Stem}$, EL, PLD and stem diameter recovery capacity (RC) on the probability of mortality using a four-parameter logistic regression, a method appropriate for binary outcome such as life or death (Menard, 2002; Hammond *et al.*, 2019) using Sigma Plot 12.3 ®. By analogy to what was done by Hammond *et al.* (2019) and by using the inflection point of the logistic regression, we determined the lethal threshold at which 50% of trees would die in terms of RWC ($LD_{50}$-RWC) and RC ($LD_{50}$-RC) for both species and in terms of hydraulic failure ($LD_{50}$) and EL ($LD_{50}$-EL) for *A. concolor* and in term of loss of stem diameter ($LD_{50}$-PLD) for *F. sylvatica*.

Statistical analyses consisted of paired *t*-test (after testing for normality and homogeneity of variances) and Wilcoxon test (for non-normal distribution) and were performed using R programs to compare the set before the drought event (Control) and BRW. All tests were performed using a level of significance $\alpha = 0.05$.

The dataset was subjected to principal component analysis (PCA) and the Kaiser-Mayer-Olkin index (KMO) was calculated to measure the sampling adequacy to PCA (the ability to summarize the information contained in the dataset) (Kaiser, 1974).

## 3. Results

### 3.1. Vulnerability curves to cavitation and cellular death

Vulnerability curves reported $P_{50}$ values of -3.8 and -2.5 MPa for *A. concolor* and *F. sylvatica*, respectively (Figure 59). *A. concolor* individuals were thus rehydrated once they reached $\Psi_{Stem}$ values of ranging from -3.3 to −8.0MPa, that is from $P_{30}$ to $P_{100}$. *F. sylvatica* were rehydrated once showing $\Psi_{Stem}$ values ranging from −2.9 to −7.0 MPa, that is from $P_{70}$ to $P_{100}$.

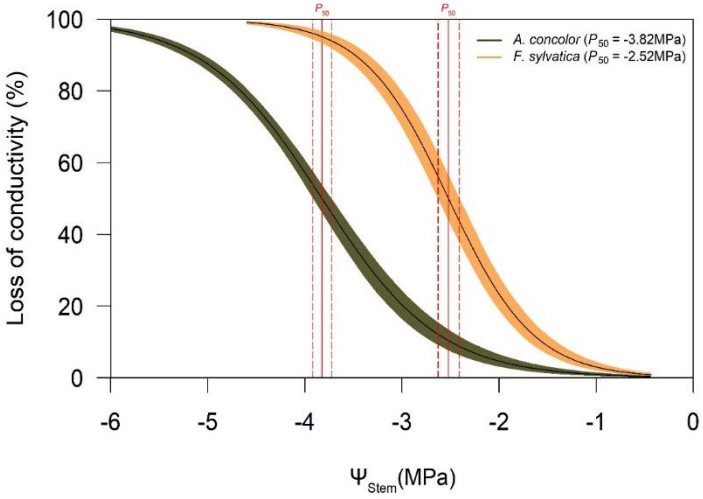


**Figure 59.** Vulnerability curves to cavitation for *Abies concolor* stems and *Fagus sylvatica* stems.
Both vulnerability curves were obtained on five different samples using the Cavitron technique developed by Cochard in 2002.
The $P_{50}$ is evaluated at -3.8MPa for *A. concolor* and -2.5MPa for *F. sylvatica*.
Red solid lines represent the $P_{50}$ for each species while red dashed lines represent the confidence interval around $P_{50}$ at 95%.

*A. concolor* which reported the highest resistance to cavitation presented the lowest critical RWC value before suffering cellular damages ($RWC_{crit}$ = 78%) whereas *F. sylvatica* which showed the lowest resistance to cavitation presented a higher $RWC_{crit}$ (88%) (Figure 60). The $EL_{50}$ was calculated as 43.5±4.1% for *A. concolor* whereas it was computed at 47.5±4.2% for *F. sylvatica* thus showing no differences between species. The slope of the regression was calculated at 2.5±1.1 for *A. concolor* and was of 2.8±1.0 for *F. sylvatica* once again showing no differences across species.

**Figure 60.** Dynamic of cellular damages (EL) regarding stem relative water content ($RWC_{Stem}$). Triangles represent the $RWC_{crit}$ identified for each species.

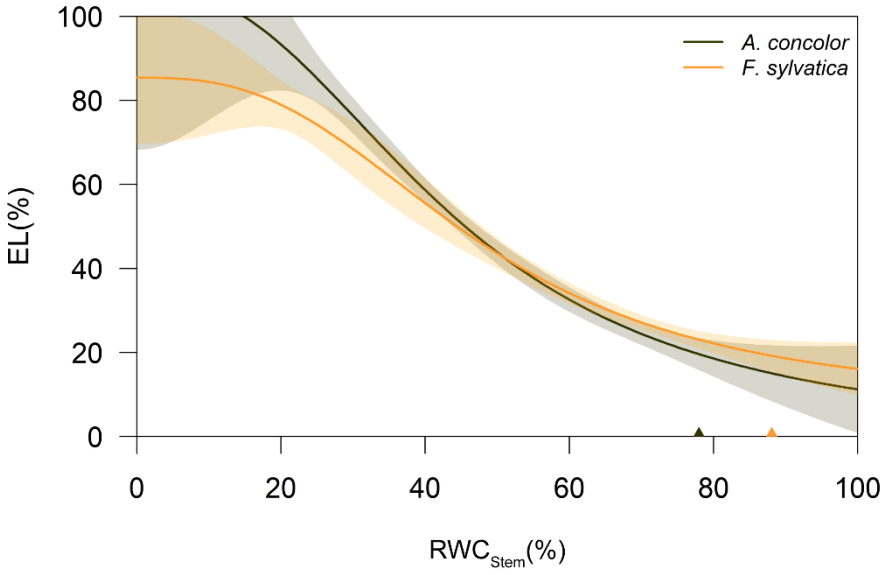

### 3.2. Effect of drought on stem diameter variation

Stem showed a noticeable shrinkage for both species during the time course of the dehydration for all individuals (Figure 61 and Figure 62). After re-watering and according to the LVDT dynamic, we observed three different types of responses for the two species studied: full stem diameter recovery, partial recovery of stem diameter and no recovery of stem diameter. We calculated a percentage of stem recovery capacity (%RC) and determined a recovery type according to the %RC. Type 1 (T1) trees showed an increase in stem diameter in the following day after re-watering (full stem diameter recovery) and were able to recover their diameter until reaching more than 95% of the stem initial diameter (RC > 95%) (Figure 61b and Figure 62b). Type 2 (T2) trees only partially recovered their stem initial diameter (i.e., RC > 5% but <100%) (Figure 61c and Figure 62c) and type 0 (T0) trees were not able to recover their stem initial diameter and showed a RC < 5% (Figure 61d and Figure 62d). We observed for *A. concolor* 13 T0 trees, 12 T1 trees and 23 T2 trees whereas the re-watering experiment of *F. sylvatica* showed 16 T0 trees, 17 T1 trees and 12 T2 trees.

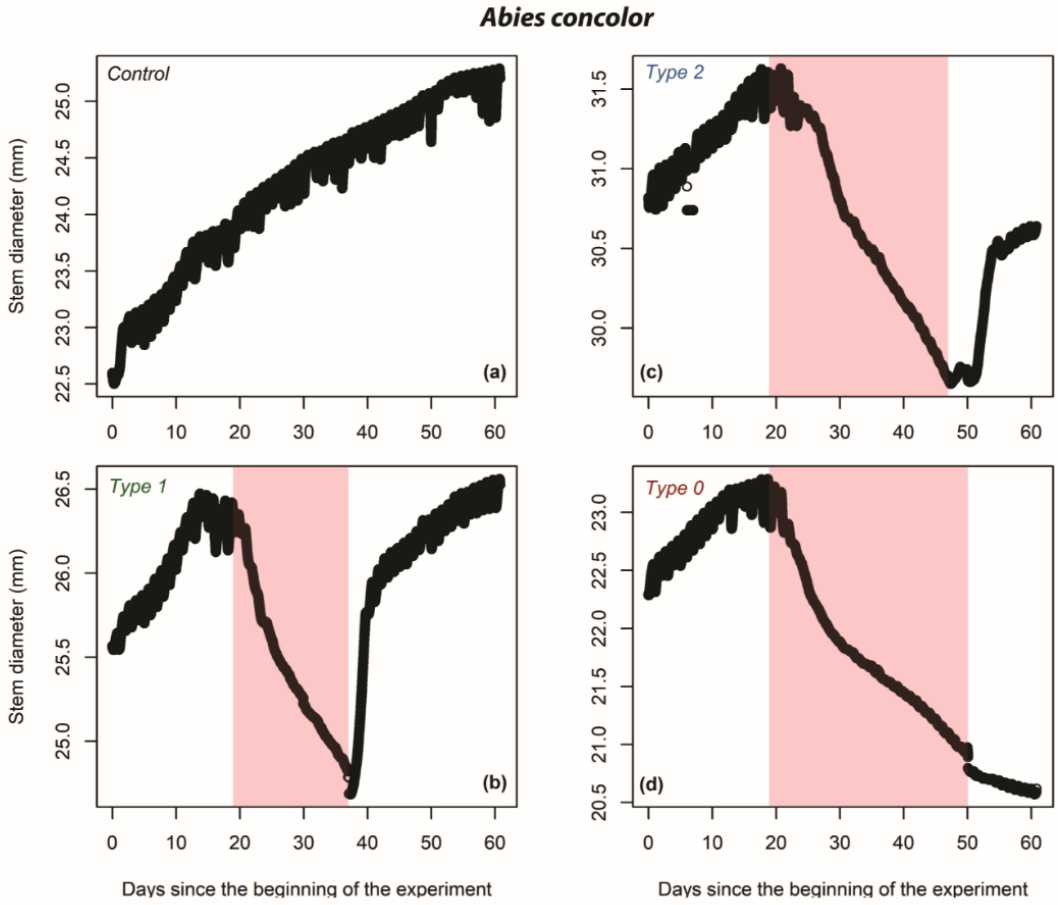


**Figure 61.** Variation of stem diameter during the time-course of the experiment for *Abies concolor*.
Stem diameter (in mm) was recorded by Linear Variable Differential Transformer (LVDT). The light red rectangles represent the period where water was withheld to simulate an extreme drought event.
Panel **(a)** represents a tree in control conditions, **(b)** a Type 1 tree, i.e., a tree that fully recovered its initial diameter after being re-watered. **(c)** Type 2 tree, i.e., here a tree that recovered 49% of its initial diameter, **(d)** a Type 0 tree, i.e., a tree that did not recovered its initial diameter.

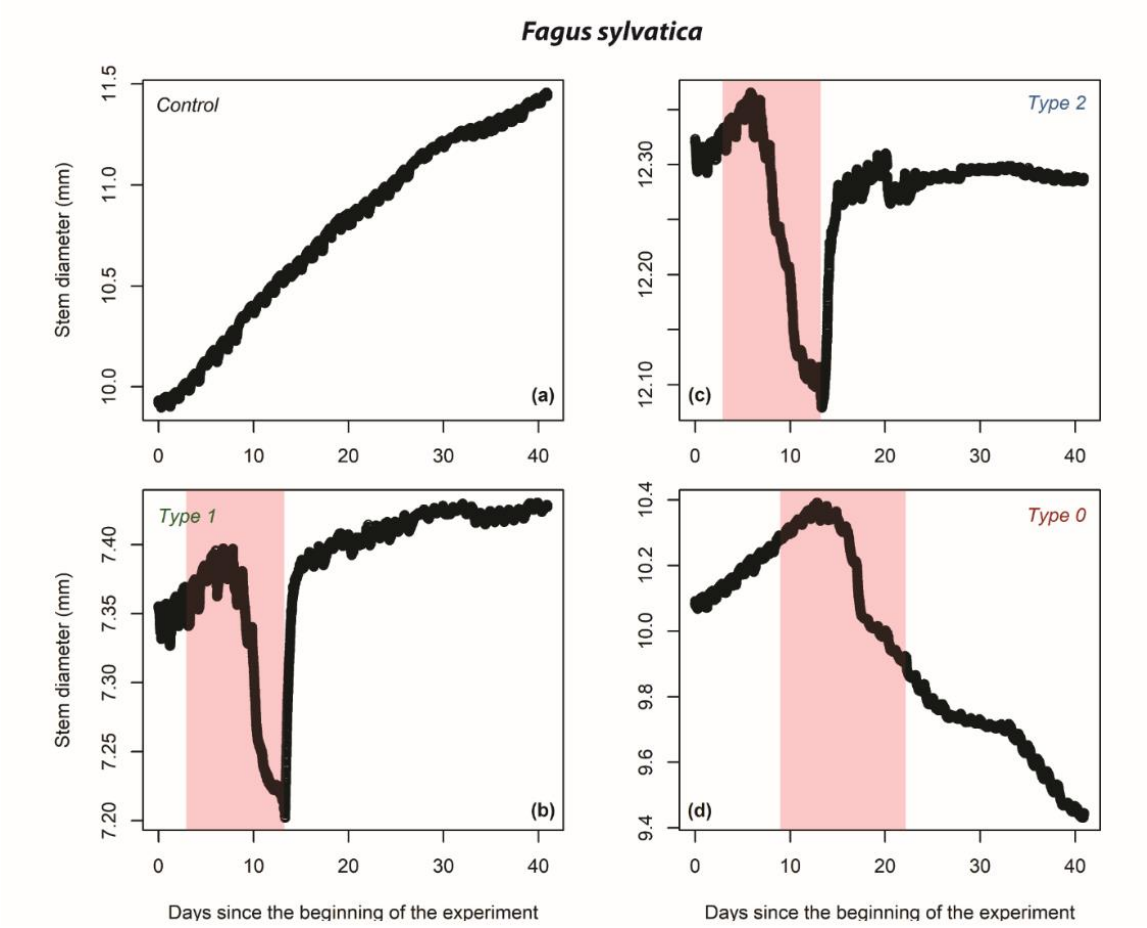


**Figure 62.** Variation of stem diameter during the time-course of the experiment for *Fagus sylvatica*.
Stem diameter (in mm) was recorded by Linear Variable Differential Transformer (LVDT). The light red rectangles represent the period where water was withheld to simulate an extreme drought event. Panel **(a)** represents a tree in control conditions, **(b)** a Type 1 tree, i.e., a tree that fully recovered its initial diameter after being re-watered. **(c)** Type 2 tree, i.e., a tree that recovered 80% of its initial diameter, **(d)** a Type 0 tree, i.e., a tree that did not recovered its initial diameter.

## *3.3. Capacity of recovery from drought and variation of physiological traits at the time of re-watering*

### *3.3.1. Die or survive?*

Globally, for *A. concolor*, 26 trees died and 24 survived during the following year of the drought experiment. For *F. sylvatica*, 14 trees died whereas 26 survived during the following year of the drought experiment. For both species, one of the control trees died the year following the experiment. Looking more in detail and according to the different types defined earlier, for both species, T1 trees (RC>95%) showed a survival rate after one year of 100%. T0 trees (RC<5%) all died after a year of re-watering. The survival rate of T2 trees varied across species. For *A. concolor*, 10 trees out of 23 survived the drought experiment after a year. For *F. sylvatica*, 9 trees out of 12 survived after a year of re-watering.

### 3.3.2. *Stem water potential, PLC and tree survival*

Before re-watering we noticed for *A. concolor* and *F. sylvatica*, that the trees that died from the experiment presented lower $\Psi_{Stem}$ values than the trees that survived the drought event (Figure 63).

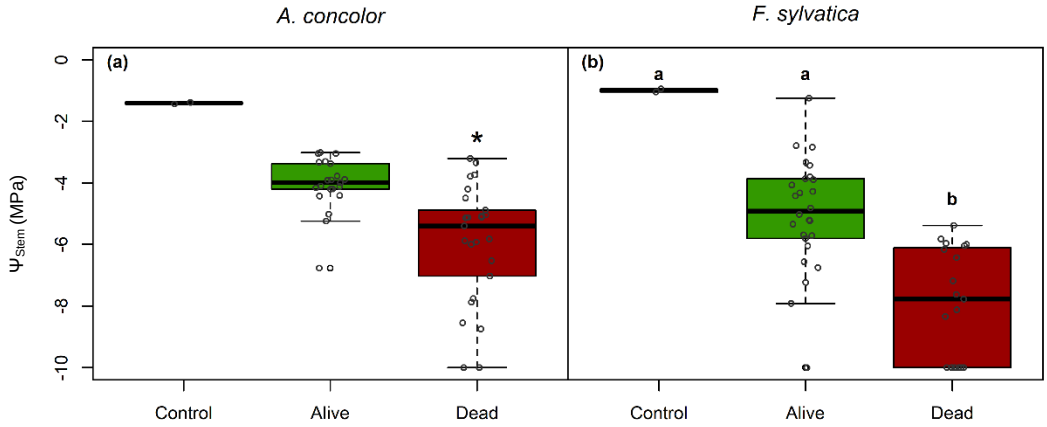


**Figure 63.** Levels of stem water potential ($\Psi_{Stem}$) for **(a)** *Abies concolor* and **(b)** *Fagus sylvatica* in control conditions (Control) or at the time of re-watering for trees that survived the experiment (Alive) and trees that died from drought (Dead). Stars (for *A. concolor*) and letters (for *F. sylvatica*) represent statistical differences between the groups (*a=0.05*).

In control conditions, the mean levels of PLC in the stem for *A. concolor* and *F. sylvatica* were of 1.6±1.2 and 30.9±3.8 respectively. Before re-watering, the PLC measured in the stems of the trees exposed to drought varied from 15 to 100 for *A. concolor* whereas it went from 11.3 to 99.8 for *F. sylvatica*. In the case of *A. concolor*, the trees that survived the experiment also presented lower PLC values than the ones that died from the experiment (Figure 64a). However, this was not the case for *F. sylvatica* trees which showed no differences in PLC levels BRW between the surviving and dying trees (Figure 64b).

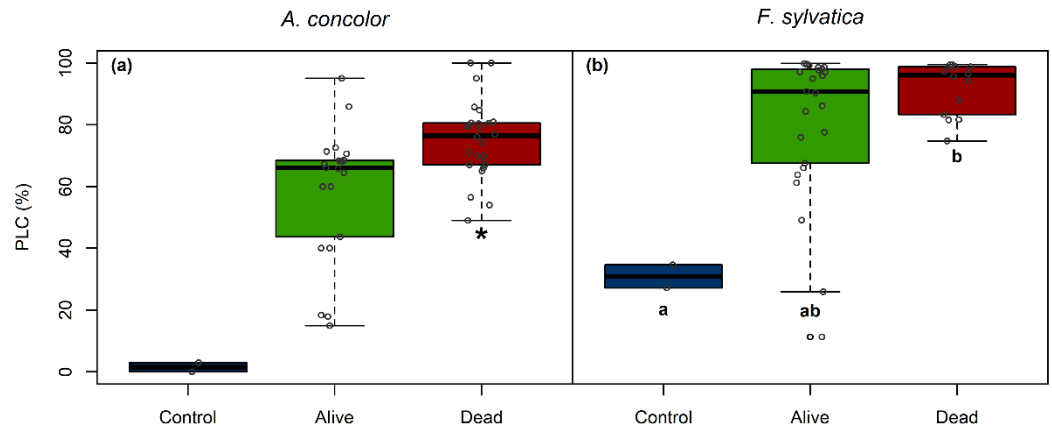


**Figure 64.** Levels of loss in hydraulic conductance (PLC) for **(a)** *Abies concolor* and **(b)** *Fagus sylvatica* trees in control conditions (Control) or at the time of re-watering for trees that survived the experiment (Alive) and trees that died from drought (Dead).
Stars (for *A. concolor*) and letters (for *F. sylvatica*) represent statistical differences between the groups (*a=0.05*).

The trees exposed to drought could be divided into 10% classes (Table 2) and the results evidenced, for *A. concolor*, that a single tree dying before reaching a PLC level of 50%. Most of the trees died when presenting a PLC > 50% but could survive until very high level of loss of conductance (PLC > 90%) (Table 2). For *F. sylvatica*, 5 trees died before attaining PLC levels of 88% whereas most of the trees survived even at very high level of PLC (PLC > 90%) and could even survive when showing almost full embolization of their xylem vessels, i.e., when presenting a PLC level of 99% BRW (Table 2).

| | PLC | 0-10% | 10-20% | 20-30% | 30-40% | 40-50% | 50-60% | 60-70% | 70-80% | 80-90% | 90-100% |
|---|---|---|---|---|---|---|---|---|---|---|---|
| A. concolor (N) | Alive | 3 | 3 | 0 | 0 | 3 | 0 | 10 | 3 | 1 | 1 |
| | Dead | 0 | 0 | 0 | 0 | 1 | 2 | 7 | 7 | 6 | 3 |
| F. sylvatica (N) | Alive | 1 | 0 | 2 | 0 | 1 | 0 | 4 | 2 | 2 | 14 |
| | Dead | 0 | 0 | 0 | 0 | 0 | 0 | 0 | 1 | 4 | 9 |

**Table 2.** PLC variability across classes of 10% for *Abies concolor* and *Fagus sylvatica* trees before re-watering.

### 3.3.3. *Cellular damages and tissue dehydration at the time of re-watering and their effect on tree survival*

When looking at the $RWC_{Stem}$ values at the stem level BRW, our results show that, for both species, on average trees that survived the drought event presented higher $RWC_{Stem}$ values than tree that subsequently died. Indeed, for *A. concolor*, the recovering trees presented a mean $RWC_{Stem}$ value of 53.9±8.1% against 43.6±7.8% for dying trees (Figure 65a). In the case of *F. sylvatica*, surviving trees presented a mean $RWC_{Stem}$ value of 71.0±4.3% whereas dying trees showed a mean $RWC_{Stem}$ value of 52.6±19.3% (Figure 65b).

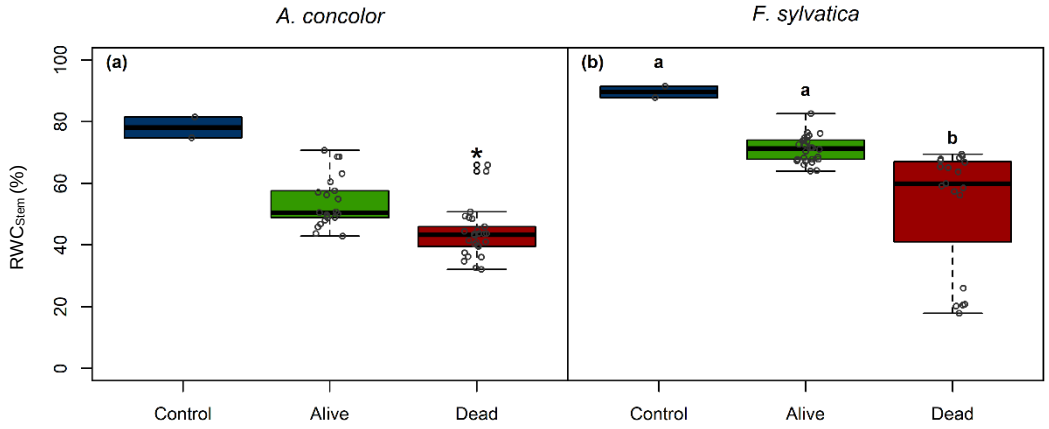


**Figure 65.** Levels of stem relative water content ($RWC_{Stem}$) for **(a)** *Abies concolor* and **(b)** *Fagus sylvatica* trees in control conditions (Control) and right before re-watering for trees that survived the experiment (Alive) and trees that died from drought (Dead).
Stars (for *A. concolor*) and letters (for *F. sylvatica*) represent statistical differences between the groups (*a=0.05*).

At the time of re-watering, *A. concolor* recovering trees showed, on average, a lower level of cellular damages than dying trees (Alive: EL=56.2±14.0%; Dead: EL=72.6±13.7%) (Figure 66a). This was not the case for *F. sylvatica* trees that showed no differences in their level of stem cellular damages BRW (Alive: EL=31.4±8.4%; Dead: EL=42.0±21.5%) (Figure 66b).

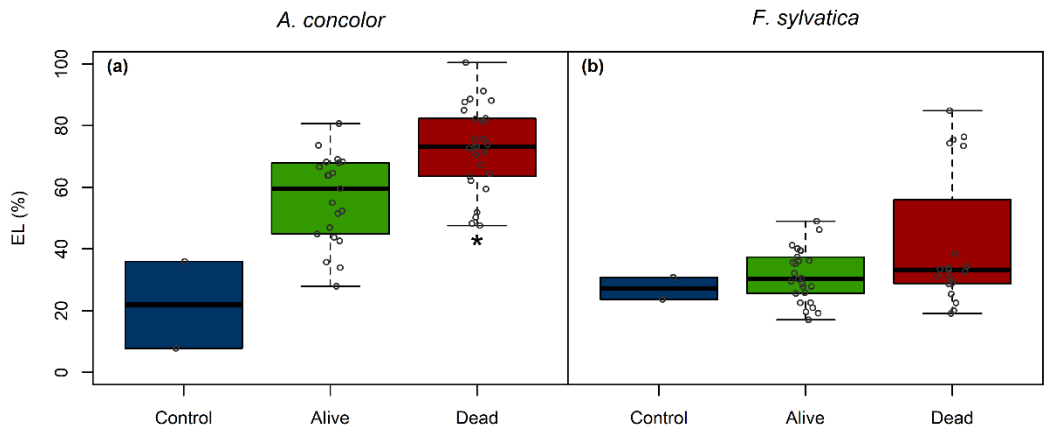


**Figure 66.** Levels of cellular damages (EL) for **(a)** *Abies concolor* and **(b)** *Fagus sylvatica* trees in control conditions (Control) and right before re-watering for trees that survived the experiment (Alive) and trees that died from drought (Dead). Stars (for *A. concolor*) represent statistical differences between the groups (*a=0.05*).

### *3.3.4. Loss of stem diameter during dehydration and stem diameter recovery capacity after re-watering and their effect on tree survival*

During dehydration, stems showed a noticeable shrinkage (PLD) according to the LVDT dynamic. Alive trees showed, for *A. concolor* an average PLD of 6.3±1.7% lower than the one of dying trees (PLD = 7.9±2.3%) (Figure 67a). For *F. sylvatica* the average PLD value of surviving trees was calculated as 2.6±0.8% which was lower than the PLD of dying trees (6.0±4.7%) BRW (Figure 67b).

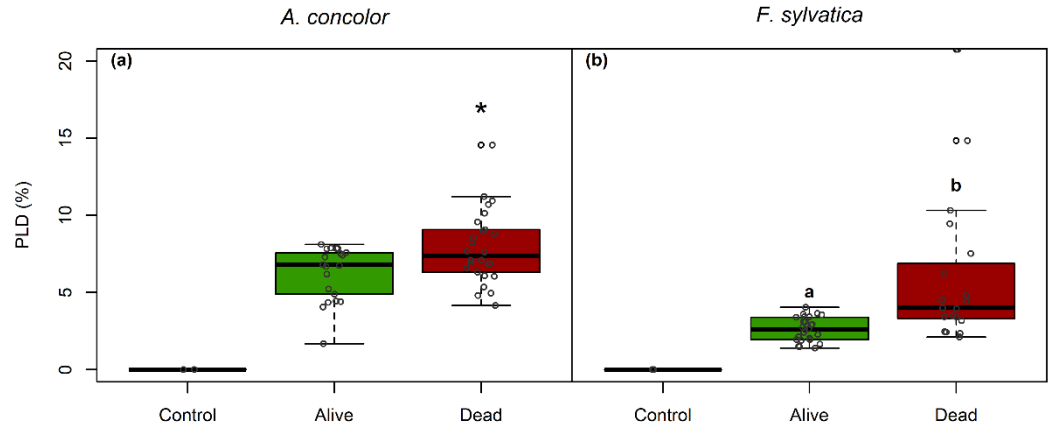


**Figure 67.** Percentage loss of stem diameter (PLD) for **(a)** *Abies concolor* and **(b)** *Fagus sylvatica* trees in control conditions (Control) and right before re-watering for trees that survived the experiment (Alive) and trees that died from drought (Dead). Stars (for *A. concolor*) and letters (for *F. sylvatica*) represent statistical differences between the groups (*a=0.05*).

After re-watering the pots, the stem RC for *A. concolor* differed between trees that survived the experiment and the ones that did not. Alive trees showed higher RC values (86.2±19.2%) than dying trees (25.2±33.3%) (Figure 68a). The same conclusion was obtained for *F. sylvatica* trees whose surviving trees were able to recover 91.7±13.6% of their initial stem diameter when dying trees only recovered 7.9±20.1% of their initial stem diameter (Figure 68b).

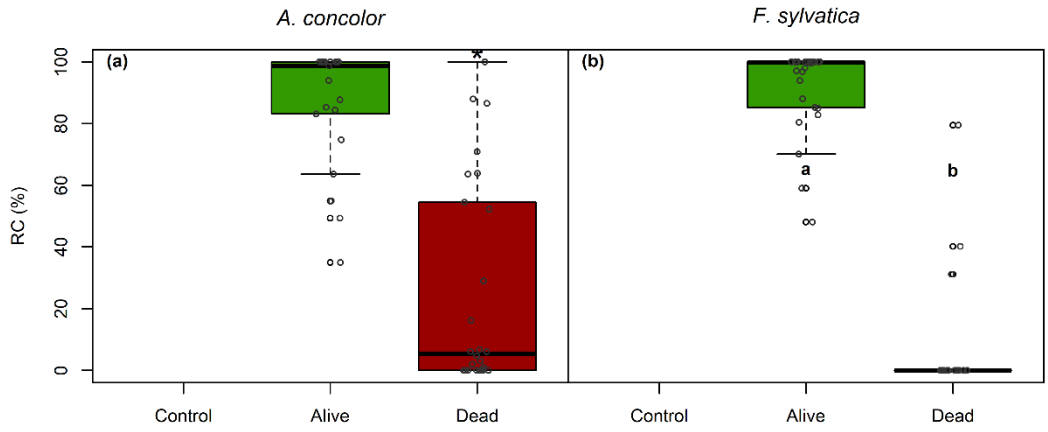


**Figure 68.** Percentage of stem recovery capacity (RC) for **(a)** *Abies concolor* and **(b)** *Fagus sylvatica* trees in control conditions (Control) and after re-watering for trees that survived the experiment (Alive) and trees that died from drought (Dead). Stars (for *A. concolor*) and letters (for *F. sylvatica*) represent statistical differences between the groups (*a=0.05*).

### *3.4.A multi-explanation for tree survival under drought conditions? A PCA analysis*

The contrasted dynamics observed in $\Psi_{Stem}$, PLC, $RWC_{Stem}$, EL, PLD and RC suggest that the survival after a drought event may result from a combination of different traits. Indeed, none of the previously presented physiological parameter could set a threshold that allowed the distinction of the binary response of the tree after re-watering. Thus, the variability in the survival response to drought has been explored through multivariate principal component analysis (PCA) with respect to the survival response (i.e., alive, or dead). The *A. concolor* dataset exhibited an overall Kaiser-Mayer-Olkin (KMO) index of 0.782. The *F. sylvatica* dataset exhibited an overall KMO index of 0.694. Both KMO suggested that PCA had a good ability to summarize the information contained in the datasets and that PCA was usable on such dataset.

For *A. concolor*, the first four components contributed to 93.3% of cumulated variance (from 61.2 to 7.1% for each component; Table 3) but the first two components explained 76.6% of the cumulated variance. $RWC_{Stem}$, $\Psi_{Stem}$, PLC, RC and EL mainly contributed to the first component (Dimension 1: Dim-1, Figure 69a). PLD mainly contributed to the second component (Dimension 2: Dim-2, Figure 69b).

| Principal components | Eigenvalue | Percentage of variance | Cumulative percentage of variance |
|---|---|---|---|
| comp 1 | 3.67 | 61.24 | 61.24 |
| comp 2 | 0.92 | 15.39 | 76.63 |
| comp 3 | 0.58 | 9.63 | 86.26 |
| comp 4 | 0.42 | 7.05 | 93.31 |
| comp 5 | 0.29 | 4.88 | 98.19 |
| comp 6 | 0.11 | 1.81 | 100 |

**Table 3.** Table representing the contribution of the different components to the cumulated variance for *Abies concolor*.

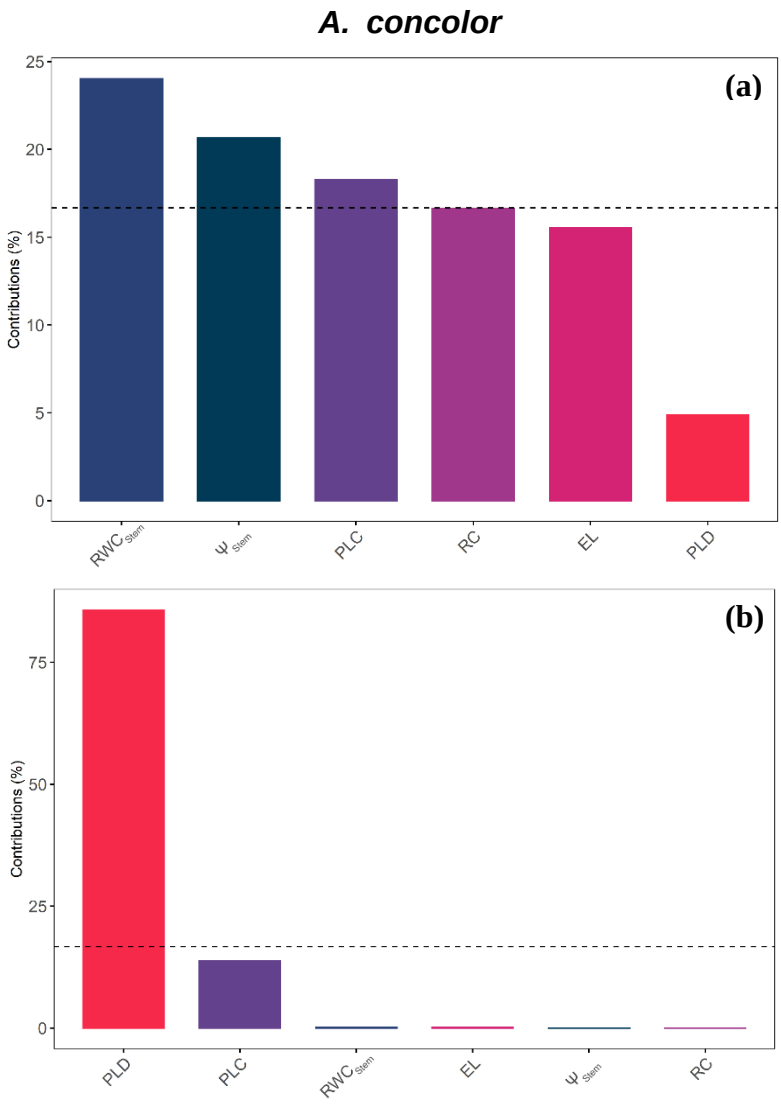


**Figure 69.** Contribution of each parameter measured right before re-watering to **(a)** Dimension 1 (Dim-1) and **(b)** Dimension 2 (Dim-2) of the PCA analysis run for *Abies concolor*.
Each colour represents one parameter.

According to Dim-1 and Dim-2, trees were discriminated from left to right along the x line. Trees that survived the drought event were located on the right of the x line, towards $RWC_{Stem}$, $\Psi_{Stem}$ and RC whereas trees that died consequently to the drought event were located on the left towards EL and PLC (Figure 70).

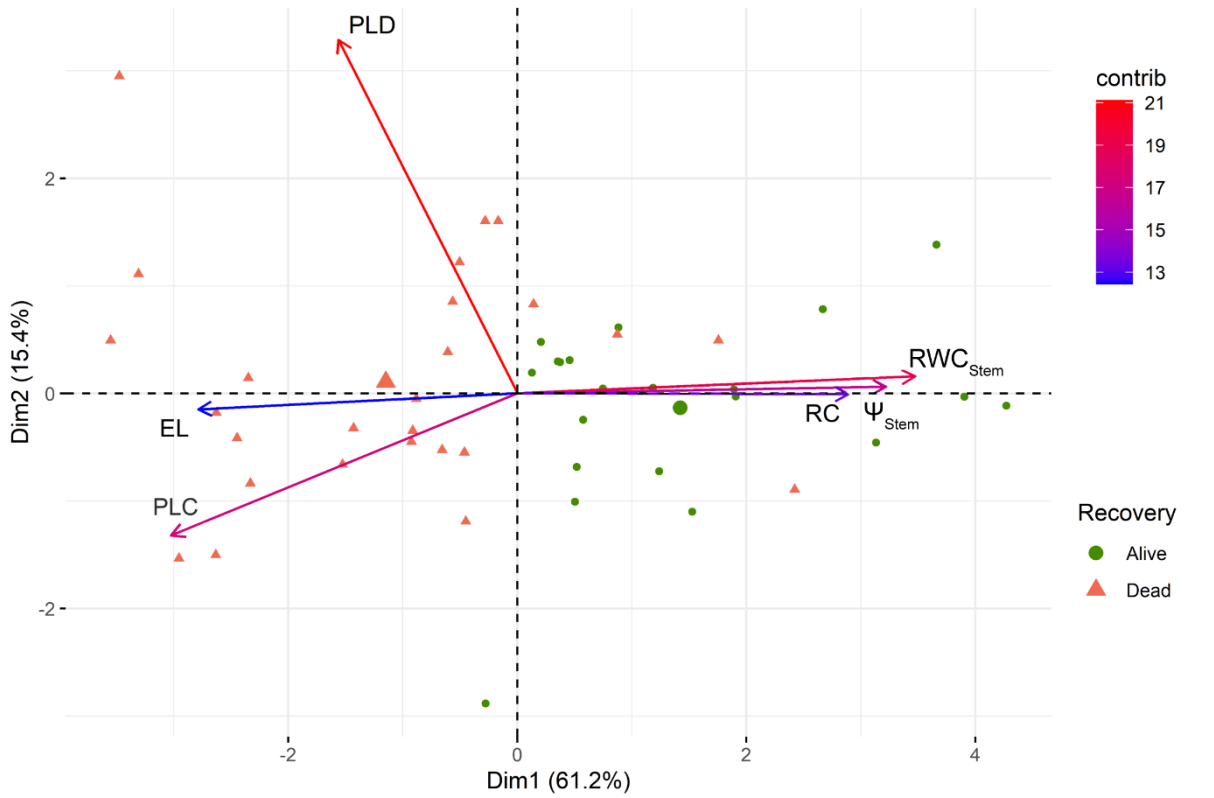


**Figure 70.** Principal Component Analysis (PCA) based on the survival response from drought after a year of re-watering for *Abies concolor*. The green dots represent the individuals that survived from the drought-event while the red triangles represent the individual that died from drought. Dimensions 1 and 2 are represented as they maximize the discrimination between alive and dead individuals.
The "contrib" scale represents the contribution of each parameter to Dim1-2.
EL = cellular damages, PLC = Percentage Loss of hydraulic Conductance, PLD = Percentage Loss of stem Diameter, RC = stem diameter Recovery Capacity, $RWC_{Stem}$ = Stem Relative Water Content, $\Psi_{Stem}$ = Stem Water Potential.

For *F. sylvatica*, the first four components contributed to 89.8% of cumulated variance (from 45.4 to 8.1% for each component; Table 4) but the first two components explained 66.8% of the cumulated variance. $RWC_{Stem}$, RC, $\Psi_{Stem}$ and PLD mainly contributed to the first component (Dimension 1: Dim-1, Figure 71a). EL and PLC mainly contributed to the second component (Dimension 2: Dim-2, Figure 71b).

| Principal components | Eigenvalue | Percentage of variance | Cumulative percentage of variance |
|---|---|---|---|
| comp 1 | 2.73 | 45.44 | 45.44 |
| comp 2 | 1.28 | 21.33 | 66.76 |
| comp 3 | 0.9 | 15.01 | 81.77 |
| comp 4 | 0.48 | 8.07 | 89.84 |
| comp 5 | 0.4 | 6.62 | 96.46 |
| comp 6 | 0.21 | 3.54 | 100 |

**Table 4.** Table representing the contribution of the different components to the cumulated variance for *Fagus sylvatica*.

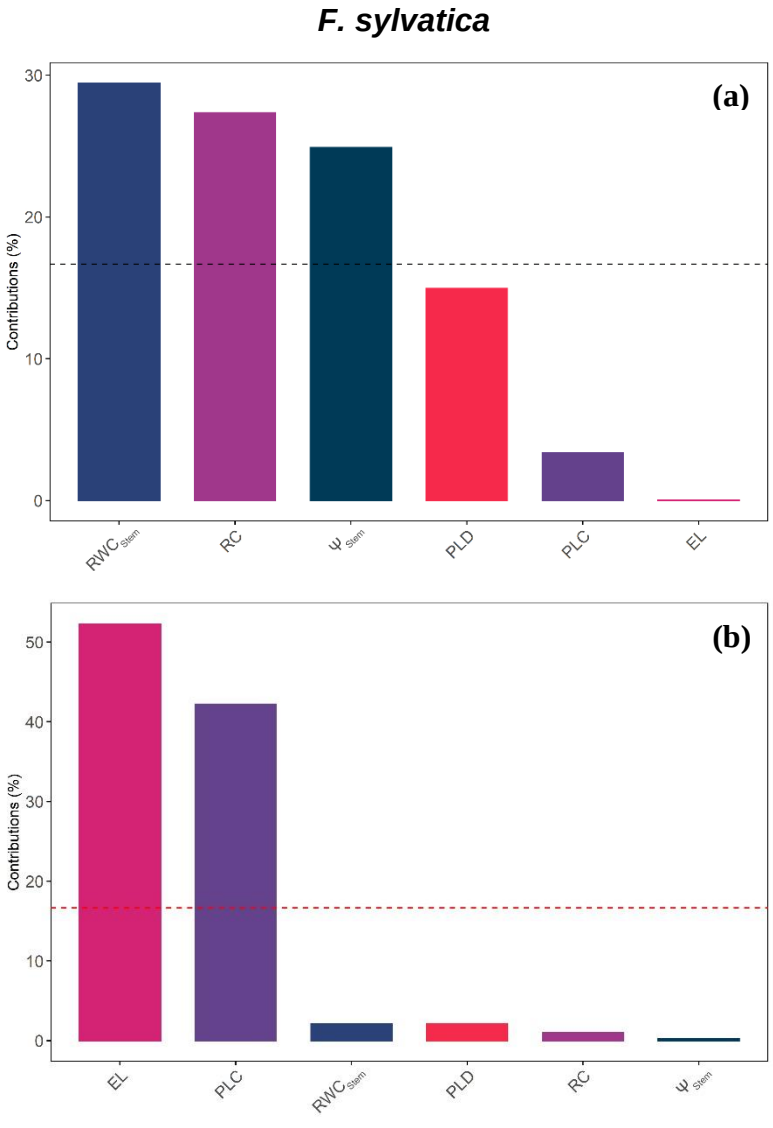


**Figure 71.** Contribution of each parameter measured right before re-watering to **(a)** Dimension 1 (Dim-1) and **(b)** Dimension 2 (Dim-2) of the PCA analysis run for *Fagus sylvatica*. Each colour represents one parameter.

According to Dim-1 and Dim-2, trees were discriminated from left to right along the x line. Trees that survived the drought event were located on the right of the x line, towards $RWC_{Stem}$, $\Psi_{Stem}$ and RC whereas trees that died consequently to the drought event were located on the left towards PLD (Figure 72).

A correlation matrix established between the different traits measured BRW and after re-watering, shows that the traits explaining tree survival according to the PCA analyses (i.e., RC, $RWC_{Stem}$ and $\Psi_{Stem}$) were correlated positively between them for both species (Figure S6). A positive correlation was also observed within the traits explaining tree death for *A. concolor* (i.e., EL and PLC) (Figure S6a). For *F. sylvatica,* no positive correlation could be observed for the traits explaining tree death as only the PLD explained tree death (Figure S6b). For both species, traits explaining tree survival and tree death were negatively correlated (Figure S6).

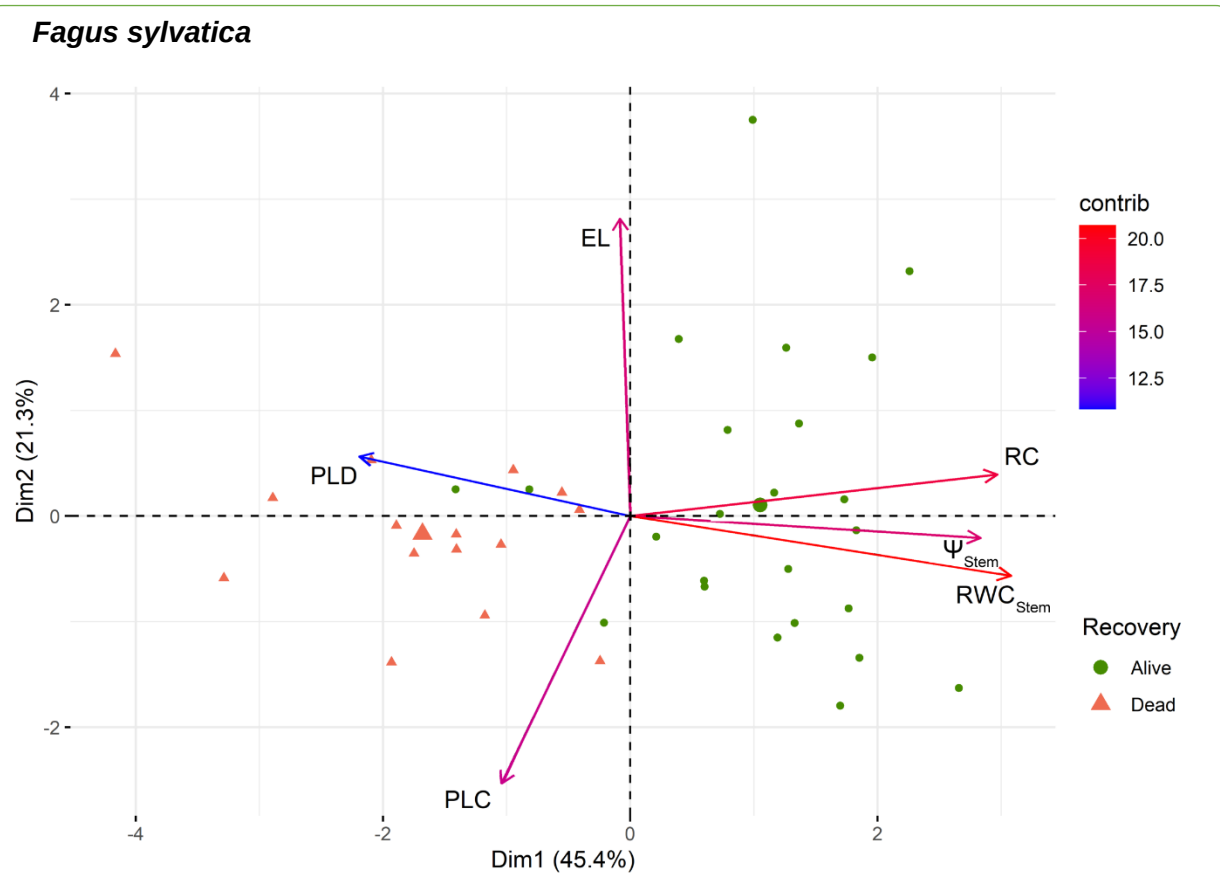


**Figure 72.** Principal Component Analysis (PCA) based on the survival response from drought after a year of re-watering for *Fagus sylvatica*. The green dots represent the individuals that survived from the drought-event while the red triangles represent the individual that died from drought. Dimensions 1 and 2 are represented as they maximize the discrimination between alive and dead individuals.
The "contrib" scale represents the contribution of each parameter to Dim1-2.
EL = cellular damages, PLC = Percentage Loss of hydraulic Conductance, PLD = Percentage Loss of stem Diameter, RC = stem diameter Recovery Capacity, $RWC_{Stem}$ = Stem Relative Water Content, $\Psi_{Stem}$ = Stem Water Potential.

### *3.5.Other thresholds for predicting tree survival?*

For *A. concolor*, it seems that, according to the PCA analysis (Figure 70), $RWC_{Stem}$, PLC, RC and EL could explain tree survival or death from drought a year after-rewatering. Using logistic regressions, we determined the lethal threshold for $RWC_{Stem}$ at which 50% of trees would die ($LD_{50}$-RWC) to be 46.9±1.8% (*Figure S7*). We also determined the lethal threshold for hydraulic failure at which 50% of the tree died ($LD_{50}$) at 58.1±3.5% (Figure S8). We also calculated the $LD_{50}$-RC, i.e., the lethal threshold for stem recovery at which 50% of trees would die, at 71.1±2.7% (Figure S9). Finally, we determined the $LD_{50}$-EL, i.e., the lethal threshold in EL at which 50% of the trees died, at 60.1±3.4% (Figure S10).

For *F. sylvatica*, according to the PCA analysis (Figure 72), $RWC_{Stem}$, RC and PLD explained tree survival or death from drought after re-watering. Using logistic regressions, we determined the $LD_{50}$-RWC at 63.5±1.9% (Figure S11), the $LD_{50}$-RC at 45.9±4.4% (Figure S12) and the $LD_{50}$-PLD, i.e., the lethal threshold in PLD at which 50% of the trees died, at 3.5±0.3% (Figure S13).

### *3.6.Cambium damages as a key for determining tree survival?*

For both species in control conditions, the cambial cells showed that the whole cytoplasm was occupied with large vacuoles (Figure 73a and f; Figure 74a and f). The plasmalemma was closely attached to the cell walls in all cambial cells. BRW, the different types of trees, according to their RC, showed different cambial cells ultrastructure. For *A. concolor* T1 trees (Figure 73b and g), some ultrastructural changes were observed. The plasmalemma was not in contact with the cell wall in most of the cells, making the cytoplasm visible, however, vacuoles were still present showing a certain level of hydration of those cells. For *F. sylvatica* T1 trees (Figure 74b and g), no ultrastructural differences could be observed compared with control plants. The same observations were made for T2 trees that were able to survive the drought event for both species (Figure 73c and h; Figure 74c and h). When looking at T2 trees that did not recover from drought, a disintegration of the cambial cells was observed for both species (Figure 73d and i; Figure 74d and i). For *A. concolor*, almost no vacuoles were noticed in the cambial zone of those trees whereas a visible plasmalemma collapse, i.e., a detachment from the inner cell wall, was noticed in the cambial cells of *F. sylvatica* trees. For T0 trees, in both species (Figure 73e and j; Figure 74e and j), about ~80%-90% of the cambial cells showed complete cellular failure, with a distinctly shrunken cytoplasm and almost no vacuoles.

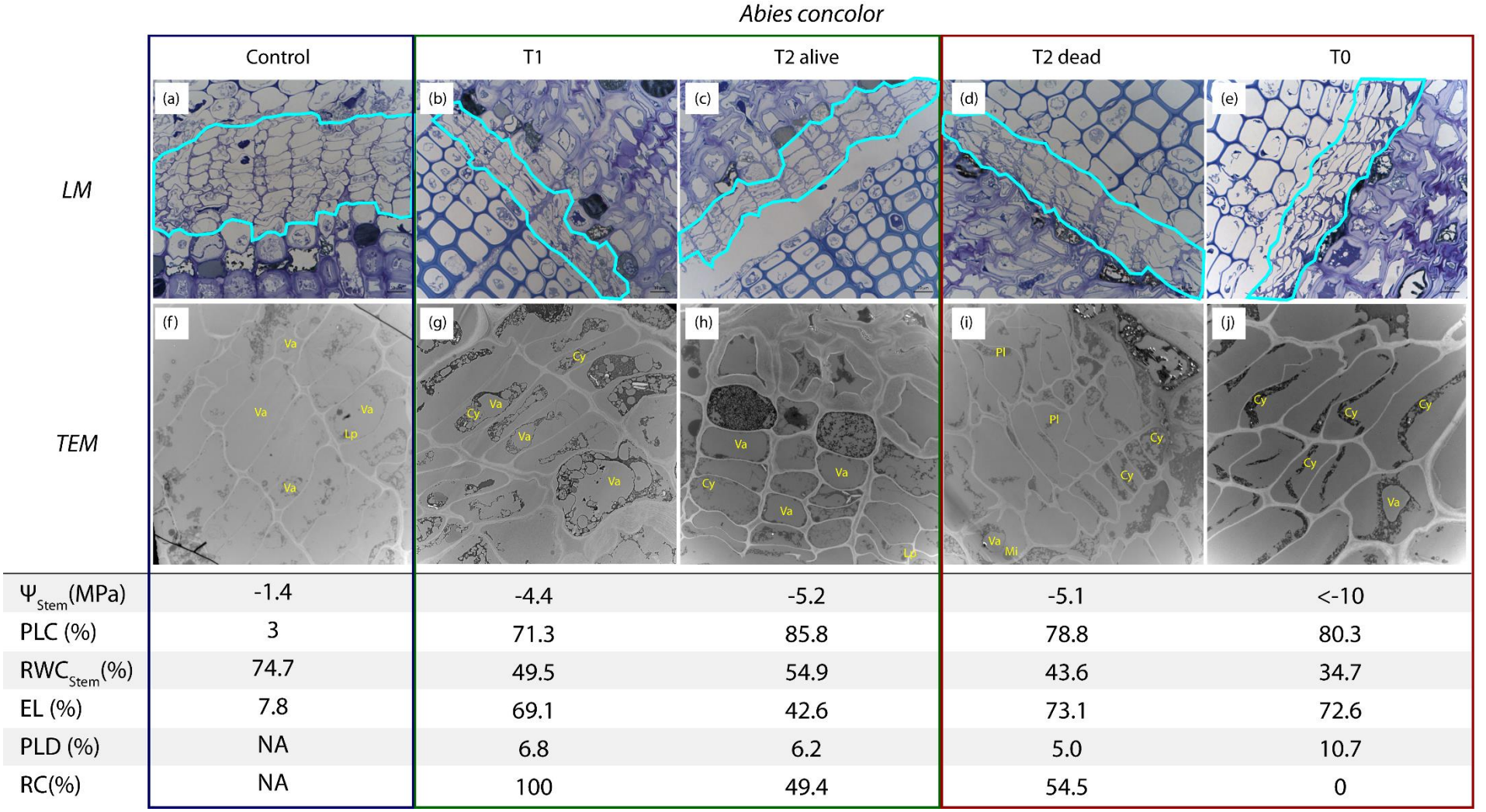


| | Control | T1 | T2 alive | T2 dead | T0 |
|---|---|---|---|---|---|
| $\Psi_{Stem}$(MPa) | -1.4 | -4.4 | -5.2 | -5.1 | <-10 |
| PLC (%) | 3 | 71.3 | 85.8 | 78.8 | 80.3 |
| $RWC_{Stem}$(%) | 74.7 | 49.5 | 54.9 | 43.6 | 34.7 |
| EL (%) | 7.8 | 69.1 | 42.6 | 73.1 | 72.6 |
| PLD (%) | NA | 6.8 | 6.2 | 5.0 | 10.7 |
| RC(%) | NA | 100 | 49.4 | 54.5 | 0 |

**Figure 73.** Transverse light microscopy (LM) and Transmission Electron Microscopy (TEM) images of the vascular cambium in stems of *Abies concolor* in control conditions (Control) and before re-watering after a drought period (T1; T2 alive; T2 dead and T0) associated with their measured physiological parameters at the time of re-watering after re-watering for RC. T1 refers to trees that fully recovered their stem diameter after re-watering, T2 trees partially recovered their stem diameter after re-watering and T0 trees did not recover their stem diameter after re-watering. Surrounded in light blue on the LM images are the cambial cells. Surrounded in blue is the control tree, in green are the samples of trees that survived after a year of re-watering and in red are the samples of trees that died consequently of the drought experiment. T1 and T2 alive trees shows moderately damaged cells whereas T2 dead and T0 shows fully collapse ultrastructure.
Cy = Cytoplasm; Mi = mitochondria; Pl = Plasmalemma; Va = Vacuole.

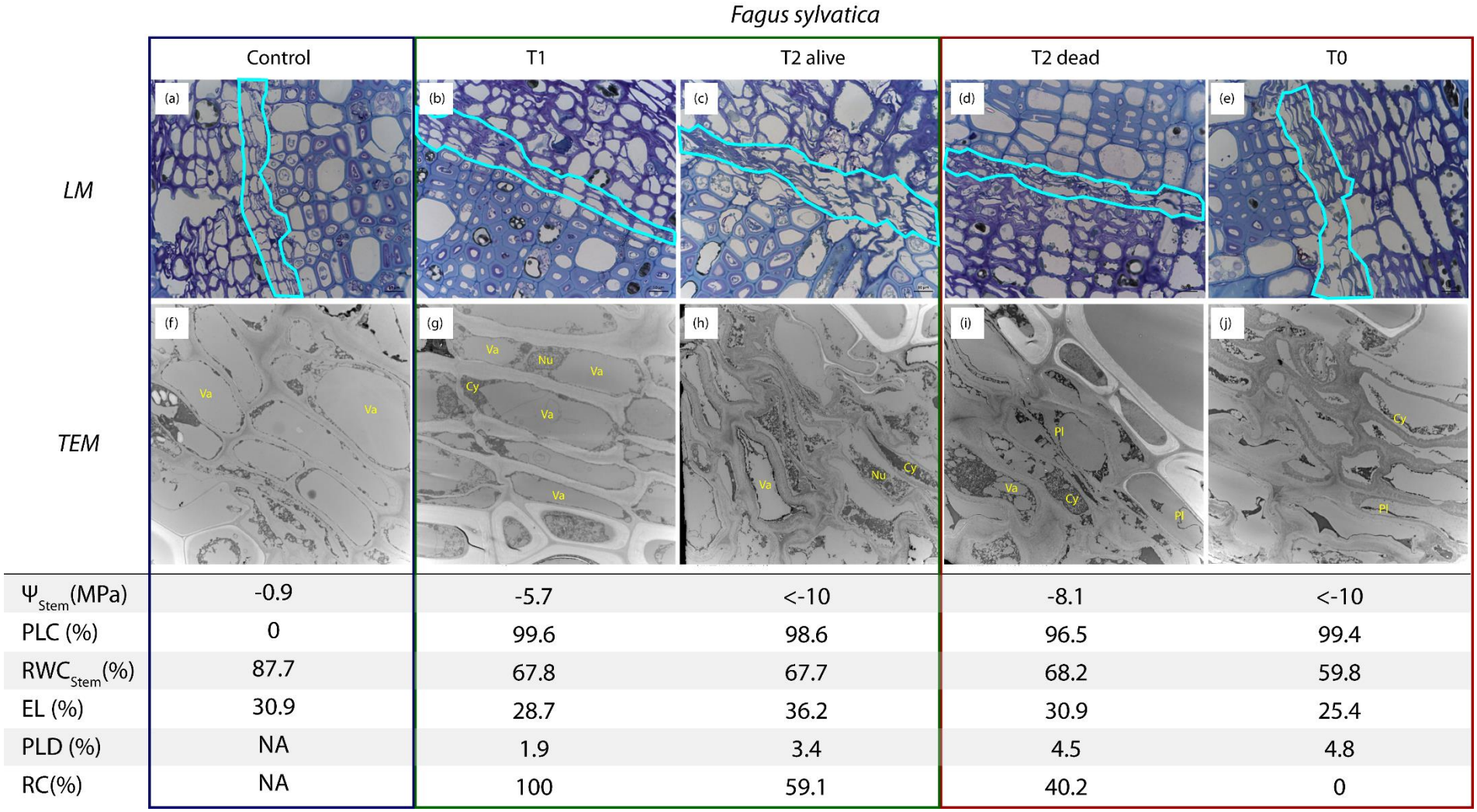


| | Control | T1 | T2 alive | T2 dead | T0 |
|---|---|---|---|---|---|
| $\Psi_{Stem}$(MPa) | -0.9 | -5.7 | <-10 | -8.1 | <-10 |
| PLC (%) | 0 | 99.6 | 98.6 | 96.5 | 99.4 |
| $RWC_{Stem}$(%) | 87.7 | 67.8 | 67.7 | 68.2 | 59.8 |
| EL (%) | 30.9 | 28.7 | 36.2 | 30.9 | 25.4 |
| PLD (%) | NA | 1.9 | 3.4 | 4.5 | 4.8 |
| RC(%) | NA | 100 | 59.1 | 40.2 | 0 |

**Figure 74.** Transverse light microscopy (LM) and Transmission Electron Microscopy (TEM) images of the vascular cambium in stems of *Fagus sylvatica* in control conditions (Control) and before re-watering after a drought period (T1; T2 alive; T2 dead and T0) associated with their measured physiological parameters at the time of re-watering or after re-watering for RC. T1 refers to trees that fully recovered their stem diameter after re-watering, T2 trees partially recovered their stem diameter after re-watering and T0 trees did not recover their stem diameter after re-watering. Surrounded in light blue on the LM images are the cambial cells. Surrounded in blue is the control tree, in green are the samples of trees that survived after a year of re-watering and in red are the samples of trees that died consequently of the drought experiment. T1 and T2 alive trees shows moderately damaged cells whereas T2 dead and T0 shows fully collapse ultrastructure.
Cy = Cytoplasm; Nu = Nucleus; Pl = Plasmalemma; Va = Vacuole.

## 4. Discussion

### *4.1.Plant survival is not necessarily correlated to high losses of hydraulic conductance*

Our results provide strong evidence that plant survival is not necessarily correlated to high losses of hydraulic conductance. Indeed, our results shows that trees can recover from drought even when surpassing the $P_{50}$ for conifers (*A. concolor*) and the $P_{88}$ for angiosperms (*F. sylvatica*). Those results agree with the ones obtained by Hammond *et al.* (2019) on *Pinus taeda* L. and by Mantova *et al.* (2021) on *Prunus lusitanica* L. (an angiosperm) and *Pseudotsuga menziesii* M. (a conifer). However, according to our PCA analyses, high levels of PLC only play a role in determining the survival capacity for *A. concolor* and does not appear as a triggering factor for plant death in the case of *F. sylvatica*, probably because of the small range of PLC values reported for dying or surviving trees (PLC mostly varied from 80 to 100% for the angiosperm in our study). Therefore, we determined, according to Hammond *et al.* (2019), the $LD_{50}$, i.e., the lethal death threshold above which the probability to die is higher than the one to survive, at 58PLC for *A. concolor*. This result, although higher than the conventional $P_{50}$ value used for predicting tree death (Brodribb & Cochard, 2009), appears as lower than the one calculated by Hammond *et al.* (2019) on *P. taeda* that presented a $LD_{50}$ of 80.2PLC and thus question the variability of this lethal threshold across species.

*F. sylvatica* trees could recover from the drought event even until reaching almost full embolization. Those results agree with our previous study (Mantova *et al.*, 2021) that demonstrated how some *P. lusitanica* were able to survive from a drought event even if the stem xylem was nearly fully embolized (PLC=99.8) and with the results of Vilagrosa *et al.* (2003) where only trees presenting PLC levels of 100% would die from the drought event. However, these important levels of embolism measured at the time of re-watering may be overestimated. Indeed, in our study the PLC was measured in lateral branches, at the nearest point of the main stem. However, trees might be subjected to within-plant hydraulic segmentation with distal plant parts, such as leaves or small branches being more vulnerable to drought-induced xylem embolism than central parts such as trunk and would suggest that the actual PLC of the trunk is probably lower than the measured PLC value in the lateral branches (Tyree & Zimmermann, 2002; Johnson *et al.*, 2016). Also, during transpiration $\Psi_{xylem}$ should always be lower in more distal parts of the hydraulic pathway, generating a greater tension and exacerbating the risk of xylem cavitation (Charrier *et al.*, 2016). Considering this, the PLC measured in the branches might also have been overestimated. This would suggest that, in order to predict tree mortality under drought conditions, measuring the PLC in a single point would not be sufficient and it would be necessary to consider the PLC level of the whole plant when implementing models.

### *4.2.Having access to the water present in the soil might be as important as maintaining hydraulic functioning to survive from a drought event*

More surprisingly, our results on *F. sylvatica* indicate that a few numbers of trees could die even when presenting PLC level <88% while only one tree of *A. concolor* died before attaining a PLC value above 50%. The fact that some plants with PLC levels lower than the ones considered for hydraulic failure were not able to recover and survive from the drought event

despite having, *in theory*, access to water suggest that some global irreversible hydraulic disconnection between the tree and the soil had already happen during the drought event. Indeed, even though at the time of rewatering, our PLC measurements, where they were performed, showed not yet a local hydraulic failure, the recovery observations demonstrated that there was already a global hydraulic disfunction that broke the hydraulic continuum between the soil and the plant. This could be due to the hair shrinkage that happens during drought and that can hydraulically disconnect the tree from the soil (Duddek *et al.*, 2022). Indeed, if under mild drought conditions the hair shrinkage could accelerate the rate of dehydration of the whole plant, it is expected that, under an extreme drought, such as the one encountered in our experiment, an important shrinkage of the roots and particularly roots hairs would happen. This shrinkage, associated with soil dehydration may lead tree to death through the disruption of the capillary continuum from the soil to the root (Körner, 2019), making the disponible water in the soil inaccessible to the tree and provoking fatally its full embolization and death. In addition, as water movements to the roots depend on the hydraulic conductivity of the soil and the distance between the soil and the root, and as these parameters are themselves influenced by the soil composition and texture (Nobel & Cui, 1992), a difference in soil composition between the pots of the trees in our experiment could have been at the origin of the differences in response at the time of rehydration. Indeed, it is possible that some trees had a more clayey substrate than others and that these substrates were more prone to shrinkage during drought and less prone to return quickly to their initial state (Fernandes *et al.*, 2015) during rewatering, thus favouring a hydraulic disconnection between the roots and the soil for some individuals. Furthermore, the same result could also have been observed if the tree underwent fine roots failure as it was the case for *Juniperus* trees where the roots were the first to cavitate under drought conditions, condemning the recovery of the tree even if water was made available before the hydraulic failure of the aerial part (Johnson *et al.*, 2018). Therefore, this would highlight the fact that, in order to recover from drought, water not only needs to be available in the soil but also needs to be accessible for the plant. Thus, if a tree is able to maintain a minimal hydraulic functioning with PLC greater than 50% for conifers and of almost 100% for angiosperms, they should be able to recover from the drought event if the soil to root to plant continuum is maintained. Therefore, considering a value of global hydraulic functioning of the tree integrating, at the same time, soil hydraulic disconnection and root hydraulic functioning as well as the hydraulic functioning of the aerial part of the tree would help to better predict the recovery of trees after a drought event.

### *4.3.Seeking new physiological thresholds*

#### *4.3.1. High levels of $RWC_{Stem}$ correlate with tree capacity to recover from drought*

Our PCA analyses identified $RWC_{Stem}$ as the main parameter contributing to the distinction between surviving and dying trees. In fact, $RWC_{Stem}$ contributed to dimension-1 (i.e., alive or dead distinction) for ~25% for *A. concolor* and for ~30% for *F. sylvatica*. Those results agree with the ones from Mantova *et al.* (2021) and Sapes & Sala (2021) where RWC appeared as a potential threshold for predicting tree mortality under drought conditions. They also comfort the position taken by Martinez-Vilalta *et al.* (2019) which advocated for a better focus on water pools when trying to understand and predict tree mortality from drought.

Our calculation of a $LD_{50}$-RWC evidenced that the possibility to die became predominant when the level of $RWC_{Stem}$ went below 47% for *A. concolor* and of 63% for *F. sylvatica*. Those values appear as a lot lower than the critical RWC ($RWC_{crit}$) values identified for the onset of cellular mortality, that were of 78% for *A. concolor* and 88% for *F. sylvatica*. This suggest that, with all trees of both species presenting lower $RWC_{Stem}$ than their $RWC_{crit}$ at the time of re-watering, trees can recover from drought even if the $RWC_{crit}$ for cellular integrity is overpassed. Because $RWC_{crit}$ only represents the onset of cellular damages when a tissue undergoes a dehydration, and because it has been demonstrated that high levels of cellular damages were needed to incur tree death (Mantova *et al.*, 2021), our results show that the $RWC_{crit}$ value below which cellular integrity begins to be compromised cannot act as a good threshold when trying to implement mechanistic models for predicting tree mortality. However, it could help comparing the cellular resistance to dehydration across species and tissues. Nevertheless, the $LD_{50}$-RWC might help predicting tree probability of survival for both species.

#### *4.3.2. Level of EL is not always a good indicator for predicting tree mortality from drought*

Our results show that the level of EL before re-watering might be a good indicator to discriminate trees that will or will not survive from drought in the case of conifer trees but not in the case of angiosperms. Those results agree with the ones obtained on both conifers and angiosperms by Mantova *et al.* (2021). Indeed, in this study, *P. menziesii* recovering trees consistently showed lower EL values than the ones that did not recover from the drought event immediately after re-watering. However, no EL changes were observed for *P. lusitanica* recovering or dead trees. These results obtained on the angiosperm species, both in this experiment and in the study by Mantova *et al.* (2021), might be explained by the fact that the EL method might not be sensitive enough to detect changes in the number of dead cells during a short dehydration. Indeed, the magnitude of the changes in EL for *F. sylvatica* trees was only of 32% during the time-course of the experiment whereas it was of 93% for *A. concolor* ones. However, after weeks of dehydration, the EL method could detect significant changes in the number of dead cells even in the case of *F. sylvatica*. Therefore, this suggest that most of the cells within our *F. sylvatica* samples were probably not dead at the time of sampling, but the survival of the trees was already hindered by the death of very specific cells whom changes were not detectable using the EL method or other factors such as the hydraulic failure of the whole hydraulic pathway. Indeed, even though trees can rely on their own water reserves under drought conditions which could maintain the metabolism of the cells a bit longer (Epila *et al.*, 2017) and explain the important amount of living cells BRW, if the plant cannot absorb water after re-hydrating the soil, the water reserves will ultimately dry and cells would die from dehydration.

#### *4.3.1. The percentage loss of stem diameter might correlate with tree death in the case of angiosperms*

Our results show that the PLD described by Lamacque *et al.* (2020) on lavender species (i.e., on an angiosperm woody species) could work as a proxy to identify tree death in the case of *F. sylvatica* but not in the case of *A. concolor*. Indeed, the PLD contributed to ~15% of the dimension-1 of the PCA analysis discriminating dead and alive trees. However, if those results

agree with the ones of Lamacque *et al.* (2020), the PLD value that we calculated during our study, above which trees will die from drought, appears as much lower than the one encountered in their study. Indeed, if Lamacque *et al.* (2020) evidenced a PLD threshold at 21% for Lavender species, our study on *F. sylvatica* reveals that once the PLD has reached 10%, no surviving trees are observed. This would suggest that such PLD threshold would vary importantly across species. Thus, if the PLD were to become a new standard to assess tree death, broader studies would be required to characterize the lethal PLD for different species.

More surprisingly, our results on *A. concolor* did not evidence any PLD threshold for drought-induced tree mortality which is to be discussed and corroborated with future studies as none, to date, has tried to evidence a PLD on conifer species. The difference between this conifer and the angiosperm species studied could be explained by the capacitance of the stems. Indeed, stem capacitance is the amount of water released as stem xylem pressure become more negative and contributes to embolism avoidance and therefore hydraulic safety through transient release of stored water into the transpiration stream (Johnson *et al.*, 2012). Indeed, it has been demonstrated that in order to achieve higher resistance to embolism (more negative $P_{50}$) in wood, species must construct a network of fibres and conduits with thick walls (Pratt *et al.*, 2007) which precludes them from presenting large volumes of living parenchyma cells, which may be a source of capacitance (Johnson *et al.*, 2012) and thus water movement and stem shrinkage. Here, as *A. concolor* presented a lower $P_{50}$ than *F. sylvatica*, we can hypothesize that the hydraulic capacitance of *F. sylvatica* would be higher than the one of *A. concolor*. Therefore, *F. sylvatica* trees would be able to show a distinguishable loss in stem diameter before dying from water depletion, whereas changes in stem diameter of *A. concolor* between recovering and dying trees would be small and make it difficult to distinguish between those able to recover and those that are not.

#### *4.3.2. The recovery capacity of the stems could help predicting the possibility of tree survival*

Our results showed that the recovery capacity of the stems after re-watering is correlated with the survival of the trees for both species, contributing to almost 20% and 27% of the survival explanation for *A. concolor* and *F. sylvatica* respectively according to the PCA analyses. Thus, we determined that the probability to die from the drought event increases when the stem diameter after re-watering does not reach 71% for *A. concolor* and 45% of their initial diameter for *F. sylvatica*.

The loss in the capacity of the tree to fully recover its initial diameter, i.e., showing an irreversible shrinkage after alleviating the stress conditions, has been considered as a reliable indicator of frost damage (Améglio *et al.*, 2003; Lintunen *et al.*, 2015) and associated with cell damage in the elastic compartments of the plants under drought conditions (Lamacque *et al.*, 2020). However, by investigating thoroughly the physiology after re-watering and testing the relationship between loss of recovery capacity and tree survival as suggested by Lamacque *et al.* (2020), our results show that the RC of the stem only correlates with a probability of survival and does not always explain, in the absolute, the tree survival on the longer term. Indeed, our results evidenced that trees presenting exactly the same RC were not always able to survive.

### *4.4.Surviving from drought: when meristems matter*

Despite showing good correlation between the RC, $RWC_{Stem}$ and the survival probability for both species, none of the indicators followed during our experiment could exactly identify the time at which trees died from drought and thus function as a binary response when implemented in a model. However, our experiment showed that the main difference between two trees presenting nearly the same physiological traits values (i.e., $\Psi_{Stem}$, PLC, $RWC_{Stem}$, RC, EL and PLD) remained at the level of integrity of the cambial cells. Indeed, for both species, trees that were able to recover from drought presented cambial cells that still evinced the presence of a vacuole, stating their hydrated status and their ability to maintain turgor, whereas trees that did not survive the drought event presented disintegrated cambial cells with shrunken protoplast and collapse of the cytoplasm. These results agree with the ones provided by Li & Jansen (2017) where plants that were water stressed beyond their lethal level showed, in their cambial cells, non-reversible failure. These results therefore lend some empirical support to the opinion piece of Mantova *et al.* (2022) and the renewed framework proposed by (McDowell *et al.*, 2022) that suggest that the causal link between hydraulic failure and tree mortality might be through the disintegration of meristematic cell causing their death and preventing new growth and/or resprout the following year.

However, despite our results shading lights on the importance of meristems when trying to assess tree death, they cannot exactly evaluate the relationship between the loss of hydraulic conductance at the xylem level and meristem mortality. Indeed even if hydraulic failure should provoke meristematic cell death by disrupting their water supply (Mantova *et al.*, 2022), our result show that trees with similar level of hydraulic dysfunction can present various levels of cambial cell disintegration and therefore very different responses once drought is alleviated. Thus, the sequence of events enrolling cambial cells to death remains unknown and it is still unclear if cambial cell integrity is predominantly linked with the level of PLC or with the ability or inability of the tree to mobilize water and protect those crucial cells for survival. Furthermore, as discussed earlier, maintaining the hydraulic continuum is crucial for a plant to survive. Therefore, since our measurements were made at a single point within the plant, they cannot be representative of this hydraulic pathway and future research should consider the different parts of the hydraulic pathway when trying to assess a level of hydraulic failure that will disrupt plant metabolism and growth.

## 5. Conclusion and perspectives

Our results provide evidence that tree mortality at high level of PLC is linked to meristem integrity. Indeed, multiple trees presenting similar values for the different physiological traits measured during the time course of this experiment only differed in the level of cellular disintegration of their cambium. However, despite our results shading lights on the importance of meristems when trying to assess tree death, they cannot totally explain the relationship between the loss of hydraulic conductance at the xylem level and the loss of meristem integrity. Indeed, even though our results show that hydraulic failure remains a strong marker of tree dysfunction during drought, trees presenting similar PLC levels could present very different ultrastructure integrity in their cambium cells. Therefore, focusing on the water relocation, and particularly the water relocation towards cambial cells, during a

drought event could help decipher whether the water impairment through cavitation is the triggering factor causing meristem mortality or if the water storage depletion, caused by cavitation, would provoke meristem mortality and thus tree death. Finally, after evaluation of the multiple traits followed during our experiment with a PCA analysis, it seems that a combination of high levels of $RWC_{Stem}$ and stem RC after re-watering could mainly correlate with tree survival on the longer term for both species. Although both of those traits could help determining a probability survival for angiosperms and conifers after a drought event, none of them would act as a binary parameter for exactly assessing and predicting tree death. However, this could be the case for the cambial cellular integrity where trees presenting mainly disintegrated cambial cells are not able to survive the drought event.

## 6. Authors contribution

Marylou Mantova, Hervé Cochard and José M. Torres-Ruiz conceived and designed the experiment. Marylou Mantova was responsible for running the measurements and carried out the data analysis. Steven Jansen, Nicole Brunel and Claire Szczepaniak elaborated the TEM protocol. Claire Szczepaniak prepared the thin and ultrathin sections used for TEM observations. Marylou Mantova, Nicole Brunel, José M. Torres-Ruiz and Steven Jansen ran the TEM observation. Andrew King and Sylvain Delzon supervised the setting up of the micro-CT scans. Sylvain Delzon, Hervé Cochard and José M. Torres-Ruiz ran the micro-CT scans. Marylou Mantova, José M. Torres-Ruiz, Hervé Cochard and Steven Jansen interpreted the results. Marylou Mantova wrote the first manuscript draft. All authors assisted substantially with manuscript development.

## 7. Acknowledgements

This research was supported by La Région Auvergne-Rhône-Alpes “Pack Ambition International 2020” through the project ‘ThirsTree’20-006175-01, 20-006175-02, and the Agence Nationale de la Recherche, Grant/Award Number ANR-18-CE20-0005, ‘Hydrauleaks’.

## 8. Supplementary data

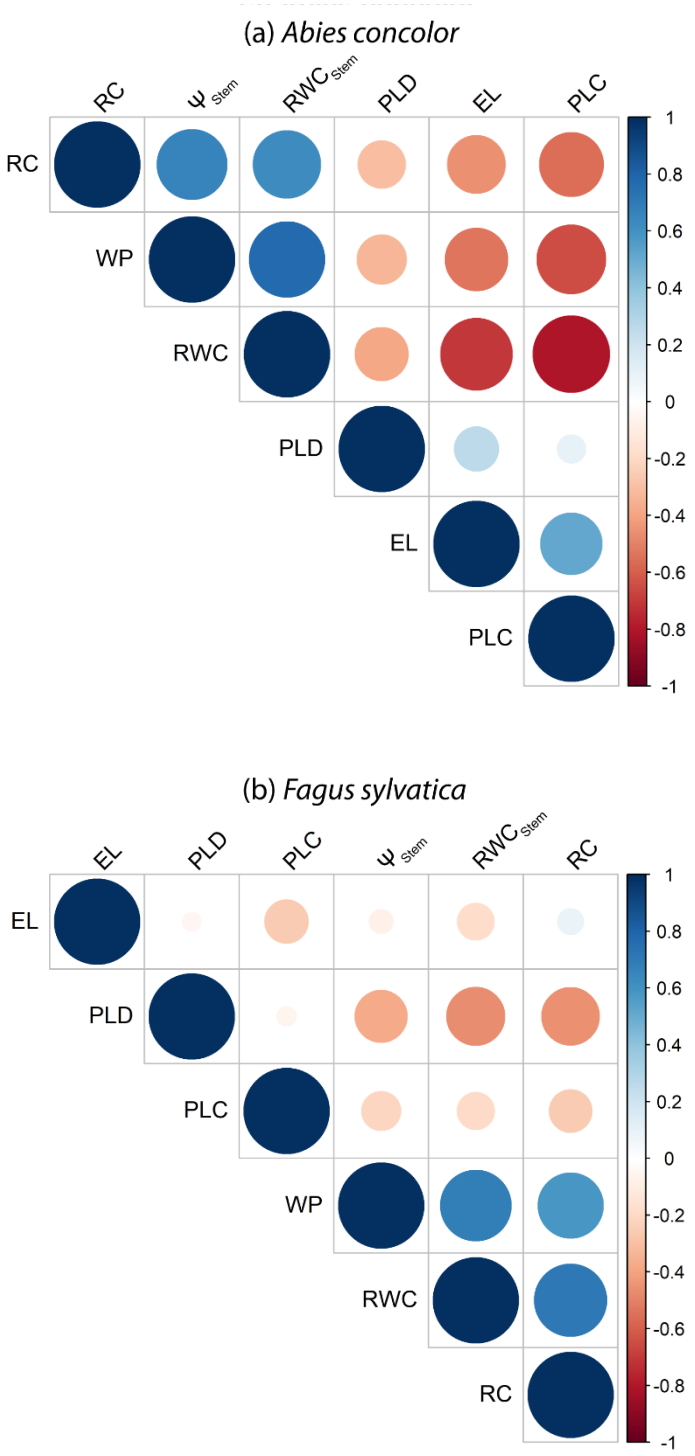


**Figure S6.** Correlation matrix between the different traits measured right before rewatering for cellular damages (EL), percentage loss of diameter (PLD), loss of hydraulic conductance (PLC), stem relative water content ($RWC_{Stem}$) and stem water potential ($\Psi_{Stem}$) or after rehydration for the stem recovery capacity (RC) for **(a)** *Abies concolor* and **(b)** *Fagus sylvatica*.

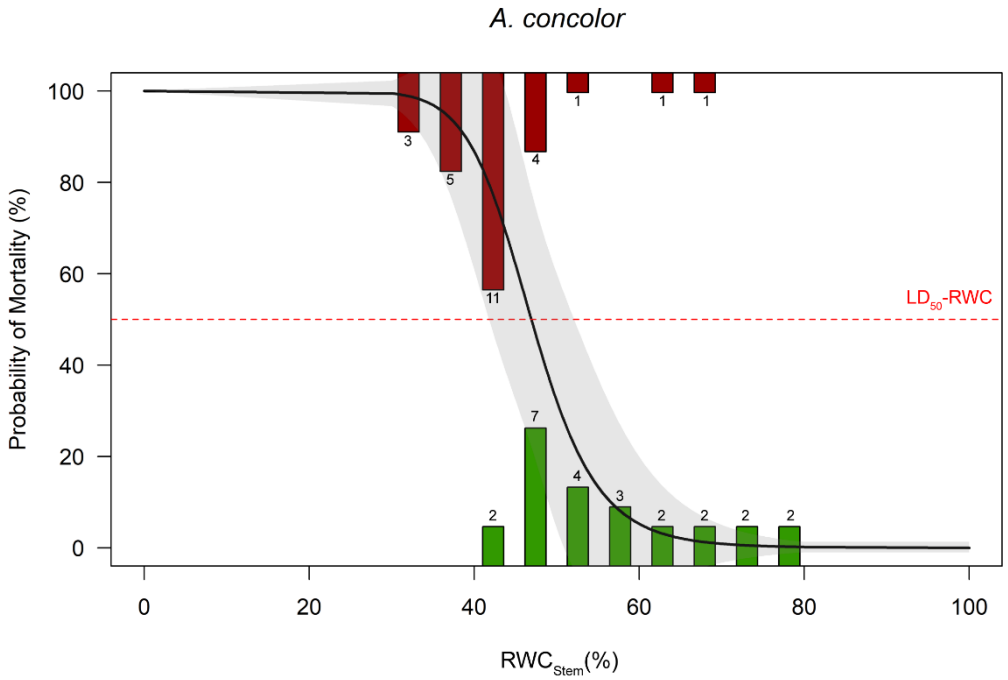


**Figure S7.** Logistic regression to determine the 50% lethal dose ($LD_{50}$-RWC, dashed red line) of stem relative water content ($RWC_{Stem}$) during drought for *Abies concolor*.
$LD_{50}$-RWC was computed at 46.9±1.8%. Bars represent the number of trees that survived (green bars) or died (red bars) from the drought event in each 5% RWC bin. The solid black line represents the logistic regression fit with a shaded grey area representing a 95% confidence interval for the logistic regression.

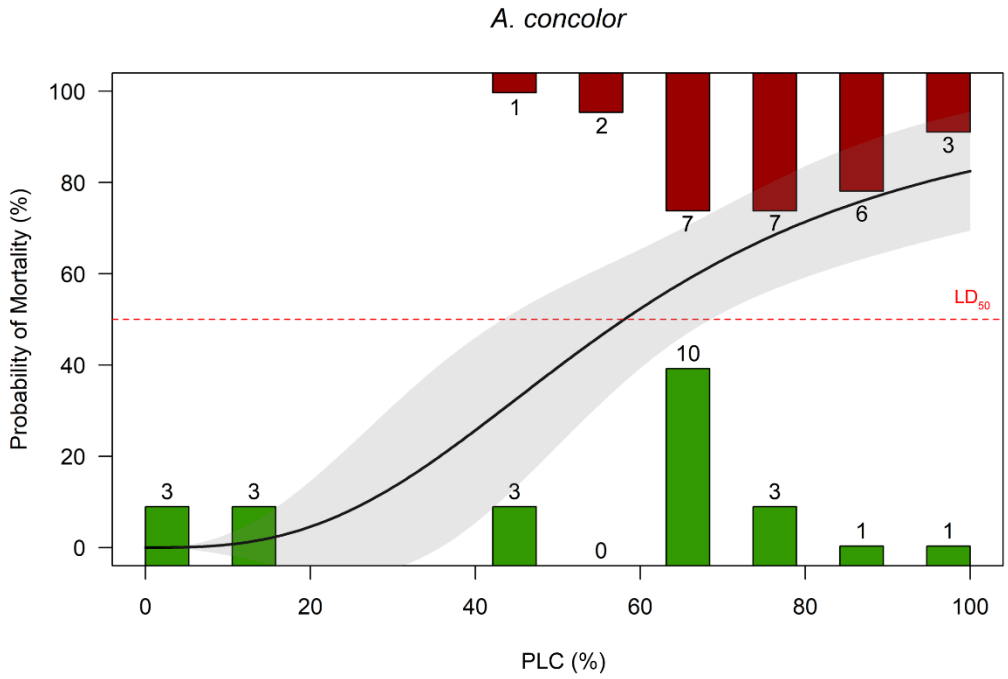


**Figure S8.** Logistic regression to determine the 50% lethal dose ($LD_{50}$, dashed red line) of percentage loss of hydraulic conductance (PLC) during drought for *Abies concolor*. $LD_{50}$ was computed at 58.1±3.5%. Bars represent the number of trees that survived (green bars) or died (red bars) from the drought event in each 10% PLC bin. The solid black line represents the logistic regression fit with a shaded grey area representing a 95% confidence interval for the logistic regression.

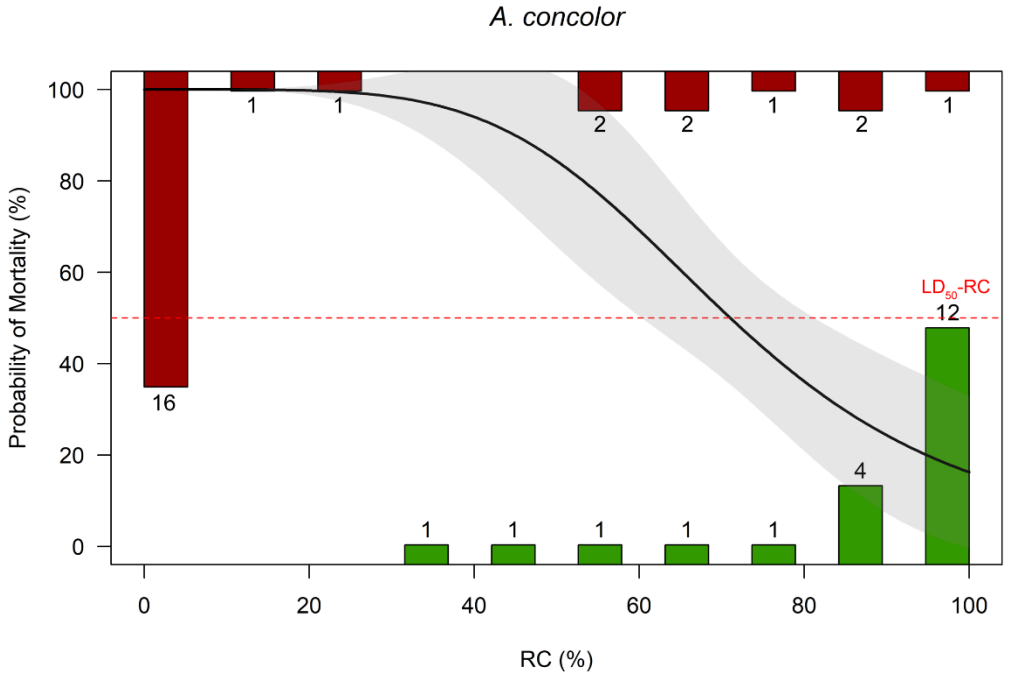


**Figure S9.** Logistic regression to determine the 50% lethal dose ($LD_{50}$-RC, dashed red line) of stem recovery capacity (RC) during drought for *Abies concolor*.
$LD_{50}$-RC was computed at 71.1±2.7%. Bars represent the number of trees that survived (green bars) or died (red bars) from the drought event in each 10% RC bin. The solid black line represents the logistic regression fit with a shaded grey area representing a 95% confidence interval for the logistic regression.

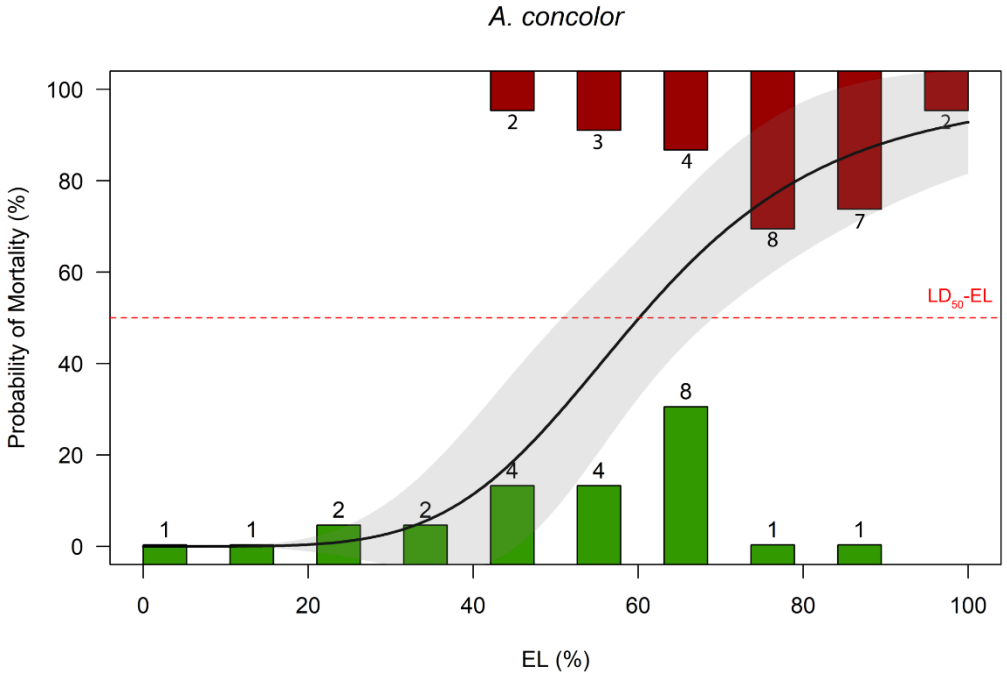


**Figure S10.** Logistic regression to determine the 50% lethal dose ($LD_{50}$-EL, dashed red line) of cellular damages (EL) during drought for *Abies concolor*.
$LD_{50}$-EL was computed at 60.1±3.4%. Bars represent the number of trees that survived (green bars) or died (red bars) from the drought event in each 10% EL bin. The solid black line represents the logistic regression fit with a shaded grey area representing a 95% confidence interval for the logistic regression.

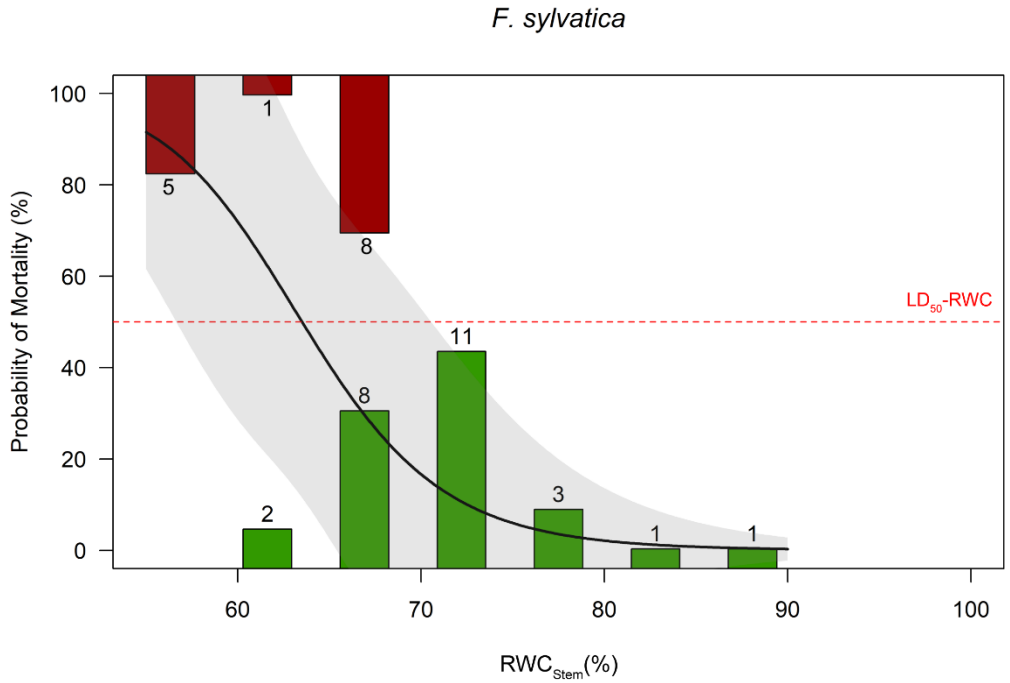


**Figure S11.** Logistic regression to determine the 50% lethal dose ($LD_{50}$-RWC, dashed red line) of stem relative water content ($RWC_{Stem}$) during drought for *Fagus sylvatica*. $LD_{50}$-RWC was computed at 63.5±1.9%. Bars represent the number of trees that survived (green bars) or died (red bars) from the drought event in each 5% RWC bin. The solid black line represents the logistic regression fit with a shaded grey area representing a 95% confidence interval for the logistic regression.

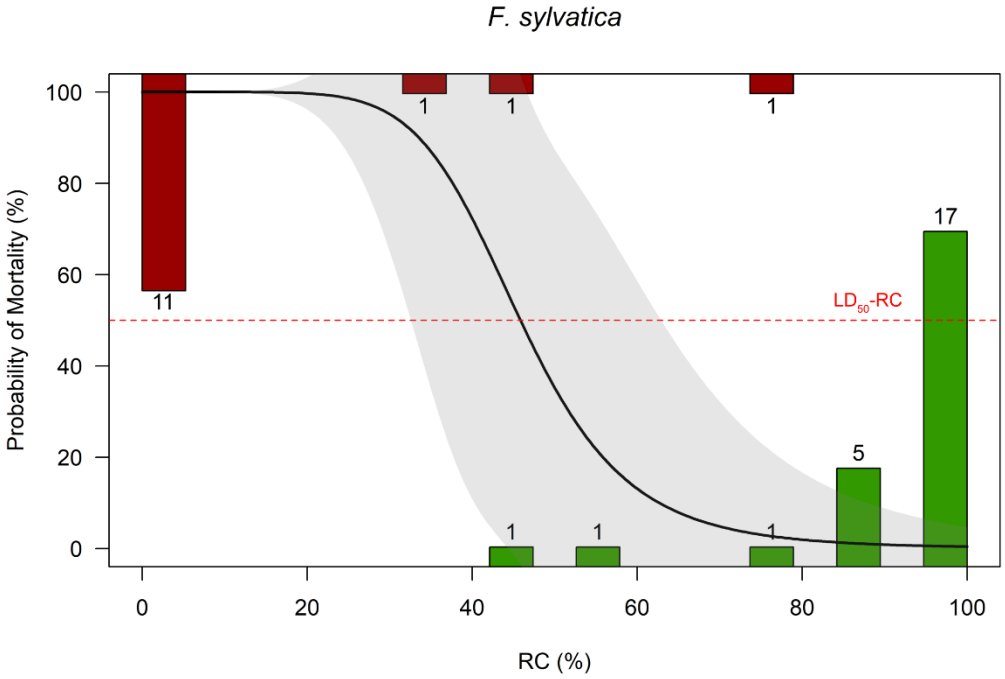


**Figure S12.** Logistic regression to determine the 50% lethal dose ($LD_{50}$-RC, dashed red line) of stem recovery capacity (RC) during drought for *Fagus sylvatica*.
$LD_{50}$-RC was computed at 45.9±4.4%. Bars represent the number of trees that survived (green bars) or died (red bars) from the drought event in each 10% RC bin. The solid black line represents the logistic regression fit with a shaded grey area representing a 95% confidence interval for the logistic regression.

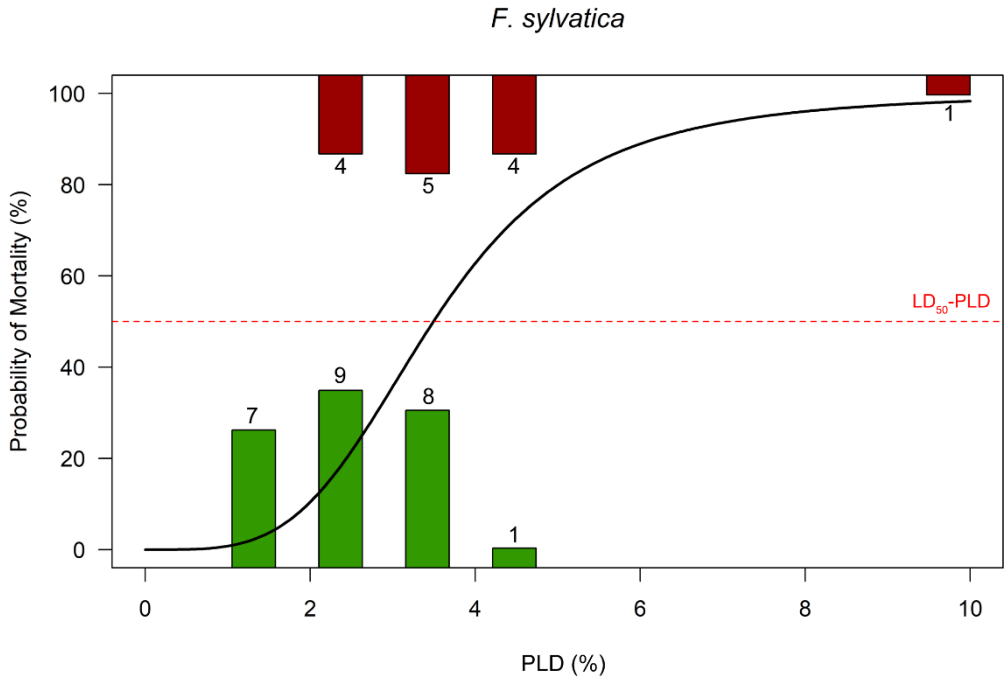


**Figure S13.** Logistic regression to determine the 50% lethal dose ($LD_{50}$-PLD, dashed red line) of percentage loss of stem diameter (PLD) during drought for *Fagus sylvatica*.
$LD_{50}$-PLD was computed at 3.5±0.3%. Bars represent the number of trees that survived (green bars) or died (red bars) from the drought event in each 1% PLD bin. The solid black line represents the logistic regression fit.

# *General Discussion*

# General Discussion

In the context of climate change, where tree mortality is already notable and is expected to become increasingly frequent, the thesis work presented above aimed to (i) understand the causal link between hydraulic failure and tree mortality and (ii) identify the key physiological traits that would determine a tree's ability to recover from a drought event.

## 1. Contribution of the study to the understanding of the causal link between hydraulic failure and tree mortality

### *1.1.Hydraulic failure triggers cell mortality*

Although hydraulic failure had been identified as a ubiquitous factor in tree death and McDowell *et al.* (2008, 2022) have proposed a hypothesis that hydraulic failure leads to tree mortality by leading to complete dehydration and cell death, the mechanistic link between hydraulic failure and cell death has only been weakly investigated before (Figure 75).

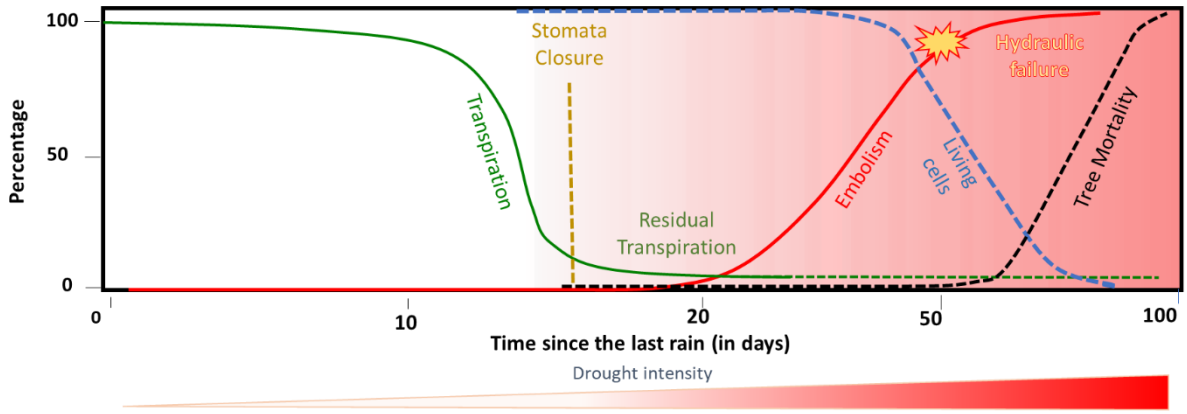


**Figure 75.** Theoretical framework linking the increment in embolism (solid red line), the decrease in the amount of living cells (dashed blue line) and the consequent tree mortality (dashed black line). Continuous lines represent what is already demonstrated whereas dashed lines represent what is, to date, a simple correlation and has not been demonstrated yet. (Adapted from Delzon & Cochard, 2014)

Indeed, only a study by Brodribb *et al.* (2021) had shown, at a very local level in a leaf, how xylem cavitation led to a loss of fluorescence of the cells connected to it. Thus, by precisely studying the kinetics of the different cavitation and cell death events, first at the leaf level (see Chapter 2.), then at the stem level (see Appendix 1, Figure S14), our studies showed that hydraulic failure is indeed a precursor of cell death and thus, *in fine*, of the organ, therefore confirming the observations of Brodribb *et al.* (2021). In fact, by combining different techniques for monitoring the propagation of cavitation events, the decrease in tissue water content (*via* RWC (Barrs & Weatherley, 1962; Martinez-Vilalta *et al.*, 2019; Trueba *et al.*, 2019; Sapes & Sala, 2021)) and the follow-up of cell mortality (using electrolyte leakage measurements as a proxy for membrane dysfunction (Sutinen *et al.*, 1992; Chaturvedi *et al.*, 2014; Guadagno *et al.*, 2017)) our studies revealed that the onset of cavitation events within the leaf or within the stem always occurred at higher (for leaves) or similar (for stems) RWC than the ones causing cell death in the respective organs, and thus that cell death was inherent to a drop in water content

caused by a hydraulic dysfunction. If Lamacque *et al.* (2022) have shown that stem contraction was associated with two relatively temporally separated mechanisms: the onset of embolism and cell death, we were unable to discern these two processes using stem dendrometers signals during our Chapter 1. and Chapter 3. experiments. However, by using other techniques, our studies confirmed that the propagation of embolism did precede cell death and thus, these novel results demonstrated the sequence of events that had been, until now, theoretical (Figure 76).

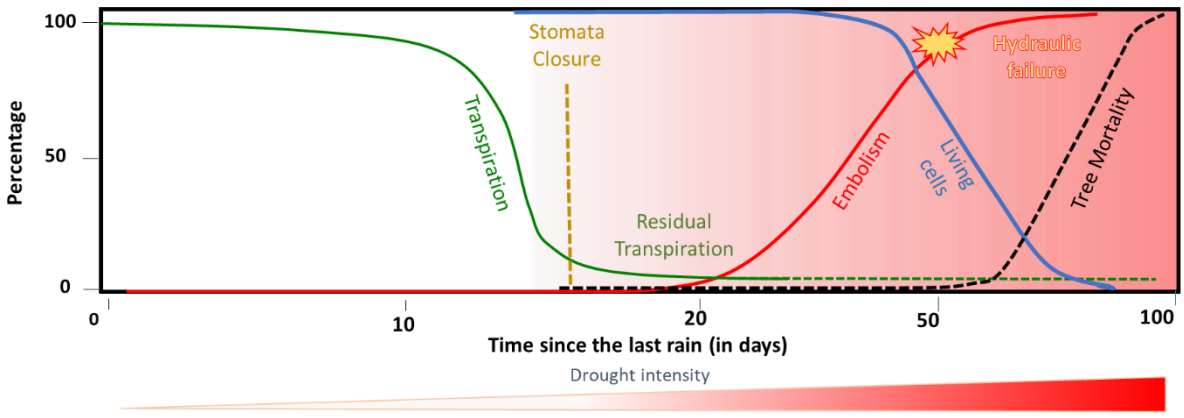


**Figure 76.** Theoretical framework linking the increment in embolism (solid red line), the decrease in the amount of living cells (solid blue line) and the consequent tree mortality (dashed black line).
Continuous lines represent what is already demonstrated whereas dashed lines represent what is, to date, a simple correlation and has not been demonstrated yet.
Here, as a difference from figure 75, the link between embolism and amount of living cells has been demonstrated. Now, only the causal link with tree mortality remains under-explored. (Adapted from Delzon & Cochard, 2014)

### *1.2. Cell mortality occurs at different RWC values across species*

Based on the study of the decrease in RWC, which has the advantage of being a metric that directly reflects the state of dehydration of our tissues (Barrs & Weatherley, 1962; Martinez-Vilalta *et al.*, 2019), our experiments have highlighted an important dehydration threshold, that we have called the $RWC_{crit,}$ corresponding to the critical RWC below which cell mortality increased significantly (see Chapter 2.) These $RWC_{crit}$ determination carried out both at leaf level (see Chapter 2.) and at stem level (see Chapter 3.) showed that the $RWC_{crit}$ varied across species. Indeed, we noticed that the most vulnerable to xylem cavitation species also tended to present cells more vulnerable to cavitation, i.e., with a higher $RWC_{crit}$ than the others, thus maybe highlighting a common evolutionary pathway on drought-tolerance strategies.

This differential tolerance to cell dehydration could be due to, as discussed earlier in this thesis report, cell properties *per se* and particularly to the cell wall properties. Indeed, as it has been shown that the greater resistance of xylem to cavitation is probably due to a greater strengthening of their vessel walls (Hacke *et al.*, 2001; Cochard *et al.*, 2008), by extension, it would be likely that the cells of the different parenchyma may have more or less thick walls and/or different composition therefore playing an important role in their mechanical

deformation and thus probability of death (Mantova *et al.*, 2022). For example, it has been shown, in the case of thick non-lignified seed walls, that richer in mannose-containing hemicelluloses (Harris, 2005) would make the cells less vulnerable to dehydration. This type of cell wall composition could, thus, provide a better resistance to deformation, thus preventing cytorrhysis (Oertli, 1986), or cell cavitation (Llorens *et al.*, 2016; Sakes *et al.*, 2016).

More surprisingly, our study showed that as soon as the $RWC_{crit}$ was reached, cell death spread at the same rate in the leaves of the studied species if the RWC kept declining. This therefore highlighted that the vulnerability to death under water stress did not only depend on the cells' composition and tolerance to dehydration but also on the pace of the dehydration, and particularly to the time it takes to reach the $RWC_{crit}$. Thus, as the time-dependence of hydraulic failure has been highlighted as an important but too often overlooked piece of the puzzle in understanding response to drought (Blackman *et al.*, 2016), it highlights the importance of considering all the processes that occurs at the very beginning of the drought event as e.g., the time required to reach stomata closure and turgor loss point or also the dynamic of residual transpiration once stomata are closed (Billon *et al.*, 2020) and therefore the time to $RWC_{crit}$ when trying to model drought-induced cell death. Unfortunately, as the dehydration rate varied between the different individuals in our study due to the variability between trees in terms of rhizosphere or leaf area, we could not evaluate the time to $RWC_{crit}$. However, it could be hypothesized that the species that present a lower $RWC_{crit}$, would take a longer time to reach their $RWC_{crit}$ as traits involved in reducing rates of water loss could influence how long it takes to a tree to reach lethal water stress levels (Blackman *et al.*, 2016) and as lethal water stress levels are associated with cell mortality (Mantova *et al.*, 2021).

### *1.3.The meristems, the key to life or death of trees*

The main hypothesis of this thesis work was based on meristem survival (Mantova *et al.*, 2022). Indeed, while McDowell *et al.* (2008) had hypothesised that tree mortality under drought conditions was probably caused by hydraulic failure leading to cell death, we had clarified this hypothesis by arguing that this mortality was most likely related to meristem mortality which were key elements allowing organ development and regeneration in subsequent years following a drought event (Mantova *et al.*, 2022). However, very few studies, only one by Li & Jansen (2017), had attempted to establish the link between hydraulic failure and mortality of these meristems, probably because of the extreme difficulty to access them.

Thus, in the quest to understand drought-induced tree mortality, our study showed that cambium survival was indeed the key element when determining whether a tree could survive a drought event or not (Figure 77). Indeed, using transmission electron microscopy (TEM) techniques, our study was able to show a destruction of the ultrastructure of most of the cambial cells in the case of trees that were not able to recover from the drought event but not in the case of surviving trees. By transposing our results to the aerial organs and not only to the roots as it was done by Li & Jansen (2017), our study confirmed their results, i.e., that trees with intact cambial cells survive the drought event, and allowed us to elucidate more precisely the mortality mechanisms of the aerial part of trees under drought conditions. However, our study could not exactly determine what was influencing cambium survival. Indeed, none of the followed physiological traits could strongly determine the faith of the cambium cells.

Therefore, even when the stem presented a low RWC, meristematic mortality might have been avoided by mobilising water reserves as hypothesized by Mantova *et al.* (2022). Indeed, it has been demonstrated with X-ray micro-CT that the water contained in the xylem matrix embedding xylem vessels was usually released to the adjacent tissues (i.e., for a stem: in meristematic tissues) concomitant with stem shrinkage and the formation of embolism, and not before the onset of cavitation (Tyree & Yang, 1990; Knipfer *et al.*, 2019). Also, it has been shown that as the xylem tension increases, numerous cavitation events are observed in the xylem vessels located close to the vascular cambium (Knipfer *et al.*, 2019). Thus, this would suggest that the mobilization of these water reserves could partially buffer the water depletion caused by cavitation in the symplastic tissues and protect the key cells for survival that are the meristems. In addition, the expression of aquaporins in rays may have increased radial flow from xylem and phloem to the cambial region, therefore sustaining cambial cells metabolism (Almeida-Rodriguez & Hacke, 2012). Considering this, different trees showing similar RWC and cellular damages levels at the stem level before re-watering might have had different water relocation strategies, probably because of the differential aquaporins activation as it has been demonstrated in *Eucalyptus globulus* (Feltrim *et al.*, 2021), and thus have presented different cambium cells ultrastructure. Thus, further studies on water relocation during a drought event would be required to determine exactly the parameters influencing cambium survival and, *in fine*, tree survival (Figure 77).

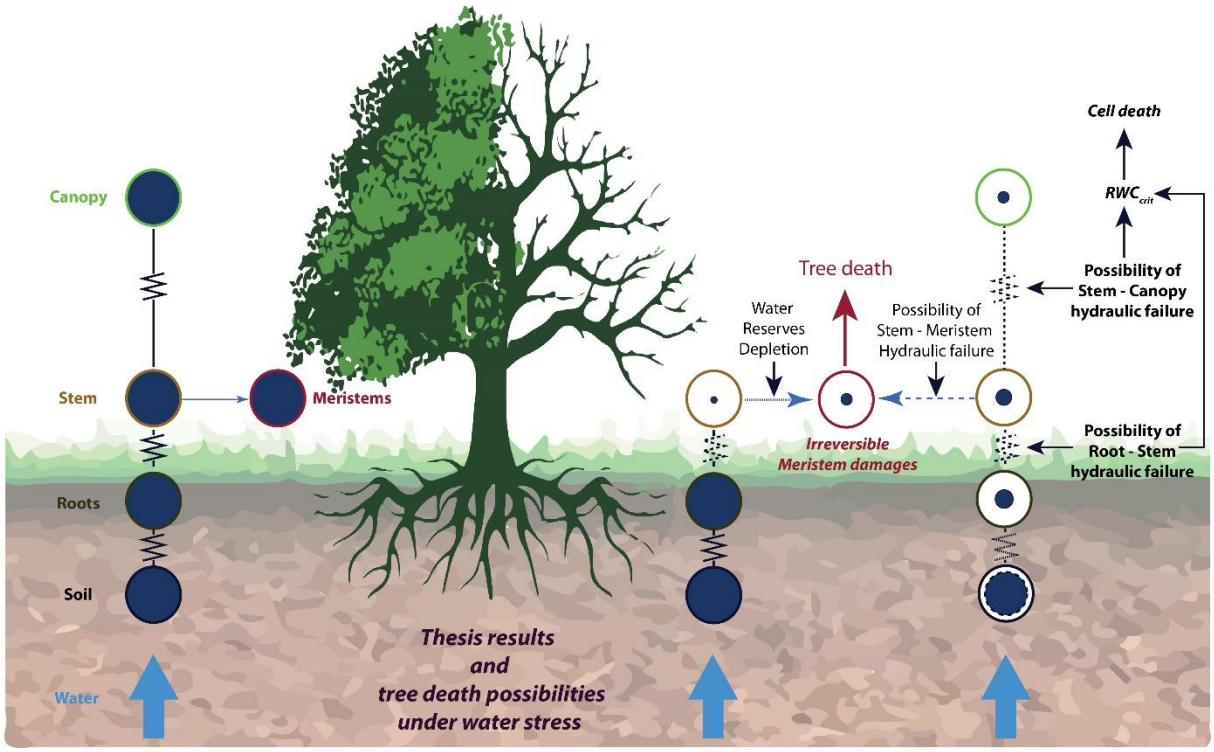


**Figure 77.** Summary diagram part 1.
Meristems vitality represents the key to life or death after a drought event for trees.

### *1.4.Having access to water is as important as maintaining stem hydraulic functioning*

The results obtained during this thesis showed that high levels of hydraulic failure were not necessarily responsible for plant mortality and that some plants, particularly *F. sylvatica*, some angiosperms, may be unable to recover from the drought event even though they theoretically had enough stem xylem conductivity and abundant water in their soil. Indeed, despite having many living cells and a relatively low PLC at the point measured, some trees were not able to recover from the drought event meaning that the disruption of their water transport was located upstream in the hydraulic pathway. Thus, if the presence of large number of living cells can be explained by the plant's ability to survive on its water reserves (Epila *et al.*, 2017) which would maintain the plant's metabolism a little longer until being depleted and going below a critical RWC as demonstrated in Chapter 2., the incapacity of the tree to recover from drought even when presenting a sufficient xylem hydraulic functioning must be linked to their inability to either draw water from the soil or to conduct it to the stem. In fact, the inability to access water in the soil or to conduct it to the stem might be linked to the hair shrinkage that happens during drought and that can hydraulically disconnect the tree from the soil (Duddek *et al.*, 2022) or to the fine root failure hypothesis presented by Johnson *et al.* (2018). Indeed, the root shrinkage, independent to shrinkage to lethal level, associated with soil dehydration may lead tree to death through the disruption of the hydraulic continuum from the soil to the root (Körner, 2019) (Figure 78), making the disponible water in the soil inaccessible to the tree and provoking fatally its full embolization and death. In addition, a hydraulic segmentation where roots are more vulnerable to drought than the aerial part could provoke the hydraulic failure of the whole tree by disrupting the plant water supply (Johnson *et al.*, 2018) (Figure 78). Therefore, this highlight the fact that, in order to recover from drought, water not only needs to be available in the soil but also needs to be accessible and transportable for and within the tree.

Thus, if we have seen in Chapter 3. that trees with a PLC <88 at the stem level may not survive the drought event after rehydration of their soil and that this may be explained by their inability to mobilise water from the soil due to a hydraulic failure located further upstream of the measurement point within the xylem as discussed in the previous paragraph, **it raises the question of at what level, or within which organ, PLC measurements should be made and/or simulated when predicting tree mortality under drought conditions**. Thus, it appears, after this thesis work, that if measurements are made only at the stem level when the Achilles heel of the hydraulic system is located further upstream in the hydraulic continuum, then the prediction of mortality would be biased and underestimated. Indeed, although measurements at the stem level would not identify the plant as dead, it would already be doomed due to its inability to mobilise water from the soil and would therefore be dying and not dead. Thus, our results provide evidence that, in order to accurately predict tree mortality under drought-conditions using PLC values, it is necessary to take into consideration the PLC of the whole hydraulic pathway and not only a very local PLC value (Figure 78).

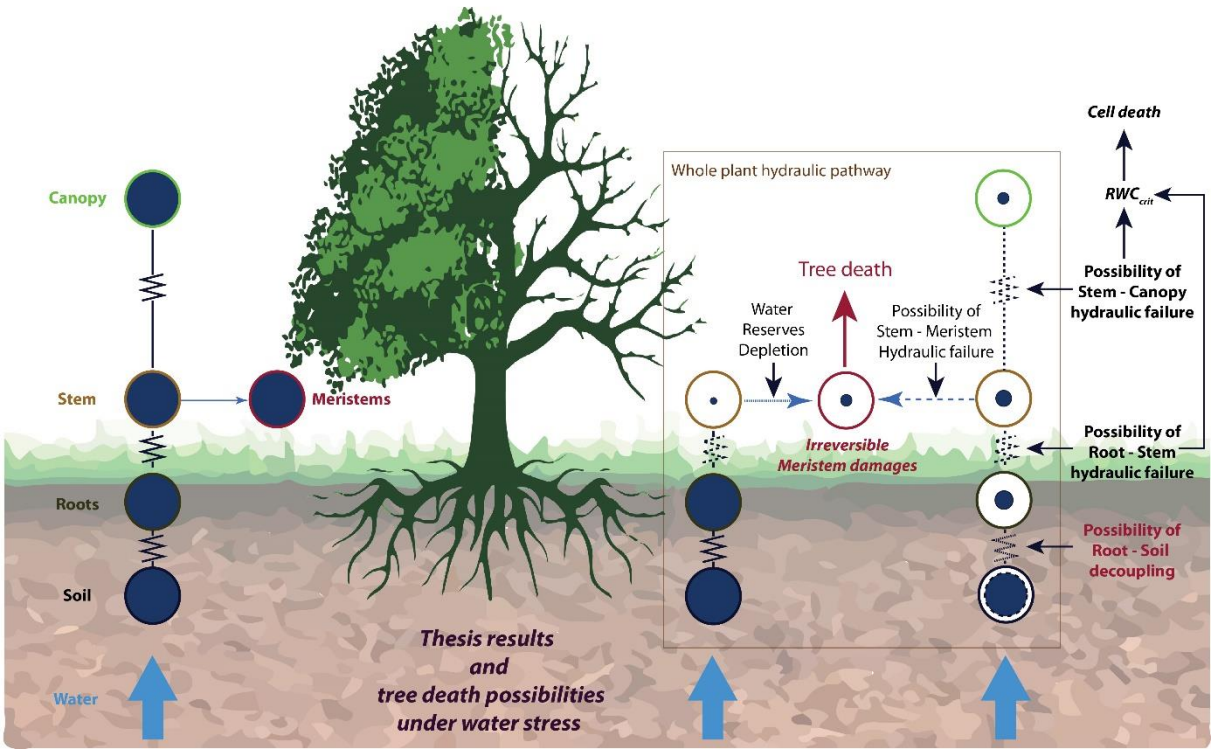


**Figure 78.** Summary diagram part 2.
Having access to water is as important as presenting a conductive pathway in order to survive from drought. Thus, if the hydraulic pathway is somewhat disrupted along the soil-plant-atmosphere continuum, the tree might ultimately desiccate and die from drought. Therefore, in order to predict tree risk of mortality, it is important to consider the PLC of the whole hydraulic pathway.

## 2. Identification of the key physiological traits for assessing tree mortality

### *2.1.A paradigm shift, high losses of hydraulic functioning are not the best indicators of tree survival under drought conditions*

For about ten years, the loss of hydraulic conductance and more particularly the values of $P_{50}$ and $P_{88}$, most of the time defined at the stem level, have been considered as the gold standard for determining tree mortality under drought conditions (Brodribb & Cochard, 2009; Barigah *et al.*, 2013b; Urli *et al.*, 2013). They have even been used as indicators in various models to assess the impact of future climate change on tree survival (Brodribb *et al.*, 2020; Lemaire *et al.*, 2021). However, since 2019, it seems that this paradigm is slowly changing as $P_{50}$ (Hammond *et al.*, 2019; Mantova *et al.*, 2021) and $P_{88}$ (Mantova *et al.*, 2021) seem to no longer be the most accurate indicators of whether a tree will survive the drought event or not. Indeed, while Hammond *et al.* (2019) have already shown that $P_{50}$ could not function as an indicator of mortality on *P. taeda* (a conifer, also known under the common name Loblolly pine), our studies presented in Chapter 1. and Chapter 3. confirmed that the survival of conifers after a drought event was not solely related to level of hydraulic failure of 50%. Thus, even though it is certain that trees with a PLC of 100% will not be able to recover from the drought event, it seems that a minimal hydraulic connection would be sufficient to allow trees to survive if they

have access to water. In fact, our studies (see Chapter 1. and Chapter 3.) have shown that, in angiosperms, trees with levels of PLC higher than $P_{88}$ and even reaching levels of almost 100% could recover from a drought event and even produce new leaves and organs the following years if they have access to water.

However, the ability of trees to recover from the drought event when presenting PLC values very close to 100% remains questionable. Indeed, it remains unknown how a tree presenting such minimal hydraulic functioning could meet his water needs even under mild VPD conditions. In fact, in our studies, the measurements were conducted on potted plants that were rehydrated to field capacity after the dehydration phase and thus, it is important to remember that such rehydration phenomena rarely occur in nature and that they could have increased the probability of plant survival by allowing the plant to equilibrate their water balance by compensating the evaporative demand even when presenting low level of hydraulic functioning. Secondly, our PLC measurements were carried out on lateral branches and thus might be overestimated. Indeed, lateral branches may be subject to within-plant segmentation phenomena, either due to the fact that $\Psi_{xylem}$ values would be more negative in distal parts of the tree (e.g., branches or leaves) than in central parts (e.g., the trunk) (Tyree & Zimmermann, 2002), or to highest vulnerability to cavitation in distal parts (Charrier *et al.*, 2016), which would certainly, in both cases, overestimate the PLC we measured (Tyree & Zimmermann, 2002; Johnson *et al.*, 2016). This would mean that the PLC of the tree would be generally lower than the one we measured and therefore provide a higher hydraulic conductivity than the one we estimated during our study. In addition, contrary to our study which focused on stem hydraulic failure, a study on drought-driven tree mortality in Texas suggested that the fine root failure was probably more related to mortality than stem hydraulic failure (Johnson *et al.*, 2018). Indeed, the trees which suffers the most important mortality rates (i.e., *Juniperus*) presented lower (more negative) stem $P_{88}$ values (i.e., more resistance to embolism) than those showing lower mortality rates (i.e., *Quercus*) (Johnson *et al.*, 2018). Therefore, considering the existence of the hydraulic segmentation, it would seem judicious to take into consideration the whole hydraulic vulnerability of the soil-plant-atmosphere continuum when trying to predict tree mortality. Indeed, if the soil-plant continuum is at some point disrupted, the plant will fatally reach a full level of embolization and consequently die from drought. Indeed, even if the disruption of the continuum does not occur at the soil-root interaction level, a hydraulic disruption downstream, for example in the main stem, could also lead tree to death *via* meristem death (McDowell *et al.*, 2022; Mantova *et al.*, 2022). Therefore, when trying to predict tree mortality using PLC thresholds, we should not focus on a special organ but on the whole hydraulic functioning of the soil-plant-atmosphere continuum (Figure 78).

### *2.2.Identifying tree mortality by focusing on water pools*

In their 2019 viewpoint Martinez-Vilalta *et al.* suggested that focusing on water pools and not only on the PLC would allow a better understanding and anticipation of tree mortality under drought conditions. They then outlined the properties of a good predictor of drought-induced mortality and stated that an indicator should be **sensitive** and specific under very different conditions, **widely applicable**, have a **mechanistic basis**, implying a link with the water status of the plant, be **integrative**, i.e., able to incorporate spatio-temporal variability,

**threshold-prone**, i.e., allow the determination of the point initiating mortality and finally, **scalable**, i.e., applicable at the level of the cell and the organ as well as at the ecosystem level. Thus, RWC appeared to one of the ideal candidates for determining a tree death threshold. Indeed, as a direct measure of the hydration or dehydration state of the cell or organ, RWC had a mechanistic basis. In addition, considering that, at the leaf level, large variations in water potential led to small variations in RWC, especially at the turgor loss point (Bartlett *et al.*, 2012), Martinez-Vilalta *et al.* (2019) hypothesised that RWC would be more constant than water potential across species and would therefore make it easier to compare organ resistance to dehydration. Indeed, by incorporating net changes in tissue water content over time, RWC appeared to be more integrative than the flux measurements that could be perform on different individuals. More importantly, empirical evidence had shown that RWC at turgor loss point appeared to be constant across species even though they have very different resistances to xylem cavitation (Bartlett *et al.*, 2012 - see also Chapter 2.). Thus, RWC could be subject to large and abrupt variations in the moments before plant death and especially when cell integrity is compromised.

In our study, RWC at the stem level appeared as a good indicator of tree probability of survival. Indeed, the recovering trees, either angiosperms (*P. lusitanica* and *F. sylvatica*) or conifers (*P. menziesii* or *A. concolor*) consistently showed higher $RWC_{Stem}$ than the trees that did not recover from drought. Considering this, we defined, in Chapter 3., a threshold below which the trees were more likely to die than to survive from drought ($LD_{50}$-RWC) and we noticed that, despite turgor loss point being relatively constant across species (Bartlett *et al.*, 2012), the defined $LD_{50}$-RWC value varied across species with conifers generally tolerating a higher decrease in $RWC_{Stem}$ before suffering from drought. However, even though our results in Chapter 2. evidenced a critical RWC for cellular integrity ($RWC_{crit}$), which was also determined in Chapter 3., we noticed during our recovery experiment in Chapter 3. that this value was not a good indicator of tree mortality. Indeed, the onset of tree mortality occurred at lower RWC than the onset of cellular mortality suggesting that trees can lose a large amount of their cell vitality before dying from drought which agrees with our results on *P. menziesii* in Chapter 1. Thus, if $RWC_{crit}$ would not work as a threshold when implementing models for predicting tree mortality, this value could still be helpful to compare the tolerance of cells to dehydration across species. Finally, even though RWC appeared as a good indicator when trying to understand tree death from drought, our results failed to identify a RWC threshold, that could determine a binary response (i.e., life or death) across species, but succeeded in providing a $LD_{50}$-RWC value helpful to predict if a tree has a more important chance to die than to survive from drought. This value, however, varied across species which highlighted the importance of integrating more species when trying to predict the future of our forests' ecosystems.

### *2.3. Stem diameter variation and recovery capacity as predictors of tree capacity of survival*

During our study, stem diameter variations were used twice to determine the ability of trees to survive the drought event (see Chapter 1. and Chapter 3.). As observed by Lamacque *et al.* (2020), stem diameter variations recorded with dendrometers proved to be very useful when determining tree survival and more specifically tree mortality. Indeed, while recovery

of part of the initial diameter was not always correlated with tree survival (see Chapter 3.), a lack of diameter recovery after re-watering was systematically associated with tree mortality, confirming the observations made by Lamacque *et al.* (2020). While Lamacque *et al.* (2020) had succeeded in showing on lavender and lavandin species that a loss of diameter (PLD) of at least 21% was systematically associated with individual mortality, our results could not be as convincing on our studied species. Indeed, PLD appeared as a factor influencing tree survival only in the case of *F. sylvatica* (an angiosperm) and not in *A. concolor* (a conifer). Unfortunately, the lack of recovering trees (only one for each species) in Chapter 1. did not allow us to determine if the PLD was influencing the survival capacity of the plant. Yet, the PLD value of 21% found on lavender and lavandin species (Lamacque *et al.*, 2020) was not found in *F. sylvatica* where a decrease in diameter equal to or greater than 3.5% led in more than one case out of two to the death of the tree.

Furthermore, it has been shown that under natural conditions, i.e., in semi-arid forests, stem diameter variations could be used to identify tree mortality long before visual signs of mortality appear (e.g., canopy browning) (Preisler *et al.*, 2021). Unfortunately, this thesis work did not focus on identifying signals that predict tree mortality within the LVDT signals recorded throughout the extreme drought experiments. However, as presented by Preisler *et al.* (2021) a cessation of daily diameter variation, reflecting a loss of stem radial water flow, could possibly be identified in dying trees. Therefore, a more detailed analysis of the LVDT signals could possibly confirm this observation made on on-site forest drought and transpose it on rapid and extreme drought. Perhaps, if we observed the same cessation of daily diameter variation in dying trees, meaning that water relocation is not happening anymore (*see* 1.3. The meristems, the key to life or death of trees *above*), this could probably explain why some cambium mortality occurred in some individuals and not in others that presented the same physiological traits before re-watering.

# *Perspectives*

# Perspectives

The results obtained during this thesis have led to several open questions, ranging from the understanding of cellular death mechanisms to the influence of recurring drought on tree survival and acclimation, and to the possibility of transposition of the results and techniques used in the previous experiments in the monitoring of not just an organ or a tree but an entire ecosystem. Therefore, this last part aims to propose avenues of reflection at different scales, their potential implication for modelling and to determine the follow-up to be given to this work.

## 1. Dying of thirst: how can cells succumb and what implications for predicting tree mortality?

### *1.1.Identification of the physical mechanisms inducing cellular death*

One of the first questions that emerged in this thesis work was the understanding of the mechanisms inducing cell death and how these could be influenced by cell composition and structure. To date, two main mechanisms have been put forward to explain cell death during water stress. Firstly, cells could die due to **cavitation**, i.e., when a critical pressure is encountered inside the cell causing the cytoplasm to fracture and a gas bubble to form inside it (Sakes *et al.*, 2016). While this phenomenon has been observed theoretically in the catapult mechanism of fern spores (Noblin *et al.*, 2012; Llorens *et al.*, 2016), it has never been linked empirically to cell death and therefore needs to be studied. Secondly, cells could die of **cytorrhysis** (Oertli, 1986; Choat *et al.*, 2016b) that consists in the deformation of the cell wall when the cell loses volume due to dehydration, thus leading to the collapse of the cell as a unit and its shrinkage to lethal levels. However, like cell cavitation, no empirical results have been found to support this theory.

Thus, our results from Chapter 2. and more particularly the observations made with the Synchrotron SOLEIL x-ray microtomograph led us to question not only the mechanisms of cell death but also the factors influencing the establishment of one or the other phenomenon. We therefore conducted a preliminary study using a Cryo-SEM in conjunction with the Holbrook laboratory at Harvard which aimed to identify the mechanisms behind cellular death under drought conditions. In fact, Cryo-SEM is a microscopy technique that allows capturing images without altering the water content of the samples and thus avoiding the dehydration artefacts that can exist when using other conventional microscopy techniques. Furthermore, Cryo-SEM and more specifically the cryo-fracture technique has the advantage of preserving cells' 3D structure, making it the ideal tool to perform our observations. Thus, we performed, on two evergreen species with contrasting resistance to xylem cavitation (i.e., *Hibiscus rosa-sinensis* and *Laurus nobilis*), transverse cryofractures on leaves at different RWC, in an attempt to elucidate the existence of one or both of the mechanisms that can cause cell death.

Our observations using Cryo-SEM allowed us to observe that the majority of cells seemed to suffer from the phenomenon of cytorrhysis during dehydration, and this, at early stage of dehydration. Indeed, the majority of cells, whether from the palisade parenchyma or the

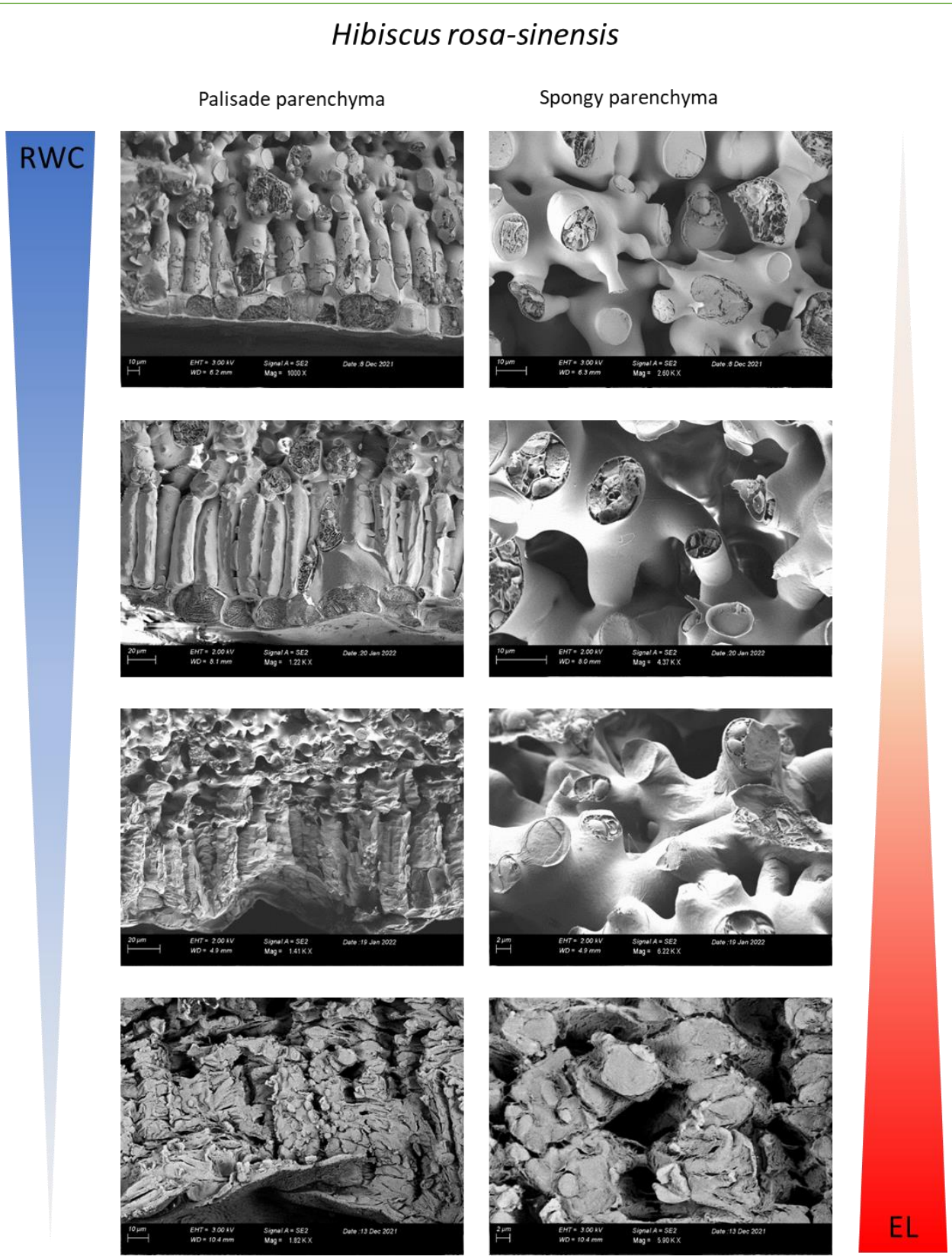


**Figure 79.** Cryo-SEM observation of transversal cryofractures of *Hibiscus rosa-sinensis* leaves along a decrease in their relative water content (RWC) and a conjoint increase in cellular damages (EL).

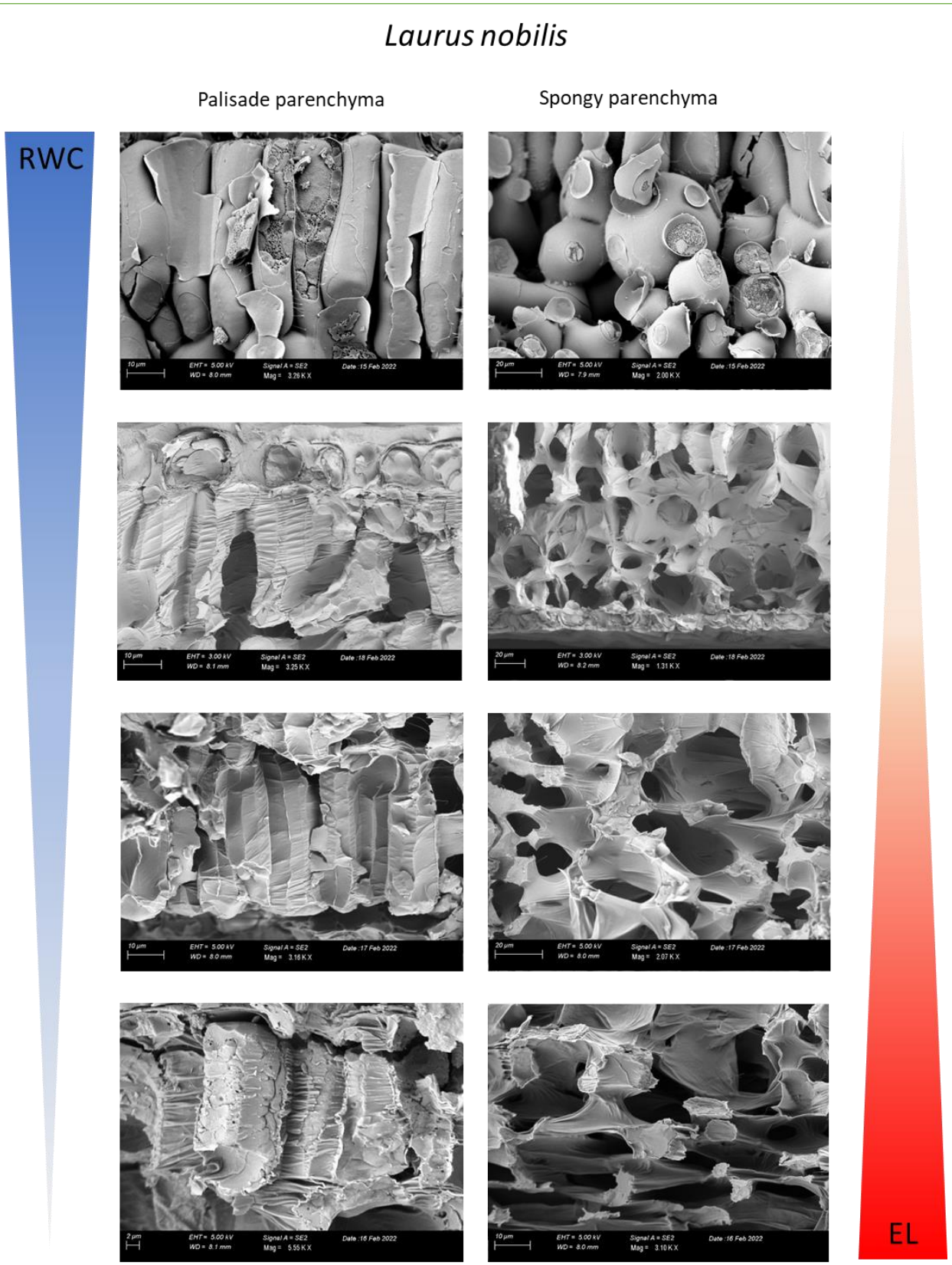


**Figure 80.** Cryo-SEM observation of transversal cryofractures of *Laurus nobilis* leaves along a decrease in their relative water content (RWC) and a conjoint increase in cellular damages (EL).

spongy parenchyma, seemed to collapse on themselves during dehydration in the case of both species (Figure 79 and Figure 80). Furthermore, as observed in the Chapter 2. of this thesis, we noted that changes in the epidermis only occurred at very low RWC values probably due to their role in maintaining leaf structure (Evert, 2006). In addition, we observed a difference in the mechanical reaction of the epidermis between the two studied species. Indeed, while *H. rosa-sinensis* seemed to show only very slight changes in their epidermis during dehydration, the epidermis of *L. nobilis* seemed to show a sequence of events that could suggest cell cavitation, indeed, at very low RWC, the epidermis cells of *L. nobilis* seemed to be empty or filled with gas what could suggest cell cavitation (Figure 81). As it is known that the epidermis cell walls vary in thickness (Evert, 2006), further studies focused on measuring the cell wall thickness could help deciphering if it plays a role in the deformation and further destruction of the cell under drought-stress.

Finally, this preliminary work allowed us to confirm the sequence of events leading to the death of the different cells' layers in *L. nobilis* leaves and to elucidate this sequence in *H. rosa-sinensis*. Indeed, in both species, it seems that the palisade parenchyma was the first affected by dehydration, followed by the spongy parenchyma and finally by the epidermis. However, although our preliminary study confirmed that there were indeed cytorrhysis phenomena at the leaf level and perhaps cellular cavitation phenomena within the epidermis of *L. nobilis*, it did not allow us to determine which cellular factors were at play during deformation. Thus, making cross-sections of leaves would allow us to measure precisely the thickness of the cell walls; to compare between different tissues if this value changes and finally to compare between species if this value has an influence on the attainment of the $RWC_{crit}$.

Although both processes (i.e., cell cavitation and cytorrhysis) were found to exist, our preliminary results did not yet show whether these mechanical deformations were the cause of cell death. Thus, assuming that a dead cell cannot recover its initial volume due to the absence of a plasma membrane, it would be necessary to perform a forced rehydration of the leaves at different RWC to determine until what level of deformation the cells are able to recover their initial volume. If the results show that as soon as a cell is deformed, it cannot rehydrate, then we could conclude that the deformation of the cell is a very important element in determining its survival and thus that of the plant. On the other hand, if extremely deformed cells could all recover their initial volume, meaning that the plasma membrane was not affected, then we could conclude that cell deformation is not the cause of cell death, which would mean that biochemical processes are more important in determining cell death (Figure 82).

### *1.2.What about reactive oxygen species?*

Another possibility presented as potentially responsible for cell and tree death under drought conditions was the destruction of the plasma membrane caused by the accumulation of reactive oxygen species. Indeed, during abiotic stresses, an accumulation of ROS can occur in the cell leading to oxidative stress. This oxidative stress is then at the origin of numerous biochemical changes leading in particular to lipid peroxidation (Suzuki *et al.*, 2012; Petrov *et al.*, 2015) and the rupture of the plasma membrane causing the death of the cell (Guadagno *et al.*, 2017). However, the thesis work did not focus on the biochemical aspects of cell death. Nevertheless, it would seem necessary to not only study the production of ROS throughout

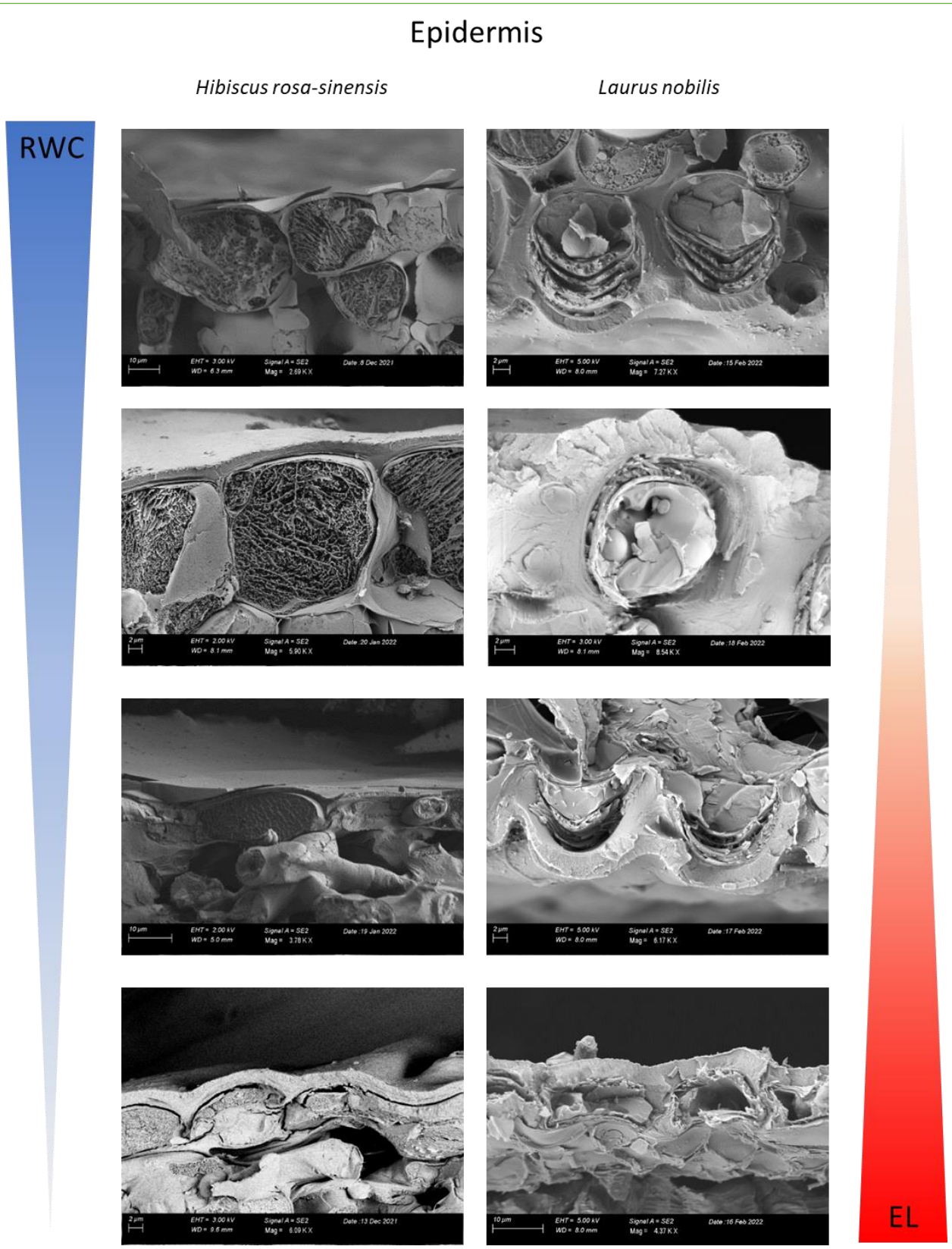


**Figure 81.** Cryo-SEM observation of transversal cryofractures of *Hibiscus rosa-sinensis* and *Laurus nobilis* epidermis cells along a decrease in their relative water content (RWC) and a conjoint increase in cellular damages (EL).

the drought but also to evaluate the management of oxidative stress by plants. Indeed, it has been shown in plants that are able to tolerate extreme drought, such as resurrection plants, that ROS accumulation can be countered by an increase in the production of ROS-scavenging enzymes and antioxidants (Singh *et al.*, 2015) leading to the protection of the cell integrity (Ingle *et al.*, 2007). Therefore, it would seem appropriate to compare ROS and antioxidants production across species with different drought-tolerant cells and identify their role in cellular death under extreme drought conditions (Figure 82).

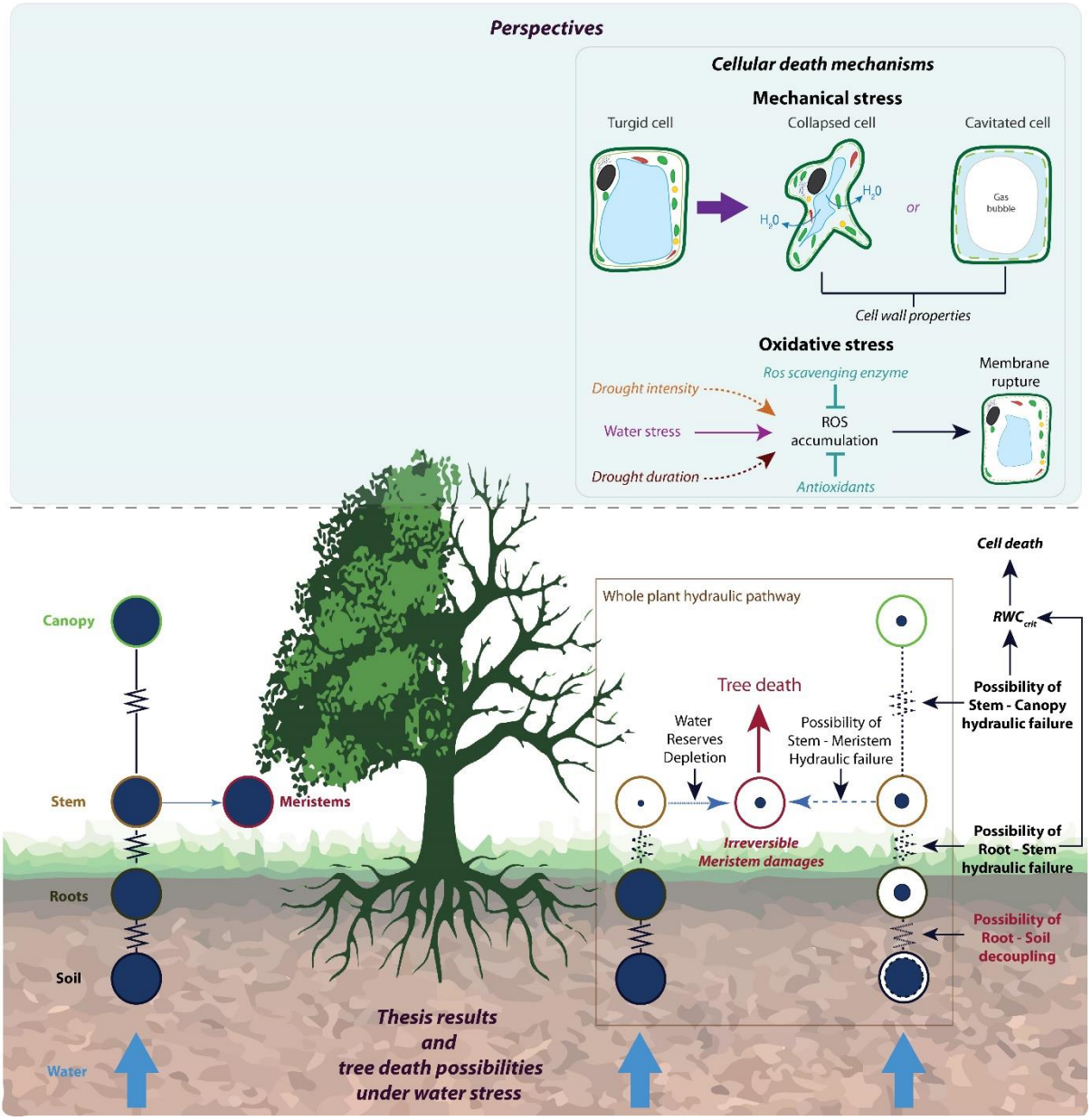


**Figure 82.** Summary diagram part 3.
Here, the first perspectives to this thesis are presented at the cellular level. A future direction to give to this work would be to elucidate the mechanisms behind cellular death and how they are affected by the cell wall properties. On the biochemical level, understanding how drought intensity and duration affect reactive oxygen species (ROS) production and thus membrane rupture and cellular death is a promising direction to get a better knowledge of drought-induced cell mortality and thus tree mortality.

Furthermore, it was also shown in anhydrobiotic aquatic moss that the rate of dehydration imposed on the plant during a drought event was of great importance in the induction of cell damage (Cruz De Carvalho *et al.*, 2012). Indeed, it has been shown that in anhydrobiotic organisms, slow dehydration would protect cells from ROS production and allow them to survive in the presence of very little water (Cruz De Carvalho *et al.*, 2012). Thus, experiments varying the dehydration rate of plants, for example by varying the VPD of the drying environment using the same principle as the drought-box (Billon *et al.*, 2020) but this time for potted plants, could lead to the elucidation of the role of ROS in cell mortality under drought conditions (Figure 82). However, transposing those ROS effects at the cells level to the individual level might remain challenging in practice. Indeed, it remains tricky to work at the meristem levels as the cambium only represents three to four layers of cells. Thus, evaluating the amount of ROS in the cambial cells themselves seems very difficult in practice. Therefore, the determination of the amount of ROS needed to provoke meristem death seems only possible by working by proxy at the stem level.

### *1.3. Is the prediction of meristematic cells mortality inevitable when trying to predict tree mortality?*

One of the questions that arose from this thesis work was whether it would be necessary to predict cell mortality or whether the prediction of hydraulic failure alone would determine when a tree might die from a drought event. Indeed, the results reported in Chapter 3. demonstrated that maintaining cambial integrity was one of the most important elements for allowing a tree to recover from the drought event and produce new organs and continue to grow the following vegetative season. These results supported the assumptions made by Körner (2019) where high level of hydraulic functioning would not allow to save a tree if its tissues were already damaged. However, our results do not exactly corroborate with all the hypothesis launched by Körner (2019). Indeed, the results of Chapter 3. also showed that some trees, although presenting a large number of living cells, might not survive the drought event suggesting that a hydraulic failure located upstream in the hydraulic pathway and upstream of the measurement point had already occurred, thus dooming the future of these trees. Thus, hydraulic failure therefore seems to be the process that triggers tree death in an inexorable manner, although on the longer or shorter term.

Therefore, in view of our results, it seems that in order to predict tree mortality from drought, **considering the interplay of hydraulic failure and meristematic cells integrity** could help improving model predictions and their accuracy. However, we suggest taking into consideration the PLC of the whole hydraulic pathway instead of the PLC of a single point when running predictions. Thus, in order to implement the models we suggest running more experiments such as those carried out in Chapter 3. but, this time, taking into account the PLC of the whole hydraulic pathway and the status of the root-soil hydraulic connection in order to try to link the hydraulic failure with the level of cell death within the meristems. In addition, as our study was only interested in the survival of the cambium and neglected the other meristems (i.e., bud, roots and shoot apical meristems), we suggest taking them into consideration as it has been shown that bud break quality was strongly dependant on the previous year's environmental conditions (Escobedo & Crabbé; Herter *et al.*, 1988; Egea & Burgos, 1993; Cook & Jacobs, 2000) and that drought stress may impact their survival capacity

and thus hinder the future growth and development of the tree (Barigah *et al.*, 2013a). Taking all these elements into consideration, it would be possible to compare between individuals and to check if two trees, with the same global PLC, present identical levels of cell damage within their meristems. **If this were the case, then it would no longer be necessary to model meristematic cells mortality but only the overall hydraulic failure level of the individual**. (Figure 83).

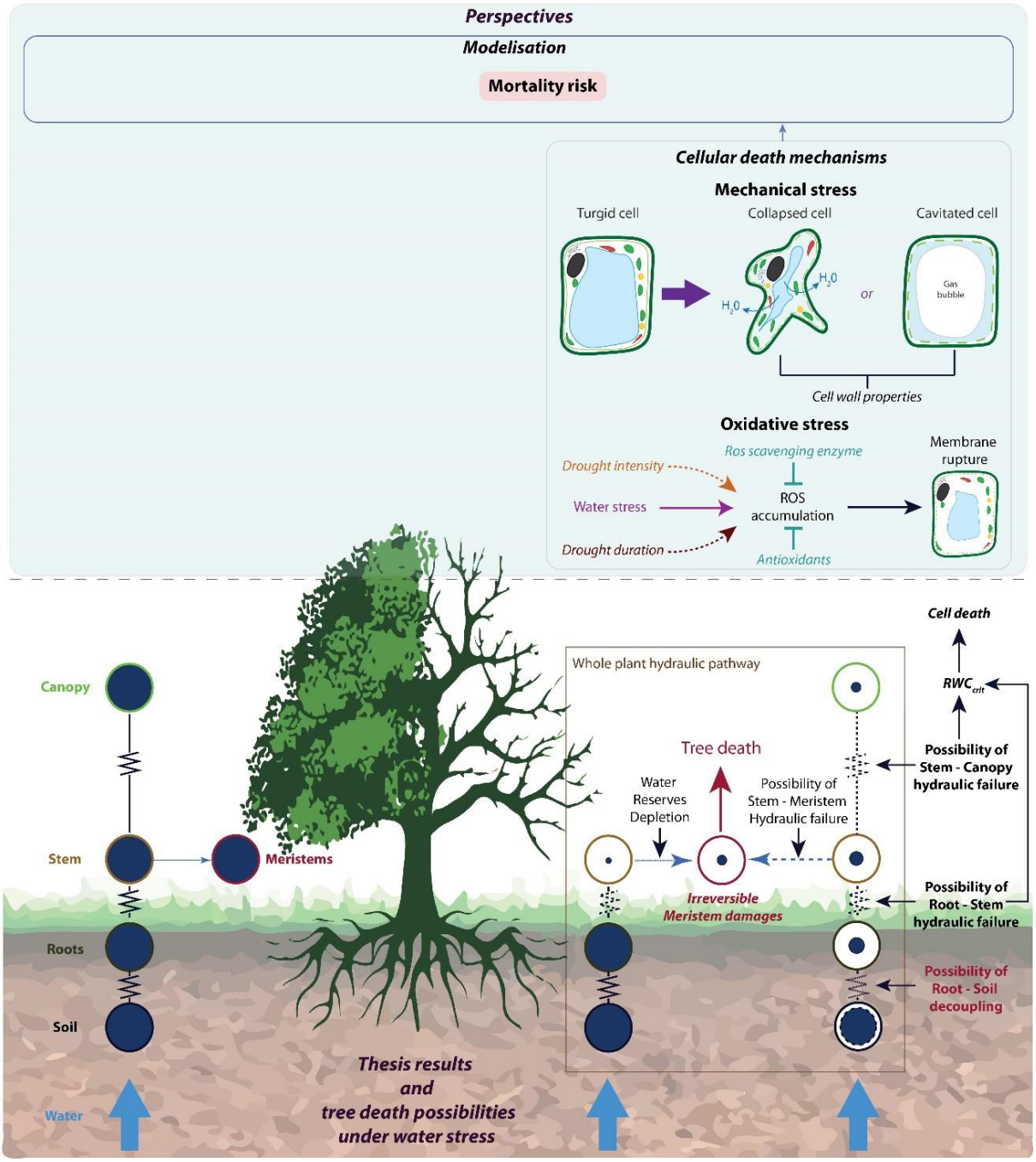


**Figure 83.** Summary diagram part 4.
While the first perspectives to this thesis were presented at the cellular level, the findings could also help implementing models and predicting tree mortality risk through either the prediction of xylem hydraulic failure at the whole hydraulic pathway level or through the prediction of cell mortality.

## 2. Considering the recurrence of drought stress on individual survival

Another point worth considering in the study of tree mortality under drought conditions, and that was not at all addressed through this thesis, is that an individual tree under natural conditions will, in general, face several drought events during their lifetime. As global climate models predict an increment in the frequency of droughts in the coming years (IPCC, 2022), this recurrence of drought events is expected to increase globally. Therefore, when trying to predict tree mortality under drought conditions, the resilience and acclimation of individuals to these drought events within a population appears as crucial in order to be able to withstand the recurrence of these events and thus survive in the long term (DeSoto *et al.*, 2020; Lemaire *et al.*, 2021). Indeed, **resilience** describes the capacity of a system to maintain its functions after the impact of an exogenous disturbance (Holling, 1973), while **acclimation** through phenotypic plasticity is defined as the ability of the plant to improve a given trait in response to changes in its environment (Nicotra *et al.*, 2010). If some studies have suggested that low resilience to drought could increase the risk of tree mortality (DeSoto *et al.*, 2020), others have also mentioned that the acclimation could represent a major source of uncertainty when trying to determine the risk of mortality during a drought and that this process have not been sufficiently taken into account in models probably because we lack knowledge about which traits are likely to acclimate and to what extent (McDowell *et al.*, 2022).

In terms of resilience it has been shown that gymnosperm species, such as *Pinaceae*, tend to show stronger and longer-term **legacy effects** on their radial growth after drought (Anderegg *et al.*, 2015b) thus recovering slower and therefore being more vulnerable to new drought episodes than some Angiosperm species, such as the *Fagaceae,* which recovered quicker from drought and thus cope better when facing a new episode of water shortage (Gazol *et al.*, 2017). However, if the resilience in term of growth resilience has been largely studied in the past years (Lloret *et al.*, 2011; Martínez-Vilalta *et al.*, 2012; Carnwath & Nelson, 2017), none of the studies on trees have evaluated the resilience of cells to a drought event. In fact, none of them has tried, for example, to see if a cell that was extremely dehydrated and presented a shrunken protoplast, which was the case in our cambial TEM observation in Chapter 3., could swing back to its original shape if the water stress was alleviated. In addition, none of them has tried to estimate the legacy effect directly at the meristems level and if the trees would keep a reduced number of meristematic cells after a drought event or if numerous meristematic cell divisions would happen once the stress is alleviated, thus allowing a faster recovery of the trees and, in the end, a better resilience.

The acclimation of various physiological and morphological traits, such as the change in resource allocation to branches at the expense of leaves or the plasticity of the turgor loss point, has already been well documented (Mencuccini & Bonosi, 2001; Martínez-Vilalta *et al.*, 2009; Rosas *et al.*, 2019). Recently, the plasticity and acclimation of hydraulic traits, in response to water stress, has been assessed in practice by Lemaire *et al.* (2021) that have shown that a significant increase in xylem resistance to cavitation was possible when growing trees of *P. tremula x alba* under a mild water stress, i.e., at only 25-30% of soil field capacity. In addition, they have shown that this increased resistance to xylem cavitation, conjoint with the other acclimated traits, was responsible, in simulations run with the SurEau model (Cochard *et al.*,

2021), for a time needed to reach the hydraulic failure 200% longer than that of plants not acclimated to drought, i.e., grown under non-water limited conditions. Thus, these results suggest that understanding and taking into account the acclimation of species following moderate water stress is an essential parameter for improving predictions of tree mortality risk under drought conditions. Therefore, although our studies did not attempt to investigate the effects of acclimation on tree survival, we could suggest, in view of our results, that there is a need to assess the capacity of cell acclimation after a moderate water stress. Indeed, considering that, for conifers, high level of cellular mortality is linked with lower probability to survive a drought event (Chapter 1. and Chapter 3.) and that this cellular mortality occurs after a defined dehydration threshold ($RWC_{crit}$) (Chapter 2. And Chapter 3.), one question that now arises is whether an individual exposed to a first moderate drought event would present cells that are more tolerant to dehydration afterwards, meaning that the cells produced during the moderate drought event would present a lower $RWC_{crit}$. Thus, it would be interesting to evaluate the $RWC_{crit}$ of clone individuals that have either been grown under moderate water stress or at field capacity to check if an acclimation at the cell level is possible. As studies of $P_{50}$ acclimation suggest that this trait acclimation is only possible in angiosperms (Sorek *et al.*, 2021) and not in conifers (Hudson *et al.*, 2018), probably because of the ability of some angiosperms to repair embolism, if not routinely for all tree species (Cochard & Delzon, 2013), at least regularly and on a daily basis for some grapevine species (Zufferey *et al.*, 2011; Knipfer *et al.*, 2019), another question that arise is to know if this observed non-acclimating pattern at the hydraulic level for conifers would also be observed at the cellular level.

Thus, as resilience and acclimation, appears as a key factor for surviving a recurrence of drought-event, particularly in angiosperms, considering it when implementing mechanistic models aiming at predicting drought-induced tree mortality, would allow an important leap forward in the predictions and thus forest management for the future (Figure 84). However, it is important to keep in mind that intense droughts may occur too quickly to allow acclimation of trees and thus exacerbate their mortality risk (McDowell *et al.*, 2022), therefore the acclimation and resilience components should be implemented as variable factors when predicting tree mortality by using mechanistic models.

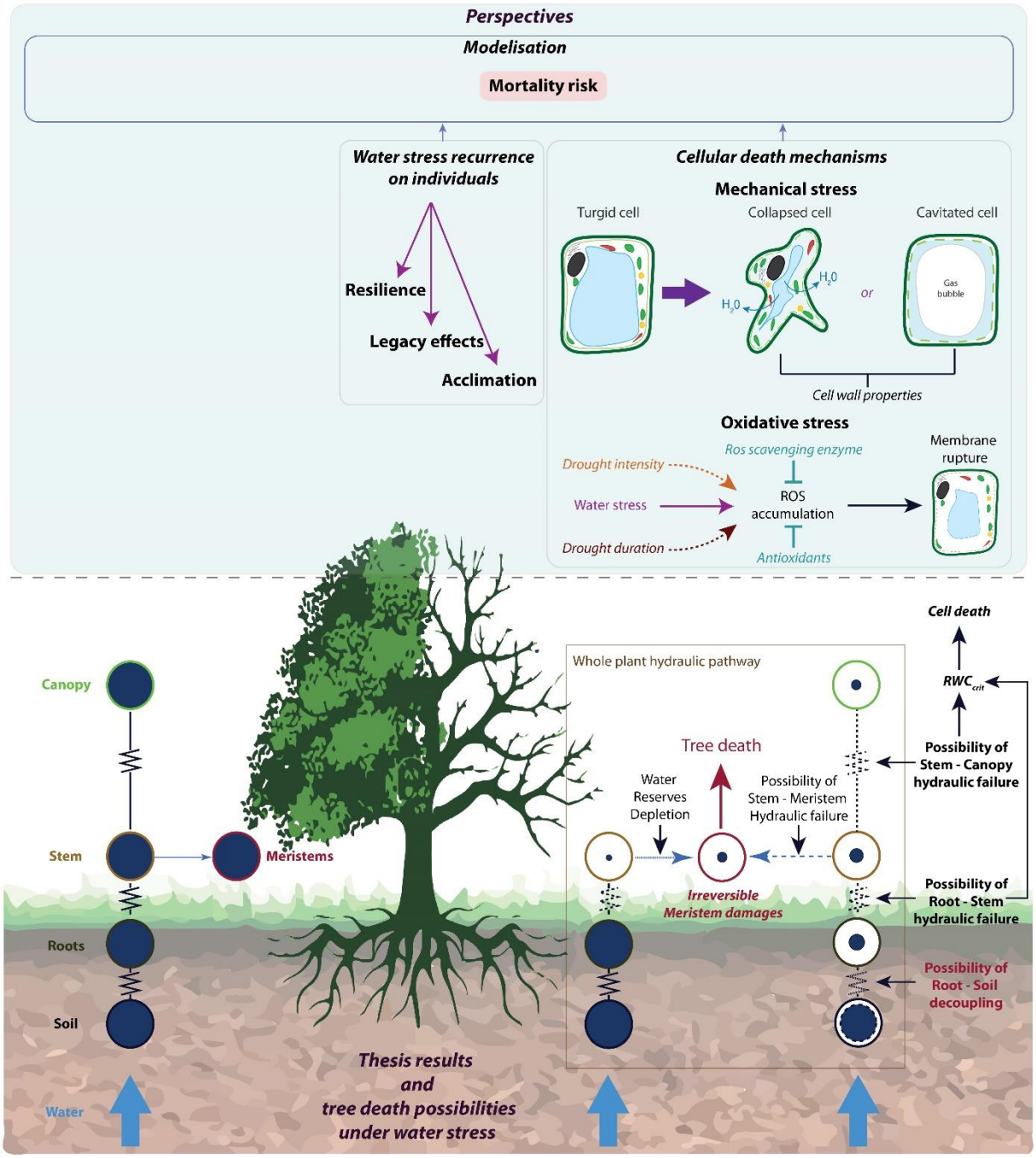


**Figure 84.** Summary diagram part 5.
Another perspective to this thesis work is presented at the individual level. A future direction to give to this work would be to elucidate the importance of water stress recurrence on individuals and how their resilience, legacy effect, and acclimation, particularly at the cellular level, could influence tree survival. In order to better predict tree mortality under the recurrence of droughts that is expected for the future climate, those elements should also appear in future models which, for now, lack of knowledge about these processes.

## 3. Results extrapolation: from cells to ecosystem management

A unanimous conclusion of the last years of research concerns the need to characterise water stress responses at a larger scale by conducting field studies in different environments and across different developmental levels (Matallana-Ramirez *et al.*, 2021). Indeed, most studies in the last decades have been conducted on small plants in pots exposed to extreme drought (Choat *et al.*, 2018), and this was also the case in this thesis work. Therefore, studies that incorporate the effects of long droughts (several years) on mature trees appear essential to understand and predict tree mortality under drought conditions. In addition, in recent years, modelling of plant hydraulics and more specifically plant mortality under drought conditions has been done at large scales (Tai *et al.*, 2017). However, very few studies have been conducted to ensure the accuracy of these predictions. Thus, this has led to an increasing need for large-scale observations, i.e., at the forest or ecosystem level.

Although many studies, including the results from this thesis, have shown that (i) plants that survive the drought event generally have a higher RWC than trees that do not (Mantova *et al.*, 2021; Sapes & Sala, 2021) and (ii) there is a $RWC_{crit}$ below which cells in different organs start to be damaged by water stress (see Chapter 2.), frequent and widespread measurements of RWC in the field have remained a challenge in practice and should be an important focus for the future studies. Indeed, RWC has been presented as scalable from organ to ecosystem (Martinez-Vilalta *et al.*, 2019) and has been shown to be of great interest when assessing water stress in forests *via* **remote sensing** (Van Emmerik *et al.*, 2017; Konings *et al.*, 2019; Rao *et al.*, 2019; Marusig *et al.*, 2020). Thus, if remote sensing tools have already been used to record the effects of drought at the global level using satellite sensors (McDowell *et al.*, 2015) and at the regional level *via* aircraft sensors (Asner *et al.*, 2016) we suggest that using a combination of the measurements carried out during the thesis (e.g., PLC, RWC, EL…) and remote sensing ones, such as the estimation of canopy water content (CWC) (Baeza *et al.*, 2021), would be a way to monitor the risk of tree mortality on a large scale, i.e., at the level of the forest or even the ecosystem (Figure 85). In addition, the remote sensing techniques would help working on both young individuals (saplings) and mature trees at the same time and thus compare their vulnerabilities, determine the crucial stages for forest development, and better manage the forest ecosystems. Indeed, depending on the resolution that we would like to give to our observations, it would be possible to use radar techniques (up to 1 metre in accuracy) (Van Emmerik *et al.*, 2017) or radiometry techniques that can have a resolution of 10km (Konings *et al.*, 2019) to screen forests from the individual to the ecosystem level and identify the risk of drought-induced mortality.

In addition, the use of remote-sensing techniques and particularly the interplay between the **spectrum analysis** and ground measurements would certainly allow the parametrization of new models, or improve already existing model like SurEau (Cochard *et al.*, 2021) that can predict the tree mortality risk (Figure 85). Indeed, remote-sensing tools would be an efficient way to detect alive and dead trees rapidly within a forest and therefore lead to more effective ground measurements such as water potential, RWC or meristem vitality on those detected trees. Thus, after characterization of those traits, it should be possible to obtain a correlation with the spectrum obtained with remote-sensing tools and thus accelerate the detection of

vulnerable trees to drought. In addition, the combination of the ground measurements and spectrum measurements should allow the calibration of a model that would explore the vulnerability of tree to drought at a large scale and thus be able to better predict the risks of mortality linked to climate change in future years. Those remote-sensing measurements coupled with modelling of future response of trees under drought conditions would therefore enable better forest management by, for example, providing useful information as to when a **rescue irrigation** is needed or if trees are already condemned by water-stress and needs to be harvested (Figure 85). In addition, this type of approach could also be used for orchard management which are, to date, most often irrigated on the basis of decision support systems based on indirect data such as meteorological data, (Allen *et al.*, 1998) or on the water status of the soil (Jones, 2004) and not on the basis of the water status of the trees, even though this water status would provide useful information on the physiological performance of the trees (Boini *et al.*, 2019). Therefore, the use of data obtained *via* remote sensing could permit better management of these orchards by limiting irrigation to the strict minimum without sacrificing productivity, but above all by allowing producers to carry out rescue irrigation if the water status of the trees becomes critical and threatens trees' survival.

Finally, the spectrum analysis would allow the detection of the trees with the best probability to survive a drought event and could lead to their **genetic screening**. Thus, by detecting, using remote-sensing, the trees with the best genotype-environment-survival interaction and by analyzing the genome of those trees, remote sensing technique could help identify "elite" trees that would lead to (i) a better thinning of the forest by keeping the most promising trees, which could also apply for orchards or (ii) a selection of the best genotypes (Figure 85) in order to plant the future forests and increase/or maintain wood production, or generate the best clones and cultivars, that will, by reducing the mortality rate under drought conditions, limit yield loss, an essential parameter in orchards (Dalal *et al.*, 2017). Thus, a combination of *in situ* measurements, remote-sensing techniques and model predictions could ultimately improve forests ecosystems and orchards management by providing useful information about individuals and population water-stress or identify climate-resilient traits that will guide future breeding efforts and thus have an important economic impact (Figure 85 and Figure 86).

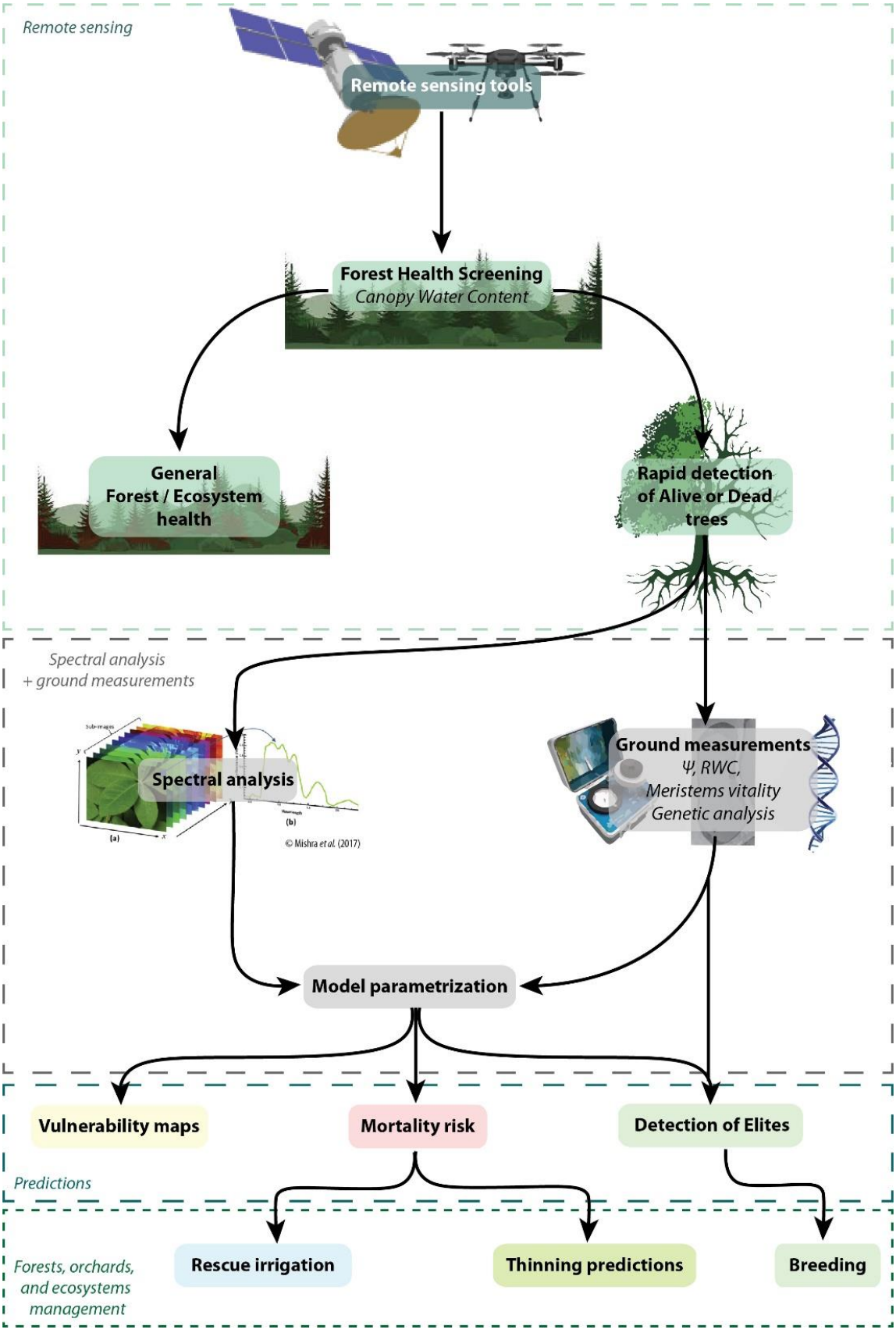


**Figure 85.** Diagram demonstrating the advantages of remote sensing tools for model parameterisation and forests, orchards, and ecosystems management.

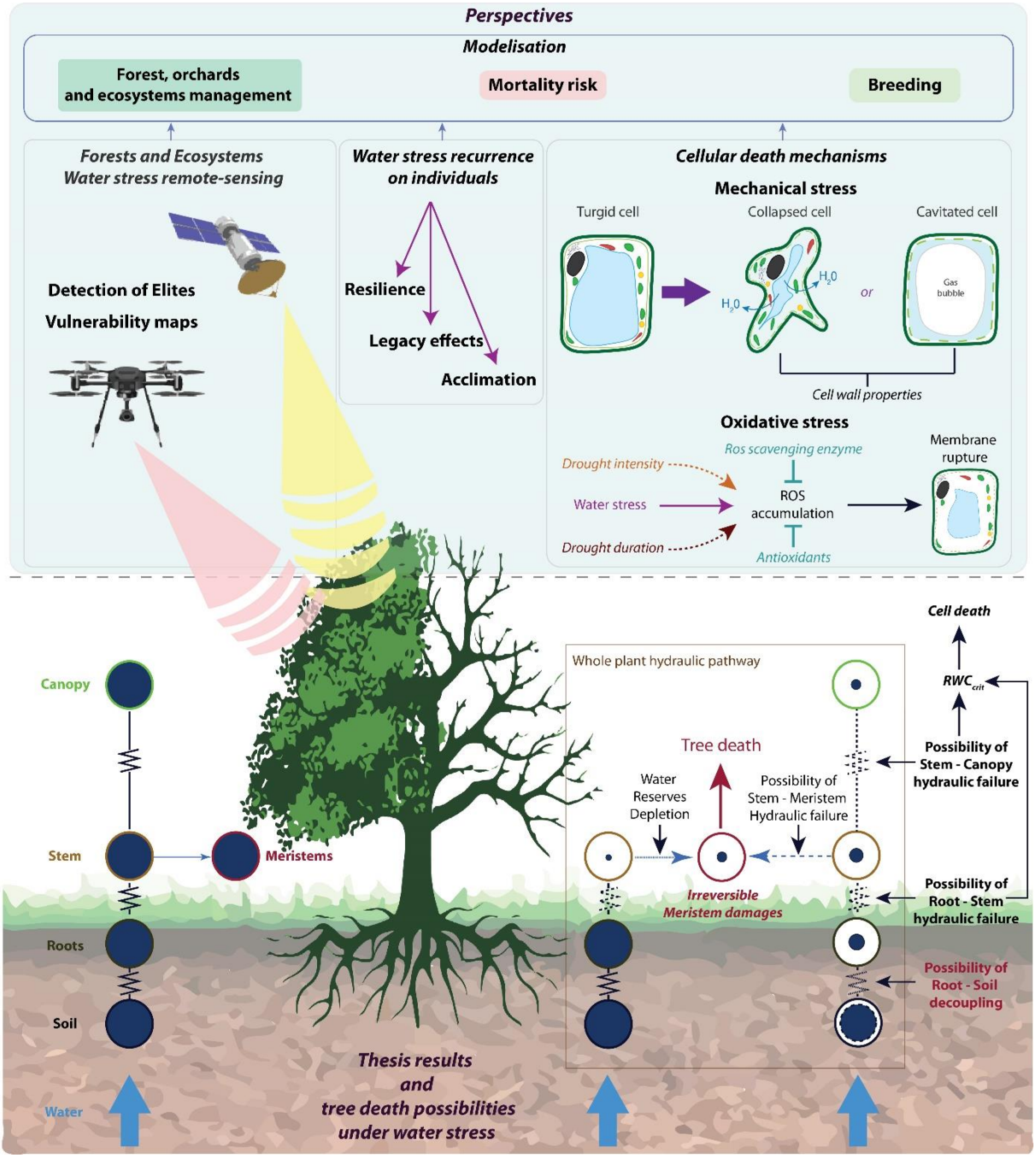


**Figure 86.** Final summary diagram and perspectives of the thesis.

# *Literature cited*

**Adams HD, Zeppel MJB, Anderegg WRL, Hartmann H, Landhäusser SM, Tissue DT, Huxman TE, Hudson PJ, Franz TE, Allen CD, *et al.* 2017**. A multi-species synthesis of physiological mechanisms in drought-induced tree mortality. *Nature Ecology and Evolution* **1**: 1285–1291.

**Algeo TJ, Scheckler SE, Maynard JB**. **2016**. 12. Effects of the Middle to Late Devonian Spread of Vascular Land Plants on Weathering Regimes, Marine Biotas, and Global Climate. *Plants Invade the Land*: 213–236.

**Allen CD, Breshears DD, McDowell NG**. **2015**. On underestimation of global vulnerability to tree mortality and forest die-off from hotter drought in the Anthropocene. *Ecosphere* **6**: 1–55.

**Allen CD, Macalady AK, Chenchouni H, Bachelet D, McDowell N, Vennetier M, Kitzberger T, Rigling A, Breshears DD, Hogg EH (Ted., *et al.* 2010**. A global overview of drought and heat-induced tree mortality reveals emerging climate change risks for forests. *Forest Ecology and Management* **259**: 660–684.

**Allen RG, Pereira LS, Raes D, Smith M**. **1998**. Crop evapotranspiration-Guidelines for computing crop water requirements-FAO Irrigation and drainage paper 56. *Fao, Rome* **300**: D05109.

**Almeida-Rodriguez AM, Hacke UG**. **2012**. Cellular localization of aquaporin mRNA in hybrid poplar stems. *American Journal of Botany* **99**: 1249–1254.

**Améglio T, Cochard H, Ewers FW**. **2003**. Gelista$^{TM}$: A new tool for testing frost hardiness by stem diameter variations on walnut. *Acta Horticulturae* **618**: 509–514.

**Ameglio T, Cruiziat P**. **1992**. Daily Variations of Stem and Branch Diameter: Short Overview from a Developed Example BT - Mechanics of Swelling. In: Karalis TK, ed. Berlin, Heidelberg: Springer Berlin Heidelberg, 193–204.

**Anderegg WRL, Berry JA, Field CB**. **2012a**. Linking definitions, mechanisms, and modeling of drought-induced tree death. *Trends in Plant Science* **17**: 693–700.

**Anderegg WRL, Berry JA, Smith DD, Sperry JS, Anderegg LDL, Field CB**. **2012b**. The roles of hydraulic and carbon stress in a widespread climate-induced forest die-off. *Proceedings of the National Academy of Sciences* **109**: 233–237.

**Anderegg WRL, Flint A, Huang CY, Flint L, Berry JA, Davis FW, Sperry JS, Field CB**. **2015a**. Tree mortality predicted from drought-induced vascular damage. *Nature Geoscience* **8**: 367–371.

**Anderegg WRL, Schwalm C, Biondi F, Camarero JJ, Koch G, Litvak M, Ogle K, Shaw JD, Shevliakova E, Williams AP, *et al.* 2015b**. Pervasive drought legacies in forest ecosystems and their implications for carbon cycle models. *Science* **349**: 528–532.

**Antoni V, Baude M, Calatayud P, Cerisier-Auger A, Christmann P, Colas S, Dossa-Thauvin V, Eumont D, Gauche M, Guzmove L, *et al.* 2020**. Focus ‘Ressources Naturelles’ - 2ème partie. In: CGDD, ed. L’environnement en France - Focus ‘Ressources Naturelles’.

**Arias PA, Bellouin N, Coppola E, Jones RG, Krinner G, Marotzke J, Naik V, Palmer MD, Plattner G-K, Rogelj J, *et al.* 2021**. 2021: Technical Summary. In: Masson-Delmotte, V., P. Zhai, A. Pirani, S.L. Connors, C. Péan, S. Berger, N. Caud, Y. Chen, L. Goldfarb MIG, M. Huang, K. Leitzell, E. Lonnoy, J.B.R. Matthews, T.K. Maycock, T. Waterfield, O. Yelekçi, R. Yu and BZ, eds. In Climate Change 2021: The Physical Science Basis. Contribution of Working Group I to the Sixth Assessment Report of the Intergovernmental Panel on Climate

Change. Cambridge, UK and New York, USA: Cambridge University Press, 33–144.

**Arndt SK, Irawan A, Sanders GJ**. **2015**. Apoplastic water fraction and rehydration techniques introduce significant errors in measurements of relative water content and osmotic potential in plant leaves. *Physiologia Plantarum* **155**: 355–368.

**Asner GP, Brodrick PG, Anderson CB, Vaughn N, Knapp DE, Martin RE**. **2016**. Progressive forest canopy water loss during the 2012–2015 California drought. *Proceedings of the National Academy of Sciences* **113**: E249–E255.

**Ayres MP, Lombardero MJ**. **2000**. Assessing the consequences of global change for forest disturbance from herbivores and pathogens. *Science of the Total Environment* **262**: 263–286.

**Baas P, Wheeler EA**. **1996**. Parallelism and reversibility in xylem evolution a review. *IAWA Journal* **17**: 351–364.

**Baeza A, Martin RE, Stephenson NL, Das AJ, Hardwick P, Nydick K, Mallory J, Slaton M, Evans K, Asner GP**. **2021**. Mapping the vulnerability of giant sequoias after extreme drought in California using remote sensing. *Ecological Applications* **31**: 1–14.

**Barigah TS, Bonhomme M, Lopez D, Traore A, Douris M, Venisse JS, Cochard H, Badel E**. **2013a**. Modulation of bud survival in Populus nigra sprouts in response to water stress-induced embolism. *Tree Physiology* **33**: 261–274.

**Barigah TS, Charrier O, Douris M, Bonhomme M, Herbette S, Améglio T, Fichot R, Brignolas F, Cochard H**. **2013b**. Water stress-induced xylem hydraulic failure is a causal factor of tree mortality in beech and poplar. *Annals of Botany* **112**: 1431–1437.

**Barley ME, Bekker A, Krapež B**. **2005**. Late Archean to Early Paleoproterozoic global tectonics, environmental change and the rise of atmospheric oxygen. *Earth and Planetary Science Letters* **238**: 156–171.

**Barrs H., Weatherley PE**. **1962**. A Re-Examination of the Relative Turgidity Techniques for Estimating Water Deficits in Leaves. *Australian Journal of Biological Sciences* **15**: 413–428.

**Bartlett MK, Klein T, Jansen S, Choat B, Sack L**. **2016**. The correlations and sequence of plant stomatal, hydraulic, and wilting responses to drought. *Proceedings of the National Academy of Sciences* **113**: 13098–13103.

**Bartlett MK, Scaffoni C, Sack L**. **2012**. The determinants of leaf turgor loss point and prediction of drought tolerance of species and biomes : a global meta-analysis. *Ecology Letters* **15**: 393–405.

**Beck EH, Fettig S, Knake C, Hartig K, Bhattarai T**. **2007**. Specific and unspecific responses of plants to cold and drought stress. *Journal of Biosciences* **32**: 501–510.

**Berner RA, Kothavala Z**. **2001**. Geocarb III: A revised model of atmospheric CO2 over phanerozoic time. *American Journal of Science* **301**: 182–204.

**Berry JA, Beerling DJ, Franks PJ**. **2010**. Stomata: Key players in the earth system, past and present. *Current Opinion in Plant Biology* **13**: 233–240.

**Bigler C, Bräker OU, Bugmann H, Dobbertin M, Rigling A**. **2006**. Drought as an inciting mortality factor in scots pine stands of the Valais, Switzerland. *Ecosystems* **9**: 330–343.

**Billon LM, Blackman CJ, Cochard H, Badel E, Hitmi A, Cartailler J, Souchal R, Torres-Ruiz JM**. **2020**. The DroughtBox: A new tool for phenotyping residual branch conductance

and its temperature dependence during drought. *Plant Cell and Environment*: 1–11.

**Biswas C, Johri BM**. **1997**. Cordaitales. In: The Gymnosperms. Berlin, Heidelberg: Springer Berlin Heidelberg, 127–136.

**Blackman CJ, Pfautsch S, Choat B, Delzon S, Gleason SM, Duursma RA**. **2016**. Toward an index of desiccation time to tree mortality under drought. *Plant Cell and Environment* **39**: 2342–2345.

**Blin F, Lafaye M, Vaurs P**. **2019**. *Bilan de la santé des forêts Puy-de-Dôme*.

**Blum A, Tuberosa R**. **2018**. Dehydration survival of crop plants and its measurement. *Journal of Experimental Botany* **69**: 975–981.

**Boini A, Manfrini L, Bortolotti G, Corelli-Grappadelli L, Morandi B**. **2019**. Monitoring fruit daily growth indicates the onset of mild drought stress in apple. *Scientia Horticulturae* **256**: 108520.

**Bolte A, Czajkowski T, Cocozza C, Tognetti R, De Miguel M, Pšidová E, Ditmarová L, Dinca L, Delzon S, Cochard H, *et al.* 2016**. Desiccation and mortality dynamics in seedlings of different European beech (Fagus sylvatica L.) populations under extreme drought conditions. *Frontiers in Plant Science* **7**: 1–12.

**Bouche PS, Larter M, Domec JC, Burlett R, Gasson P, Jansen S, Delzon S**. **2014**. A broad survey of hydraulic and mechanical safety in the xylem of conifers. *Journal of Experimental Botany* **65**: 4419–4431.

**Breashears DD, Cobb NS, Rich PM, Price KP, Allen CD, Balice RG, Romme WH, Kastens JH, Floyd ML, Belnap J, *et al.* 2005**. Tree die-off in response to global change-type drought: mortality insights from a decade of plant water potential measurements. *Proceedings of the National Academy of Sciences* **102**: 15144–15148.

**Briggs LJ, Shantz H. 1913**. *The water requirements of plants*. Washington, DC: US Department of Agriculture.

**Brodersen CR, McElrone AJ, Choat B, Matthews MA, Shackel KA**. **2010**. The dynamics of embolism repair in xylem: In vivo visualizations using high-resolution computed tomography. *Plant Physiology* **154**: 1088–1095.

**Brodribb TJ**. **2017**. Progressing from 'functional' to mechanistic traits. *New Phytologist* **215**: 9–11.

**Brodribb TJ, Bowman DJMS, Nichols S, Delzon S, Burlett R**. **2010**. Xylem function and growth rate interact to determine recovery rates after exposure to extreme water deficit. *New Phytologist* **188**: 533–542.

**Brodribb T, Brodersen CR, Carriqui M, Tonet V, Rodriguez Dominguez C, McAdam S**. **2021**. Linking xylem network failure with leaf tissue death. *New Phytologist*.

**Brodribb TJ, Carriqui M, Delzon S, Lucani C**. **2017**. Optical Measurement of Stem Xylem Vulnerability. *Plant Physiology* **174**: 2054–2061.

**Brodribb TJ, Cochard H**. **2009**. Hydraulic Failure Defines the Recovery and Point of Death in Water-Stressed Conifers. *Plant Physiology* **149**: 575–584.

**Brodribb TJ, Holbrook NM, Edwards EJ, Gutiérrez M V. 2003**. Relations between stomatal closure, leaf turgor and xylem vulnerability in eight tropical dry forest trees. *Plant, Cell and*

*Environment* **26**: 443–450.

**Brodribb TJ, Powers J, Cochard H, Choat B**. **2020**. Hanging by a thread? Forests and drought. *Science* **368**: 261–266.

**Brodribb TJ, Skelton RP, Mcadam SAM, Bienaimé D, Lucani CJ, Marmottant P**. **2016**. Visual quantification of embolism reveals leaf vulnerability to hydraulic failure. *New Phytologist* **209**: 1403–1409.

**Brown HR**. **2013**. The Theory of the Rise of Sap in Trees: Some Historical and Conceptual Remarks. *Physics in Perspective* **15**: 320–358.

**Brugger J, Hofmann M, Petri S, Feulner G**. **2019**. On the Sensitivity of the Devonian Climate to Continental Configuration, Vegetation Cover, Orbital Configuration, CO 2 Concentration, and Insolation. *Paleoceanography and Paleoclimatology* **34**: 1375–1398.

**Buckley T**. **2005**. The control of stomata by water balance. *New Phytologist*: 275–292.

**Carnwath G, Nelson C**. **2017**. Effects of biotic and abiotic factors on resistance versus resilience of Douglas fir to drought. *PLoS ONE* **12**: 1–19.

**Chaffey N**. **1999**. Cambium: Old challenges - new opportunities. *Trees - Structure and Function* **13**: 138–151.

**Charrier G, Delzon S, Domec JC, Zhang L, Delmas CEL, Merlin I, Corso D, King A, Ojeda H, Ollat N, *et al.* 2018**. Drought will not leave your glass empty: Low risk of hydraulic failure revealed by long-term drought observations in world's top wine regions. *Science Advances* **4**: 1–10.

**Charrier G, Torres-Ruiz JM, Badel E, Burlett R, Choat B, Cochard H, Delmas CEL, Domec J-C, Jansen S, King A, *et al.* 2016**. Evidence for Hydraulic Vulnerability Segmentation and Lack of Xylem Refilling under Tension. *Plant Physiology* **172**: 1657–1668.

**Chaturvedi AK, Patel MK, Mishra A, Tiwari V, Jha B**. **2014**. The SbMT-2 Gene from a Halophyte Confers Abiotic Stress Tolerance and Modulates ROS Scavenging in Transgenic Tobacco. *PLoS ONE* **9**.

**Choat B, Badel E, Burlett R, Delzon S, Cochard H, Jansen S**. **2016a**. Noninvasive Measurement of Vulnerability to Drought-Induced Embolism by X-Ray Microtomography. *Plant Physiology* **170**: 273–282.

**Choat B, Brodersen CR, Mcelrone AJ**. **2015**. Synchrotron X-ray microtomography of xylem embolism in Sequoia sempervirens saplings during cycles of drought and recovery. *New Phytologist* **205**: 1095–1105.

**Choat B, Brodribb TJ, Brodersen CR, Duursma RA, López R, Medlyn BE**. **2018**. Triggers of tree mortality under drought. *Nature* **558**: 531–539.

**Choat B, Jansen S, Brodribb TJ, Cochard H, Delzon S, Bhaskar R, Bucci SJ, Feild TS, Gleason SM, Hacke UG, *et al.* 2012**. Global convergence in the vulnerability of forests to drought. *Nature* **491**: 752–755.

**Choat B, Lahr EC, Melcher PJ, Zwieniecki MA, Holbrook NM**. **2005**. The spatial pattern of air seeding thresholds in mature sugar maple trees. *Plant, Cell and Environment* **28**: 1082–1089.

**Choat B, Munns R, McCully M, Passioura J, Tyerman S, Bramley H, Canny M**. **2016b**.

Chapter 3 - Water movement in plants Chapter 3 - Water movement in plants. : 1–95.

**CNRTL**. **2012**. Végétal, -ale, -aux.

**Cochard H**. **1992**. Vulnerability of several conifers to air embolism. *Tree Physiology* **11**: 73–83.

**Cochard H**. **2002a**. A technique for measuring xylem hydraulic conductance under high negative pressures. *Plant, Cell and Environment* **25**: 815–819.

**Cochard H**. **2002b**. How to measure xylem embolism with the XYL ' EM apparatus. : 1–7.

**Cochard H**. **2019**. A new mechanism for tree mortality due to drought and heatwaves. *bioRxiv*: 531632.

**Cochard H, Badel E, Herbette S, Delzon S, Choat B, Jansen S**. **2013**. Methods for measuring plant vulnerability to cavitation: A critical review. *Journal of Experimental Botany* **64**: 4779–4791.

**Cochard H, Barigah ST, Kleinhentz M, Eshel A**. **2008**. Is xylem cavitation resistance a relevant criterion for screening drought resistance among Prunus species? *Journal of Plant Physiology* **165**: 976–982.

**Cochard H, Cruiziat P, Tyree MT**. **1992**. Use of Positive Pressures to Establish Vulnerability Curves : Further Support for the Air-Seeding Hypothesis and Implications for Pressure-Volume Analysis. *Plant Physiology* **100**: 205–209.

**Cochard H, Delzon S**. **2013**. Hydraulic failure and repair are not routine in trees. *Annals of Forest Science* **70**: 659–661.

**Cochard H, Delzon S, Badel E**. **2015**. X-ray microtomography (micro-CT): A reference technology for high-resolution quantification of xylem embolism in trees. *Plant, Cell and Environment* **38**: 201–206.

**Cochard H, Herbette S, Hernández E, Hölttä T, Mencuccini M**. **2009**. The effects of sap ionic composition on xylem vulnerability to cavitation. *Journal of Experimental Botany* **61**: 275–285.

**Cochard H, Pimont F, Ruffault J, Martin-StPaul N**. **2021**. SurEau: a mechanistic model of plant water relations under extreme drought. *Annals of Forest Science* **78**.

**Cook C, Jacobs G**. **2000**. Progression of apple (Malus× domestica Borkh.) bud dormancy in two mild winter climates. *The Journal of Horticultural Science and Biotechnology* **75**: 233–236.

**Creek D, Lamarque LJ, Torres-Ruiz JM, Parise C, Burlett R, Tissue DT, Delzon S**. **2020**. Xylem embolism in leaves does not occur with open stomata: evidence from direct observations using the optical visualization technique. *Journal of experimental botany* **71**: 1151–1159.

**Crowe JH, Hoekstra FA, Crowe LM**. **1992**. John H. Crowe, Folkert. *Annu. Rev. Physiol* **54**: 579–99.

**Cruz de Carvalho R, Catalá M, Branquinho C, Marques da Silva J, Barreno E**. **2017**. Dehydration rate determines the degree of membrane damage and desiccation tolerance in bryophytes. *Physiologia Plantarum* **159**: 277–289.

**Cruz De Carvalho R, Catalá M, Marques Da Silva J, Branquinho C, Barreno E**. **2012**. The

impact of dehydration rate on the production and cellular location of reactive oxygen species in an aquatic moss. *Annals of Botany* **110**: 1007–1016.

**Dai A**. **2013**. Increasing drought under global warming in observations and models. *Nature Climate Change* **3**: 52–58.

**Dalal A, Attia Z, Moshelion M**. **2017**. To produce or to survive: How plastic is your crop stress physiology? *Frontiers in Plant Science* **8**: 1–8.

**Delzon S, Cochard H**. **2014**. Recent advances in tree hydraulics highlight the ecological significance of the hydraulic safety margin. *New Phytologist* **203**: 355–358.

**Delzon S, Douthe C, Sala A, Cochard H**. **2010**. Mechanism of water-stress induced cavitation in conifers: Bordered pit structure and function support the hypothesis of seal capillary-seeding. *Plant, Cell and Environment* **33**: 2101–2111.

**DeSoto L, Cailleret M, Sterck F, Jansen S, Kramer K, Robert EMR, Aakala T, Amoroso MM, Bigler C, Camarero JJ, *et al.* 2020**. Low growth resilience to drought is related to future mortality risk in trees. *Nature Communications* **11**: 1–9.

**Dixon H, Joly J**. **1894**. On the ascent of sap. *Philosophical Transactions of the Royal Society of London. (B.)* **186**.

**Van Doorn WG, Beers EP, Dangl JL, Franklin-Tong VE, Gallois P, Hara-Nishimura I, Jones AM, Kawai-Yamada M, Lam E, Mundy J, *et al.* 2011**. Morphological classification of plant cell deaths. *Cell Death and Differentiation* **18**: 1241–1246.

**Van Doorn WG, Woltering EJ**. **2005**. Many ways to exit? Cell death categories in plants. *Trends in Plant Science* **10**: 117–122.

**Duan H, Duursma RA, Huang G, Smith RA, Choat B, O'Grady AP, Tissue DT**. **2014**. Elevated [CO2] does not ameliorate the negative effects of elevated temperature on drought-induced mortality in Eucalyptus radiata seedlings. *Plant, Cell and Environment* **37**: 1598–1613.

**Duddek P, Carminati A, Koebernick N, Ohmann L, Lovric G, Delzon S, Rodriguez-Dominguez CM, King A, Ahmed MA**. **2022**. The impact of drought-induced root and root hair shrinkage on root–soil contact. *Plant Physiology*: 0–5.

**Duke NC, Kovacs JM, Griffiths AD, Preece L, Hill DJE, Van Oosterzee P, Mackenzie J, Morning HS, Burrows D**. **2017**. Large-scale dieback of mangroves in Australia's Gulf of Carpentaria: A severe ecosystem response, coincidental with an unusually extreme weather event. *Marine and Freshwater Research* **68**: 1816–1829.

**Duursma R, Choat B**. **2017**. fitplc - an R package to fit hydraulic vulnerability curves. *Journal of Plant Hydraulics* **4**: 002.

**Edwards D**. **2004**. Embryophytic sporophytes in the Rhynie and Windyfield cherts. *Transactions of the Royal Society of Edinburgh, Earth Sciences* **94**: 397–410.

**Egea J, Burgos L**. **1993**. CLIMA and double kerneled fruits in almond. In: I International Congress on Almond 373. 219–224.

**Van Emmerik T, Steele-Dunne S, Paget A, Oliveira RS, Bittencourt PRL, Barros F de V., van de Giesen N**. **2017**. Water stress detection in the Amazon using radar. *Geophysical Research Letters* **44**: 6841–6849.

**Epila J, De Baerdemaeker NJF, Vergeynst LL, Maes WH, Beeckman H, Steppe K**. **2017**.

Capacitive water release and internal leaf water relocation delay drought-induced cavitation in African Maesopsis eminii. *Tree Physiology* **37**: 481–490.

**Escobedo J, Crabbé J**. Golden Delicious ).

**Evert RF**. **2006**. *Esau's Plant Anatomy Meristems, Cells and Tissues of the Plant Body - Their structure, Function, and Development*. Hoboken, New Jersey: John Wiley & Sons, Ltd.

**FAO**. **2020**. Évaluation Des Ressources Forestières Mondiales 2020. *Évaluation Des Ressources Forestières Mondiales 2020*.

**Feltrim D, Pereira L, Costa MG de S, Balbuena TS, Mazzafera P**. **2021**. Stem aquaporins and surfactant-related genes are differentially expressed in two Eucalyptus species in response to water stress. *Plant Stress* **1**: 100003.

**Fernandes M, Denis A, Fabre R, Lataste JF, Chrétien M**. **2015**. In situ study of the shrinkage-swelling of a clay soil over several cycles of drought-rewetting. *Engineering Geology* **192**: 63–75.

**Finch-Savage WE**. **1992**. Embryo Water Status and Survival in the Recalcitrant Species Quercus robur L : Evidence for a Critical Moisture Content. *Journal of Experimental Botany* **43**: 663–669.

**Food and Agriculture Organization**. **2006**. Global Forest Resources Assessment 2005: Progress towards sustainable forest management. *FAO Forestry Paper 147* **147**: 11–36.

**Franklin JF, Shugart HH, Harmon ME**. **1987**. Tree Death as an Ecological Process. *BioScience* **37**: 550–556.

**Franks PJ, Adams MA, Amthor JS, Barbour MM, Berry JA, Ellsworth DS, Farquhar GD, Ghannoum O, Lloyd J, McDowell N, *et al.* 2013**. Sensitivity of plants to changing atmospheric CO2 concentration: From the geological past to the next century. *New Phytologist* **197**: 1077–1094.

**Ganthaler A, Bär A, Dämon B, Losso A, Nardini A, Dullin C, Tromba G, von Arx G, Mayr S**. **2022**. Alpine dwarf shrubs show high proportions of nonfunctional xylem: Visualization and quantification of species-specific patterns. *Plant Cell and Environment* **45**: 55–68.

**Gazol A, Camarero JJ, Anderegg WRL, Vicente-Serrano SM**. **2017**. Impacts of droughts on the growth resilience of Northern Hemisphere forests. *Global Ecology and Biogeography* **26**: 166–176.

**Gričar J, Jagodic Š, Šefc B, Trajković J, Eler K**. **2014**. Can the structure of dormant cambium and the widths of phloem and xylem increments be used as indicators for tree vitality? *European Journal of Forest Research* **133**: 551–562.

**Guadagno CR, Ewers BE, Speckman HN, Aston TL, Huhn BJ, DeVore SB, Ladwig JT, Strawn RN, Weinig C**. **2017**. Dead or alive? Using membrane failure and chlorophyll fluorescence to predict mortality from drought. *Plant Physiology* **175**: pp.00581.2016.

**Hacke UG, Sperry JS, Pockman WT, Davis SD, Mcculloh KA**. **2001**. Trends in wood density and structure are linked to prevention of xylem implosion by negative pressure. : 457–461.

**Hacke UG, Venturas MD, Mackinnon ED, Jacobsen AL, Sperry JS, Pratt RB**. **2015**. The standard centrifuge method accurately measures vulnerability curves of long-vesselled olive

stems. *New Phytologist* **205**: 116–127.

**Hammond WM, Williams AP, Abatzoglou JT, Adams HD, Klein T, López R, Sáenz-Romero C, Hartmann H, Breshears DD, Allen CD**. **2022**. Global field observations of tree die-off reveal hotter-drought fingerprint for Earth's forests. *Nature Communications* **13**.

**Hammond WM, Yu KL, Wilson LA, Will RE, Anderegg WRL, Adams HD**. **2019**. Dead or dying? Quantifying the point of no return from hydraulic failure in drought-induced tree mortality. *New Phytologist* **223**: 1834–1843.

**Harris PJ**. **2005**. Diversity in plant cell walls. *Plant diversity and evolution: genotypic and phenotypic variation in higher plants*: 201–227.

**Hartmann H, Moura CF, Anderegg WRL, Ruehr NK, Salmon Y, Allen CD, Arndt SK, Breshears DD, Davi H, Galbraith D, *et al.* 2018**. Research frontiers for improving our understanding of drought-induced tree and forest mortality. *New Phytologist* **218**: 15–28.

**Hartmann H, Ziegler W, Kolle O, Trumbore S**. **2013**. Thirst beats hunger - declining hydration during drought prevents carbon starvation in Norway spruce saplings. *New Phytologist* **200**: 340–349.

**Hasanuzzaman M, Davies NW, Shabala L, Zhou M, Brodribb TJ, Shabala S**. **2017**. Residual transpiration as a component of salinity stress tolerance mechanism: A case study for barley. *BMC Plant Biology* **17**: 1–12.

**Hasanuzzaman M, Shabala L, Zhou M, Brodribb TJ, Corkrey R, Shabala S**. **2018**. Factors determining stomatal and non-stomatal (residual) transpiration and their contribution towards salinity tolerance in contrasting barley genotypes. *Environmental and Experimental Botany* **153**: 10–20.

**Herter FG, Finardi NL, Mauget JC**. **1988**. Dormancy development in apple trees cvs. Gala, Golden and Fuji, in Pelotas, RS [Brazil]. *Acta Horticulturae (Netherlands)*.

**Hietz P, Rosner S, Sorz J, Mayr S**. **2008**. Comparison of methods to quantify loss of hydraulic conductivity in Norway spruce. *Annals of Forest Science* **65**: 502–502.

**Hochberg U, Windt CW, Ponomarenko A, Zhang Y-J, Gersony J, Rockwell FE, Holbrook NM**. **2017**. Stomatal Closure, Basal Leaf Embolism, and Shedding Protect the Hydraulic Integrity of Grape Stems. *Plant Physiology* **174**: 764–775.

**Hogg EH, Hurdle PA**. **1997**. Sap flow in trembling aspen implications for stomatal responses to VPD. *Tree Physiology* **17**: 501–509.

**Holbrook NM**. **1995**. Stem Water Storage. In: Academic Press, ed. Plant Stems: Physiology and Functional Morphology. San Diego, 151–174.

**Holling CS**. **1973**. Resilience and Stability of Ecological Systems. *Annu.Rev.Ecol.Syst.* **4**: 1–23.

**Hosking GP, Hutcheson JA**. **1988**. Mountain beech (nothofagus solandri var. cliffortioides) decline in the kaweka range, north island, new zealand. *New Zealand Journal of Botany* **26**: 393–400.

**Hudson PJ, Limousin JM, Krofcheck DJ, Boutz AL, Pangle RE, Gehres N, McDowell NG, Pockman WT**. **2018**. Impacts of long-term precipitation manipulation on hydraulic architecture and xylem anatomy of piñon and juniper in Southwest USA. *Plant Cell and Environment* **41**: 421–435.

**IGN**. **2021**. *Mémento*. Saint-Mandé.

**Ingle RA, Schmidt UG, Farrant JM, Thomson JA, Mundree SG**. **2007**. Proteomic analysis of leaf proteins during dehydration of the resurrection plant Xerophyta viscosa. *Plant, Cell and Environment* **30**: 435–446.

**IPCC**. **2007**. *Climate Change 2007 Synthesis Report [Core Writing Team, Pachauri, R.K and Reisinger, A. (eds.)]*.

**IPCC**. **2014**. *Climate Change 2014: Synthesis Report. Contribution of Working Groups I, II and III to the Fifth Assessment Report of the Intergovernmental Panel on Climate Change [Core Writing Team, R.K. Pachauri and L.A. Meyer (eds.)]*. Geneva, Switzerland: IPCC.

**IPCC**. **2018**. Annex I: Glossary. In: Masson-Delmotte V, Zhai P, Pörtner H-O, Roberts D, Skea J, Shukla PR, Pirani A, Moufouma-Okia W, Péan C, Pidcock R, et al., eds. Global Warming of 1.5°C. An IPCC Special Report on the impacts of global warming of 1.5°C above pre-industrial levels and related global greenhouse gas emission pathways, in the context of strengthening the global response to the threat of climate change,.

**IPCC**. **2021**. *Climate Change 2021: The Physical Science Basis. Contribution of Working Group I to the Sixth Assessment Report of the Intergovernmental Panel on Climate Change* (RY and BZ Masson-Delmotte, V., P. Zhai, A. Pirani, S. L. Connors, C. Péan, S. Berger, N. Caud, Y. Chen, L. Goldfarb, M. I. Gomis, M. Huang, K. Leitzell, E. Lonnoy, J.B.R. Matthews, T. K. Maycock, T. Waterfield, O. Yelekçi, Ed.). Cambridge University Press.

**IPCC**. **2022**. Climate Change 2022: Impacts, Adaptation and Vulnerability Summary for Policymakers. In: Pörtner H-O, Roberts DC, Adams H, Adler C, Aldunce P, Ali E, Begum RA, Betts R, Kerr RB, Biesbroek R, et al., eds. Water. Cambridge: Cambridge University Press, 551–715.

**Joardder MUH, Brown RJ, Kumar C, Karim MA**. **2015**. Effect of cell wall properties on porosity and shrinkage of dried apple. *International Journal of Food Properties* **18**: 2327–2337.

**Johnson DM, Domec JC, Carter Berry Z, Schwantes AM, McCulloh KA, Woodruff DR, Wayne Polley H, Wortemann R, Swenson JJ, Scott Mackay D, *et al.* 2018**. Co-occurring woody species have diverse hydraulic strategies and mortality rates during an extreme drought. *Plant Cell and Environment* **41**: 576–588.

**Johnson DM, Mcculloh KA, Woodruff DR, Meinzer FC**. **2012**. Plant Hydraulic safety margins and embolism reversal in stems and leaves: Why are conifers and angiosperms so different? Daniel. *Plant Science*.

**Johnson DM, Wortemann R, McCulloh KA, Jordan-Meille L, Ward E, Warren JM, Palmroth S, Domec JC**. **2016**. A test of the hydraulic vulnerability segmentation hypothesis in angiosperm and conifer tree species. *Tree Physiology* **36**: 983–993.

**Jones HG**. **2004**. Irrigation scheduling: Advantages and pitfalls of plant-based methods. *Journal of Experimental Botany* **55**: 2427–2436.

**Jones HG, Sutherland RA**. **1991**. Stomatal control of xylem embolism. *Plant, Cell & Environment* **14**: 607–612.

**Kaiser MO**. **1974**. Kaiser-Meyer-Olkin measure for identity correlation matrix. *Journal of the Royal Statistical Society* **52**: 296–298.

**Keenan TF, Hollinger DY, Bohrer G, Dragoni D, Munger JW, Schmid HP, Richardson**

**AD**. **2013**. Increase in forest water-use efficiency as atmospheric carbon dioxide concentrations rise. *Nature* **499**: 324–327.

**Kenrick P, Crane PR**. **1997**. The origin and early evolution of plants on land. *Nature* **389**: 33–39.

**Kerstiens G**. **1996**. Cuticular water permeability and its physiological significance. *Journal of Experimental Botany* **47**: 1813–1832.

**King M., Ludford PM**. **1983**. Chilling injury and electrolyte leakage in fruit of different tomato cultivars. *J. Am. Soc. Hort. Sci.* **108**: 74–77.

**Kirkham M. 2005**. Structure and Properties of Water. In: Principles of Soil and Plant Water Relations. Dana Dreibelbis, 27–39.

**Klepper B**. **1968**. Diurnal Pattern of Water Potential in Woody Plants. *Plant Physiology* **43**: 1931–1934.

**Klimešová J, Nobis MP, Herben T**. **2015**. Senescence, ageing and death of the whole plant: Morphological prerequisites and constraints of plant immortality. *New Phytologist* **206**: 14–18.

**Knipfer T, Reyes C, Earles JM, Berry ZC, Johnson DM, Brodersen CR, McElrone AJ**. **2019**. Spatiotemporal coupling of vessel cavitation and discharge of stored xylem water in a tree sapling. *Plant Physiology* **179**: 1658–1668.

**Konings AG, Rao K, Steele-Dunne SC**. **2019**. Macro to micro: microwave remote sensing of plant water content for physiology and ecology. *New Phytologist* **223**: 1166–1172.

**Körner C**. **2019**. No need for pipes when the well is dry - a comment on hydraulic failure in trees. *Tree Physiology*.

**Koster KL, Balsamo RA, Espinoza C, Oliver MJ**. **2010**. Desiccation sensitivity and tolerance in the moss Physcomitrella patens : assessing limits and damage. *Plant Growth Regulation* **62**: 293–302.

**Van Kranendonk MJ, Altermann W, Beard BL, Hoffman PF, Johnson CM, Kasting JF, Melezhik VA, Nutman AP, Papineau D, Pirajno F**. **2012**. The Geologic Time Scale. In: Gradstein F., Ogg J., Schmitz M., Ogg G., eds. The Geologic Time Scale. Boston, MA: Elsevier, 299–392.

**Kump LR, Barley ME**. **2007**. Increased subaerial volcanism and the rise of atmospheric oxygen 2.5 billion years ago. *Nature* **448**: 1033–1036.

**Kursar TA, Engelbrecht BMJ, Burke A, Tyree MT, El Omari B, Giraldo JP**. **2009**. Tolerance to low leaf water status of tropical tree seedlings is related to drought performance and distribution. *Functional Ecology* **23**: 93–102.

**Lamacque L, Charrier G, dos Santos Farnese F, Lemaire B, Ameglio T, Herbette S**. **2020**. Drought-induced mortality: branch diameter variation reveals a point of no recovery in lavender species. *Plant Physiology* **183**: 1638–1649.

**Lamacque L, Sabin F, Améglio T, Herbette S, Charrier G**. **2022**. Detection of acoustic events in lavender for measuring xylem vulnerability to embolism and cellular damage. *Journal of Experimental Botany* **73**: 3699–3710.

**Landmann G, Dreyer E**. **2006**. Impacts of drought and heat on forest. Synthesis of available knowledge, with emphasis on the 2003 event in Europe. *Annals of Forest Science 3* **6**: 567–

652.

**Larter M, Brodribb TJ, Pfautsch S, Burlett R, Cochard H, Delzon S**. **2015**. Extreme aridity pushes trees to their physical limits. *Plant Physiology* **168**: 804–807.

**Laux T**. **2004**. The Stem Cell Concept in Plants. *Cell* **113**: 281–283.

**Lawrence MG**. **2005**. The relationship between relative humidity and the dewpoint temperature in moist air: A simple conversion and applications. *Bulletin of the American Meteorological Society* **86**: 225–233.

**Lemaire C, Blackman CJ, Cochard H, Menezes-Silva PE, Torres-Ruiz JM, Herbette S**. **2021**. Acclimation of hydraulic and morphological traits to water deficit delays hydraulic failure during simulated drought in poplar. *Tree Physiology*: 1–14.

**Lens F, Sperry JS, Christman MA, Choat B, Rabaey D, Jansen S**. **2011**. Testing hypotheses that link wood anatomy to cavitation resistance and hydraulic conductivity in the genus Acer. *New Phytologist* **190**: 709–723.

**Lewis LA, McCourt RM**. **2004**. Green algae and the origin of land plants. *American Journal of Botany* **91**: 1535–1556.

**Lewis JD, Smith RA, Ghannoum O, Logan BA, Phillips NG, Tissue DT**. **2013**. Industrial-age changes in atmospheric [CO2] and temperature differentially alter responses of faster- and slower-growing Eucalyptus seedlings to short-term drought. *Tree Physiology* **33**: 475–488.

**Li S, Feifel M, Karimi Z, Schuldt B, Choat B, Jansen S**. **2015**. Leaf gas exchange performance and the lethal water potential of five European species during drought. *Tree Physiology* **36**: 179–192.

**Li S, Jansen S**. **2017**. The root cambium ultrastructure during drought stress in Corylus avellana. *IAWA Journal* **38**: 67–80.

**Li S, Lens F, Espino S, Karimi Z, Klepsch M, Schenk HJ, Schmitt M, Schuldt B, Jansen S**. **2016**. Intervessel pit membrane thickness as a key determinant of embolism resistance in angiosperm xylem. *IAWA Journal* **37**: 152–171.

**Lintunen A, Paljakka T, Riikonen A, Lindén L, Lindfors L, Nikinmaa E, Hölttä T**. **2015**. Irreversible diameter change of wood segments correlates with other methods for estimating frost tolerance of living cells in freeze-thaw experiment: a case study with seven urban tree species in Helsinki. *Annals of Forest Science* **72**: 1089–1098.

**Llorens C, Argentina M, Rojas N, Westbrook J, Dumais J, Noblin X**. **2016**. The fern cavitation catapult: Mechanism and design principles. *Journal of the Royal Society Interface* **13**.

**Lloret F, Keeling EG, Sala A**. **2011**. Components of tree resilience: Effects of successive low-growth episodes in old ponderosa pine forests. *Oikos* **120**: 1909–1920.

**Lwanga JS**. **2003**. Localized tree mortality following the drought of 1999 at Ngogo, Kibale National Park, Uganda. *African Journal of Ecology* **41**: 194–196.

**Maherali H, Pockman WT, Jackson RB**. **2004**. Adaptive variation in the vulnerability of woody plants to xylem cavitation. *Ecology* **85**: 2184–2199.

**Malamy JE, Benfey PN**. **1997**. Organization and cell differentiation in lateral roots of Arabidopsis thaliana. *Development (Cambridge, England)* **124**: 33–44.

**Manion PD**. **1981**. *Tree disease concepts*. Englewood Cliffs, New Jersey, USA: Prentice-Hall Inc.

**Mantova M, Herbette S, Cochard H, Torres-Ruiz JM**. **2022**. Hydraulic failure and tree mortality: from correlation to causation. *Trends in Plant Science* **27**: 335–345.

**Mantova M, Menezes-Silva PE, Badel E, Cochard H, Torres-Ruiz JM**. **2021**. The interplay of hydraulic failure and cell vitality explains tree capacity to recover from drought. *Physiologia Plantarum* **172**: 247–257.

**Martin-StPaul N, Delzon S, Cochard H**. **2017**. Plant resistance to drought depends on timely stomatal closure. *Ecology Letters* **20**: 1437–1447.

**Martinez-Vilalta J, Anderegg WRL, Sapes G, Sala A**. **2019**. Greater focus on water pools may improve our ability to understand and anticipate drought-induced mortality in plants. *New Phytologist*.

**Martínez-Vilalta J, Cochard H, Mencuccini M, Sterck F, Herrero A, Korhonen JFJ, Llorens P, Nikinmaa E, Nolè A, Poyatos R, *et al.* 2009**. Hydraulic adjustment of Scots pine across Europe. *New Phytologist* **184**: 353–364.

**Martínez-Vilalta J, López BC, Loepfe L, Lloret F**. **2012**. Stand- and tree-level determinants of the drought response of Scots pine radial growth. *Oecologia* **168**: 877–888.

**Marusig D, Petruzzellis F, Tomasella M, Napolitano R, Altobelli A, Nardini A**. **2020**. Correlation of field-measured and remotely sensed plant water status as a tool to monitor the risk of drought-induced forest decline. *Forests* **11**.

**Matallana-Ramirez LP, Whetten RW, Sanchez GM, Payn KG**. **2021**. Breeding for Climate Change Resilience: A Case Study of Loblolly Pine (Pinus taeda L.) in North America. *Frontiers in Plant Science* **12**: 1–22.

**Mayr S, Cochard H**. **2003**. A new method for vulnerability analysis of small xylem areas reveals that compression wood of Norway spruce has lower hydraulic safety than opposite wood. *Plant, Cell and Environment* **26**: 1365–1371.

**McDowell**. **2011**. Mechanisms Linking Drought, Hydraulics, Carbon Metabolism, and Vegetation Mortality. *Plant Physiology* **155**: 1051–1059.

**McDowell NG, Beerling DJ, Breshears DD, Fisher RA, Raffa KF, Stitt M**. **2011**. The interdependence of mechanisms underlying climate-driven vegetation mortality. *Trends in Ecology and Evolution* **26**: 523–532.

**McDowell NG, Coops NC, Beck PSA, Chambers JQ, Gangodagamage C, Hicke JA, Huang C ying, Kennedy R, Krofcheck DJ, Litvak M, *et al.* 2015**. Global satellite monitoring of climate-induced vegetation disturbances. *Trends in Plant Science* **20**: 114–123.

**McDowell N, Pockman WT, Allen CD, Breashears DD, Cobb N, Kolb T, Plaut J, Sperry J, West A, Williams DG, *et al.* 2008**. Mechanisms of plants survival and mortality during drought: why do some plants survive while others succumb to drought? *New Phytologist* **178**: 719–739.

**McDowell NG, Sapes G, Pivovaroff A, Adams HD, Allen CD, Anderegg WRL, Arend M, Breshears DD, Brodribb T, Choat B, *et al.* 2022**. Mechanisms of woody-plant mortality under rising drought, CO2 and vapour pressure deficit. *Nature Reviews Earth & Environment*.

**McElrone AJ, Choat B, Grambetta, Greg A. Brodersen CR**. **2013**. Water Uptake and

Transport in Vascular Plants.

**Meinzer FC, Clearwater MJ, Goldstein G**. **2001**. Water transport in trees: current perspectives, new insights and some controversies. *Environental and Experimental Botany* **45**: 239–262.

**Meinzer FC, Johnson DM, Lachenbruch B, McCulloh KA, Woodruff DR**. **2009**. Xylem hydraulic safety margins in woody plants: Coordination of stomatal control of xylem tension with hydraulic capacitance. *Functional Ecology* **23**: 922–930.

**Menard S**. **2002**. *Applied logistic regression analysis*. Sage.

**Mencuccini M, Bonosi L**. **2001**. Leaf/sapwood area ratios in Scots pine show acclimation across Europe. *Canadian Journal of Forest Research* **31**: 442–456.

**Meyer-Berthaud B, Decombeix AL**. **2009**. L'évolution des premiers arbres : les stratégies dévoniennes. *Comptes Rendus - Palevol* **8**: 155–165.

**Meyer-Berthaud B, Scheckler SE, Bousquet JL**. **2000**. The development of Archaeopteris: New evolutionary characters from the structural analysis of an Early Famennian trunk from Southeast Morocco. *American Journal of Botany* **87**: 456–468.

**Meyer-Berthaud B, Scheckler SE, Wendt J**. **1999**. Archaeopteris is the earliest known modern tree. *Nature* **398**: 700–701.

**Miao S, Zou CB, Breshears DD**. **2009**. Vegetation Responses to Extreme Hydrological Events: Sequence Matters. *The American Naturalist* **173**: 113–118.

**Milburn J, Johnson R**. **1966**. The conduction of sap : II. Detection of vibrations produced by sap cavitation in Ricinus xylem. *Planta* **69 (1)**: 43:52.

**Mirone A, Brun E, Gouillart E, Tafforeau P, Kieffer J**. **2014**. The PyHST2 hybrid distributed code for high speed tomographic reconstruction with iterative reconstruction and a priori knowledge capabilities. *Nuclear Instruments and Methods in Physics Research, Section B: Beam Interactions with Materials and Atoms* **324**: 41–48.

**Mirzaie M, Darvishzadeh R, Shakiba A, Matkan AA, Atzberger C, Skidmore A**. **2014**. Comparative analysis of different uni- and multi-variate methods for estimation of vegetation water content using hyper-spectral measurements. *International Journal of Applied Earth Observation and Geoinformation* **26**: 1–11.

**Momayyezi M, Borsuk AM, Brodersen CR, Gilbert ME, Théroux-Rancourt G, Kluepfel DA, McElrone AJ**. **2022**. Desiccation of the leaf mesophyll and its implications for CO2 diffusion and light processing. *Plant Cell and Environment* **45**: 1362–1381.

**Moore JP, Vicré-Gibouin M, Farrant JM, Driouich A**. **2008**. Adaptations of higher plant cell walls to water loss: Drought vs desiccation. *Physiologia Plantarum* **134**: 237–245.

**Nicotra AB, Atkin OK, Bonser SP, Davidson AM, Finnegan EJ, Mathesius U, Poot P, Purugganan MD, Richards CL, Valladares F, *et al.* 2010**. Plant phenotypic plasticity in a changing climate. *Trends in Plant Science* **15**: 684–692.

**Niklas KJ**. **1994**. The Allometry of Safety-Factors for Plant Height. *American Journal of Botany* **81**: 345–351.

**Nobel PS**. **2009**. Chapter 2 - Water. In: Nobel PSBT-P and EPP (Fourth E, ed. San Diego: Academic Press, 44–99.

**Nobel PS, Cui M**. **1992**. Hydraulic conductances of the soil, the root-soil air gap, and the root: Changes for desert succulents in drying soil. *Journal of Experimental Botany* **43**: 319–326.

**Noblin X, Rojas NO, Westbrook J, Llorens C, Argentina M, Dumais J**. **2012**. The fern sporangium: A unique catapult. *Science* **335**: 1322.

**Nolf M, Rosani A, Ganthaler A, Beikircher B, Mayr S**. **2016**. Herb hydraulics: Inter-and intraspecific variation in three ranunculus species. *Plant Physiology* **170**: 2085–2094.

**Oertli JJ**. **1986**. The Effect of Cell Size on Cell Collapse under Negative Turgor Pressure. *Journal of Plant Physiology* **124**: 365–370.

**Oren R, Pataki DE**. **2001**. Transpiration in response to variation in microclimate and soil moisture in southeastern deciduous forests. *Oecologia* **127**: 549–559.

**Paganin D**. **2006**. *Coherent X-ray optics, Vol. 6 of Oxford series on synchrotron radiation* (OU Press, Ed.). Oxford, UK.

**Palmer WC**. **1965**. Meteorological Drought. *U.S. Departmente of Commerce* **45**: 58.

**Pammenter NW, Berjak P**. **2014**. Physiology of desiccation-sensitive (recalcitrant) seeds and the implications for cryopreservation. *International Journal of Plant Science* **175**: 21–28.

**Pammenter N., Vander Willigen C**. **1998**. A mathematical and statistical analysis of the curves illustrating vulnerability of xylem to cavitation. *Tree Physiology* **18**: 589–593.

**Pan Y, Birdsey RA, Fang J, Houghton R, Kauppi PE, Kurz WA, Phillips OL, Shvidenko A, Lewis SL, Canadell JG**. **2011**. A large and persistent carbon sink in the world's forests. *Science* **333**: 988–993.

**Pearce RS**. **2001**. Plant freezing and damage. *Annals of Botany* **87**: 417–424.

**Pederson BS**. **1998**. the Role of Stress in the Mortality of Midwestern Oaks As Indicated By Growth Prior To Death. *Ecology* **79**: 79–93.

**Petrov V, Hille J, Mueller-Roeber B, Gechev TS**. **2015**. ROS-mediated abiotic stress-induced programmed cell death in plants. *Frontiers in Plant Science* **6**: 1–16.

**Pfautsch S, Hölttä T, Mencuccini M**. **2015**. Hydraulic functioning of tree stems - Fusing ray anatomy, radial transfer and capacitance. *Tree Physiology* **35**: 706–722.

**Ponomarenko A, Vincent O, Pietriga A, Cochard H, Badel E, Marmottant P**. **2014**. Ultrasonic emissions reveal individual cavitation bubbles in water-stressed wood. *Journal of the Royal Society Interface* **11**: 1–7.

**Pratt RB, Jacobsen AL, Ewers FW, Davis SD**. **2007**. Relationships among xylem transport, biomechanics and storage in stems and roots of nine Rhamnaceae species of the California chaparral. *New Phytologist* **174**: 787–798.

**Preisler Y, Tatarinov F, Grünzweig JM, Yakir D**. **2021**. Seeking the "point of no return" in the sequence of events leading to mortality of mature trees. *Plant, Cell & Environment* **44**: 1315–1328.

**Rajashekar CB, Lafta A**. **1996**. Cell-wall changes and cell tension in response to cold acclimation and exogenous abscisic acid in leaves and cell cultures. *Plant Physiology* **111**: 605–612.

**Rao K, Anderegg WRL, Sala A, Martínez-Vilalta J, Konings AG**. **2019**. Satellite-based

vegetation optical depth as an indicator of drought-driven tree mortality. *Remote Sensing of Environment* **227**: 125–136.

**Raven JA**. **2018**. Evolution and palaeophysiology of the vascular system and other means of long-distance transport. *Philosophical Transactions of the Royal Society B: Biological Sciences* **373**.

**Reichstein M, Bahn M, Ciais P, Frank D, Mahecha MD, Seneviratne SI, Zscheischler J, Beer C, Buchmann N, Frank DC, *et al.* 2013**. Climate extremes and the carbon cycle. *Nature* **500**: 287–295.

**Riederer M**. **2006**. Thermodynamics of the water permeability of plant cuticles: Characterization of the polar pathway. *Journal of Experimental Botany* **57**: 2937–2942.

**Rodriguez-Dominguez CM, Forner A, Martorell S, Choat B, Lopez R, Peters JMR, Pfautsch S, Mayr S, Carins-Murphy MR, McAdam SAM, *et al.* 2022**. Leaf water potential measurements using the pressure chamber: Synthetic testing of assumptions towards best practices for precision and accuracy. *Plant Cell and Environment*: 0–25.

**Roland J-C, Roland F, Bouteau F, El Maarouf Bouteau H**. **2008**. *Atlas Biologie végétale – Tome 2 – Organisation des plantes à fleurs*.

**Rosas T, Mencuccini M, Barba J, Cochard H, Saura-Mas S, Martínez-Vilalta J**. **2019**. Adjustments and coordination of hydraulic, leaf and stem traits along a water availability gradient. *New Phytologist* **223**: 632–646.

**Saatchi S, Asefi-Najafabady S, Malhi Y, Aragão LEOC, Anderson LO, Myneni RB, Nemani R**. **2013**. Persistent effects of a severe drought on Amazonian forest canopy. *Proceedings of the National Academy of Sciences of the United States of America* **110**: 565–570.

**Sack L, Dietrich EM, Streeter CM, Sánchez-Gómez D, Holbrook NM**. **2008**. Leaf palmate venation and vascular redundancy confer tolerance of hydraulic disruption. *Proceedings of the National Academy of Sciences of the United States of America* **105**: 1567–1572.

**Sack L, John GP, Buckley TN**. **2018**. ABA accumulation in dehydrating leaves is associated with decline in cell volume, not turgor pressure. *Plant Physiology* **176**: 489–493.

**Sack L, Pasquet-Kok J, Bartlett M**. **2010**. Leaf pressure-volume curve parameters. *Prometheus Protocols*.

**Sakes A, Van Wiel M Der, Henselmans PWJ, Van Leeuwen JL, Dodou D, Breedveld P**. **2016**. Shooting mechanisms in nature: A systematic review. *PLoS ONE* **11**.

**Salmon Y, Torres-Ruiz JM, Poyatos R, Martinez-Vilalta J, Meir P, Cochard H, Mencuccini M**. **2015**. Balancing the risks of hydraulic failure and carbon starvation: A twig scale analysis in declining Scots pine. *Plant Cell and Environment* **38**: 2575–2588.

**Sapes G, Roskilly B, Dobrowski S, Maneta M, Anderegg WRL, Martinez-Vilalta J, Sala A**. **2019**. Plant water content integrates hydraulics and carbon depletion to predict drought-induced seedling mortality. *Tree Physiology* **39**: 1300–1312.

**Sapes G, Sala A**. **2021**. Relative water content consistently predicts drought mortality risk in seedling populations with different morphology, physiology, and times to death. *Plant, Cell & Environment*: 1–14.

**Schindelin J, Arganda-Carreras I, Frise E, Kaynig V, Longair M, Pietzsch T, Preibisch S,**

**Rueden C, Saalfeld S, Schmid B, *et al.* 2012**. Fiji: An open-source platform for biological-image analysis. *Nature Methods* **9**: 676–682.

**Scoffoni C, Vuong C, Diep S, Cochard H, Sack L**. **2014**. Leaf shrinkage with dehydration: Coordination with hydraulic vulnerability and drought tolerance. *Plant Physiology* **164**: 1772–1788.

**Scott I, Logan DC**. **2008**. Mitochondrial morphology transition is an early indicator of subsequent cell death in Arabidopsis. *New Phytologist* **177**: 90–101.

**Scott C, Lyons TW, Bekker A, Shen Y, Poulton SW, Chu X, Anbar AD**. **2008**. Tracing the stepwise oxygenation of the Proterozoic ocean. *Nature* **452**: 456–459.

**Simonin KA, Roddy AB**. **2018**. Genome downsizing, physiological novelty, and the global dominance of flowering plants. *PLoS Biology* **16**: 1–15.

**Singh S, Ambastha V, Levine A, Sopory SK, Yadava PK, Tripathy BC, Tiwari BS**. **2015**. Anhydrobiosis and programmed cell death in plants: Commonalities and Differences. *Current Plant Biology* **2**: 12–20.

**Sorek Y, Greenstein S, Netzer Y, Shtein I, Jansen S, Hochberg U**. **2021**. An increase in xylem embolism resistance of grapevine leaves during the growing season is coordinated with stomatal regulation, turgor loss point and intervessel pit membranes. *New Phytologist* **229**: 1955–1969.

**Speck D -Biol T, Vogellehner D**. **1988**. Biophysical Examinations of the Bending Stability of Various Stele Types and the Upright Axes of Early "Vascular" Land Plants. *Botanica Acta* **101**: 262–268.

**Sperry JS**. **2003**. Evolution of water transport and xylem structure. *International Journal of Plant Sciences* **164**.

**Sperry JS, Donnelly JR, Tyree MT**. **1988**. *A method for measuring hydraulic conductivity and embolism in xylem*.

**Sperry JS, Love DM**. **2015**. What plant hydraulics can tell us about responses to climate-change droughts. *New Phytologist* **207**: 14–27.

**Stein WE, Berry CM, Hernick LV, Mannolini F**. **2012**. Surprisingly complex community discovered in the mid-Devonian fossil forest at Gilboa. *Nature* **483**: 78–81.

**Stojnić S, Suchocka M, Benito-Garzón M, Torres-Ruiz JM, Cochard H, Bolte A, Cocozza C, Cvjetković B, De Luis M, Martinez-Vilalta J, *et al.* 2018**. Variation in xylem vulnerability to embolism in European beech from geographically marginal populations. *Tree Physiology* **38**: 173–185.

**Suarez ML, Ghermandi L**. **2004**. Factors predisposing episodic drought-induced tree mortality in Nothofagus – site , climatic sensitivity and. *Journal of Ecology*: 954–966.

**Sutinen M-L, Palta JP, Reich PB**. **1992**. Seasonal differences in freezing stress resistance of needles of Pinus nigra and Pinus resinosa: evaluation of the electrolyte leakage method. *Tree Physiology* **11**: 241–254.

**Suzuki N, Koussevitzky S, Mittler R, Miller G**. **2012**. ROS and redox signalling in the response of plants to abiotic stress. *Plant, Cell and Environment* **35**: 259–270.

**Swetnam TW, Betancourt JL**. **1998**. Mesoscale Disturbance and Ecological Response to

Decadal Climatic Variability in the American Southwest. *Journal of Climate* **11**: 3128–3147.

**Tai X, Mackay DS, Anderegg WRL, Sperry JS, Brooks PD**. **2017**. Plant hydraulics improves and topography mediates prediction of aspen mortality in southwestern USA. *New Phytologist* **213**: 113–127.

**Taiz L, Zeiger E**. **2006**. Plant Physiology. In: Sinauer Associates I, ed. 46–47.

**Taiz L, Zeiger E**. **2010**. *Plant physiology*.

**Tardieu F**. **1996**. Drought perception by plants: Do cells of draughted plants experience water stress? *Plant Growth Regulation* **20**: 93–104.

**Thomas H**. **2013**. Senescence, ageing and death of the whole plant. **197**: 696–711.

**Torres-Ruiz JM, Cochard H, Choat B, Jansen S, López R, Tomášková I, Padilla-Díaz CM, Badel E, Burlett R, King A, *et al.* 2017**. Xylem resistance to embolism: presenting a simple diagnostic test for the open vessel artefact. *New Phytologist* **215**: 489–499.

**Torres-Ruiz JM, Cochard H, Mayr S, Beikircher B, Diaz-Espejo A, Rodriguez-Dominguez CM, Badel E, Fernández JE**. **2014**. Vulnerability to cavitation in Olea europaea current-year shoots: Further evidence of an open-vessel artifact associated with centrifuge and air-injection techniques. *Physiologia Plantarum* **152**: 465–474.

**Torres-Ruiz JM, Diaz-Espejo A, Morales-Sillero A, Martín-Palomo MJ, Mayr S, Beikircher B, Fernández JE**. **2013**. Shoot hydraulic characteristics, plant water status and stomatal response in olive trees under different soil water conditions. *Plant and Soil* **373**: 77–87.

**Torres-Ruiz JM, Jansen S, Choat B, McElrone AJ, Cochard H, Brodribb TJ, Badel E, Burlett R, Bouche PS, Brodersen CR, *et al.* 2015**. Direct X-Ray Microtomography Observation Confirms the Induction of Embolism upon Xylem Cutting under Tension. *Plant Physiology* **167**: 40–43.

**Trenberth KE, Dai A, Van Der Schrier G, Jones PD, Barichivich J, Briffa KR, Sheffield J**. **2014**. Global warming and changes in drought. *Nature Climate Change* **4**: 17–22.

**Trueba S, Pan R, Scoffoni C, John GP, Davis SD, Sack L**. **2019**. Thresholds for leaf damage due to dehydration: declines of hydraulic function, stomatal conductance and cellular integrity precede those for photochemistry. *New Phytologist* **223**: 134–149.

**Trumbore S, Brando P, Hartmann H**. **2015**. Forest health and global change. *Science* **349**: 814–818.

**Tyree MT**. **1997**. The Cohesion-Tension theory of sap ascent: Current controversies. *Journal of Experimental Botany* **48**: 1753–1765.

**Tyree MT, Sperry JS**. **1989**. Vulnerability of xylem to cavitation and embolism. *Annual Review of Plant Physiology and Plant Molecular Biology* **40**: 19–36.

**Tyree MT, Yang S**. **1990**. Water-storage capacity of Thuja, Tsuga and Acer stems measured by dehydration isotherms - The contribution of capillary water and cavitation. *Planta* **182**: 420–426.

**Tyree MT, Zimmermann MH**. **2002**. *Xylem structure and the ascent of sap*. Springer, New York, NY.

**Ullah S, Skidmore AK, Naeem M, Schlerf M**. **2012**. An accurate retrieval of leaf water content from mid to thermal infrared spectra using continuous wavelet analysis. *Science of the Total Environment* **437**: 145–152.

**United Nations Department of Economic and Social Affairs UNF on FS**. **2021**. *The Global Forest Goals Report 2021*. United Nations.

**Urli M, Porté AJ, Cochard H, Guengant Y, Burlett R, Delzon S**. **2013**. Xylem embolism threshold for catastrophic hydraulic failure in angiosperm trees. *Tree Physiology* **33**: 672–683.

**Vandegehuchte MW, Guyot A, Hubau M, De Groote SRE, De Baerdemaeker NJF, Hayes M, Welti N, Lovelock CE, Lockington DA, Steppe K**. **2014**. Long-term versus daily stem diameter variation in co-occurring mangrove species: Environmental versus ecophysiological drivers. *Agricultural and Forest Meteorology* **192**–**193**: 51–58.

**Verslues PE, Agarwal M, Katiyar-Agarwal S, Zhu J, Zhu JK**. **2006**. Methods and concepts in quantifying resistance to drought, salt and freezing, abiotic stresses that affect plant water status. *Plant Journal* **45**: 523–539.

**Vilagrosa A, Bellot J, Vallejo VR, Gil-Pelegrín E**. **2003**. Cavitation, stomatal conductance, and leaf dieback in seedlings of two co-occurring Mediterranean shrubs during an intense drought. *Journal of Experimental Botany* **54**: 2015–2024.

**Vilagrosa A, Morales F, Abadía A, Bellot J, Cochard H, Gil-Pelegrin E**. **2010**. Are symplast tolerance to intense drought conditions and xylem vulnerability to cavitation coordinated? An integrated analysis of photosynthetic, hydraulic and leaf level processes in two Mediterranean drought-resistant species. *Environmental and Experimental Botany* **69**: 233–242.

**Wang Q, Li P**. **2012**. Identification of robust hyperspectral indices on forest leaf water content using PROSPECT simulated dataset and field reflectance measurements. *Hydrological Processes* **26**: 1230–1241.

**Wang C-R, Yang A-F, Yue G-D, Gao Q, Yin H-Y, Zhang J-R**. **2008**. Enhanced expression of phospholipase C 1 ( ZmPLC1 ) improves drought tolerance in transgenic maize. *Planta* **227**: 1127–1140.

**Wang M, Zheng Q, Shen Q, Guo S**. **2013**. The critical role of potassium in plant stress response. *International Journal of Molecular Sciences* **14**: 7370–7390.

**Wertin TM, McGuire MA, Teskey RO**. **2010**. The influence of elevated temperature, elevated atmospheric CO2 concentration and water stress on net photosynthesis of loblolly pine (Pinus taeda L.) at northern, central and southern sites in its native range. *Global Change Biology* **16**: 2089–2103.

**Widholm J**. **1972**. The use of FDA and phenosafranine for determining viability of cultured plant cells. *Stain technology* **47**: 189–94.

**Wilhite DA, Glantz MH**. **1987**. Chapter 2: Understanding the Drought Phenomenon: The Role of Definitions. *Planning for Drought: Toward a Reduction of Societal Vulnerability*: 11–27.

**Willis K, McElwain J**. **2014**. *The evolution of plants*. Oxford University Press.

**Wortemann R, Herbette S, Barigah TS, Fumanal B, Alia R, Ducousso A, Gomory D, Roeckel-Drevet P, Cochard H**. **2011**. Genotypic variability and phenotypic plasticity of cavitation resistance in Fagus sylvatica L. across Europe. *Tree Physiology* **31**: 1175–1182.

**Yang D, Pan S, Ding Y, Tyree MT**. **2017**. Experimental evidence for negative turgor pressure

in small leaf cells of Robinia pseudoacacia L versus large cells of Metasequoia glyptostroboides Hu et W.C.Cheng. 1. Evidence from pressure-volume curve analysis of dead tissue. *Plant Cell and Environment* **40**: 351–363.

**Zhang MIN, Willison JHM**. **1987**. An improved conductivity method for the measurement of frost hardiness. *Canadian Journal of Botany* **65**: 710–715.

**Zhu JK**. **2016**. Abiotic Stress Signaling and Responses in Plants. *Cell* **167**: 313–324.

**Zimmermann MH**. **1983**. *Xylem Structure and the Ascent of Sap*. Berlin, Heidelberg: Springer Berlin Heidelberg.

**Zimmermann MH**. **1984**. Xylem Structure and the Ascent of Sap. *Biologia Plantarum* **26**: 165.

**Zufferey V, Cochard H, Ameglio T, Spring JL, Viret O**. **2011**. Diurnal cycles of embolism formation and repair in petioles of grapevine (Vitis vinifera cv. Chasselas). *Journal of Experimental Botany* **62**: 3885–3894.

# *Appendix*

# Appendix 1: Dynamic of embolism and cellular damages in stems

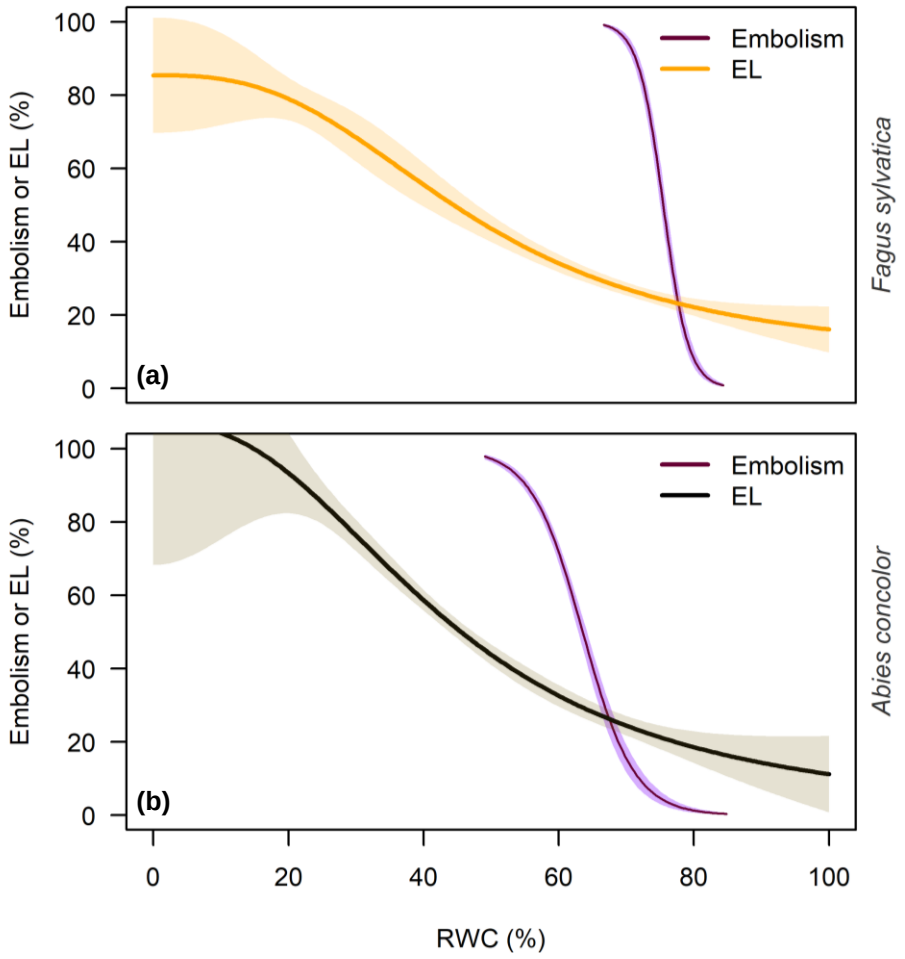


**Figure S14.** Dynamic of embolism and cellular damages (EL) regarding a decrease in stem relative water content (RWC) for **(a)** *Fagus sylvatica* and **(b)** *Abies concolor*.
The percentage of embolism has been evaluated with the cavitron technique and using a regression of RWC regarding stem water potential evaluated throughout the dehydration on seven *F. sylvatica* trees (75 samplings) and 10 *A. concolor* trees (129 samplings) exposed to a total bench dehydration. The critical RWC for cellular integrity ($RWC_{crit}$) has been evaluated at 88.1% for *F. sylvatica* and 78.0% for *A. concolor*. $EL_{50}$ has been calculated at 43.5±4.1% for *A. concolor* whereas it was computed at 47.5±4.2% for *F. sylvatica*.
$P_{12}$ has been evaluated at 79.2% and 71.1% for *F. sylvatica* and *A. concolor* respectively. $P_{50}$ has been evaluated at 75.5% and 63.5% for *F. sylvatica* and *A. concolor* respectively. $P_{88}$ has been evaluated at 71.8% and 56.0% for *F. sylvatica* and *A. concolor* respectively.
For both species, $RWC_{crit}$ appear as concomitant to the onset of embolism whereas 50% of cellular damages occur at lower RWC values than the one inducing 88% of embolism for both species.

# Appendix 2: Mechanisms of woody-plant mortality under rising drought, $CO_2$ and vapor pressure deficit

REVIEWS



## Mechanisms of woody-plant mortality under rising drought, $CO_2$ and vapour pressure deficit

Nate G. McDowell[1,2]✉, Gerard Sapes[3], Alexandria Pivovaroff[1], Henry D. Adams[4], Craig D. Allen[5], William R. L. Anderegg[6], Matthias Arend[7], David D. Breshears[8], Tim Brodribb[9], Brendan Choat[10], Hervé Cochard[11], Miquel De Cáceres[12], Martin G. De Kauwe[13,14,15], Charlotte Grossiord[16,17], William M. Hammond[18], Henrik Hartmann[19], Günter Hoch[7], Ansgar Kahmen[7], Tamir Klein[20], D. Scott Mackay[21,22], Marylou Mantova[11], Jordi Martínez-Vilalta[12,23], Belinda E. Medlyn[10], Maurizio Mencuccini[12,24], Andrea Nardini[25], Rafael S. Oliveira[26], Anna Sala[27], David T. Tissue[10], José M. Torres-Ruiz[11], Amy M. Trowbridge[28], Anna T. Trugman[29], Erin Wiley[30] and Chonggang Xu[31]

Abstract | Drought-associated woody-plant mortality has been increasing in most regions with multi-decadal records and is projected to increase in the future, impacting terrestrial climate forcing, biodiversity and resource availability. The mechanisms underlying such mortality, however, are debated, owing to complex interactions between the drivers and the processes. In this Review, we synthesize knowledge of drought-related tree mortality under a warming and drying atmosphere with rising atmospheric $CO_2$. Drought-associated mortality results from water and carbon depletion and declines in their fluxes relative to demand by living tissues. These pools and fluxes are interdependent and underlay plant defences against biotic agents. Death via failure to maintain a positive water balance is particularly dependent on soil-to-root conductance, capacitance, vulnerability to hydraulic failure, cuticular water losses and dehydration tolerance, all of which could be exacerbated by reduced carbon supply rates to support cellular survival or the carbon starvation process. The depletion of plant water and carbon pools is accelerated under rising vapour pressure deficit, but increasing $CO_2$ can mitigate these impacts. Advancing knowledge and reducing predictive uncertainties requires the integration of carbon, water and defensive processes, and the use of a range of experimental and modelling approaches.

**Mortality**
The irreversible cessation of metabolism and the associated inability to regenerate.

**Die-off**
Widespread and rapid mortality of a species or community.

✉e-mail: nate.mcdowell@pnnl.gov

https://doi.org/10.1038/s43017-022-00272-1

Woody-plant mortality results in the irreversible cessation of metabolism and the resultant inability to regenerate. Since widespread observations began in the 1960s, there has been evidence of increasing background tree mortality in many regions of the world[1–6] (FIG. 1a), including regional-scale die-off events[7–15] (widespread, rapid tree loss). Large mortality events have been recorded in dry tropical forests[15], tropical rainforests[16–18], temperate rainforests[19,20], semi-arid woodland and savannahs[8,13,21], boreal forests[22–24] and temperate deciduous to evergreen forests[12,25]. Such mortality is insidious in the case of the slowly but steadily increasing background mortality and dramatic in the case of die-off events.

These contemporary increases in background tree mortality and extreme regional die-off events are associated with atmospheric warming and a corresponding increase in vapour pressure deficit (VPD) and evapotranspiration[26–29] (FIG. 1b). As a result of greater water loss from foliage and soil surfaces, historically, non-lethal soil droughts have become lethal[29,30]. With anthropogenic forcing anticipated to further increase warming, as well as the frequency and duration of heatwaves and soil drought[10,30–33] (FIG. 1c), tree mortality is also expected to increase in the future[34,35]. However, rising $CO_2$ (FIG. 1b) can mitigate the negative impacts of increased VPD through higher carbon uptake and reduced water loss, affording potential water savings[36,37]. Contemporary observations suggest that rising VPD could be increasingly offsetting $CO_2$ benefits[38–40], and, so, the net balance might be in favour of either greater survival or mortality[37,41–44].

Background mortality
Mortality rates in the absence of disturbances.

Droughts
Periods of anomalously low precipitation.

Hydraulic failure
The accumulation of emboli within the sapwood past a threshold after which water transport is irrecoverable.

Threshold
The magnitude or intensity that must be exceeded to cause a reaction or change.

Mechanistic understanding of such drought-related and heat-related mortality is limited. Hydraulic failure, the accumulation of sapwood emboli past a threshold after which water transport is irrecoverable, and carbon starvation, the process by which a limited supply of carbohydrate impairs maintenance of carbon-dependent metabolic, defence or hydraulic functions, have both been proposed as key processes[45–47]. These processes are both challenged by a lack of clear definitions and hypotheses and the large range of experimental conditions under which they have been studied, leading to a wide range of results regarding their occurrence[48]. Though recent models have incorporated these potential processes of mortality[49–54], their interdependent contributions to drought-induced mortality of woody plants remains uncertain.

Given that tree mortality leads to substantial changes in the structure and function of ecosystems, understanding drought-related mortality is fundamental to basic biology, ecosystem management and climate-feedback predictions[55,56]. Changes in ecosystem structure and function due to mortality lead to large ecohydrologic shifts, with abrupt and potentially sustained changes in streamflow[57], as well as downstream water quality, quantity and timing[58,59]. Long-term shifts in forest demographics might also result from shifts in tree mortality rates[60], with corresponding limitations to net terrestrial carbon storage[11]; a doubling of mortality halves forest carbon storage over 50 years if net primary production doesn't equally increase. Resulting impacts on biodiversity might be large and surprisingly unpredictable at regional and global scales, and likely depend on disturbance type, biome and species, among other factors[61,62]. Moreover, the economic impacts of forest loss, particularly in regions where wood production is vital to societal well-being, could be substantial[63].

In this Review, we synthesize understanding of woody-plant mortality under rising VPD and $CO_2$. We begin with a discussion of contemporary, observed drought-associated tree mortality. We follow with consideration of three general, interdependent mechanisms of tree mortality — water relations, carbon relations and defensive failure — and propose an integrative, predictive framework for mortality under a changing global climate. We subsequently examine how such processes might interact to promote vulnerability and influence future projections. We end with recommendations for future research. Throughout the Review, all mechanisms are treated as part of the mortality process: that is, from failure of root water uptake through to hydraulic failure, carbon starvation and irreversible cell dehydration. We consider a plant in the 'dying' phase to have passed a point of no return or a threshold[64–70], beyond which mortality of the organ (branch dieback)[71] or the entire plant is certain. Processes that occur before the dying phase can be critical in promoting or delaying mortality, whereas those that occur thereafter can be considered consequences, not causes.

**Author addresses**

[1]Atmospheric Sciences and Global Change Division, Pacific Northwest National Laboratory, Richland, WA, USA.
[2]School of Biological Sciences, Washington State University, Pullman, WA, USA.
[3]Department of Ecology, Evolution, and Behavior, University of Minnesota, St. Paul, MN, USA.
[4]School of the Environment, Washington State University, Pullman, WA, USA.
[5]Department of Geography and Environmental Studies, University of New Mexico, Albuquerque, NM, USA.
[6]School of Biological Sciences, University of Utah, Salt Lake City, UT, USA.
[7]Department of Environmental Sciences — Botany, University of Basel, Basel, Switzerland.
[8]School of Natural Resources and the Environment, University of Arizona, Tucson, AZ, USA.
[9]School of Natural Sciences, University of Tasmania, Hobart, Tasmania, Australia.
[10]Hawkesbury Institute for the Environment, Western Sydney University, Richmond, New South Wales, Australia.
[11]Université Clermont-Auvergne, INRAE, PIAF, Clermont-Ferrand, France.
[12]Centre for Research on Ecology and Forestry Applications (CREAF), Bellaterra, Spain.
[13]School of Biological Sciences, University of Bristol, Bristol, UK.
[14]ARC Centre of Excellence for Climate Extremes, Sydney, New South Wales, Australia.
[15]Climate Change Research Centre, University of New South Wales, Sydney, New South Wales, Australia.
[16]Plant Ecology Research Laboratory (PERL), École Polytechnique Fédérale de Lausanne (EPFL), Lausanne, Switzerland.
[17]Community Ecology Unit, Swiss Federal Institute for Forest, Snow and Landscape Research (WSL), Lausanne, Switzerland.
[18]Agronomy Department, University of Florida, Gainesville, FL, USA.
[19]Department of Biogeochemical Processes, Max Planck Institute for Biogeochemistry, Jena, Germany.
[20]Department of Plant and Environmental Sciences, Weizmann Institute of Science, Rehovot, Israel.
[21]Department of Geography, University at Buffalo, Buffalo, NY, USA.
[22]Department of Environment and Sustainability, University at Buffalo, Buffalo, NY, USA.
[23]Universitat Autònoma de Barcelona, Bellaterra, Spain.
[24]Institució Catalana de Recerca i Estudis Avançats (ICREA), Barcelona, Spain.
[25]Department of Life Sciences, University of Trieste, Trieste, Italy.
[26]Department of Plant Biology, University of Campinas — UNICAMP, Campinas, Brazil.
[27]Division of Biological Sciences, University of Montana, Missoula, MT, USA.
[28]Department of Entomology, University of Wisconsin-Madison, Madison, WI, USA.
[29]Department of Geography, University of California, Santa Barbara, Santa Barbara, CA, USA.
[30]Department of Biology, University of Central Arkansas, Conway, AR, USA.
[31]Earth and Environmental Sciences Division, Los Alamos National Laboratory, Los Alamos, NM, USA.

## Background mortality and regional die-off

The regionally distributed trends of increasing background tree mortality[1–6] (FIG. 1a) — as observed throughout western and boreal North America[1,2], the Amazon basin[6] and Europe[11] — indicate that a common driver underlies changes in woody-plant mortality. The degree of increase in mortality rates varies with region, including a non-significant change in the Congo, the underlying climatic and physiological processes of which remain relatively unknown[72]. Elsewhere, these background rate increases could reflect increasing VPD impacts[26,29,73], and, under wetter conditions, might also reflect elevated productivity and turnover[74,75]. However, there is little evidence for increasing competition-induced mortality[18,37]. Additionally, when water is ample, rising $CO_2$ and warming could provide conditions for structural overshoot, where forests rapidly gain biomass and leaf area (at the individual plant and the stand scales) to levels not hydraulically sustainable during the eventual hotter droughts[76,77], which could, likewise, promote increasing mortality.

Regional die-off events are now also being observed across both warm and dry and wet and cool biomes[7–25],

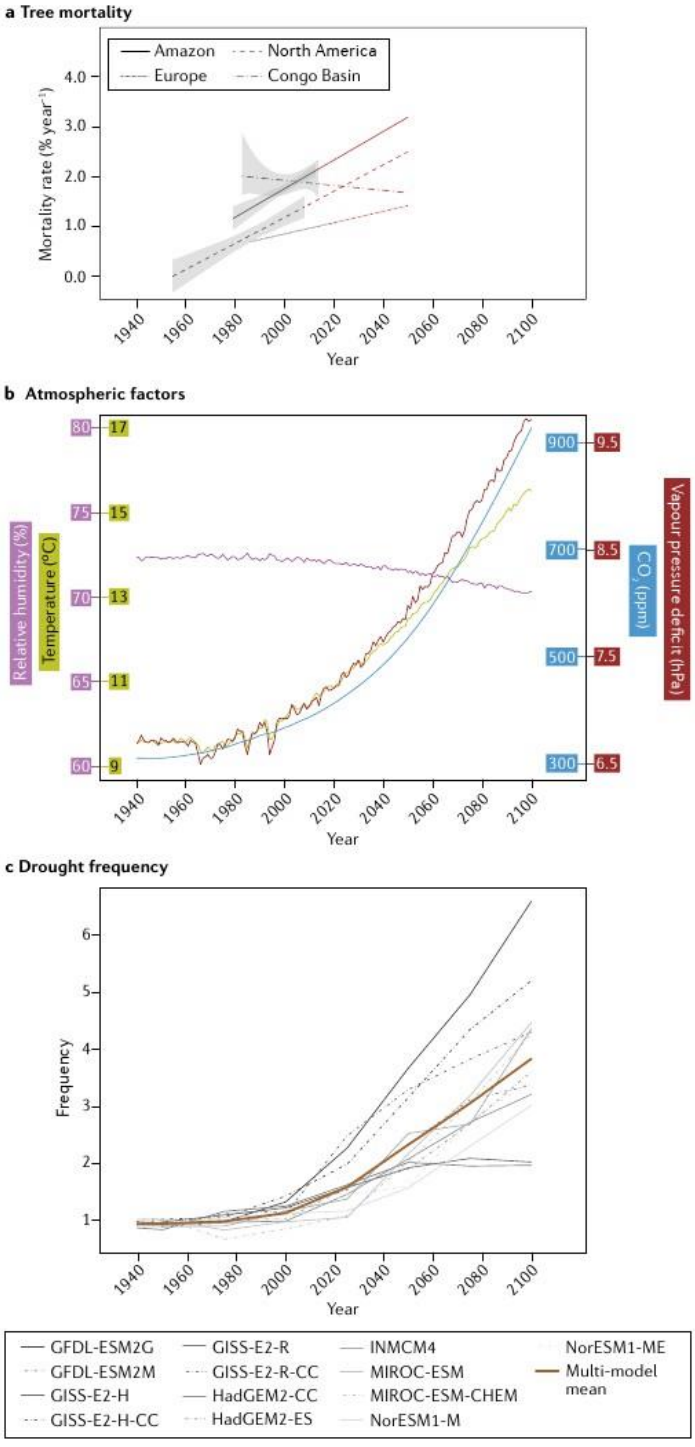


Fig. 1 | **Changing tree mortality and climate variables.** **a** | Observed (grey) and linearly projected (red) tree mortality rates for North America[1,2], the Amazon[5], Europe[11] and the Congo Basin[6]. Grey shading represents 95% confidence intervals. **b** | Average simulated $CO_2$, surface temperature, relative humidity and vapour pressure deficit for grid points only over global vegetated land. Projections are based on RCP8.5. **c** | Simulated drought frequencies relative to the historical mean (1850–1999); values <1 indicate lower frequency compared with historical and those >1 indicate greater frequency compared with historical. Drought frequency is based on extreme plant-available soil water as <2 percentile of the 1850–1999 period. Projections follow RCP8.5 using 13 models from CMIP5. See REF.[34] for details of calculations. Increasing atmospheric drivers of mortality are consistent with increasing mortality rates, except in the Congo.

even following decades of productive growth[78], indicating that no biome is invulnerable. Die-off events are regional in scale, can kill one or more species and occur rapidly[14]. This global distribution of die-off events is associated with global increases in temperature and VPD[14]. Droughts eventually occur everywhere, but now with warmer temperature and higher VPD than historically[28].

## Drivers and mechanisms of mortality

Understanding and predicting mortality under future climate requires a framework that provides unambiguous definitions, generates testable hypotheses and identifies uncertainties. In the case of drought-associated woody-plant mortality, this framework is expected to also identify pools and fluxes of critical resources and their potential lethal thresholds, and to be relevant across different biomes and environmental conditions. Previous frameworks have advanced knowledge of drought-related mortality[45–47,79]. However, existing frameworks grapple with the complexity of the interdependent processes that occur while trees are dying[45–47,80], including hydraulic failure, carbon starvation and attack by biotic agents[81,82] (FIG. 2). Overall, there remains a lack of consensus on the appropriate terminology, mechanisms and, ultimately, a clear set of hypotheses.

Owing to consistent evidence of deteriorating water status during death[45–47,80] and widespread prevalence of hydraulic dysfunction in drought-associated mortality[13,14,22,23], the mechanisms underlying woody-plant mortality originate from a whole-plant water-relations backbone. Examining mortality can start from a basic end point in the process: the rupture of cell membranes owing to water content falling below a critical threshold, preventing plant recovery[65,68] (FIGS 2,3). Crossing this critical threshold depends, in part, on the absolute water content below which the cells cannot survive, the osmoregulation potential of the cells and the capacity to provide substrates and energy for continuous membrane maintenance and osmolyte production[68]. Such cellular death must manifest across tissues at the whole-plant scale and eventually impact all meristematic cells needed for growth and reproduction before organismal mortality has occurred. Thus, while plant water relations are the keystone process for drought-associated mortality, hydraulic function and associated failure might also depend on starch and sugar availability, thus, water and carbon supply, and their respective cellular reservoir size, might be critical for survival[83].

**Carbon starvation**
The process whereby a limited carbohydrate supply rate impairs maintenance of carbon-dependent metabolic, defence or hydraulic functions.

**Process**
A series of mechanisms that leads to an end point.

**Mechanisms**
Systems of parts working together within a process; pieces of the machinery.

**Dying**
Committed to death; beyond the point of no return; to have passed a threshold beyond which mortality is certain.

**Biotic agents**
Living organisms — especially fungi, bacteria and insects — that interdependently impact the water and carbon economies of plants.

**Meristematic cells**
Undifferentiated cells capable of division and formation into new tissues.

**Cytorrhysis**
Irreparable damage to cell walls after cellular collapse from the loss of internal positive pressure.

Likewise, biotic attack is also highly likely to interact with physiological declines given defensive dependency on water and carbon relations[47,81]. The mortality process is now discussed in terms of whole-plant water relations, water–carbon dependencies and water–carbon–biotic dependencies.

***Whole-plant water relations preceding mortality.*** Failure of whole-plant water relations and subsequent mortality occurs through a series of sequential and interdependent mechanisms (FIG. 3). First, a severe decline in root water uptake, whole-plant hydraulic conductance and associated stomatal closure[84,85] occurs, causing the water and carbon pools to become finite and exhaustible. The depletion of water pools is followed by continued loss of water through evaporation from plant surfaces and, subsequently, increasing occurrence of sapwood embolism as water pools are depleted[86,87]. Ultimately, hydraulic failure occurs and subsequent downstream mortality ensues as water pools deplete below the threshold for irreversible cell death[46,64–68], known as cell wall rupture or cytorrhysis[88,89]. In this view, hydraulic failure is a mechanism within the larger process of mortality, rather than a sole cause in itself. Hydraulic failure in woody plants, strictly defined, is the accumulation of emboli within conduits causing a decline in conductance and an increase in tension of the remaining conduits, creating a feedback loop of runaway cavitation and, subsequently, insufficient distal water supply relative to water loss. By definition, hydraulic failure includes a threshold resulting from the whole-plant processes of water flow, that is, a threshold beyond which recovery of flow is impossible due to emboli accumulation within conduits. Critically, the importance of fluxes and pools of water to survival increases as drought progresses[83] (FIG. 3). The sequence of events that promotes a constraint upon survival through failure of whole-plant water relations and associated hydraulic failure is now discussed.

Drying soil demands a steep increase in the amount of tension, or water potential gradient, that plants must withstand to extract soil water[90]. The soil–root interface becomes a primary limitation on whole-plant

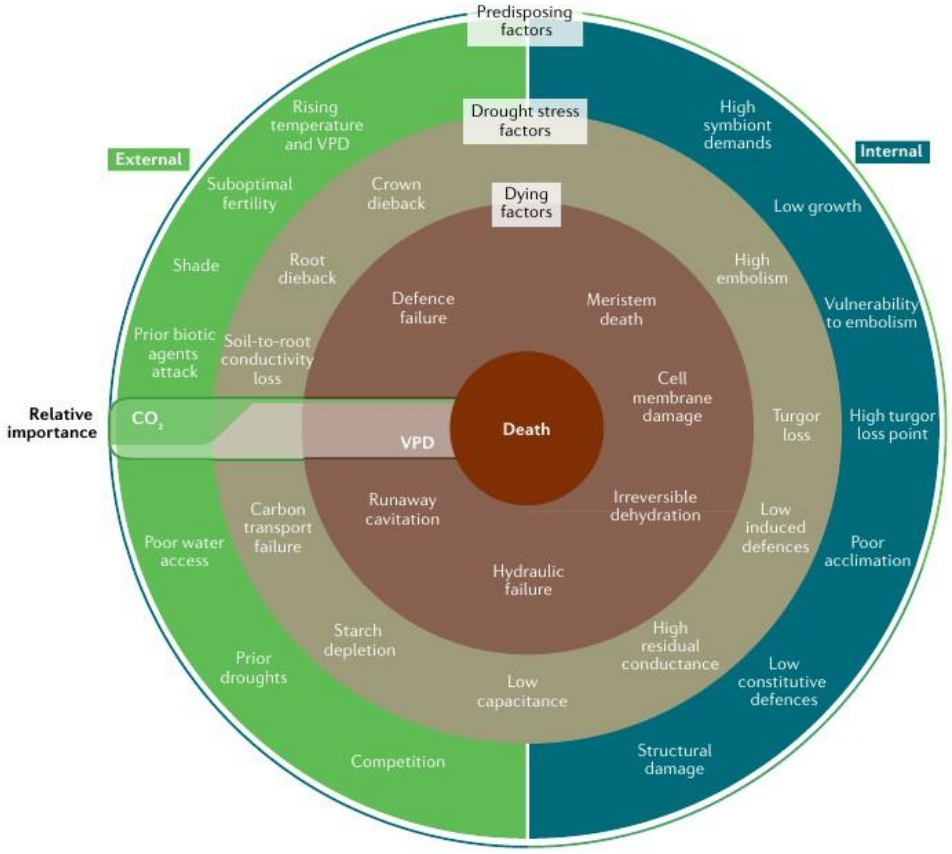


Fig. 2 | **The interconnected mortality process.** A hypothetical representation of the mortality processes from predisposing factors to death. Predisposing factors are linked to mortality via the mechanisms in the second innermost ring, which subsequently cause a plant to pass a threshold beyond which mortality is inevitable. The death spiral results from the interaction of external drivers, the processes of hydraulic failure and carbon starvation, and their underlying, interdependent mechanisms. VPD, vapour pressure deficit. Figure inspired by REF.[80].

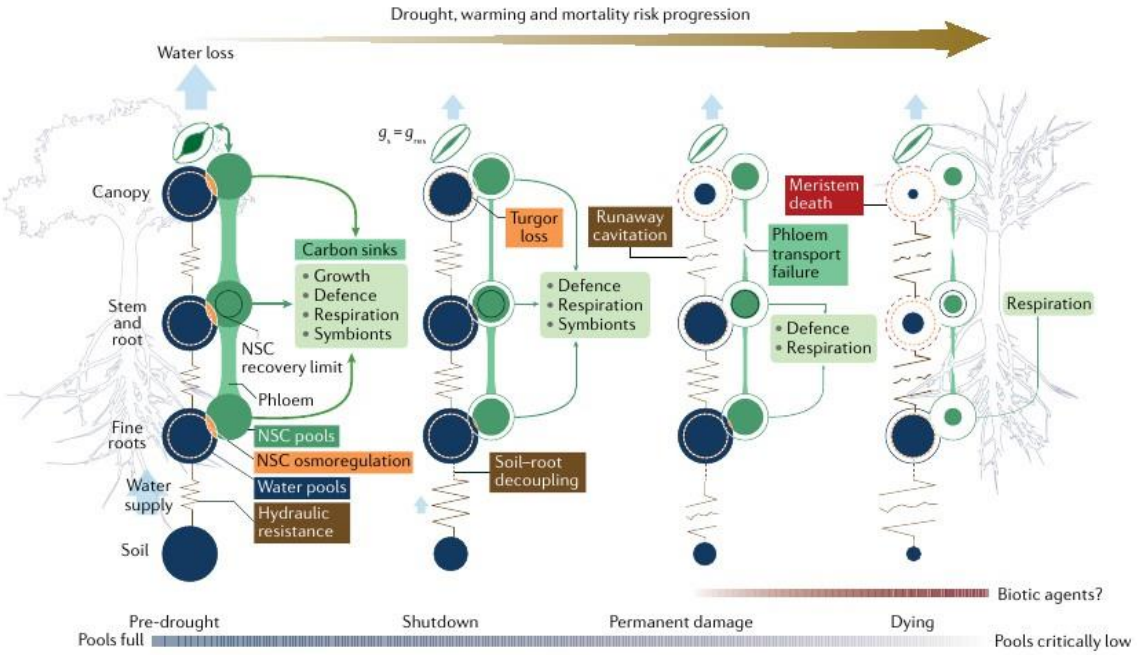


Fig. 3 | **Mechanisms that lead towards mortality.** Hypothesized mechanisms, including pools and fluxes, that influence mortality as drought progresses. Primary water and carbohydrate pools are in blue and green circles, respectively, with their fluxes as resistors and green arrows. Interactions between water and carbon pools are in orange. As drought progresses, stomatal and belowground conductance decline to near zero. $g_{res}$ (residual conductance from foliage and bark post-stomatal closure) then dominates water loss and plant survival depends on the finite, stored carbon and water pools. Ultimately, dehydration and depletion of these pools promotes sustained negative turgor (dashed orange circles), followed by meristem death (dashed red circles) from the cellular water content falling below a threshold for cellular rupture. The black circle within the stem and root carbohydrate pools indicates the point at which there is insufficient carbohydrates to recover via regrowth. $g_s$, stomatal conductance; NSC, non-structural carbohydrate.

conductance under these conditions and can constitute >95% of whole-plant resistance[91,92]. Complete hydraulic disconnection between the soil and roots has been demonstrated in mature woody plants, including during drought-associated mortality[93,94], although the frequency of such disconnection during drought is unknown. Under these conditions, stomatal conductance declines to near zero[91], reducing water loss and photosynthesis[95]. Near-zero belowground (soil–root) conductance and stomatal conductance mark a transition point[56,58] when the individual plant becomes solely reliant on its limited water stores[96,97]. The size of these stores, their net depletion rate and the tissue-level and cell-level tolerances for depletion define the likelihood of mortality[98] (FIG. 3).

As hydraulic failure and cytorrhysis ensue for some tissues, crown dieback (foliage and branch loss) and root loss will advance, and, if the damage proceeds to destroy all meristematic tissues, individual mortality occurs (FIG. 3). Such cellular failure can occur at organ (dieback) or individual (mortality) levels, depending on its extent and the degree of hydraulic segmentation within the plant. Variation in cellular thresholds for survival is likely substantial and could be important in regulating where and when woody-plant mortality occurs. The threshold for cellular cytorrhysis is above 0% water content[89] and might vary with species, genotypes, phenotypes, tissue and cell types, but remains relatively unexplored in woody plants.

Evaporative losses after stomatal closure are dominated by residual vapour fluxes through leaky stomata, cuticle, bark and possibly roots[99–103] (residual conductance ($g_{res}$)). The evaporative flux through $g_{res}$ becomes the dominant path of whole-plant water loss during a severe drought and is exacerbated at high air temperatures[86,87]. Continued water loss (which is not replaced) results in declining water pools and increasing embolism (FIG. 3). Even under situations where the soil–root connection is maintained, if the fluxes of water to the plant are smaller than those lost through $g_{res}$, the stored pools of water will deplete and embolisms will develop.

The bidirectional feedbacks between the depletion of water pools and irreparable hydraulic failure is a logical and testable hypothesis for mortality progression. However, a water-only perspective ignores the potentially critical roles of carbon and defence against biotic agents during drought, both of which could promote failure of water relations if they individually fail. During short and hotter droughts, failure to maintain the critical water supply can dominate the mortality process because of the rapid rate of water loss relative to the rate of carbohydrate and defensive losses[104–107]. In longer droughts, or in cases of mortality years after drought, the role of carbon supply to critical survival processes should increase[104–107] due to the far longer residence time and slower changes in carbohydrates than in water pools[108,109].

**Dieback**
The partial loss of canopy or root biomass, without whole-plant mortality.

**Failure of water relations**
Impairment of the interacting water and carbon processes that forces declines in water supply and subsequent dehydration.

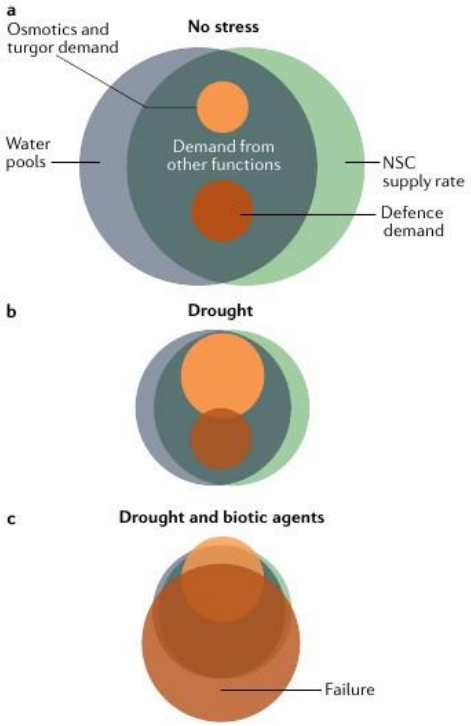


Fig. 4 | **The linkage between woody plant's defence systems and biotic attack. a** | Pre-drought, water and carbon pools and supply rates are sufficient to support the demand for defence, osmotic regulation, metabolism and other functions. **b** | During drought, the demand for osmotic regulation increases as water and carbon pools and supply rates decline. **c** | Once biotic agents attack, the demand for defence increases, potentially beyond that which can be supported by the water and carbon pools and fluxes. This viewpoint suggests that, if any component of the system fails, it can lead to the cessation of the interdependent distal processes critical to survival. NSC, non-structural carbohydrate.

***The water–carbon interdependency.*** The process by which plants' carbon economy has a role in mortality before, during and after lethal droughts involves multiple potential mechanisms. These include those associated with decreased photosynthetic gain[45], reduced xylem and constitutive defensive compound production[110–113], initial carbohydrate storage increases and then decreases prior to death[11,47–114], a critical increasing role of carbohydrates in osmoregulation and cellular maintenance[115–122], and possible carbohydrate feedbacks upon hydraulic and defensive function[47]. In this view, carbon starvation, or the steps by which metabolic functions are impaired by limitations in the supply rate of carbohydrates, is a mechanism within the larger process of carbon limitations upon mortality. These mechanisms are described chronologically from pre-drought through the dying phases (FIGS 2,3).

There is evidence that water–carbon-related factors that occur prior to drought can promote mortality (FIG. 2). Decades-long reductions in carbon allocation to stem wood and resin ducts within dying conifer species indicate potential roles of pre-drought allocation to mortality[105–107,110–113]. Low growth preceding death can be a lingering consequence of prior climate or injuries that predispose trees to carbon constraints[79] (FIG. 2). By contrast, shifts in allocation towards greater pre-drought growth can also influence mortality owing to reduced allocation to defence at the expense of growth[123–127] or from over-allocation to aboveground biomass (in particular, leaf area at the individual and stand levels) during favourable conditions, which cannot be sustained during subsequent hotter droughts (structural overshoot)[76]. A feedback loop can be created, in which pre-drought factors can predispose plants to mortality during drought (FIG. 2). Indeed, declines in growth, hydraulic function and defence can be a function of reductions in crown leaf area owing to crown dieback or root loss from prior drought, lightning, wind damage and defoliating or root-feeding insects or pathogens[128–133]. However, declining leaf area can also promote survival by reducing water loss during drought[134,135]. The net consequence of pre-drought shifts in carbon and water pools and fluxes remains a research challenge.

Once drought has become sufficiently severe and/or prolonged such that photosynthesis has declined to near zero, the starvation process can promote mortality through water relations or defensive failure (FIG. 3). Carbon starvation is the process by which carbon-dependent metabolism, defence and possibly hydraulic maintenance are shifted owing to limited carbon supply rate relative to demand (FIG. 4). This definition is consistent with the literature on starvation across global animal and plant taxa[136–138], which characterize starvation as causing significant shifts in metabolism, which are reversible, until a threshold is passed, after which the interdependent processes required for survival are not met. Carbon starvation is considered to occur nightly in plants[139], though for the purposes of drought-associated mortality, this process becomes relevant when stomatal closure precludes photosynthesis relative to carbon demand for abnormally prolonged periods (months to years). Starvation manifests at the cellular scale but can occur widely throughout an organism. As starvation progresses, the supply rate and/or pool of carbohydrates (sugars derived from starch, lipid and hemicellulose breakdown, as well as products derived from autophagy)[140–142] could possibly decline below the threshold at which cellular to whole-tree mortality is promoted. Such thresholds can include the minimum metabolism required for survival, failure to maintain membrane stability, inability to maintain the osmotic functions for the hydraulic system or failure to maintain the defence system (FIGS 3,4).

It is the interplay between the available carbon pools, their fluxes and the demands for survival that cause carbohydrate supply rates to not meet the requirements to avoid hydraulic failure[105,143–145] or insect and/or pathogen defence failure[79,146,147] (FIGS 3,4). If an insufficient supply rate of carbon substrates to required metabolic processes[115] results from short-distance or long-distance transport constraints, for example, through source

strength impacts upon phloem loading and viscosity challenges[148–151], failure of carbon-dependent processes could be promoted. Declining resistance to xylem embolism has been associated with low carbohydrate concentrations[145]. Reduced carbon supply rates can promote osmoregulation failure, loss of protein and membrane stability, failure to scavenge free radicals and reductions in cross-membrane transport of ions and amino acids[115–122]. Simultaneously, the carbon requirements for these processes increase with drought stress[45,152–157], thus, the carbon safety margin, or the difference between carbon availability and demand, decreases with drought. Therefore, failure to maintain hydraulic integrity and cellular water content appear directly linked to the carbon economy of plants (FIG. 3), particularly under longer droughts.

***The water–carbon–defence interdependency.*** Attacks by biotic agents such as insects or pathogens are frequently concomitant with drought-associated mortality prior to, during or shortly after the drought event[81,158–160], and are likely interdependently associated with impacts on carbon and water relations (FIGS 3,4). When a biotic attack occurs prior to drought, it can impact plants through defoliation or root loss, predisposing plants to subsequent mortality if the attack impaired their water and carbon economies (FIGS 3,4). When drought stress predisposes trees to attack, it can lead to hydraulic failure if the vascular system is infected[161–163]. Biotic agents can disrupt carbon uptake and transport through leaf loss[164] or depletion of carbohydrate reserves via direct consumption[165,166], and they can stimulate a plant's induced defence response[167,168].

The initiation of regional-scale outbreaks typically occurs during or after drought when the defensive capacity of host trees is constrained, and a critical number of vulnerable trees becomes susceptible across the landscape[169–171]. The level of stress that limits defensive function remains unknown owing to a lack of empirical evidence linking carbohydrates, hydraulics and defences in field experiments with mature trees[172]. Experiments that preclude biotic attack, however, such as caging, insecticide/fungicide and anti-aggregation pheromones, have demonstrated that some insects, fungi and other pathogens have the potential to directly move drought-weakened plants into the dying phase, while those free of biotic attack survive[47] (FIG. 3). In these cases, the roles of the plant water and carbon economies in defensive failure can be substantial.

The water and carbon economies directly impact the defensive system, such that failure of one component can lead to failure of another (FIG. 4). The relative water content and water potential of cells directly impacts turgor pressure and the substrate transport critical to defence[173,174]. Synthesis of secondary metabolites and metabolic transport costs of the defensive system depend directly on labile carbon availability for induced defences[173–176] (FIG. 4). Higher sugar concentrations are associated with reduced attack by insects and fungi, demonstrating the potential role of carbohydrates in defence, perhaps through fuelling induced responses[174,176]. Defensive compounds have a particularly high carbon concentration[177] and tend to be upregulated at the transcriptional level during drought[178,179]. Similarly, a rapid increase in defensive allocation upon attack has been associated with declining local carbohydrates[168]. Thus, defence incurs a substantial carbon cost[180] (FIG. 4), suggesting that reduced carbohydrate supply rates could render the plant susceptible to biotic attack[181,182]. For example, conifers with fewer resin ducts formed in years prior to drought are frequently more likely to die during beetle attack[111,167,183–186], consistent with a carbon constraint inducing defensive failure. When insects and pathogens reach epidemic levels, the attacks might switch from the poorly defended to the faster-growing, well-defended plants due to the higher availability of resources available to the attacking agents[127]. Thus, defensive failure can be both a cause and a consequence of impaired water and carbon economies during drought (FIG. 3).

***The interdependent framework of mechanisms.*** This framework (FIGS 2–4) outlines the individual mechanisms within the larger processes that lead plants into the dying phase. As a plant enters a hotter drought with higher VPD, it must manage limited water resources amidst the edaphic and structural conditions that it enters the drought with (FIG. 2), including defensive dependence and hydraulic dependence on carbon allocation to sapwood, roots and foliage prior to the drought. As drought ensues and belowground and stomatal conductance declines to near zero, embolisms can accumulate, thus, reducing whole-plant conductance and photosynthesis, setting up a feedback cycle. Once water fluxes approach zero, the finite pools and fluxes of water and carbon become exhaustible, while demands for allocation of carbohydrates to osmoregulation and maintenance of cellular, defensive and, potentially, hydraulic metabolism rise (FIG. 3). Thus, allocation to sapwood, roots, foliage and carbohydrates prior to drought, and to osmoregulation, cytorrhysis tolerance and defence during drought, can all feed back directly upon the likelihood of hydraulic failure, with rising VPD causing a smaller threshold between survival and mortality. However, rising $CO_2$ might influence such mortality either through promoting structural overshoot or water use benefits, either promoting or delaying mortality as VPD rises (BOX 1).

Potential thresholds also emerge from the mortality mechanisms framework. A decline in cellular water pools below the threshold for cytorrhysis is a clear point of no return of lethal dehydration, which results from the chain of hydraulic events that leads to a threshold amount of hydraulic failure, after which the cytorrhysis threshold was exceeded. The maintenance of the hydraulic system, avoidance of hydraulic failure and minimization and tolerance of cellular dehydration might all depend directly on carbon pool sizes and fluxes to sites of demand. Likewise, induced defensive responses depend on localized fluxes of both water and carbohydrates. These are all possible key failure points within the system — the loss of one can trigger a cascade of losses in the others. These individual or interdependent

failures at small scales (tissue to organ), with VPD and $CO_2$ dependencies, will reduce survival likelihood at the whole-plant level.

Box 1 | **The impact of rising VPD and $CO_2$ on mortality risk**

Increasing cumulative vapour pressure deficit (VPD) exposure (such as temperature degree days)[128] ultimately causes plant water content (see the figure, blue line) and carbon supply (see the figure, green line) to decrease towards a threshold of lethal dehydration during drought. The mortality thresholds (see the figure, blue and green dashed lines) vary with cellular resistance to cytorrhysis from water and carbon supply limitations. The mortality threshold for water content is assumed to be unchanging with accumulating VPD and, for carbon supply, is assumed to increase with VPD due to increased maintenance requirements[229]. There is a wide range of functional spaces that the curves and mortality thresholds could occupy, with edaphic, taxa, VPD and $CO_2$ all having a regulatory role. While not represented, temperature causes a small range of negative responses due to its impacts on water and carbon demand (residual conductance ($g_{res}$) and respiration rates, respectively). The hypothesized responses shown here have been rarely tested, owing to limited research that has manipulated either VPD or $CO_2$ under drought.

The figure, built upon the proposed mechanistic framework (FIGS 2–4), presents hypotheses regarding the interdependency of the carbon-related and water-related processes, their thresholds and their responses to VPD and $CO_2$.

- Hypothesis 1: accumulating greater exposure to VPD, particularly during drought, reduces plant water content because it increases the demand for transpiration relative to supply.
- Hypothesis 2: as water content declines, the risk of hydraulic failure increases, leading to a feedback loop of increasing dehydration.
- Hypothesis 3: greater VPD exposure reduces whole-plant carbon supply through reduced stomatal conductance to $CO_2$.
- Hypothesis 4: rising cumulative VPD forces a decline in photosynthesis to near zero as transpiration increases to an upper threshold, exacerbating both carbon supply and water pool declines. However, under particularly high temperature and VPD, transpiration can decline as hydraulic failure progresses.
- Hypothesis 5: reduced $CO_2$ supply at plant and tissue levels pushes the plant towards the lethal threshold.
- Hypothesis 6: elevated $CO_2$ shifts the trajectory of the response of water content and carbon supply to accumulating VPD exposure.
- Hypothesis 7: water pools could increase if rising $CO_2$ reduces transpiration.
- Hypothesis 8: plant-level carbon supply rate increases via $CO_2$-induced photosynthetic stimulation.
- Hypothesis 9: if structural overshoot[73] occurs such that the shoot-to-root ratio increases, larger biomass requires water and carbon during droughts and heatwaves, accelerating progression towards the lethal thresholds. Higher leaf area can increase carbon uptake prior to drought however, shifting the carbon supply rate above the assumed trajectory.
- Hypothesis 10: overshoot at the stand level through increasing plant density should also reduce water and carbon supply demand through increased competition for finite resources.

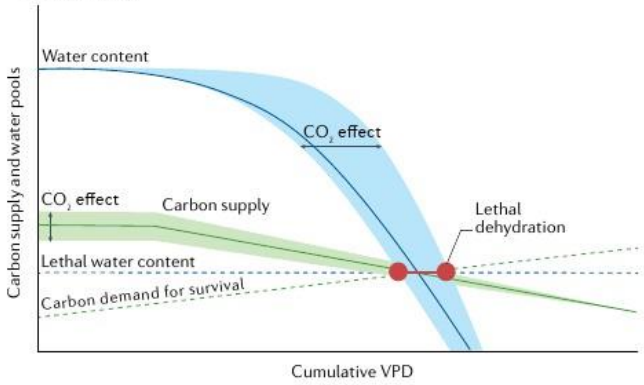


**Environmental change impacts on mortality**

The observed increase in tree mortality (FIG. 1a) makes it imperative to further understand the potential impacts of rising $CO_2$ and VPD. Projections of future woody plant loss are now discussed, highlighting the potential roles of a changing environment on mortality and outlining the strengths and challenges facing the current generation of models for simulating mortality.

***Modelling climate impacts on drought-induced mortality.*** Existing predictions of future forest mortality are limited, but all point to a common threat of increasing background mortality and die-off events. For example, according to an empirical model, regional-scale conifer loss is predicted across the Southwestern USA by 2050 owing to increases in VPD, along with periodic droughts[29]. These findings were confirmed using multiple tree-scale and ecosystem-scale process models, with Earth system models predicting widespread conifer mortality throughout the Northern Hemisphere, again due to drying[35]. Predictions of increasing future mortality also exist for aspen, eucalypts, conifers and a broad suite of ecosystems under climate change[187–189]. While these models point to threats of woody-plant mortality under warming and droughts, they are challenged in simulation of the combined impacts of rising VPD and $CO_2$.

To highlight how some potential mortality mechanisms respond to changing climate, a multi-model analysis of mortality likelihood under the independent and combined impacts of rising VPD and $CO_2$ is provided (FIG. 5; Supplementary Information). Trees are simulated in a Swiss forest where there were physiological observations of both dying and surviving Norway spruce (*Picea abies*) during a severe drought in 2018 (REF.[104]). Model-predicted percentage loss of whole-tree conductance ($PLC_{plant}$) is used as an index of the risk of mortality as prognostic of drought-associated mortality[18,80,189]; higher $PLC_{plant}$ indicates greater loss of conductance and a greater likelihood of hydraulic failure. Predicting mortality from PLC assumes that $PLC_{plant}$ captures any changes in carbon metabolism that might drive variation in PLC (FIG. 3). Model-data evaluation suggests that models simulated surviving trees better than dying trees (FIG. 5a), particularly late in the mortality process, and, so, estimates of PLC in dying trees are conservative.

The ensemble-mean results indicate several key roles of the changing atmosphere on drought-associated mortality. Firstly, surviving trees with deeper root systems and/or more resistant xylem exhibit similar responses to dying trees but with one distinction: surviving trees consistently have lower $PLC_{plant}$ than dying trees (FIG. 5b,c). Secondly, relative to the baseline 2018 simulations, elevated $CO_2$ consistently alleviates mortality risk (FIG. 5) by reducing water loss through stomatal closure, prolonging maintenance of belowground conductance, increasing xylem water potentials and, hence, reducing $PLC_{plant}$ (REF.[189]) (FIGS 3,5). Simulated water savings are consistent with observations of decreased stomatal conductance with increasing $CO_2$ (REFS[190–192]), potentially reducing water loss and slowing the depletion of both plant and soil water pools. However, such maintenance of soil water pools arising from reduced transpiration is

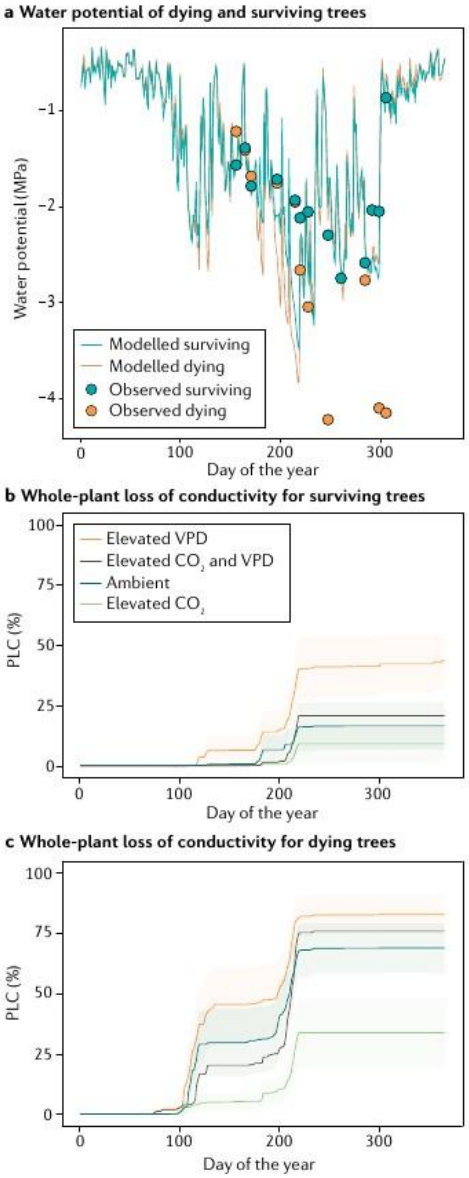


Fig. 5 | **Simulated whole-plant hydraulic failure during drought-associated mortality. a** | Multi-model ensemble-mean predictions of plant water potential compared with observed values in a mature Norway spruce forest during a drought-associated mortality event separated by surviving and dying trees. **b** | Model predictions of mortality via elevated percentage loss of conductance (PLC) under varying $CO_2$ and vapour pressure deficit (VPD) for those trees that survived the 2018 drought. Lines represent the ensemble-mean values for each climate scenario, where ambient represents the control simulation using 2018 observed climate. The shaded areas represent the standard error around the ensemble mean. Future $CO_2$, VPD, temperature and relative humidity are derived for the region using downscaled simulations from EURO-CORDEX[227]. **c** | As in panel **b** but for dying trees (those that did not survive the 2018 drought). The models and modelling approach are described in the Supplemental Information. Elevated $CO_2$ could alleviate mortality risk, while elevated VPD can increase it.

not frequently observed[193–196] due to the compensating effects of increased crown leaf area on water use. Beyond what was modelled, rising $CO_2$ also increases photosynthetic rates[37] and defensive allocation[197], and influences hydraulic architecture[198], mitigating the risk of carbon limitations and defensive failure. Carbohydrate pools are generally reduced by drought and increased by elevated $CO_2$ (REF.[199]), thus, potentially balancing each other.

VPD can act in the opposite direction of $CO_2$ in its impact on mortality likelihood. The model simulations indicate that elevated VPD induces higher $PLC_{plant}$ compared with the 2018 scenario (FIG. 5) owing to increased evaporation from foliage and soils[32], and, thus, decreased belowground conductance. When belowground conductance approaches zero and stomata are closed (FIG. 3), the benefits of $CO_2$ are manifest to a lesser extent. Furthermore, once the plant is relatively disconnected from external resources and is dependent on its internal resource pools, elevated VPD acts to accelerate the depletion of internal water reserves through evaporation via $g_{res}$. This evaporative loss is accentuated during heatwaves owing to the temperature sensitivity of $g_{res}$, in which the cuticular permeability can dramatically increase above 40 °C (REFS[86,87]).

The ensemble-mean simulation results for the elevated $CO_2$ and elevated VPD combined scenario suggest a slight increase in mortality likelihood (FIG. 5). However, given the inter-model variability, such a slight increase might be insignificant and within the variation across the models. Nonetheless, these results suggest that warming-based VPD increases could balance the ameliorating gains from elevated $CO_2$. This balancing of the benefits of elevated $CO_2$ with the consequences of elevated VPD is consistent with the shared time to death of elevated $CO_2$ and ambient $CO_2$ drought experiments[200,201], but contrasts with the increases in mortality observed globally (FIG. 1a). Given that the model-data evaluation revealed an overestimation of the water potential of dying trees (FIG. 5a), it is possible that the predicted increases in mortality under the elevated $CO_2$ and VPD scenario are underestimated.

While not modelled in the simulations, it is important to note that the impact of rising $CO_2$ on photosynthesis and carbohydrate pools also has implications for defence against biotic attack. Defensive failure can occur via shifts in total nonstructural carbohydrates, specific leaf area and reallocation of leaf nitrogen, all of which alter plant host quality, and thus, suitability for herbivores[202]. Elevated $CO_2$ also affects host susceptibility and resistance to biotic attack by altering the synthesis or downregulation of phytochemical defence compounds[203]. However, complete resource budgets that document the fluxes and pools of carbon to and from the defence system has not been done, potentially limiting the capacity of models to forecast future mortality.

***Mortality mechanisms under rising VPD and $CO_2$.*** When examined within the context of rising VPD and $CO_2$, several clear hypotheses originate from the proposed drought-associated mortality framework (FIGS 2–4) and the model results (FIG. 5). Perhaps the most critical hypotheses are that drought-associated mortality is triggered physiologically by severe declines in belowground hydraulic conductance, with the concurrent water loss, and the water-based and carbon-based thresholds for cytorrhysis, all linking together to drive plants into the dying stage (FIGS 2–4). Further, the logical emergent hypothesis is that rising VPD negatively impacts plant survival during drought, whereas rising $CO_2$ can have both positive and negative impacts on mortality likelihood (BOX 1). These hypotheses are well supported by non-mortality research but have rarely been examined in relation to drought-induced death[200,201].

Hypothesized mechanisms underlying these responses also emerge. As exposure to VPD accumulates, both through prolonged chronic rises and extreme events, water loss increases, which, if not met by increased belowground supply, forces plant water pools to decline. Furthermore, rising VPD promotes stomatal closure, which reduces carbon supply at the whole-plant scale. Rising $CO_2$, by contrast, can reduce water loss through stomatal closure and increase photosynthetic rates, leading to higher water content and carbon supply, subsequently reducing mortality likelihood (BOX 1). However, structural overshoot leading to reduced root allocation relative to shoot allocation can predispose trees to mortality through reductions in both water and carbon supply demand during drought. Structural overshoot could also potentially happen at the stand level, in which larger biomass leads to more competition for finite resources (including water and nutrients)[204] during drought.

The interdependency between carbon-related and water-related mechanisms of drought-associated mortality suggest that cytorrhysis occurs when the carbon supply rate needed to maintain hydraulic function exceeds a minimum threshold for survival (BOX 1). An equally likely hypothesis is that water content can fall below the threshold for cytorrhysis before the minimum carbon supply rate is surpassed. Both scenarios could occur depending on the length of the drought and the accumulated exposure to VPD. For example, particularly severe droughts with higher cumulative VPD might promote more rapid drops in water content than in carbon supply rate, thus, exceeding the water content threshold for mortality prior to that for carbon supply rate. Therefore, an associated critical test is to determine the water content and carbon supply rate thresholds and how they respond to increasing cumulative VPD and $CO_2$.

## Challenges to modelling mortality

Models provide useful hypothesis-generating tools for understanding the impacts of a changing environment on mortality (FIG. 5). Models have improved considerably in the representation of water and carbohydrate dynamics at the organ to whole-plant level, and implemented at scales from individual plants to the terrestrial biosphere[49–54,86,205–207]. The coupling between carbon and water at both long and short timescales can now be represented[205,206], although many of the carbon–water interdependencies in the proposed framework (FIG. 3) are either not yet developed or remain untested. Furthermore, gas exchange is represented ever more elegantly[189]. Some models also represent cuticular fluxes and their temperature sensitivity and the subsequent drawdown of internal water pools[86] (FIG. 3). Many models are also trait based and incorporate parameters that are potentially critical to mortality (FIG. 3), some of which can be empirically measured a priori, allowing mechanistically constrained parameterization and large scaling potential[188].

Nevertheless, there remain numerous modelling challenges for those processes that are represented and those that are not, owing, in part, to the interactive nature of mortality drivers and mechanisms. These challenges are highlighted by the model analyses, which, in some cases, failed to capture the particularly negative water potentials of dying trees (FIG. 5a). For those processes captured by models, there can be difficulty in constraining the response functions. For example, belowground conductance is poorly constrained, owing to a lack of empirical measurements. Furthermore, some processes that might be critical to mortality are not yet represented by ecosystem-process models, notably, biotic agents, the attacks of which often coincide with drought[167]. Few models additionally represent the starvation-related mechanisms that could promote the mortality process, including the carbohydrate dependency of metabolism, osmoregulation and hydraulic and defensive functions. Failure of phloem transport can exacerbate localized carbon starvation[130,144,208] but is rarely modelled (but see REF.[149]). Representation of these processes will require more empirical and numerical testing to justify their inclusion in already complex modelling schemes.

A further challenge in modelling woody-plant mortality is the absence of acclimation, partly related to a lack of knowledge of what parameters acclimate and at what rate. If acclimation keeps pace with changes in climate and $CO_2$, multiple traits could enhance survival likelihood. Some traits that could acclimate to reduced water loss under elevated $CO_2$ and VPD include reductions in maximum stomatal conductance ($g_{max}$), $g_{res}$ and individual plant leaf area, along with increases in embolism resistance (estimated as the pressure at which 50% of conductance is lost (P50)).

The impacts of these trait shifts on mortality likelihood were assessed using the SurEau model, representing a spruce tree in the year 2100 (FIG. 6). In this set of scenarios, if $g_{res}$ and P50 decline by 10%, PLC declines (within distal branches) from >90% to ~35%. Similar 10% declines in $g_{max}$ and individual leaf area push PLC likelihood from >90% all the way to 0%. These declines in PLC likelihood translate into declining risk of mortality. Accordingly, reductions in these traits are beneficial to survival under a changing environment (though reductions in all but $g_{res}$ will constrain carbon uptake). $g_{max}$ might acclimate[190,191,209], while P50 has exhibited acclimation potential in angiosperms[210] but less so in gymnosperms[211]. Acclimation to elevated $CO_2$ results in larger leaf area[200,201,212], which would increase the likelihood of elevated mortality. Acclimation of $g_{res}$ to

Acclimation
Structural or physiological shifts in response to external drivers.

long-term warming is unlikely to buffer plants from hydraulic risks during punctuated heatwaves[87]. These shifts can all reduce the likelihood of critical dehydration through reductions in water demand per unit leaf area, but they have potential negative consequences on the carbon economy through reductions in whole-plant photosynthesis (via reduced leaf area and $g_{max}$).

Ultimately, acclimation could be important in survival over longer time periods. However, punctuated droughts and heatwaves can occur much too rapidly for acclimation to manifest (except in the case of leaf loss, which occurs in angiosperms during droughts and heatwaves)[212,213] and exacerbate mortality[33]. Heatwaves are of particular concern because they dramatically increase VPD and leaf temperature when water availability is limited, with foliage typically dying at temperatures above 54 °C (REF.[214]). Beyond acclimation, the extension of the phenological cycle through elevated temperature in temperate and boreal regions could, however, mitigate some of the above-mentioned challenges to the potential of acclimation to mitigate mortality likelihood[215–217], with complicated impacts on mortality–reproduction relationships in masting species[218]. A longer growing season can also promote greater water loss, so the net impacts remain unknown.

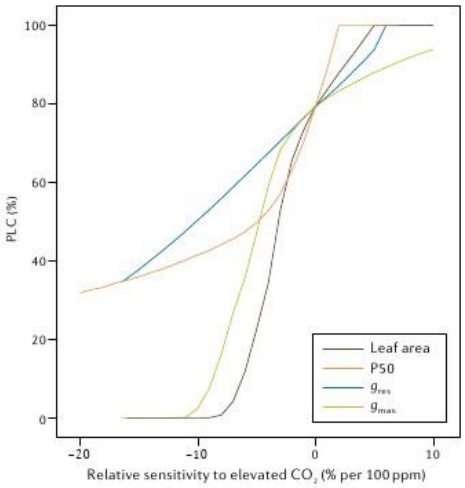


Fig. 6 | **Trait acclimation can reduce mortality likelihood.** Sensitivity analysis, using the SurEau model, in which a spruce tree under elevated $CO_2$ and vapour pressure deficit (from FIG. 5) is allowed to shift traits as $CO_2$ rises. The individually shifted parameters are leaf area, P50, $g_{res}$ and $g_{max}$. If any of these parameters decline as $CO_2$ rises, they are predicted to reduce the likelihood of mortality, indexed as percentage loss of conductance (PLC), through the influences upon water loss (leaf area, $g_{res}$ and $g_{max}$) and tolerance to water loss (P50).

**Summary and future perspectives**

Increasing background mortality rates (FIG. 1a) are alarming in the context of the strong current and future increases in their environmental drivers (FIG. 1b,c). The broad geographic distribution of rising mortality suggests a globally distributed driver, which is consistent with physiological theory (FIGS 2–4) and model results (FIG. 5) that suggest elevated $CO_2$ and VPD could be critical drivers (BOX 1). Mortality appears to be initiated by severe reductions in belowground conductance and subsequent increased risk of hydraulic failure as embolism increases with continued water loss from $g_{res}$ and carbon starvation as stomata shut and, thus, curtail photosynthesis (FIG. 3). Lost hydraulic conductance most immediately increases the risk of hydraulic failure, but if drought is sufficiently prolonged, can deplete carbohydrate stores and fluxes required to maintain metabolism and defence (FIG. 4). Acclimation to drought, $CO_2$ and VPD could provide some buffering of mortality against environmental change, if such acclimation is of sufficient magnitude and speed to accommodate the rapid rate of climate change (FIGS 1b,c,5). The emergent framework generates a set of hypotheses that require testing if understanding and simulation of woody-plant mortality is to be improved under a changing climate.

The proposed framework identifies considerable experimental challenges, particularly for quantifying the key mortality mechanisms and thresholds, and the carbon–water–defence interdependencies that matter most to survival. For example, we must identify the point-of-no-return value for each critical pool and flux (FIGS 2–4), their timing of achieving the threshold and their dependence upon interacting mechanisms. Identifying these thresholds and their underlying mechanisms is achievable through detailed experimentation that investigates the dynamics and interdependencies of the hydraulic, carbon and defensive mechanisms, pools and fluxes, during the dying process.

In addition to experimental challenges, multiple steps can be taken to test the hypotheses regarding mortality mechanisms (FIGS 2–4). Understanding the predisposing factors, such as differences in carbon allocation to water conduction traits and how they predispose or protect plants from drought-associated death, will require long-term observational and experimental studies. Examining the timing and magnitudes of hydraulic limitations (FIG. 3) and the hydraulic point of no return is feasible[66]. However, a substantial challenge remains to quantify belowground hydraulic dynamics accurately[80], including xylary and extra-xylary components of the pathway. Identifying when and where belowground conductance approaches zero is critical, as it sets the rest of the mortality mechanisms into motion[98] (FIG. 3) and is likely essential to accurate modelling (FIG. 5). Likewise, identifying dehydration thresholds and quantifying how long plants can survive on water stores, while losing water to $g_{res}$ under a warming atmosphere, is a large but critical challenge.

Many components of the proposed carbon failure process are also possible to measure. However, identifying the key carbon-based mechanisms leading to mortality will require substantial investment in developing detailed carbon budgets at both the whole-plant and the cellular scales, as has been done for *Arabidopsis* under mild drought[219]. Such carbon budgets must integrate and quantify the fluctuating carbon demands for metabolic and defensive maintenance, osmoregulation and hydraulic function, and can use metabolomic, transcriptomic and proteomic approaches.

The role of biotic agents is also crucial to test but is challenged, in particular, by the lack of knowledge on the exact role of specific defence compounds[220–222]. Nonetheless, manipulative exclusion and inclusion experiments with biotic agents coupled to detailed defensive-carbon budgets could be used to advance understanding of failure to defend against biotic attack. Ultimately, all of these thresholds can be used to identify the mechanism underlying the mortality threshold, or the point of no return.

The role of temporal and spatial shifts in mechanisms that lead to mortality (FIGS 2–4) are a largely unexplored frontier that must be addressed to reduce model uncertainty. We must determine to what degree can acclimation promote survival and to what degree does a lack of acclimation promote mortality. For plants that can adjust rooting depths, $g_{res}$, $g_{smax}$, P50, leaf area (FIG. 6) and other critical variables prior to severe droughts, survival likelihood is increased. If they shift at all[212], the rate of shifts in these variables must be quantified to enable improved predictions. However, non-adaptive acclimation is also a threat, in which extended periods of mesic conditions could promote carbon allocation to increased leaf area and decreased root area (or decreased sapwood area or a myriad of other shifts) that predispose the plant to death when water limitations are severe[76,213]. Scaling of predictions to the ecosystem, region and globe requires consideration of the distinct allometries and allocation patterns of different species/plant functional types[134] and on the distribution of plant roots relative to ephemeral versus constant water sources[206,223,224]. Furthermore, the role of stand density remains a large question[18,225]. If rising $CO_2$ promotes increasing stand density during periods of abundant precipitation, then when a drought occurs, the stand might be overstocked relative to the site's ability to provide water, thus, promoting mortality. This process, however, is not observed in all regional situations[18,225].

Ultimately, the model predictions of tree mortality are critical to estimates of the future terrestrial carbon sink, land–atmosphere interactions and, hence, the rate of climate warming[226]. Maximizing predictive accuracy requires understanding the mechanistic basis for mortality and simultaneously identifying the simplest and most parsimonious approach to modelling mortality at broad scales. Models should be validated at each temporal and spatial scale and applied to aid understanding of future mortality risks. Understanding and predicting the interdependent mechanisms of mortality under climate warming is a critical research priority for disciplines ranging from tissue-level physiology to global-scale prediction.

## Data availability

All data from the simulations can be obtained from the lead author.

Published online: 29 March 2022


1. van Mantgem, P. J. et al. Widespread increase of tree mortality rates in the western United States. *Science* **323**, 521–524 (2009).
2. Peng, C. et al. A drought-induced pervasive increase in tree mortality across Canada's boreal forests. *Nat. Clim. Chang.* **1**, 467–471 (2011).
3. Brienen, R. J. et al. Long-term decline of the Amazon carbon sink. *Nature* **519**, 344–348 (2015).
4. Klein, T., Cahanovitc, R., Sprintsin, M., Herr, N. & Schiller, G. A nation-wide analysis of tree mortality under climate change: forest loss and its causes in Israel 1948–2017. *For. Ecol. Manag.* **432**, 840–849 (2019).
5. Yu, K. et al. Pervasive decreases in living vegetation carbon turnover time across forest climate zones. *Proc. Natl Acad. Sci. USA* **116**, 24662–24667 (2019).
6. Hubau, W. et al. Asynchronous carbon sink saturation in African and Amazonian tropical forests. *Nature* **579**, 80–87 (2020).
7. Kharuk, V. I. et al. Climate-driven conifer mortality in Siberia. *Glob. Ecol. Biogeogr.* **30**, 543–556 (2021).
8. Breshears, D. D. et al. Regional vegetation die-off in response to global-change-type drought. *Proc. Natl Acad. Sci. USA* **102**, 15144–15148 (2005).
9. Lewis, S. L., Brando, P. M., Phillips, O. L., van der Heijden, G. M. & Nepstad, D. The 2010 amazon drought. *Science* **331**, 554 (2011).
10. Ruthrof, K. X. et al. Subcontinental heat wave triggers terrestrial and marine, multi-taxa responses. *Sci. Rep.* **8**, 13094 (2018).
11. Senf, C. et al. Canopy mortality has doubled in Europe's temperate forests over the last three decades. *Nat. Commun.* **9**, 4978 (2018).
12. Schuldt, B. et al. A first assessment of the impact of the extreme 2018 summer drought on Central European forests. *Basic Appl. Ecol.* **45**, 86–103 (2020).
13. Kannenberg, S. A., Driscoll, A. W., Malesky, D. & Anderegg, W. R. Rapid and surprising dieback of Utah juniper in the southwestern USA due to acute drought stress. *For. Ecol. Manag.* **480**, 118639 (2021).
14. Allen, C. D., Breshears, D. D. & McDowell, N. G. On underestimation of global vulnerability to tree mortality and forest die-off from hotter drought in the Anthropocene. *Ecosphere* **6**, 1–55 (2015).
15. Powers, J. S. et al. A catastrophic tropical drought kills hydraulically vulnerable tree species. *Glob. Change Biol.* **26**, 3122–3133 (2020).
16. Werner, W. L. Canopy dieback in the upper montane rain forests of Sri Lanka. *GeoJournal* **17**, 245–248 (1988).
17. Feldpausch, T. R. et al. Amazon forest response to repeated droughts. *Glob. Biogeochem. Cycles* **30**, 964–982 (2016).
18. Esquivel-Muelbert, A. et al. Tree mode of death and mortality risk factors across Amazon forests. *Nat. Commun.* **11**, 5515 (2020).
19. Werner, R. A. & Holsten, E. H. Mortality of white spruce during a spruce beetle outbreak on the Kenai Peninsula in Alaska. *Can. J. For. Res.* **13**, 96–101 (1983).
20. Suarez, M. L., Ghermandi, L. & Kitzberger, T. Factors predisposing episodic drought-induced tree mortality in Nothofagus: site, climatic sensitivity and growth trends. *J. Ecol.* **92**, 954–966 (2004).
21. Swemmer, A. M. Locally high, but regionally low: the impact of the 2014–2016 drought on the trees of semi-arid savannas, South Africa. *Afr. J. Range Forage Sci.* **37**, 31–42 (2020).
22. Michaelian, M., Hogg, E. H., Hall, R. J. & Arsenault, E. Massive mortality of aspen following severe drought along the southern edge of the Canadian boreal forest. *Glob. Chang Biol.* **17**, 2084–2094 (2011).
23. Kharuk, V. I. et al. Climate-induced mortality of Siberian pine and fir in the Lake Baikal Watershed, Siberia. *For. Ecol. Manag.* **384**, 191–199 (2017).
24. Kharuk, V. I., Ranson, K. J., Oskorbin, P. A., Im, S. T. & Dvinskaya, M. L. Climate induced birch mortality in Trans-Baikal lake region, Siberia. *For. Ecol. Manag.* **289**, 385–392 (2013).
25. Crouchet, S. E., Jensen, J., Schwartz, B. F. & Schwinning, S. Tree mortality after a hot drought: distinguishing density-dependent and -independent drivers and why it matters. *Front. For. Glob. Change* **2**, 21 (2019).
26. Breshears, D. D. et al. The critical amplifying role of increasing atmospheric moisture demand on tree mortality and associated regional die-off. *Front. Plant Sci.* **4**, 266 (2013).
27. Grossiord, C. et al. Plant responses to rising vapor pressure deficit. *New Phytol.* **226**, 1550–1566 (2020).
28. Trenberth, K. E. et al. Global warming and changes in drought. *Nat. Clim. Chang.* **4**, 17–22 (2014).
29. Williams, A. P. et al. Temperature as a potent driver of regional forest drought stress and tree mortality. *Nat. Clim. Chang.* **3**, 292–297 (2013).
30. Xu, C. et al. Increasing impacts of extreme droughts on vegetation productivity under climate change. *Nat. Clim. Chang.* **9**, 948–953 (2019).
31. Dore, M. H. Climate change and changes in global precipitation patterns: what do we know? *Environ. Int.* **31**, 1167–1181 (2005).
32. Ukkola, A. M., De Kauwe, M. G., Roderick, M. L., Abramowitz, G. & Pitman, A. J. Robust future changes in meteorological drought in CMIP6 projections despite uncertainty in precipitation. *Geophys. Res. Lett.* **31**, e2020GL087820 (2020).
33. Breshears, D. D. et al. Underappreciated plant vulnerabilities to heat waves. *New Phytol.* **231**, 32–39 (2021).
34. Adams, H. D. et al. Temperature response surfaces for mortality risk of tree species with future drought. *Environ. Res. Lett.* **12**, 115014 (2017).
35. McDowell, N. G. et al. Multi-scale predictions of massive conifer mortality due to chronic temperature rise. *Nat. Clim. Chang.* **6**, 295–300 (2016).
36. Keenan, T. F. et al. Increase in forest water-use efficiency as atmospheric carbon dioxide concentrations rise. *Nature* **499**, 324–327 (2013).
37. Walker, A. P. et al. Integrating the evidence for a terrestrial carbon sink caused by increasing atmospheric $CO_2$. *New Phytol.* **229**, 2413–2445 (2020).
38. Long, S. P. Modification of the response of photosynthetic productivity to rising temperature by atmospheric $CO_2$ concentrations: has its importance been underestimated? *Plant Cell Environ.* **14**, 729–739 (1991).
39. Hickler, T. et al. $CO_2$ fertilization in temperate FACE experiments not representative of boreal and tropical forests. *Glob. Change Biol.* **14**, 1531–1542 (2008).
40. Baig, S., Medlyn, B. E., Mercado, L. & Zaehle, S. Does the growth response of woody plants to elevated $CO_2$ increase with temperature? A model-oriented meta-analysis. *Glob. Change Biol.* **21**, 4303–4319 (2015).
41. Peñuelas, J. et al. Shifting from a fertilization-dominated to a warming-dominated period. *Nat. Ecol. Evol.* **1**, 1438–1445 (2017).
42. Belmecheri, S. et al. Precipitation alters the $CO_2$ effect on water-use efficiency of temperate forests. *Glob. Change Biol.* **27**, 1560–1571 (2021).

43. Duffy, K. A. et al. How close are we to the temperature tipping point of the terrestrial biosphere? *Sci. Adv.* **7**, eaay1052 (2021).
44. De Kauwe, M. G., Medlyn, B. E. & Tissue, D. T. To what extent can rising [$CO_2$] ameliorate plant drought stress? *New Phytol.* **231**, 2118–2124 (2021).
45. Martınez-Vilalta, J., Piñol, J. & Beven, K. A hydraulic model to predict drought-induced mortality in woody plants: an application to climate change in the Mediterranean. *Ecol. Model.* **155**, 127–147 (2002).
46. McDowell, N. et al. Mechanisms of plant survival and mortality during drought: why do some plants survive while others succumb to drought? *New Phytol.* **178**, 719–739 (2008).
47. McDowell, N. G. et al. The interdependence of mechanisms underlying climate-driven vegetation mortality. *Trends Ecol. Evol.* **26**, 523–532 (2011).
48. Adams, H. D. et al. A multi-species synthesis of physiological mechanisms in drought-induced tree mortality. *Nat. Ecol. Evol.* **1**, 1285–1291 (2017).
49. Fisher, R. et al. Assessing uncertainties in a second-generation dynamic vegetation model caused by ecological scale limitations. *New Phytol.* **187**, 666–681 (2010).
50. McDowell, N. G. et al. Evaluating theories of drought-induced vegetation mortality using a multimodel–experiment framework. *New Phytol.* **200**, 304–321 (2013).
51. Anderegg, W. R. L. et al. Hydraulic diversity of forests regulates ecosystem resilience during drought. *Nature* **561**, 538–541 (2018).
52. Christoffersen, B. O. et al. Linking hydraulic traits to tropical forest function in a size-structured and trait-driven model (TFS v. 1-Hydro). *Geosci. Model Dev.* **9**, 4227–4255 (2016).
53. Kennedy, D. et al. Implementing plant hydraulics in the community land model, version 5. *J. Adv. Model. Earth Syst.* **11**, 485–513 (2019).
54. Koven, C. D. et al. Benchmarking and parameter sensitivity of physiological and vegetation dynamics using the Functionally Assembled Terrestrial Ecosystem Simulator (FATES) at Barro Colorado Island, Panama. *Biogeosciences* **17**, 3017–3044 (2020).
55. Anderegg, W. R., Kane, J. M. & Anderegg, L. D. Consequences of widespread tree mortality triggered by drought and temperature stress. *Nat. Clim. Chang.* **3**, 30–36 (2013).
56. Hartmann, H. et al. Research frontiers for improving our understanding of drought-induced tree and forest mortality. *New Phytol.* **218**, 15–28 (2018).
57. Adams, H. D. et al. Ecohydrological consequences of drought- and infestation-triggered tree die-off: insights and hypotheses. *Ecohydrology* **5**, 145–159 (2012).
58. Bearup, L. A., Maxwell, R. M., Clow, D. W. & McCray, J. E. Hydrological effects of forest transpiration loss in bark beetle-impacted watersheds. *Nat. Clim. Chang.* **4**, 481–486 (2014).
59. Bennett, K. E. et al. Climate-driven disturbances in the San Juan River sub-basin of the Colorado River. *Hydrol. Earth Syst. Sci.* **22**, 709–725 (2018).
60. Lutz, J. A. & Halpern, C. B. Tree mortality during early forest development: a long-term study of rates, causes, and consequences. *Ecol. Monogr.* **76**, 257–275 (2006).
61. Clark, J. S. et al. The impacts of increasing drought on forest dynamics, structure, and biodiversity in the United States. *Glob. Change Biol.* **22**, 2329–2352 (2016).
62. McDowell, N. G. et al. Pervasive shifts in forest dynamics in a changing world. *Science* **368**, eaaz9463 (2020).
63. Waring, K. M. et al. Modeling the impacts of two bark beetle species under a warming climate in the southwestern USA: ecological and economic consequences. *Environ. Manag.* **44**, 824–835 (2009).
64. Barigah, T. S. et al. Water stress-induced xylem hydraulic failure is a causal factor of tree mortality in beech and poplar. *Ann. Bot.* **112**, 1431–1437 (2013).
65. Guadagno, C. R. et al. Dead or alive? Using membrane failure and chlorophyll *a* fluorescence to predict plant mortality from drought. *Plant Physiol.* **175**, 223–234 (2017).
66. Hammond, W. M. et al. Dead or dying? Quantifying the point of no return from hydraulic failure in drought-induced tree mortality. *New Phytol.* **223**, 1834–1843 (2019).
67. Sapes, G. et al. Plant water content integrates hydraulics and carbon depletion to predict drought-induced seedling mortality. *Tree Physiol.* **39**, 1300–1312 (2019).
68. Mantova, M., Menezes-Silva, P. E., Badel, E., Cochard, H. & Torres-Ruiz, J. M. The interplay of hydraulic failure and cell vitality explains tree capacity to recover from drought. *Physiol. Plant.* **172**, 247–257 (2021).
69. Kono, Y. et al. Initial hydraulic failure followed by late-stage carbon starvation leads to drought-induced death in the tree *Trema orientalis*. *Commun. Biol.* **2**, 8 (2019).
70. Preisler, Y. et al. Seeking the "point of no return" in the sequence of events leading to mortality of mature trees. *Plant Cell Environ.* **44**, 1315–1328 (2020).
71. Allen, C. D. et al. A global overview of drought and heat-induced tree mortality reveals emerging climate change risks for forests. *For. Ecol. Manag.* **259**, 660–684 (2010).
72. Bennett, A. C. et al. Resistance of African tropical forests to an extreme climate anomaly. *Proc. Natl Acad. Sci. USA* **118**, e2003169118 (2021).
73. McDowell, N. G. & Allen, C. D. Darcy's law predicts widespread forest mortality under climate warming. *Nat. Clim. Chang.* **5**, 669–672 (2015).
74. Stephenson, N. L. & van Mantgem, P. J. Forest turnover rates follow global and regional patterns of productivity. *Ecol. Lett.* **8**, 524–531 (2005).
75. Zhu, K. C. et al. Dual impacts of climate change: forest migration and turnover through life history. *Glob. Change Biol.* **20**, 251–264 (2014).
76. Jump, A. S. et al. Structural overshoot of tree growth with climate variability and the global spectrum of drought-induced forest dieback. *Glob. Change Biol.* **23**, 3742–3757 (2017).
77. Trugman, A. T. et al. Tree carbon allocation explains forest drought-kill and recovery patterns. *Ecol. Lett.* **21**, 1552–1560 (2018).
78. Hartmann, H. et al. Climate change risks to global forest health – emergence of unexpected events of elevated tree mortality world-wide. *Annu. Rev. Plant Biol.* https://doi.org/10.1146/annurev-arplant-102820-012804 (2022).
79. Manion, P. D. *Tree Disease Concepts* (Prentice-Hall, 1981)
80. Brodribb, T. J. Learning from a century of droughts. *Nat. Ecol. Evol.* **4**, 1007–1008 (2020).
81. Anderegg, W. R. et al. Tree mortality from drought, insects, and their interactions in a changing climate. *New Phytol.* **208**, 674–683 (2015).
82. Huang, J. et al. Tree defence and bark beetles in a drying world: carbon partitioning, functioning and modelling. *New Phytol.* **225**, 26–36 (2019).
83. Martinez-Vilalta, J., Anderegg, W. R., Sapes, G. & Sala, A. Greater focus on water pools may improve our ability to understand and anticipate drought-induced mortality in plants. *New Phytol.* **223**, 22–32 (2019).
84. Cuneo, I. F., Knipfer, T., Brodersen, C. R. & McElrone, A. J. Mechanical failure of fine root cortical cells initiates plant hydraulic decline during drought. *Plant Physiol.* **172**, 1669–1678 (2016).
85. Johnson, D. M. et al. Co-occurring woody species have diverse hydraulic strategies and mortality rates during an extreme drought. *Plant Cell Environ.* **41**, 576–588 (2018).
86. Cochard, H. A new mechanism for tree mortality due to drought and heatwaves. *Peer Community J.* **1**, e36 (2021).
87. Duursma, R. A. et al. On the minimum leaf conductance: its role in models of plant water use, and ecological and environmental controls. *New Phytol.* **221**, 693–705 (2019).
88. Beckett, R. P. Pressure–volume analysis of a range of poikilohydric plants implies the existence of negative turgor in vegetative cells. *Ann. Bot.* **79**, 145–152 (1997).
89. Ding, Y., Zhang, Y., Zheng, Q. S. & Tyree, M. T. Pressure–volume curves: revisiting the impact of negative turgor during cell collapse by literature review and simulations of cell micromechanics. *New Phytol.* **203**, 378–387 (2014).
90. Sperry, J. S., Adler, F. R., Campbell, G. S. & Comstock, J. P. Limitation of plant water use by rhizosphere and xylem conductance: results from a model. *Plant Cell Environ.* **21**, 347–359 (1998).
91. Rodriguez-Dominguez, C. M. & Brodribb, T. J. Declining root water transport drives stomatal closure in olive under moderate water stress. *New Phytol.* **225**, 126–134 (2020).
92. Carminati, A. & Javaux, M. Soil rather than xylem vulnerability controls stomatal response to drought. *Trends Plant Sci.* **25**, 868–880 (2020).
93. Maseda, P. H. & Fernandez, R. J. Stay wet or else: three ways in which plants can adjust hydraulically to their environment. *J. Exp. Bot.* **57**, 3963–3977 (2006).
94. Plaut, J. A. et al. Hydraulic limits preceding mortality in a piñon–juniper woodland under experimental drought. *Plant Cell Environ.* **35**, 1601–1617 (2012).
95. Creek, D. et al. Xylem embolism in leaves does not occur with open stomata: evidence from direct observations using the optical visualization technique. *J. Exp. Bot.* **71**, 1151–1159 (2020).
96. Choat, B. et al. Triggers of tree mortality under drought. *Nature* **558**, 531–539 (2018).
97. Hammond, W. M. & Adams, H. D. Dying on time: traits influencing the dynamics of tree mortality risk from drought. *Tree Physiol.* **39**, 906–909 (2019).
98. Körner, C. No need for pipes when the well is dry — a comment on hydraulic failure in trees. *Tree Physiol.* **39**, 695–700 (2019).
99. Machado, R. et al. Where do leaf water leaks come from? Trade-offs underlying the variability in minimum conductance across tropical savanna species with contrasting growth strategies. *New Phytol.* **229**, 1415–1430 (2021).
100. Burghardt, M. & Riederer, M. in *Biology of the Plant Cuticle* (eds Riederer, M. & Müller, C.) 292–311 (Blackwell, 2006).
101. Billon, L. M. et al. The DroughtBox: a new tool for phenotyping residual branch conductance and its temperature dependence during drought. *Plant Cell Environ.* **43**, 1584–1594 (2020).
102. Wolfe, B. T. Bark water vapour conductance is associated with drought performance in tropical trees. *Biol. Lett.* **16**, 20200263 (2020).
103. Martín-Gómez, P., Serrano, L. & Ferrio, J. P. Short-term dynamics of evaporative enrichment of xylem water in woody stems: implications for ecohydrology. *Tree Physiol.* **37**, 511–522 (2017).
104. Arend, M. et al. Rapid hydraulic collapse as cause of drought-induced mortality in conifers. *Proc. Natl Acad. Sci. USA* **118**, e2025251118 (2021).
105. Wang, W. et al. Mortality predispositions of conifers across western USA. *New Phytol.* **229**, 831–844 (2020).
106. Christiansen, E., Waring, R. H. & Berryman, A. A. Resistance of conifers to bark beetle attack: searching for general relationships. *For. Ecol. Manag.* **22**, 89–106 (1987).
107. Bigler, C., Bräker, O. U., Bugmann, H., Dobbertin, M. & Rigling, A. Drought as an inciting mortality factor in Scots pine stands of the Valais, Switzerland. *Ecosystems* **9**, 330–343 (2006).
108. Richardson, A. D. et al. Seasonal dynamics and age of stemwood nonstructural carbohydrates in temperate forest trees. *New Phytol.* **197**, 850–861 (2013).
109. Meinzer, F. C. et al. Dynamics of water transport and storage in conifers studied with deuterium and heat tracing techniques. *Plant Cell Environ.* **29**, 105–114 (2006).
110. McDowell, N. G., Allen, C. D. & Marshall, L. Growth, carbon-isotope discrimination, and drought-associated mortality across a *Pinus ponderosa* elevational transect. *Glob. Change Biol.* **16**, 399–415 (2010).
111. Kane, J. M. & Kolb, T. E. Importance of resin ducts in reducing ponderosa pine mortality from bark beetle attack. *Oecologia* **164**, 601–609 (2010).
112. Ferrenberg, S., Kane, J. M. & Mitton, J. B. Resin duct characteristics associated with tree resistance to bark beetles across lodgepole and limber pines. *Oecologia* **174**, 1283–1292 (2014).
113. Cailleret, M. et al. A synthesis of radial growth patterns preceding tree mortality. *Glob. Change Biol.* **23**, 1675–1690 (2017).
114. Muller, B., Pantin, F., Génard, M., Turc, O., Freixes, S., Piques, M. & Gibon, Y. Water deficits uncouple growth from photosynthesis, increase C content, and modify the relationships between C and growth in sink organs. *J. Exp. Bot.* **62**, 1715–1729 (2011).
115. Yu, S. Cellular and genetic responses of plants to sugar starvation. *Plant Physiol.* **121**, 687–693 (1999).
116. Koster, K. L. & Leopold, A. C. Sugars and desiccation tolerance in seeds. *Plant Physiol.* **88**, 829–832 (1988).
117. Sapes, G., Demaree, P., Lekberg, Y. & Sala, A. Plant carbohydrate depletion impairs water relations and spreads via ectomycorrhizal networks. *New Phytol.* **229**, 3172–3183 (2021).
118. Hoekstra, F. A., Golovina, E. A. & Buitink, J. Mechanisms of plant desiccation tolerance. *Trends Plant Sci.* **6**, 431–438 (2001).
119. Van den Ende, W. & Valluru, R. Sucrose, sucrosyl oligosaccharides, and oxidative stress: scavenging and salvaging? *J. Exp. Bot.* **60**, 9–18 (2009).

120. Matros, A., Peshev, D., Peukert, M., Mock, H.-P. & Ende, W. Vden Sugars as hydroxyl radical scavengers: proof-of-concept by studying the fate of sucralose in Arabidopsis. *Plant J.* **82**, 822–839 (2015).
121. Rolland, F., Baena-González, E. & Sheen, J. Sugar sensing and signaling in plants: conserved and novel mechanisms. *Annu. Rev. Plant Biol.* **57**, 675–709 (2006).
122. Ramel, F., Sulmon, C., Bogard, M., Couée, I. & Gouesbet, G. Differential patterns of reactive oxygen species and antioxidative mechanisms during atrazine injury and sucrose-induced tolerance in *Arabidopsis thaliana* plantlets. *BMC Plant Biol.* **9**, 28 (2009).
123. Fine, P. V. A. et al. The growth–defense trade-off and habitat specialization by plants in Amazonian forests. *Ecology* **87**, S150–S162 (2006).
124. Huot, B., Yao, J., Montgomery, B. L. & He, S. Y. Growth–defense tradeoffs in plants: a balancing act to optimize fitness. *Mol. Plant* **7**, 1267–1287 (2014).
125. Ouédraogo, D.-Y., Mortier, F., Gourlet-Fleury, S., Freycon, V. & Picard, N. Slow-growing species cope best with drought: evidence from long-term measurements in a tropical semi-deciduous moist forest of Central Africa. *J. Ecol.* **101**, 1459–1470 (2013).
126. de la Mata, R., Hood, S. & Sala, A. Insect outbreak shifts the direction of selection from fast to slow growth rates in the long-lived conifer Pinus ponderosa. *Proc. Natl Acad. Sci. USA* **114**, 7391–7396 (2017).
127. Roskilly, B., Keeling, E., Hood, S., Giuggiola, A. & Sala, A. Conflicting functional effects of xylem pit structure relate to the growth-longevity trade-off in a conifer species. *Proc. Natl Acad. Sci. USA* **116**, 15282–15287 (2019).
128. Snyder, K. A. & Williams, D. G. Defoliation alters water uptake by deep and shallow roots of *Prosopis velutina* (Velvet Mesquite). *Funct. Ecol.* **17**, 363–374 (2003).
129. Eyles, A., Pinkard, E. A. & Mohammed, C. Shifts in biomass and resource allocation patterns following defoliation in *Eucalyptus globulus* growing with varying water and nutrient supplies. *Tree Physiol.* **29**, 753–764 (2009).
130. Hillabrand, R. M., Hacke, U. G. & Lieffers, V. J. Defoliation constrains xylem and phloem functionality. *Tree Physiol.* **39**, 1099–1108 (2019).
131. Landhäusser, S. M. & Lieffers, V. J. Defoliation increases risk of carbon starvation in root systems of mature aspen. *Trees* **26**, 653–661 (2012).
132. Poyatos, R., Aguadé, D., Galiano, L., Mencuccini, M. & Martínez-Vilalta, J. Drought-induced defoliation and long periods of near-zero gas exchange play a key role in accentuating metabolic decline of Scots pine. *New Phytol.* **200**, 388–401 (2013).
133. Cardoso, A. A., Batz, T. A. & McAdam, S. A. Xylem embolism resistance determines leaf mortality during drought in *Persea americana*. *Plant Physiol.* **182**, 547–554 (2020).
134. Mencuccini, M. et al. Leaf economics and plant hydraulics drive leaf:wood area ratios. *New Phytol.* **224**, 1544–1556 (2019).
135. Cochard, H., Pimont, F., Ruffault, J. & Martin-St Paul, N. SurEau: a mechanistic model of plant water relations under extreme drought. *Ann. Forest Sci.* **78**, 1–23 (2021).
136. Yin, M. C. & Blaxter, J. H. S. Temperature, salinity tolerance, and buoyancy during early development and starvation of Clyde and North Sea herring, cod, and flounder larvae. *J. Exp. Mar. Biol. Ecol* **107**, 279–290 (1987).
137. Cahill, G. F. Jr. Fuel metabolism in starvation. *Annu. Rev. Nutr.* **26**, 1–22 (2006).
138. Yandi, I. & Altinok, I. Irreversible starvation using RNA/DNA on lab-grown larval anchovy, *Engraulis encrasicolus*, and evaluating starvation in the field-caught larval cohort. *Fish. Res.* **201**, 32–37 (2018).
139. Smith, A. M. & Stitt, M. Coordination of carbon supply and plant growth. *Plant Cell Environ.* **30**, 1126–1149 (2007).
140. Schädel, C., Richter, A., Blöchl, A. & Hoch, G. Hemicellulose concentration and composition in plant cell walls under extreme carbon source–sink imbalances. *Physiol. Plant.* **139**, 241–255 (2010).
141. Tsamir-Rimon, M. et al. Rapid starch degradation in the wood of olive trees under heat and drought is permitted by three stress-specific beta amylases. *New Phytol.* **229**, 1398–1414 (2020).
142. McLoughlin, F. et al. Autophagy plays prominent roles in amino acid, nucleotide, and carbohydrate metabolism during fixed-carbon starvation in maize. *Plant Cell* **32**, 2699–2724 (2020).
143. Quirk, J., McDowell, N. G., Leake, J. R., Hudson, P. J. & Beerling, D. J. Increased susceptibility to drought-induced mortality in *Sequoia sempervirens* (Cupressaceae) trees under Cenozoic atmospheric carbon dioxide starvation. *Am. J. Bot.* **100**, 582–591 (2013).
144. Sevanto, S., Mcdowell, N. G., Dickman, L. T., Pangle, R. & Pockman, W. T. How do trees die? A test of the hydraulic failure and carbon starvation hypotheses. *Plant Cell Environ.* **37**, 153–161 (2014).
145. Tomasella, M., Petrussa, E., Petruzzellis, F., Nardini, A. & Casolo, V. The possible role of non-structural carbohydrates in the regulation of tree hydraulics. *Int. J. Mol. Sci.* **21**, 144 (2020).
146. Gaylord, M. L. et al. Drought predisposes piñon–juniper woodlands to insect attacks and mortality. *New Phytol.* **198**, 567–578 (2013).
147. Dickman, L. T., McDowell, N. G., Sevanto, S., Pangle, R. E. & Pockman, W. T. Carbohydrate dynamics and mortality in a piñon-juniper woodland under three future precipitation scenarios. *Plant Cell Environ.* **38**, 729–739 (2015).
148. Ruehr, N. K. et al. Drought effects on allocation of recent carbon: from beech leaves to soil $CO_2$ efflux. *New Phytol.* **184**, 950–961 (2009).
149. Mencuccini, M., Minunno, F., Salmon, Y., Martínez-Vilalta, J. & Hölttä, T. Coordination of physiological traits involved in drought-induced mortality of woody plants. *New Phytol.* **208**, 396–409 (2015).
150. Hagedorn, F. et al. Recovery of trees from drought depends on belowground sink control. *Nat. Plants* **2**, 16111 (2016).
151. Hesse, B. D., Goisser, M., Hartmann, H. & Grams, T. E. E. Repeated summer drought delays sugar export from the leaf and impairs phloem transport in mature beech. *Tree Physiol.* **39**, 192–200 (2019).
152. Wiley, E., Hoch, G. & Landhäusser, S. M. Dying piece by piece: carbohydrate dynamics in aspen (*Populus tremuloides*) seedlings under severe carbon stress. *J. Exp. Bot.* **68**, 5221–5232 (2017).
153. Weber, R. et al. Living on next to nothing: tree seedlings can survive weeks with very low carbohydrate concentrations. *New Phytol.* **218**, 107–118 (2018).
154. Hasanuzzaman, M. & Tanveer, M. (eds) *Salt and Drought Stress Tolerance in Plants: Signaling Networks and Adaptive Mechanisms* (Springer, 2020)
155. O'Brien, M. J., Leuzinger, S., Philipson, C. D., Tay, J. & Hector, A. Drought survival of tropical tree seedlings enhanced by non-structural carbohydrate levels. *Nat. Clim. Chang.* **4**, 710–714 (2014).
156. Nardini, A. et al. Rooting depth, water relations and non-structural carbohydrate dynamics in three woody angiosperms differentially affected by an extreme summer drought. *Plant Cell Environ.* **39**, 618–627 (2016).
157. Zinselmeier, C., Westgate, M. E., Schussler, J. R. & Jones, R. J. Low water potential disrupts carbohydrate metabolism in maize (*Zea mays* L.) ovaries. *Plant Physiol.* **107**, 385–391 (1995).
158. Desprez-Loustau, M.-L., Marçais, B., Nageleisen, L.-M., Piou, D. & Vannini, A. Interactive effects of drought and pathogens in forest trees. *Ann. For. Sci.* **63**, 597–612 (2006).
159. Oliva, J., Stenlid, J. & Martínez-Vilalta, J. The effect of fungal pathogens on the water and carbon economy of trees: implications for drought-induced mortality. *New Phytol.* **203**, 1028–1035 (2014).
160. Kolb, T. et al. Drought-mediated changes in tree physiological processes weaken tree defenses to bark beetle attack. *J. Chem. Ecol.* **45**, 888–900 (2019).
161. Croize, L., Lieutier, F., Cochard, H. & Dreyer, E. Effects of drought stress and high density stem inoculations with *Leptographium wingfieldii* on hydraulic properties of young Scots pine trees. *Tree Physiol.* **21**, 427–436 (2001).
162. Wullschleger, S. D., McLaughlin, S. B. & Ayres, M. P. High-resolution analysis of stem increment and sap flow for loblolly pine trees attacked by southern pine beetle. *Can. J. For. Res.* **34**, 387–2393 (2004).
163. Hubbard, R. M., Rhoades, C. C., Elder, K. & Negron, J. Changes in transpiration and foliage growth in lodgepole pine trees following mountain pine beetle attack and mechanical girdling. *For. Ecol. Manag.* **289**, 312–317 (2013).
164. Manter, D. K. & Kavanagh, K. L. Stomatal regulation in Douglas fir following a fungal-mediated chronic reduction in leaf area. *Trees* **17**, 485–491 (2003).
165. Lahr, E. L. & Sala, A. Sapwood stored resources decline in whitebark and lodgepole pines attacked by mountain pine beetles (Coleoptera: Curculionidae). *Environ. Entomol.* **45**, 1463–1475 (2016).
166. Marler, T. E. & Cascasan, A. N. Carbohydrate depletion during lethal infestation of *Aulacaspis yasumatsui* on *Cycas revoluta*. *Int. J. Plant Sci.* **179**, 497–504 (2018).
167. Hood, S. & Sala, A. Ponderosa pine resin defenses and growth: metrics matter. *Tree Physiol.* **35**, 1223–1235 (2015).
168. Roth, M., Hussain, A., Cale, J. A. & Erbilgin, N. Successful colonization of lodgepole pine trees by mountain pine beetle increased monoterpene production and exhausted carbohydrate reserves. *J. Chem. Ecol.* **44**, 209–214 (2018).
169. Raffa, K. F. et al. Cross-scale drivers of natural disturbances prone to anthropogenic amplification: the dynamics of bark beetle eruptions. *Bioscience* **58**, 501–517 (2008).
170. Seidl, R., Schelhaas, M. J., Rammer, W. & Verkerk, P. J. Increasing forest disturbances in Europe and their impact on carbon storage. *Nat. Clim. Chang.* **4**, 806–810 (2014).
171. Ryan, M. G., Sapes, G., Sala, A. & Hood, S. M. Tree physiology and bark beetles. *New Phytol.* **205**, 955–957 (2015).
172. Huang, J. et al. Tree defence and bark beetles in a drying world: carbon partitioning, functioning and modelling. *New Phytol.* **225**, 26–36 (2020).
173. Goodsman, D. W., Lusebrink, I., Landhäusser, S. M., Erbilgin, N. & Lieffers, V. J. Variation in carbon availability, defense chemistry and susceptibility to fungal invasion along the stems of mature trees. *New Phytol.* **197**, 586–594 (2013).
174. Wiley, E., Rogers, B. J., Hodgkinson, R. & Landhäusser, S. M. Nonstructural carbohydrate dynamics of lodgepole pine dying from mountain pine beetle attack. *New Phytol.* **209**, 550–562 (2016).
175. Netherer, S. et al. Do water-limiting conditions predispose Norway spruce to bark beetle attack? *New Phytol.* **205**, 1128–1141 (2015).
176. Rissanen, K. et al. Drought effects on carbon allocation to resin defences and on resin dynamics in old-grown Scots pine. *Environ. Exp. Bot.* **185**, 104410 (2021).
177. Gershenzon, J. Metabolic costs of terpenoid accumulation in higher plants. *J. Chem. Ecol.* **20**, 1281–1328 (1994).
178. Navarro, L. et al. DELLAs control plant immune responses by modulating the balance of jasmonic acid and salicylic acid signaling. *Curr. Biol.* **1**, 650–655 (2008).
179. Fox, H. et al. Transcriptome analysis of *Pinus halepensis* under drought stress and during recovery. *Tree Physiol.* **38**, 423–441 (2018).
180. Caretto, S., Linsalata, V., Colella, G., Mita, G. & Lattanzio, V. Carbon fluxes between primary metabolism and phenolic pathway in plant tissues under stress. *Int. J. Mol. Sci.* **16**, 26378–26394 (2015).
181. Franceschi, V. R., Krokene, P., Christiansen, E. & Krekling, T. Anatomical and chemical defenses of conifer bark against bark beetles and other pests. *New Phytol.* **167**, 353–376 (2005).
182. Suárez-Vidal, E. et al. Drought stress modifies early effective resistance and induced chemical defences of Aleppo pine against a chewing insect herbivore. *Environ. Exp. Bot.* **162**, 550–559 (2019).
183. Hood, S., Sala, A., Heyerdahl, E. K. & Boutin, M. Low-severity fire increases tree defense against bark beetle attacks. *Ecology* **96**, 1846–1855 (2015).
184. Zhao, S. & Erbilgin, N. Larger resin ducts are linked to the survival of lodgepole pine trees during mountain pine beetle outbreak. *Front. Plant Sci.* **10**, 1459 (2019).
185. Kichas, N. E., Hood, S. M., Pederson, G. T., Everett, R. G. & McWethy, D. B. Whitebark pine (*Pinus albicaulis*) growth and defense in response to mountain pine beetle outbreaks. *For. Ecol. Manag.* **457**, 117736 (2020).
186. Gaylord, M. L., Kolb, T. E. & McDowell, N. G. Mechanisms of piñon pine mortality after severe drought: a retrospective study of mature trees. *Tree Physiol.* **35**, 806–816 (2015).
187. Anderegg, W. et al. Tree mortality predicted from drought-induced vascular damage. *Nat. Geosci.* **8**, 367–371 (2015).
188. De Kauwe, M. G. et al. Identifying areas at risk of drought-induced tree mortality across South-Eastern Australia. *Glob. Change Biol.* **26**, 5716–5733 (2020).
189. Sperry, J. S. et al. The impact of rising $CO_2$ and acclimation on the response of US forests to global warming. *Proc. Natl Acad. Sci. USA* **116**, 25734–25744 (2019).

190. Medlyn, B. E. et al. Stomatal conductance of forest species after long-term exposure to elevated $CO_2$ concentration: a synthesis. *New Phytol.* **149**, 247–264 (2001).
191. Klein, T. & Ramon, U. Stomatal sensitivity to $CO_2$ diverges between angiosperm and gymnosperm tree species. *Funct. Ecol.* **33**, 1411–1424 (2019).
192. Paudel, I. et al. Elevated $CO_2$ compensates for drought effects in lemon saplings via stomatal downregulation, increased soil moisture, and increased wood carbon storage. *Environ. Exp. Bot.* **148**, 117–127 (2018).
193. Bobich, E. G., Barron-Gafford, G. A., Rascher, K. G. & Murthy, R. Effects of drought and changes in vapour pressure deficit on water relations of *Populus deltoides* growing in ambient and elevated $CO_2$. *Tree Physiol.* **30**, 866–875 (2010).
194. Gimeno, T. E., McVicar, T. R., O'Grady, A. P., Tissue, D. T. & Ellsworth, D. S. Elevated $CO_2$ did not affect the hydrological balance of a mature native *Eucalyptus* woodland. *Glob. Change Biol.* **24**, 3010–3024 (2018).
195. Nowak, R. S. et al. Elevated atmospheric $CO_2$ does not conserve soil water in the mojave desert. *Ecology* **85**, 93–99 (2004).
196. Schäfer, K. V., Oren, R., Lai, C. T. & Katul, G. G. Hydrologic balance in an intact temperate forest ecosystem under ambient and elevated atmospheric $CO_2$ concentration. *Glob. Change Biol.* **8**, 895–911 (2002).
197. Novick, K. A., Katul, G. G., McCarthy, H. R. & Oren, R. Increased resin flow in mature pine trees growing under elevated $CO_2$ and moderate soil fertility. *Tree Physiol.* **32**, 752–763 (2012).
198. Li, X. M. et al. Temperature alters the response of hydraulic architecture to $CO_2$ in cotton plants (*Gossypium hirsutum*). *Environ. Exp. Bot.* **172**, 104004 (2020).
199. Li, W. et al. The sweet side of global change–dynamic responses of non-structural carbohydrates to drought, elevated $CO_2$ and nitrogen fertilization in tree species. *Tree Physiol.* **38**, 1706–1723 (2018).
200. Duan, H. et al. Elevated [$CO_2$] does not ameliorate the negative effects of elevated temperature on drought-induced mortality in *Eucalyptus radiata* seedlings. *Plant Cell Environ.* **37**, 1598–1613 (2014).
201. Duan, H. et al. $CO_2$ and temperature effects on morphological and physiological traits affecting risk of drought-induced mortality. *Tree Physiol.* **38**, 1138–1151 (2018).
202. Zavala, J. A., Nabity, P. D. & DeLucia, E. H. An emerging understanding of mechanisms governing insect herbivory under elevated $CO_2$. *Annu. Rev. Entomol.* **58**, 79–97 (2013).
203. Kazan, K. Plant-biotic interactions under elevated $CO_2$: a molecular perspective. *Environ. Exp. Bot.* **153**, 249–261 (2018).
204. Gessler, A., Schaub, M. & McDowell, N. G. The role of nutrients in drought-induced tree mortality and recovery. *New Phytol.* **214**, 513–520 (2017).
205. Mackay, D. S. et al. Interdependence of chronic hydraulic dysfunction and canopy processes can improve integrated models of tree response to drought. *Water Resour. Res.* **51**, 6156–6176 (2015).
206. Mackay, D. S. et al. Conifers depend on established roots during drought: results from a coupled model of carbon allocation and hydraulics. *New Phytol.* **225**, 679–692 (2020).
207. Tai, X. et al. Plant hydraulic stress explained tree mortality and tree size explained beetle attack in a mixed conifer forest. *J. Geophys. Res. Biogeosci.* **124**, 3555–3568 (2019).
208. Sala, A., Piper, F. & Hoch, G. Physiological mechanisms of drought-induced tree mortality are far from being resolved. *New Phytol.* **186**, 274–281 (2010).
209. Limousin, J. M. et al. Regulation and acclimation of leaf gas exchange in a piñon–juniper woodland exposed to three different precipitation regimes. *Plant Cell Environ.* **36**, 1812–1825 (2013).
210. Sorek, Y. et al. An increase in xylem embolism resistance of grapevine leaves during the growing season is coordinated with stomatal regulation, turgor loss point and intervessel pit membranes. *New Phytol.* **229**, 1955–1969 (2021).
211. Hudson, P. J. et al. Impacts of long-term precipitation manipulation on hydraulic architecture and xylem anatomy of piñon and juniper in Southwest USA. *Plant Cell Environ.* **41**, 421–435 (2018).
212. Warren, J. M., Norby, R. J. & Wullschleger, S. D. Elevated $CO_2$ enhances leaf senescence during extreme drought in a temperate forest. *Tree Physiol.* **31**, 117–130 (2011).
213. Matusick, G. et al. Chronic historical drought legacy exacerbates tree mortality and crown dieback during acute heatwave-compounded drought. *Environ. Res. Lett.* **13**, 095002 (2018).
214. Shirley, H. L. Lethal high temperatures for conifers, and the cooling effect of transpiration. *J. Agric. Res.* **53**, 239–258 (1936).
215. Fisher, R. A. & Koven, C. D. Perspectives on the future of land surface models and the challenges of representing complex terrestrial systems. *J. Adv. Model. Earth Syst.* **12**, e2018MS001453 (2020).
216. Menzel, A., Sparks, T. H., Estrella, N. & Roy, D. B. Altered geographic and temporal variability in phenology in response to climate change. *Glob. Ecol. Biogeogr.* **15**, 498–504 (2006).
217. Keenan, T. F. et al. Net carbon uptake has increased through warming-induced changes in temperate forest phenology. *Nat. Clim. Chang.* **4**, 598–604 (2014).
218. Nakamura, T. et al. Tree hazards compounded by successive climate extremes after masting in a small endemic tree, *Distylium lepidotum*, on subtropical islands in Japan. *Glob. Change Biol* **27**, 5094–5108 (2021).
219. Hummel, I. et al. Arabidopsis plants acclimate to water deficit at low cost through changes of carbon usage: an integrated perspective using growth, metabolite, enzyme, and gene expression analysis. *Plant Physiol.* **154**, 357–372 (2010).
220. Jamieson, M. A., Trowbridge, A. M., Raffa, K. F. & Lindroth, R. L. Consequences of climate warming and altered precipitation patterns for plant-insect and multitrophic interactions. *Plant Physiol.* **160**, 1719–1727 (2012).
221. Mithöfer, A. & Boland, W. Plant defense against herbivores: chemical aspects. *Annu. Rev. Plant Biol.* **63**, 431–450 (2012).
222. Netherer, S. et al. Interactions among Norway spruce, the bark beetle *Ips typographus* and its fungal symbionts in times of drought. *J. Pest Sci.* **94**, 591–614 (2021).
223. Love, D. M. et al. Dependence of aspen stands on a subsurface water subsidy: implications for climate change impacts. *Water Resour. Res.* **55**, 1833–1848 (2019).
224. McDowell, N. G. et al. Mechanisms of a coniferous woodland persistence under drought and heat. *Environ. Res. Lett.* **14**, 045014 (2019).
225. Rozendaal, D. M. et al. Competition influences tree growth, but not mortality, across environmental gradients in Amazonia and tropical Africa. *Ecology* **101**, e03052 (2020).
226. Friedlingstein, P. et al. Uncertainties in CMIP5 climate projections due to carbon cycle feedbacks. *J. Clim.* **27**, 511–526 (2014).
227. CH2018 Project Team. CH2018 — climate scenarios for Switzerland. *NCCS* https://doi.org/10.18751/Climate/Scenarios/CH2018/1.0 (2018).
228. McMaster, G. S. & Wilhelm, W. W. Growing degree-days: one equation, two interpretations. *Agric. For. Meteorol.* **87**, 291–300 (1997).
229. McDowell, N. G. Mechanisms linking drought, hydraulics, carbon metabolism, and vegetation mortality. *Plant Physiol.* **155**, 1051–1059 (2011).



### Acknowledgements
The authors thank C. Körner for thoughtful advice, D. Basler for providing the CH2018 data on future climate projections for Switzerland and B. Roskilly, the Montgomery Laboratory and A. Castillo for feedback on figures. N.G.M. and C.X. were supported by the Department of Energy, Office of Science project Next Generation Ecosystem Experiment–Tropics (NGEE-Tropics). G.S. was supported by the NSFBII-Implementation (2021898). D.T.T. acknowledges support from the Australian Research Council (ARC) (DP0879531, DP110105102, LP0989881, LP140100232). M.G.D.K. acknowledges support from the ARC Centre of Excellence for Climate Extremes (CE170100023), the ARC Discovery Grant (DP190101823) and the NSW Research Attraction and Acceleration Program. C.G. was supported by the Swiss National Science Foundation (PZ00P3_174068). M.Mencuccini and J.M.-V. were supported by the Spanish Ministry of Science and Innovation (MICINN, CGL2017-89149-C2-1-R). A.T.T. acknowledges funding from NSF grant 2003205, the USDA National Institute of Food and Agriculture, Agriculture and Food Research Initiative Competitive Grants Program no. 2018-67012-31496 and the University of California Laboratory Fees Research Program award no. LFR-20-652467. W.M.H. was supported by the NSF GRFP (1-746055). A.M.T. and H.D.A. were supported by the NSF Division of Integrative Organismal Systems, Integrative Ecological Physiology Program (IOS-1755345, IOS-1755346). H.D.A. also received support from the USDA National Institute of Food and Agriculture (NIFA), McIntire-Stennis Project WNP00009 and Agriculture and Food Research Initiative award 2021-67013-33716. D.D.B. was supported by NSF (DEB-1550756, DEB-1824796, DEB-1925837), USGS SW Climate Adaptation Science Center (G18AC00320), USDA NIFA McIntire-Stennis ARZT 1390130-M12-222 and a Murdoch University Distinguished Visiting Scholar award. D.S.M. was supported by NSF (IOS-1444571, IOS-1547796). R.S.O. acknowledges funding from NERC-FAPESP 19/07773-1. W.R.L.A. was supported by the David and Lucille Packard Foundation, NSF grants 1714972, 1802880 and 2003017, and USDA NIFA AFRI grant no. 2018-67019-27850. R.S.O. acknowledges funding from NERC-FAPESP 19/07773-1. B.E.M. is supported by an Australian Research Council Laureate Fellowship (FL190100003). A.S. was supported by a Bullard Fellowship (Harvard University) and the University of Montana.


### Author contributions
N.G.M. led the effort to generate this manuscript. G.S. generated the figures. A.P., H.C., M.D.C., M.G.D.K. and D.S.M. conducted the modelling simulations. The authors contributed equally to the generation of ideas and writing of the article.

### Competing interests
The authors declare no competing interests.

### Peer review information
*Nature Reviews Earth and Environment* thanks Amanda Cardoso, Teresa Gimeno and Atsushi Ishida, who co-reviewed with Shin-Taro Saiki, for their contribution to the peer review of this work.

### Publisher's note
Springer Nature remains neutral with regard to jurisdictional claims in published maps and institutional affiliations.

### Supplementary information
The online version contains supplementary material available at https://doi.org/10.1038/s43017-022-00272-1.

# *Résumé détaillé en Français*

# *Introduction*

Les changements climatiques en cours modifient la température de surface et le régime des précipitations dans de nombreuses régions du monde et ont déjà des conséquences importantes sur la survie des arbres et le dépérissement des forêts (Anderegg *et al.*, 2012a).

Les forêts sont définies par l'organisation des Nations unies pour l'alimentation et l'agriculture (FAO) comme des terres occupant une superficie de plus de 0.5 hectares comportant des arbres atteignant une hauteur supérieure à 5 mètres et un couvert forestier de plus de 10%, ou présentant des arbres capables d'atteindre ces seuils *in situ*. Elles représentent 4.06 milliards d'hectares au niveau mondial, ce qui correspond à 31% de la superficie totale terrestre (FAO, 2020), et sont réparties pour plus de la moitié dans cinq pays : la Russie, le Brésil, le Canada, les Etats-Unis et la Chine.

Bien qu'en danger de déforestation, la forêt possède une **importance économique** certaine pour l'humanité. Par exemple, la France, considérée comme le quatrième pays européen le plus boisé, dénombre en Métropole environ 16.7Ma d'hectares de forêt (Antoni *et al.*, 2020) et la filière forêt-bois génère chaque année 38.8 millions de mètres cubes de bois et 26 milliards d'euros ce qui, en 2018, correspondait à 1.1% du Produit Intérieur Brut (PIB). De plus, en employant, en France, de manière directe 392 700 personnes et de manière indirecte 62 000 autres ce sont 454 700 emplois, soit 1.4% de la population active, qui dépendent directement de l'état de santé des forêts (https://fibois-france.fr/chiffres-cles/).

Outre son fort impact économique, la forêt apporte aussi à l'humanité, de nombreux **services sociaux et écosystémiques** (Ayres & Lombardero, 2000). Par exemple, au niveau mondial, ce sont 180 millions d'hectares de forêt qui sont utilisés pour les services sociaux tels que les activités récréatives, le tourisme, la formation, la recherche et la conservation des sites d'importance culturelle ou spirituelle (Allen *et al.*, 2010; FAO, 2020). Elle fournit aussi de nombreux services écosystémiques tels que la purification de l'eau *via* les bassins de drainage, la purification de l'air et la protection des sols contre l'érosion (Ayres & Lombardero, 2000). La forêt présente aussi l'avantage d'être un réservoir pour la biodiversité de la faune et de la flore. En France métropolitaine par exemple, ce sont 138 espèces d'arbres, 73 espèces de mammifères, 120 espèces d'oiseaux, 30 000 espèces de champignons et autant d'insectes qui sont retrouvés dans les forêts (https://www.onf.fr/onf/forets-et-espaces-naturels/+/1f::comprendre-la-foret.html). Enfin, la forêt est indispensable à l'équilibre climatique planétaire par ses rôles de **puits de carbone**, de production de biomasse, de maintien des sols et de régulation du climat (Reichstein *et al.*, 2013). Il est notamment estimé que, au niveau mondial, ce sont 8 milliards de tonnes de $CO_2$ qui sont absorbés chaque année, faisant ainsi de la forêt le deuxième puits de carbone de la planète derrière les océans.

Cependant, bien que jouant un rôle crucial pour le maintien de la vie sur la planète, la forêt est **en proie à de nombreux événements destructeurs** qu'ils soient anthropiques et/ou climatiques conduisant régulièrement, en plus de la déforestation, à la mort des arbres et aux dépérissements forestiers. Cela est par exemple le cas des sécheresses, définies par le Groupe d'Experts Intergouvernemental sur l'évolution du Climat comme « une absence prolongée ou une déficience marquée des précipitations » (IPCC, 2007), qui amènent à des événements de dépérissements forestiers (Hammond *et al.*, 2022). Ainsi, puisque les modèles climatiques globaux prédisent une augmentation de la fréquence, de l'intensité et de la durée de ces

événements de sécheresse (Trenberth *et al.*, 2014), une augmentation des risques de mortalité des arbres induite par la sécheresse et donc de dépérissement des forêts est attendue pour les années futures (Hosking & Hutcheson, 1988; Lwanga, 2003; Landmann & Dreyer, 2006; Keenan *et al.*, 2013; Duan *et al.*, 2014).

La mortalité des arbres induite par la sécheresse a été définie comme liée à deux processus non mutuellement exclusifs : la carence en carbone et la défaillance hydraulique (McDowell *et al.*, 2008). Cependant, de récentes observations ont démontré que **la défaillance hydraulique du xylème était un facteur omniprésent de la mort des arbres en condition de stress hydrique** (Urli *et al.*, 2013; Salmon *et al.*, 2015; Adams *et al.*, 2017). En effet, la défaillance hydraulique du xylème se produit lorsque, dans des conditions de sécheresse intenses, la demande évaporative et le taux de transpiration de l'arbre augmentent la tension de la sève du xylème et, par conséquent, le risque de formation **d'embolies** (c'est-à-dire de bulles de gaz) dans les conduits du xylème. Au fur et à mesure que le pourcentage de conduits embolisés augmente, le fonctionnement hydraulique du xylème diminue jusqu'à l'arrêt de l'écoulement de l'eau, provoquant la dessiccation des tissus et, en dernier recours, la mort de l'arbre (McDowell *et al.*, 2008, 2022). Bien que des taux de mortalité plus élevés soient observés pour des valeurs de perte de conductance hydraulique (PLC) plus importantes (Barigah *et al.*, 2013b), **les liens entre la mortalité des arbres, le fonctionnement hydraulique et les tissus vivants ne sont toujours pas élucidés**. En effet, d'un point de vue écophysiologique, la mortalité des arbres induite par la sécheresse est liée à une diminution significative du fonctionnement hydraulique des arbres alors que d'un point de vue physiologique, la résistance des arbres à la sécheresse est liée à une teneur en eau cruciale au niveau de leurs cellules et plus particulièrement au niveau de leurs cellules clés pour la croissance et la régénération : les cellules méristématiques (Mantova *et al.*, 2022). Cependant, les seuils de fonctionnement hydraulique amenant à un contenu en eau critique pour la survie de ces cellules ne sont pas encore connus.

Jusqu'à présent, les courbes de vulnérabilité à la cavitation, représentant le pourcentage de perte de conductance hydraulique (PLC) par rapport à la tension du xylème, ont été utilisées pour déterminer le potentiel hydrique au-delà duquel les plantes étaient considérées comme incapables de survivre à un épisode de sécheresse. C'est ainsi que les valeurs de $\boldsymbol{P_{50}}$ pour les conifères (Brodribb & Cochard, 2009) et de $\boldsymbol{P_{88}}$ pour les angiospermes (Urli *et al.*, 2013), c'est-à-dire les potentiels hydriques induisant respectivement 50% et 88% de perte de conductance hydraulique du xylème, ont été utilisées comme point de non-retour et donc de mort induite par la sécheresse. Cependant, l'exactitude de ces seuils a été récemment remise en question puisqu'une étude portant sur des individus de *Pinus taeda* (un conifère) a montré que certains individus présentant une PLC > 70 (Hammond *et al.*, 2019) pouvaient se remettre avec succès de l'événement de sécheresse et même produire de nouveaux tissus l'année suivante. **Ces résultats sont alors venus questionner le lien causal entre la défaillance hydraulique et la mortalité des arbres.**

Ainsi, alors même que McDowell *et al.* (2008) avaient indiqué que la mortalité des arbres en condition de défaillance hydraulique était liée à la déshydratation de leurs cellules, l'étude du lien causal entre ces deux phénomènes n'a été que peu réalisée ces dix dernières années. De même, l'étude de la chronologie des événements conduisant à la mortalité des

individus est restée incertaine. Ainsi, dans un *Opinion paper* publié dans *Trends in Plant Science* au début de l'année 2022, **l'importance de l'étude du lien causal entre la défaillance hydraulique du xylème et la mort des arbres en appuyant sur la nécessité d'apporter des preuves fondamentales de ce lien mécaniste afin de définir des seuils physiologiques clés et d'améliorer notre capacité à prévoir les événements de mortalité** (Mantova *et al.*, 2022) a été mise en lumière. Ainsi, en se concentrant sur l'importance du contenu en eau des cellules dans le maintien de leur intégrité et en démontrant comment les cellules méristématiques sont impliquées dans le rétablissement des arbres après une sécheresse, un focus a été réalisé sur la nécessité d'étudier leur état d'hydratation en lien avec leur vitalité afin de mieux comprendre comment la défaillance hydraulique pouvait conduire à la mort des arbres.

Dès lors, bien que le lien entre la mortalité des arbres et la défaillance hydraulique du xylème soit clair et ait été largement évalué, le lien entre la mortalité des arbres et la survie des tissus vivants reste mal compris. Par exemple, le lien entre la teneur en eau des cellules vivantes, diminué lors d'un stress hydrique, et la mort cellulaire n'est pas clair et ceci est particulièrement vrai pour les cellules des méristèmes.

Par conséquent, d'un point de vue écophysiologique et physiologique, cette thèse présente trois objectifs principaux :

- Premièrement, elle cherchera à identifier les traits physiologiques clés qui pourraient déterminer la capacité des arbres à se remettre de la sécheresse.
- Secondement, elle cherchera à évaluer le lien mécaniste entre la défaillance hydraulique du xylème et la mortalité cellulaire en aval.
- Finalement, elle cherchera à déterminer les principaux changements se produisant au niveau des tissus végétaux et, en particulier au niveau d'un tissus méristématique, le cambium, expliquant le manque de récupération après une sécheresse.

Pour atteindre ces objectifs, le travail de thèse sera divisé en trois expériences différentes :

- Premièrement, en travaillant au niveau de la tige, il cherchera à **déterminer les traits physiologiques clés qui pourraient expliquer la capacité des arbres à se remettre de la sécheresse.** Ainsi, en prenant en considération le cadre théorique de la mortalité végétale proposé par Guadagno *et al.* (2017), il a été décidé de travailler principalement sur la combinaison de deux traits physiologiques : le **contenu en eau relatif** (RWC) et les **dommages aux membranes cellulaires**.
- Secondement, après avoir démontré que l'interaction entre la défaillance hydraulique et la vitalité cellulaire pourrait expliquer la capacité des arbres à se remettre de la sécheresse, **le lien mécaniste et plus particulièrement la chronologie des événements menant de la défaillance hydraulique du xylème à la mortalité cellulaire au niveau d'un organe facilement accessible : la feuille, seront évalués**.
- Enfin, en extrapolant les résultats obtenus au niveau de la feuille sur la tige, **la perte d'eau causée par l'embolisation des vaisseaux du xylème et ses conséquences sur la capacité des arbres à récupérer ou non d'une sécheresse** sera évaluée. Pour cela, en considérant les résultats obtenus au Chapitre 1 et le postulat émis dans l'*Opinion paper* signé par Mantova *et al.* (2022) et présenté précédemment, les mêmes méthodes

(mesure du contenu en eau relatif et du niveau de défaillance membranaire) seront réappliquées à une expérience comprenant un plus grand nombre d'individus. Enfin, une tentative d'explication de la capacité de survie des arbres en condition de sécheresse sera aussi effectuée en concentrant les efforts de recherche sur **l'évaluation de l'intégrité de cellules méristématiques** spécifiques : les cellules cambiales.

# *Chapitre 1.*
# L'interaction entre la défaillance hydraulique et la vitalité cellulaire explique la capacité des arbres à se remettre de la sécheresse

### *Contexte et objectifs*

Partant du postulat présenté par McDowell *et al.* (2008) indiquant que la mortalité des arbres en condition de sécheresse impliquant une défaillance hydraulique du xylème était liée à la déshydratation de leurs cellules, ce premier chapitre de thèse a cherché à identifier les traits physiologiques clés déterminant la capacité des arbres à se remettre de la sécheresse.

### *Matériel et méthodes*

Des individus de *Pseudotsuga menziesii* M., un conifère connu sous le nom vernaculaire de Douglas, et de *Prunus lusitanica* L., une angiosperme, autrement nommé Laurier du Portugal, ont été utilisés pour cette expérimentation. Leurs courbes de vulnérabilité à la cavitation ont été établies en amont de l'événement de sécheresse sur cinq individus bien hydratés en utilisant la méthode du Cavitron (Cochard, 2002a) pour *P. menziesii* et sur cinq individus subissant une déshydratation sur paillasse et par suivi de la propagation de l'embolie à l'aide de la méthode optique (Brodribb *et al.*, 2016) pour *P. lusitanica*. Ensuite, 8 arbres de chaque espèce ont été exposés à un phénomène de sécheresse par rétention de leur arrosage puis réhydratés lorsqu'ils présentaient un potentiel hydrique induisant des niveaux de PLC importants. Au cours de l'expérimentation de déshydratation et réhydratation, les variations du diamètre des troncs de chaque arbre ont été enregistrées à l'aide de dendromètres (LVDT). Immédiatement avant la réhydratation, la PLC des tiges a été estimée à l'aide d'un microtomographe à rayons X pour *P. menziesii* (Cochard *et al.*, 2015) et à l'aide du Xyl'EM pour *P. lusitanica* (Cochard, 2002b). La vitalité des cellules des tiges a, quant-à-elle, été estimée avant la réhydratation à l'aide de deux méthodes utilisées simultanément chez les deux espèces. Ainsi, la méthode de fuite d'électrolytes (EL), témoignant de l'intégrité de la membrane plasmique et fonctionnant comme un proxy de la mortalité des cellules (Guadagno *et al.*, 2017), a permis d'obtenir le pourcentage de cellules mortes d'un échantillon alors qu'une détection des cellules vivantes à l'aide d'un fluorochrome, la fluorescéine diacétate (FDA), a permis l'estimation du pourcentage de cellules vivantes de l'écorce et la localisation de ces cellules au sein de l'échantillon. Enfin, le contenu en eau relatif des feuilles ($RWC_{Leaf}$) et des tiges ($RWC_{Stem}$) a également été mesuré avant le ré-arrosage.

### *Résultats et discussion*

**Les résultats ont montré que les seuils basés sur la PLC (c'est-à-dire 50% pour les conifères et 88% pour les angiospermes) utilisés en modélisation (Brodribb *et al.*, 2020; Lemaire *et al.*, 2021) pour estimer la récupération des arbres après un événement de sécheresse ne donnaient pas un aperçu assez précis de la capacité des arbres à survivre à cet événement**. En effet, cette étude a démontré que des arbres présentant une PLC de 68% pour les conifères, c'est-à-dire largement au-dessus du seuil de mortalité de 50%, et de 99% pour les

angiospermes, c'est-à-dire au-dessus du seuil de mortalité de 88%, pouvaient récupérer de l'événement de sécheresse puisqu'ils montraient une ré-augmentation du diamètre de leur tige après ré-arrosage (Lamacque *et al.* 2020). De plus, dans le cas de *P. lusitanica,* les individus survivant à l'événement de sécheresse pouvaient produire de nouvelles feuilles une fois que la contrainte de stress hydrique était supprimée. Ainsi, les résultats obtenus dans ce chapitre sont d'abord venus confirmer les résultats obtenus par Hammond *et al.* (2019) pour les conifères et ont représenté une nouveauté pour les angiospermes. De plus, ils ont confirmé la technique d'identification de mortalité des plantes basée sur l'utilisation de dendromètres élaborée par Lamacque *et al.* (2020).

Dans la recherche de traits physiologiques clés pouvant expliquer la survie des arbres après un stress hydrique, les résultats de ce chapitre ont montré que, **pour les conifères, le niveau de RWC au niveau de la tige ($RWC_{Stem}$) et le pourcentage de cellules vivantes de la tige (EL) étaient directement liés à la capacité des arbres à récupérer de l'événement de sécheresse.** En effet, les résultats ont montré, en ce qui concerne l'intégrité cellulaire, que les arbres récupérant après une sécheresse avaient tendance à présenter des dommages cellulaires plus faibles que les arbres morts avant la remise en eau. En effet, les arbres de *P. menziesii* qui se rétablissaient ne montraient aucun changement dans leur pourcentage de cellules mortes et ce même après l'épisode de sécheresse. Les arbres morts, au contraire, présentaient constamment des valeurs de mort cellulaire plus élevées avant le ré arrosage. Bien que les différences entre les individus récupérant ou mourant de la sécheresse étaient beaucoup plus subtiles chez les angiospermes que chez les conifères, une tendance similaire à celle des conifères a été observée. En effet, même si chez ***P. lusitanica***, les arbres mourant de la sécheresse et les arbres récupérant de l'événement ne présentaient pas de différences en termes d'EL, **les arbres survivants ont été capables de produire de nouvelles tiges et de générer de nouvelles feuilles lorsque le stress a été atténué, témoignant ainsi d'un maintien de l'intégrité de leurs cellules et plus particulièrement de leurs cellules méristématiques.** Ainsi, alors que des valeurs de mort cellulaire plus élevées sont les conséquences d'une défaillance membranaire et sont associées à la mort cellulaire (Vilagrosa *et al.*, 2010; Guadagno *et al.*, 2017), les observations réalisées chez *P. lusitanica* suggèrent que la défaillance fatale à l'échelle cellulaire ne se produit pas de manière homogène dans la tige et que, comme l'ont montré Thomas (2013) et Klimešová *et al.* (2015), la repousse de la plante peut s'effectuer si le stress est atténué et si certaines cellules sont encore en vie.

### *Conclusion*

En combinant des mesures du pourcentage de cellules vivantes avec un suivi du diamètre du tronc à l'aide de dendromètres et des mesures de PLC, cette étude a montré que **les seuils connus de récupération et de mortalité considérés jusqu'à présent, c'est-à-dire la $P_{50}$ pour les conifères et la $P_{88}$ pour les angiospermes, n'étaient pas assez précis pour évaluer et prédire la mortalité des arbres induite par la sécheresse**. Même si le lien entre un niveau élevé de PLC de la tige et la mortalité des arbres reste clair à l'issue de ce chapitre, il reste urgent de définir de nouveaux seuils physiologiques pour prédire la mortalité des arbres avec des modèles mécanistes. Pour les conifères, des valeurs $RWC_{Stem}$ plus élevées et des valeurs EL plus faibles apparaissent comme liées à une plus grande capacité de survie à la sécheresse. Cependant, bien qu'une tendance similaire à celle observée pour les conifères ait été identifiée

chez les angiospermes, aucun trait physiologique n'a pu être formellement identifié comme un proxy potentiel de la capacité des arbres à se rétablir.

Ainsi, bien qu'ayant permis d'identifier, en partie, des traits physiologiques importants pour la survie des arbres en condition de sécheresse, ce chapitre n'a pas réussi à élucider le lien ou la chronologie des événements menant de l'événement de sécheresse à la perte de conductance hydraulique du xylème et à la mort cellulaire. C'est donc ce lien qui sera plus particulièrement étudié au cours du chapitre suivant.

# *Chapitre 2.* Sur le chemin de la défaillance hydraulique à la mort cellulaire

### *Contexte et objectifs*

La défaillance hydraulique du xylème a été identifiée comme un facteur omniprésent dans le déclenchement de la mortalité des arbres induite par la sécheresse au travers des dommages provoqués par la déshydratation progressive des cellules vivantes de la plante McDowell *et al.* (2008, 2022). Le chapitre précédent a mis en évidence que le niveau de vitalité cellulaire au moment de la réhydratation jouait un rôle dans la survie des arbres, particulièrement celle des conifères, après un événement de sécheresse. Cependant, **les preuves fondamentales du lien mécaniste reliant la défaillance hydraulique du xylème à la mort cellulaire n'ont pas encore été identifiées.** En effet, seule une étude récente intégrant la défaillance hydraulique et la mortalité cellulaire a montré que la défaillance du réseau vasculaire dans les feuilles conduisait à la mort des tissus reliés (Brodribb *et al.*, 2021). Ainsi, même si Brodribb *et al.* (2021) ont mis en évidence une base mécaniste solide reliant la défaillance du réseau du xylème et la mort des tissus des feuilles, **le niveau de défaillance hydraulique auquel la mort cellulaire se produit et la façon dont ce niveau varie selon les espèces restent inconnus.** De plus, la chronologie des événements, c'est-à-dire, si les cellules commencent à mourir dès le début de la cavitation du xylème ou s'il existe un délai avant de rencontrer des dommages cellulaires, reste, elle aussi, inconnue.

Cependant, il est admis que le dysfonctionnement du système de transport de l'eau (c'est-à-dire le xylème) provoque une réduction significative de la quantité d'eau fournie aux tissus vivants des arbres et, par conséquent, de la teneur en eau de tous les tissus vivants indépendamment de leur fonction (Kursar *et al.*, 2009). Dès lors, une diminution du contenu relatif en eau (RWC) au niveau des organes provoquerait un stress hydrique au niveau des cellules entrainant la perturbation de la stabilité de la membrane plasmique et conduisant donc à la mort cellulaire (Wang *et al.*, 2008; Chaturvedi *et al.*, 2014; Guadagno *et al.*, 2017). Ainsi, **une combinaison du RWC et du niveau de dommages de la membrane plasmique apparait comme pertinente pour prédire la mortalité des arbres** (Mantova *et al.*, 2021, 2022) **et élucider le lien mécaniste entre la défaillance hydraulique et la mort des cellules.**

Une étude récente a montré qu'après la cavitation de leurs vaisseaux, les feuilles présentaient à la fois un changement de leur couleur et une augmentation de leur taux de rétrécissement en raison de la déshydratation rapide du mésophylle en aval (Brodribb *et al.*, 2021). Ces changements de couleur des feuilles ont été attribués à la perte de turgescence et à l'effondrement des cellules palissadiques qui diminuent la distance entre les cellules, réduisant ainsi la transmission de la lumière (Brodribb *et al.*, 2021). Cependant, même si la déshydratation du mésophylle devrait logiquement être associée à des changements structurels se produisant au niveau du tissu foliaire et pourrait également être responsable de la mort cellulaire (Mantova *et al.*, 2022), il n'a pas encore été décrit si la mortalité cellulaire était une conséquence de la cavitation cellulaire (Rajashekar & Lafta, 1996; Sakes *et al.*, 2016) ou de l'effondrement de la paroi de la cellule provoquant la cytorrhyse de celle-ci (Oertli, 1986).

Ainsi, considérant le besoin actuel de comprendre les processus sous-jacents reliant la défaillance hydraulique, la mort des cellules, et la mortalité des arbres (Mantova *et al.*, 2022), les principaux objectifs de cette étude étaient :

(i) d'évaluer si l'altération du transport de l'eau par la cavitation était le facteur déclenchant de la mort cellulaire dans des conditions de sécheresse
(ii) d'étudier si la relation entre l'apparition de la cavitation et la mort cellulaire variait selon les espèces ayant des résistances contrastées à la sécheresse et,
(iii) d'identifier un seuil de RWC induisant des dommages aux cellules végétales lors d'un stress hydrique.

### *Matériel et méthodes*

Pour parvenir aux objectifs présentés précédemment, un organe facilement accessible, la feuille, a été étudié. Ainsi, trois espèces différentes et présentant une résistance contrastée à la cavitation ont été étudiées : *Eucalyptus viminalis*, *Laurus nobilis* et *Populus tremula x alba*.

Sept à 11 individus de chaque espèce ont été exposés à des conditions de sécheresse sévère sur paillasse en laboratoire. Les courbes de vulnérabilité à la cavitation de chaque espèce ont été construites sur deux feuilles par arbre, à l'aide de la méthode optique (Brodribb *et al.* 2016). L'utilisation de cette méthode optique a aussi permis de suivre la propagation de l'embolie dans les vaisseaux des feuilles tout au long de l'expérimentation.

De manière concomitante à la déshydratation et à la propagation de l'embolie, le statut hydrique des feuilles a été établi régulièrement *via* des mesures de potentiel hydrique foliaire ($\Psi_{Leaf}$) et de leur contenu en eau relatif ($RWC_{Leaf}$). De plus, en association avec les mesures de statut hydrique, la vitalité des cellules des feuilles a été établie en utilisant l'approche de la fuite d'électrolytes (EL) démontrée comme prometteuse dans le premier chapitre de cette thèse.

Enfin, des scans des feuilles ont été réalisés à l'aide d'un microtomographe à rayons X, localisé au Synchrotron SOLEIL, à Paris, afin de visualiser anatomiquement les conséquences d'une diminution de l'apport en eau sur les différents tissus foliaires et ainsi de déchiffrer la séquence des événements conduisant à la mort cellulaire.

### *Résultats et discussion*

*Les vaisseaux s'embolisent en premier, ensuite meurent les cellules*

Les résultats ont montré que, lors de la déshydratation progressive des arbres, la cavitation du xylème précède la mort cellulaire au niveau des feuilles. En effet, le début des dommages induits par la déshydratation des cellules se produit à des valeurs de $RWC_{Leaf}$ plus faibles ($RWC_{crit}$,) que celles auxquelles se produit le début de la cavitation du xylème ($RWC_{12}$). Ainsi, **les résultats obtenus ont montré qu'en compromettant l'apport d'eau au mésophylle de la feuille, la cavitation provoque une diminution du $RWC_{Leaf}$ qui est suivie d'une augmentation des dommages cellulaires.** Ces résultats sont en accord avec une étude récente sur des mutants de tomate montrant que la cavitation des nervures de la feuille compromet immédiatement l'approvisionnement en eau local du mésophylle de celle-ci, entraînant la mort des tissus (Brodribb *et al.*, 2021).

De plus, les résultats ont montré que **le niveau d'hydratation critique induisant des dommages cellulaires ($RWC_{crit}$), se produisait à des niveaux d'embolie variables selon l'espèce** (environ 30% pour *P. tremula x alba* et *L. nobilis*, et environ 58% pour *E. viminalis*). Ainsi, les résultats suggèrent que de faibles niveaux d'embolie n'ont pas d'effet immédiat sur le nombre de cellules vivantes et ce probablement en raison d'une tolérance à la perturbation hydraulique fournie par la redondance vasculaire des feuilles (Sack *et al.*, 2008).

*Des espèces différentes ont-elles des dynamiques de mortalité cellulaire différentes ?*

Au cours de la déshydratation, les feuilles ont d'abord rencontré une perte de pression de turgescence au niveau de leur cellules qui a ensuite été suivie d'une cavitation progressive des vaisseaux du xylème de la feuille qui a précédé l'apparition des premiers dommages structurels au niveau des cellules. Les valeurs de $RWC_{Leaf}$ auxquelles les trois processus précédents se sont produits et les différences entre elles pourraient varier d'une espèce à l'autre en fonction de leur résistance à la sécheresse. Cette séquence d'événements est cohérente avec les résultats de Creek *et al.* (2020) où la fermeture stomatique, qui se produit généralement à des valeurs de potentiel hydrique similaires à celles du point de perte de turgescence (Brodribb *et al.*, 2003; Bartlett *et al.*, 2016; Trueba *et al.*, 2019), a précédé la cavitation du xylème, et avec ceux de Guadagno *et al.*, (2017) où les dommages cellulaires se sont produits après la perte de turgescence des cellules. Ainsi, dans cette étude, **le $RWC_{crit}$ semble varier avec la résistance à la cavitation des espèces.** En effet, les espèces les plus résistantes montrent des cellules plus tolérantes à la déshydratation, c'est-à-dire présentant des dommages induits par la déshydratation à des valeurs $RWC_{Leaf}$ plus faibles. Dès lors, ces résultats soulignent que, bien que le contenu en eau relatif au point de perte de turgescence ($RWC_{TLP}$) soit relativement constant entre les espèces (Bartlett *et al.*, 2012), **le $RWC_{crit}$ pour les dommages cellulaires pourrait dépendre de l'espèce et varier avec la résistance à la cavitation**. Cette dépendance pourrait être liée à la structure et à la composition des cellules elles-mêmes et à leur capacité à répondre aux changements de turgescence en relâchant ou en resserrant la paroi cellulaire (Moore *et al.*, 2008), empêchant ainsi la déformation et le rétrécissement des cellules jusqu'à un niveau létal (Scoffoni *et al.*, 2014), et la mort par cytorrhyse, c'est-à-dire lorsque la cellule se rétrécit en tant qu'unité (Oertli, 1986; Taiz & Zeiger, 2006).

*Un regard plus attentif sur la séquence des dommages cellulaires*

Les changements de transmittance de la lumière et de la couleur des feuilles ont été attribués à l'effondrement des cellules palissadiques, servant ainsi de proxy pour déterminer la mortalité des cellules de la feuille (Brodribb *et al.*, 2021). **En fournissant une quantification de la mort cellulaire grâce aux mesures de EL, les résultats de ce chapitre confirment l'hypothèse d'une corrélation entre une diminution du $RWC_{Leaf}$ et de la transmittance de la lumière avec la mort cellulaire faite par Brodribb *et al.* (2021).** Cependant, en effectuant des mesures au niveau des différentes couches cellulaires de la feuille, l'étude menée dans ce chapitre fournit une analyse plus détaillée de la localisation des changements structurels qui se produisent pendant la déshydratation. Ainsi, ces résultats montrent que le rétrécissement cellulaire observé dans cette expérience n'est pas toujours associé à la mort cellulaire. En effet, selon les espèces, les cellules du mésophylle peuvent subir une réduction de leur volume différente avant de présenter une augmentation des dommages cellulaires. Par exemple, les

cellules du mésophylle de *P. tremula x alba* et de *E. viminalis* ont pu supporter une importante réduction de volume au début de la déshydratation sans que celle-ci ne soit associée à une mortalité cellulaire. Cependant, pour *L. nobilis*, une telle réduction du volume des cellules du mésophylle a été immédiatement corrélée à une augmentation de la mortalité cellulaire.

De plus, en examinant de plus près la séquence des événements, il est à noter que les cellules du parenchyme palissadique, du parenchyme lacuneux et de l'épiderme réagissent différemment à la déshydratation. Dans le cas de *P. tremula x alba* et de *L. nobilis*, les cellules du parenchyme palissadique ont été les premières affectées par la déshydratation, alors qu'il n'y avait pas de différences temporelles au niveau de la réduction du volume cellulaire du parenchyme lacuneux et du parenchyme palissadique chez *E. viminalis*.

Pour les trois espèces, **les cellules de l'épiderme ont été les dernières affectées par la sécheresse.** Ces différences de réponse aux changements de volume des cellules pourraient être liées à la taille, à la structure et à la composition des cellules en tant que telles, puisque ces composantes pourraient influencer la rigidité de la paroi cellulaire et ainsi favoriser ou empêcher le rétrécissement jusqu'à un niveau létal (Scoffoni *et al.*, 2014; Joardder *et al.*, 2015).

### *Conclusion*

En évaluant la variation de $RWC_{Leaf}$, EL et le niveau d'embolie dans les feuilles d'arbres exposés à une déshydratation progressive, les résultats de ce chapitre fournissent la preuve que **la défaillance hydraulique du xylème précède l'apparition de la mortalité cellulaire.** De plus, ils permettent de décrire **une valeur critique de contenu en eau ($RWC_{crit}$)**, un seuil de déshydratation important, en dessous duquel les cellules vivantes commencent à subir des dommages dus à la sécheresse, et qui correspond à un certain degré d'apparition de l'embolie. Cette valeur critique de RWC **varie selon les espèces** et en fonction de la résistance à la cavitation.

Malgré des analyses en microtomographie à rayons X montrant une corrélation claire entre les changements structurels des cellules et la mortalité au niveau du mésophylle au cours de la déshydratation, il n'a pas été possible de déterminer si les cellules mouraient à cause de la cavitation cellulaire ou de la cytorrhyse. Ainsi, d'autres techniques de microscopie seraient nécessaires pour élucider ces phénomènes. Cette approche représente donc une première étape dans le décryptage de la façon dont le dysfonctionnement hydraulique pourrait induire des dommages aux tissus vivants clés comme, par exemple, les méristèmes, et ainsi déterminer finalement le point de mort des arbres dans des conditions de sécheresse.

# *Chapitre 3.* De la mort cellulaire à la mort de l'arbre, quand les méristèmes ont de l'importance

### *Contexte et objectifs*

Pour mieux comprendre et prédire les bases physiologiques de la mortalité des arbres en condition de sécheresse, les deux premiers chapitres de ce travail de thèse se sont attachés à décrire la relation entre une perte de conductance hydraulique et la mortalité de la plante ou de l'organe. Cependant, si le Chapitre 1 a identifié quelques traits physiologiques clés qui pourraient fonctionner comme proxy pour identifier la mortalité des arbres, il n'a pas démontré explicitement le lien entre la perte de conductance hydraulique et la mortalité. C'est ce lien qui a été explicitement étudié au cours du Chapitre 2. En effet, il a été démontré que les dommages cellulaires au niveau des feuilles se produisaient systématiquement après que des niveaux élevés d'embolie aient été rencontrés et une fois que la teneur en eau des tissus et des cellules ait baissée sous une valeur critique qui variait selon les espèces et avec la résistance des arbres à la cavitation. Pris ensemble, les résultats des Chapitres 1 et 2 ont permis de progresser dans l'élucidation des bases physiologiques de la mortalité en conditions de sécheresse. **Cependant, ils n'ont pas démontré explicitement le lien de causalité entre la défaillance hydraulique et la mortalité des arbres**.

Dès lors, considérant l'hypothèse centrale de l'*Opinion paper* présentée au début de cette thèse, **le lien causal entre la cavitation du xylème et la mortalité des arbres devrait résider autour de l'intégrité méristématique.** En effet, du point de vue de la relation plante-eau, la mort de l'arbre devrait survenir lorsqu'un arbre n'est plus en mesure de maintenir ses fonctions physiologiques clés (par exemple, la croissance et/ou la reproduction). Ainsi, si une perte importante du fonctionnement hydraulique peut entraver l'intégrité des cellules méristématiques, les arbres ne devraient pas être en mesure de survivre à l'épisode de sécheresse, et ce, quel que soit le niveau de mort cellulaire ou du niveau d'eau restant dans les tissus de leur tige au moment de la remise en eau. Par conséquent, puisque seulement quelques études centrées sur les feuilles, ont essayé de démontrer le lien causal entre la défaillance hydraulique, une diminution du contenu en eau, et la mortalité des tissus (Brodribb *et al.* 2021, *voir aussi.* Chapitre 2), **le but principal de ce chapitre était de déterminer les changements principaux se produisant au niveau des tissus végétaux, et particulièrement au niveau des cellules méristématiques cambiales, expliquant le manque de récupération après un événement de sécheresse.** Ainsi, compte tenu de la nécessité actuelle de comprendre les processus sous-jacents reliant la défaillance hydraulique et la mortalité des arbres, et de l'urgence d'identifier des seuils mécanistes, intégratifs, évolutifs et faciles à mesurer et à contrôler pour prédire la mortalité des arbres (Martinez-Vilalta *et al.*, 2019), les principaux objectifs de cette étude étaient de :

(i) tester l'hypothèse selon laquelle la mortalité des arbres serait liée à la désintégration des méristèmes,

(ii) évaluer si l'altération de l'approvisionnement en eau causée par la cavitation du xylème est le facteur déclenchant de la mortalité des méristèmes et
(iii) identifier de nouveaux seuils physiologiques permettant la prédiction de la mortalité des arbres due à la sécheresse.

### *Matériel et méthodes*

Pour parvenir à ces objectifs, un ensemble d'arbres d'*Abies concolor* (Gordon & Glend) Lindl. Ex Hildebr) (Sapin du Colorado) et de *Fagus sylvatica* L. (Hêtre commun) (60 arbres par espèce), c'est-à-dire une espèce de conifère et une espèce d'angiosperme, a été utilisé.

Cinq arbres par espèce ont servi à établir la courbe de vulnérabilité à la cavitation des tiges à l'aide de la méthode du Cavitron (Cochard, 2002a).

Parmi les 55 arbres restants, 5 ont servi de témoins tout au long de l'expérience et 50 ont été exposés à des conditions de sécheresse sévère par rétention de leur irrigation et laissés à déshydrater jusqu'à l'induction de niveaux de PLC allant de 30% à 100% pour les conifères et de 70% à 100% pour les angiospermes. À ces niveaux de PLC, les arbres ont été réhydratés pour vérifier leur capacité à récupérer de la sécheresse.

Le pourcentage de perte de diamètre de la tige (PLD) (Lamacque *et al.*, 2020), la teneur en eau relative de la tige ($RWC_{Stem}$) et les dommages à la membrane plasmique prédits par la méthode de fuite des électrolytes (EL) (Guadagno *et al.*, 2017; Mantova *et al.*, 2021 - Chapitre 2) sont apparus ces dernières années comme de nouveaux traits physiologiques permettant de mieux identifier et prédire la mortalité des arbres. Ainsi, les variations de diamètre des tiges, le potentiel hydrique (Ψ), la perte de conductance hydraulique (PLC), les changements de RWC et la vitalité des cellules (EL) au niveau de la tige ont été surveillés pendant les phases de déshydratation et de récupération.

Enfin, des **prélèvements de cambium** ont été effectués et observés à l'aide d'un **microscope électronique à transmission** (MET) (Li & Jansen, 2017) afin de déterminer l'intégrité des cellules cambiales au moment de la réhydratation.

### *Résultats et discussion*

Malgré une bonne corrélation entre la capacité de récupération, le niveau de contenu en eau et la probabilité de survie pour les deux espèces, **aucun des indicateurs suivis au cours de l'expérience n'a pu identifier exactement le moment où les arbres sont morts de la sécheresse et donc fonctionner comme une réponse binaire lorsqu'implémenté dans un modèle mécaniste.** Cependant, cette expérience a montré que la principale différence entre deux arbres présentant sensiblement les mêmes valeurs de traits physiologiques (c'est-à-dire les mêmes PLC, RWC, Ψ, EL et PLD) résiderait dans l'intégrité des cellules cambiales. En effet, pour les deux espèces, les arbres ayant pu se remettre de la sécheresse, survivre et recroître l'année suivante, présentaient des cellules cambiales qui témoignaient encore de la présence de vacuoles, indiquant donc en certain état d'hydratation et leur capacité à maintenir la turgescence, tandis que les arbres qui ne survivaient pas à la sécheresse présentaient des cellules cambiales désintégrées avec un protoplaste rétréci et un effondrement du cytoplasme.

Ces résultats rencontrés dans ce chapitre étaient en accord avec ceux fournis par Li et Jansen (2017) où les plantes qui avaient été stressées au-delà de leur niveau létal montraient, dans leurs cellules cambiales racinaires, une désintégration non réversible. Ainsi, c**es résultats apportent un soutien empirique à l'*opinion paper* écrit par Mantova *et al.* (2022) et au cadre théorique de la mortalité des arbres induite par sécheresse proposé par McDowell *et al.* (2022)** qui suggèrent que le lien de causalité entre la défaillance hydraulique et la mortalité des arbres résiderait au niveau de la désintégration des cellules méristématiques empêchant une nouvelle croissance et/ou une repousse l'année suivante et causant finalement la mort des individus.

Cependant, bien que les résultats de ce chapitre mettent en lumière l'importance des méristèmes dans l'évaluation de la mortalité des arbres, **ils ne permettent pas d'évaluer précisément la relation entre la perte de conductance hydraulique au niveau du xylème et la mortalité des méristèmes.** En effet, même si la défaillance hydraulique devrait provoquer la mort des cellules méristématiques en perturbant leur alimentation en eau (Mantova *et al.*, 2022), **les résultats obtenus au cours de cette expérience montrent que des arbres présentant un niveau similaire de dysfonctionnement hydraulique peuvent présenter différents niveaux de désintégration des cellules cambiales et donc des réponses très différentes une fois la contrainte de stress hydrique levée.** Ainsi, la séquence des événements qui conduit les cellules cambiales à leur mort reste inconnue et il n'est toujours pas établi que la perte d'intégrité des cellules cambiales soit principalement liée au niveau de PLC ou à la capacité ou l'incapacité de l'arbre à mobiliser l'eau et à protéger ces cellules cruciales pour leur survie.

### *Conclusion*

En exposant les arbres à des conditions de sécheresse extrême et en évaluant la dynamique de la déshydratation de la tige, la PLC, les dommages cellulaires au niveau de la tige et du cambium, **les résultats de ce dernier chapitre fournissent la preuve que la mortalité des arbres est causée par la perte d'intégrité des cellules méristématiques.** En effet, plusieurs arbres présentant des valeurs similaires pour les différents traits physiologiques mesurés avant réhydratation ne différaient que par le niveau de désintégration cellulaire de leur cambium. Cependant, bien que les résultats mettent en évidence l'importance des méristèmes dans l'évaluation de la mort des arbres, ils ne permettent pas d'évaluer précisément la relation entre la perte de conductance hydraulique au niveau du xylème et la mortalité des méristèmes. En effet, même si les résultats montrent que la défaillance hydraulique reste un marqueur fort du dysfonctionnement de l'arbre pendant la sécheresse, des arbres présentant des niveaux de PLC similaires pourraient présenter une intégrité ultrastructurelle très différente au niveau de leurs cellules cambiales. Par conséquent, en se concentrant sur la relocalisation de l'eau, et en particulier sur la relocalisation de l'eau vers les cellules du cambium au cours d'un épisode de sécheresse, il semblerait possible de déterminer si l'altération du transport de l'eau provoquée par la cavitation des vaisseaux du xylème est directement le facteur déclenchant de la mortalité des méristèmes ou si l'épuisement des réservoirs d'eau résultant d'une diminution de l'approvisionnement en eau causée par la cavitation provoquerait la mortalité des méristèmes et donc la mort de l'arbre.

Enfin, après évaluation des multiples traits suivis au cours de cette expérience par une analyse en composantes principales, il semble qu'une combinaison de niveaux élevés de $RWC_{Stem}$ et de la capacité de récupération des tiges après réhydratation puisse principalement être corrélée à la survie des arbres à long terme, et ce, pour les deux espèces. Bien que ces deux caractéristiques puissent aider à déterminer une probabilité de survie pour les angiospermes et les conifères après un épisode de sécheresse, aucune d'entre elles n'agirait comme un paramètre binaire permettant de prédire exactement la mort des arbres. Cependant, ceci pourrait être le cas de l'intégrité cellulaire cambiale où les arbres présentant principalement des cellules cambiales désintégrées ne sont pas capables de survivre à l'événement de sécheresse.

# Discussion générale

## *Contribution de l'étude dans la compréhension des mécanismes de mortalité des arbres en condition de sécheresse*

*La défaillance hydraulique provoque la mort des cellules*

Bien que la défaillance hydraulique eût été identifiée comme un facteur omniprésent de la mort des arbres et que McDowell *et al.* (2008) eurent proposé une hypothèse selon laquelle cette défaillance hydraulique mènerait à la mortalité des arbres en conduisant à la déshydratation complète et à la mort cellulaire, le lien mécaniste entre la défaillance hydraulique et la mort des cellules n'avait que très faiblement était étudié auparavant. En effet, seule une étude de Brodribb *et al.* (2021) avait montré, au niveau très local dans une feuille, comment la cavitation d'un vaisseau du xylème conduisait à une perte de fluorescence des cellules qui lui étaient raccordées. **Ainsi, en étudiant précisément la chronologie d'apparition des différents événements de cavitation et de mortalité cellulaire, tout d'abord au niveau de la feuille, puis au niveau de la tige, les études présentées dans cette thèse ont montré que la défaillance hydraulique était bien un précurseur de la mortalité des cellules et donc, *in fine*, de l'organe venant ainsi confirmer les observations de Brodribb *et al.* (2021).**

*La mortalité cellulaire arrive à des niveaux de contenus en eau variables entre espèces*

En se basant sur l'étude du contenu en eau relatif qui présente l'avantage d'être une métrique qui reflète directement l'état de déshydratation des tissus (Barrs & Weatherley, 1962; Martinez-Vilalta *et al.*, 2019), ces études ont mis en évidence un paramètre appelé le $RWC_{crit}$ correspondant au contenu en eau relatif critique en dessous duquel la mortalité cellulaire augmente de façon significative. Ainsi, la détermination de ce $RWC_{crit}$ réalisée à la fois au niveau des feuilles et au niveau des tiges a montré que **le $RWC_{crit}$ variait entre les espèces.** Elles ont aussi montré, sur les premières espèces étudiées, que les espèces les plus vulnérables à la cavitation du xylème présenteraient aussi des cellules plus vulnérables à la déshydratation, c'est-à-dire présentant un $RWC_{crit}$ plus élevé que les autres. Comme discuté auparavant ceci pourrait être dû aux propriétés anatomiques de leurs cellules et nous pouvons émettre l'hypothèse que des espèces présentant un xylème plus résistant à la cavitation présenterait aussi des cellules moins vulnérables à la déshydratation. En effet, il a été démontré que la plus grande résistance du xylème à la cavitation était probablement due à un plus grand renforcement des parois de leur vaisseaux (Hacke *et al.*, 2001; Cochard *et al.*, 2008). Ainsi, par extension, il serait donc probable que les cellules de leurs différents parenchymes puissent présenter des parois plus épaisses empêchant leur déformation et/ou une composition différente, les rendant donc moins vulnérables à la déshydratation du fait d'une meilleure résistance à la cytorrhyse (Oertli, 1986) ou à la cavitation cellulaire (Llorens *et al.*, 2016; Sakes *et al.*, 2016).

De manière plus surprenante, le travail de thèse a montré que dès que le $RWC_{crit}$ était atteint, la propagation de la mortalité cellulaire se faisait à la même vitesse chez les espèces étudiées démontrant ainsi l'importance du temps d'atteinte du $RWC_{crit}$ pour la préservation de l'intégrité des tissus des organes et de la plante.

*Les méristèmes représenteraient la clé de la vie ou de la mort chez les arbres*

L'hypothèse principale de ce travail de thèse reposait sur la survie des méristèmes. En effet, une précision de l'hypothèse de McDowell *et al.* (2008) avait été apportée en avançant que la mortalité des arbres était très certainement liée à la mortalité des méristèmes, éléments clés permettant le développement et la régénération des organes les années suivantes. Cependant, très peu d'études, seulement une réalisée par Li et Jansen (2017), avaient tenté d'établir le lien entre la défaillance hydraulique et la mortalité de ces méristèmes, probablement car leur accès était extrêmement difficile et coûteux.

Ainsi, dans la recherche de la compréhension de la mortalité des arbres induite par sécheresse, **le dernier chapitre de cette thèse a montré que le maintien de l'intégrité du cambium représenterait bien l'élément clé lors de la détermination de la capacité d'un arbre à survivre à la suite d'un événement de sécheresse.** En effet, en utilisant des techniques de microscopie électronique à transmission, cette étude a pu mettre en évidence une destruction de l'ultrastructure des cellules cambiales dans le cas des arbres qui n'étaient pas capables de récupérer de l'événement de sécheresse mais pas dans le cas des arbres survivants. Cependant, cette étude ne s'est intéressée qu'à la survie du cambium et a négligé les autres méristèmes (Barigah *et al.*, 2013a) ou même les processus de dédifférenciation et redifférenciation cellulaire non connus chez les conifères mais bien connus chez les angiospermes (Malamy & Benfey, 1997; Laux, 2004). Ainsi, leur rôle dans la survie des arbres reste encore inconnu et requerra plus d'investigations dans le futur. En effet, nous ne savons toujours pas si les cellules vivantes isolées sont capables de se dédifférencier et de renouveler les tissus végétaux au cours de la récupération après une sécheresse.

*L'accès à l'eau est aussi important que le maintien du fonctionnement hydraulique de la tige*

Les résultats obtenus au cours de cette thèse ont montré que des niveaux élevés de défaillance hydraulique n'étaient pas nécessairement responsables de la mortalité des arbres et que certains arbres, notamment *F. sylvatica*, pouvaient être incapables de se remettre de l'événement de sécheresse même si ils avaient théoriquement un niveau de conductivité au sein du xylème de la tige suffisant et de l'eau en abondance dans leur sol. **En effet, malgré la présence de nombreuses cellules vivantes et d'une PLC relativement faible au point mesuré, certains arbres n'ont pas pu se remettre de l'épisode de sécheresse, ce qui signifie que la perturbation de leur transport d'eau était située en amont du point de mesure dans le chemin hydraulique.** Ainsi, l'incapacité d'un arbre à se remettre d'une sécheresse, même lorsque celui-ci présente un fonctionnement hydraulique du xylème suffisant, devrait être liée à son incapacité à puiser l'eau dans le sol ou à la conduire vers la tige. Cette incapacité d'accéder à l'eau dans le sol ou à la conduire jusqu'à la tige pourrait être liée au rétrécissement des poils racinaires qui se produit pendant la sécheresse et qui peut déconnecter hydrauliquement l'arbre du sol (Duddek *et al.*, 2022) ou à l'hypothèse de défaillance hydraulique des racines présentée par Johnson *et al.* (2018), rendant l'eau disponible dans le sol inaccessible à l'arbre et provoquant fatalement son embolisation complète et sa mort. Par conséquent, cela met en évidence le fait que, pour se remettre d'une sécheresse, l'eau doit non

seulement être disponible dans le sol mais aussi être accessible et transportable pour et dans l'arbre.

Ainsi, alors que les résultats du Chapitre 3 ont montré que des arbres présentant une PLC < 88 au niveau de la tige pouvaient ne pas survivre à l'événement de sécheresse après réhydratation de leur sol et que cela pouvait être expliqué par leur incapacité à mobiliser l'eau du sol en raison d'une défaillance hydraulique située plus en amont du point de mesure dans le xylème, la question de savoir à quel niveau, ou dans quel organe, les mesures de PLC devraient être effectuées et/ou simulées lors de la prédiction de la mortalité des arbres dans des conditions de sécheresse se pose. **En effet, il apparaît, à l'issue de ce travail de thèse, que si les mesures sont effectuées uniquement au niveau de la tige alors que le talon d'Achille du système hydraulique est situé plus en amont dans le continuum hydraulique, alors la prédiction de la mortalité serait biaisée et sous-estimée.** En effet, alors que les mesures au niveau de la tige ne permettent pas d'identifier la plante comme morte, celle-ci serait déjà condamnée en raison de son incapacité à mobiliser l'eau du sol et serait donc en train de mourir.

### *Détermination de traits physiologiques clés pour la prédiction de la mortalité des arbres en condition de sécheresse*

#### *De hauts niveaux de PLC ne sont pas tout le temps le meilleur indicateur de la survie des arbres après un événement de sécheresse*

Les résultats obtenus au cours de cette thèse ont montré que **de hauts niveaux de défaillance hydraulique n'étaient pas forcément responsables de la mortalité des arbres et que certains arbres, particulièrement des angiospermes, pouvaient être incapable de récupérer de l'événement de sécheresse même en ayant théoriquement accès à une eau abondante dans leur sol.** Ces résultats sont alors venus discuter l'importance d'une connexion hydraulique entre le sol, les racines et les différents tissus. En effet, bien que présentant un grand nombre de cellules vivantes et une PLC relativement faible, certains arbres n'ont pas été capable de récupérer de l'événement de sécheresse signifiant que la cause de leur mort se situait en amont. La présence de ces cellules vivantes peut être expliquée par la capacité de la plante à survivre sur ses réserves hydriques (Epila *et al.*, 2017) ce qui maintiendrait le métabolisme de la plante un peu plus longtemps. Cependant, lorsque ces réserves seraient épuisées, les cellules de la plante se déshydrateraient et finiraient par mourir comme démontré au Chapitre 2. Ainsi, la présence de cellules vivantes mais aussi d'une connexion hydraulique suffisante entre le système racinaire et les différents tissus de la plante serait nécessaire pour permettre la récupération de la plante.

#### *Identifier la mortalité des arbres en se basant sur les réservoirs d'eau*

Dans leur point de vue publié en 2019, Martinez-Vilalta *et al.* démontraient que se concentrer sur les réservoirs d'eau et non uniquement sur la PLC permettrait de mieux comprendre et anticiper les phénomènes de mortalité des arbres en condition de sécheresse. Ils énonçaient ensuite les propriétés d'un bon prédicteur de la mortalité induite par sécheresse et démontraient que le contenu en eau relatif apparaissait comme un candidat idéal pour définir un seuil de mortalité. En considérant qu'au niveau de la feuille des variations

importantes de potentiel hydrique amenaient à de faibles variations de RWC, notamment au niveau du point de perte de turgescence (Bartlett *et al.*, 2012), Martinez-Vilalta *et al.* posaient l'hypothèse que le RWC serait plus constant que le potentiel hydrique à travers les espèces et permettrait donc de comparer plus facilement la résistance des organes à la déshydratation. De plus, puisque des évidences empiriques avaient montré que le RWC au point de perte de turgescence était constant au travers les espèces même si celles-ci présentaient des résistances à la cavitation du xylème très différentes (Bartlett *et al.* 2012, Chapitre 2), le RWC pouvait donc être sujet à des variations importantes et brutales dans les moments précédents la mort de la plante et notamment lorsque l'intégrité cellulaire est compromise.

Au cours de cette thèse, **le RWC au niveau de la tige est apparu comme un bon indicateur de la probabilité de survie des plantes.** En effet, les plantes qui se rétablissaient, qu'il s'agisse d'angiospermes (*P. lusitanica* et *F. sylvatica*) ou de conifères (*P. menziesii* ou *A. concolo*r), présentaient systématiquement un $RWC_{Stem}$ plus élevé que les plantes qui ne se rétablissaient pas de la sécheresse. Cependant, même si les résultats du Chapitre 2 ont mis en évidence une valeur de RWC critique pour l'intégrité cellulaire ($RWC_{crit}$), qui a également été déterminée au Chapitre 3, il a été remarqué lors des expériences de récupération du Chapitre 3 que cette valeur n'était pas un bon indicateur de la mortalité des arbres. **En effet, le début de la mort des arbres se produisait à un RWC inférieur à celui qui marque le début des événements de mort cellulaire suggérant alors que les arbres puissent perdre une grande partie de leur vitalité cellulaire avant de mourir de la sécheresse.** Ceci était en accord avec les résultats obtenus sur les conifères au Chapitre 1. Par conséquent, même si le RWC est apparu comme un bon indicateur pour essayer de comprendre la mort des arbres due à la sécheresse, les résultats de cette thèse n'ont pas réussi à identifier un seuil de RWC, qui pourrait déterminer une réponse binaire, c'est-à-dire déterminer si un arbre est vivant ou mort, au sein d'un modèle mécaniste tel que SurEau (Cochard *et al.*, 2021).

*Les variations de diamètre et le pourcentage de récupération après une sécheresse pourraient fonctionner comme des indicateurs de la mortalité*

Durant cette thèse, les variations de diamètre des tiges ont été utilisées à deux reprises pour déterminer la capacité des arbres à survivre à l'événement de sécheresse (Chapitre 1 et Chapitre 3). Conformément à ce qui avait été observé par Lamacque *et al.* (2020), les variations de diamètres enregistrées à l'aide des dendromètres se sont révélées très utiles lors de la détermination de la survie des arbres et plus particulièrement de la mortalité de ceux-ci. En effet, si la récupération d'une partie du diamètre initial n'a pas toujours était corrélée à la survie des arbres (*voir* Chapitre 3), un manque de récupération de diamètre après réarrosage a systématiquement été associé à la mortalité de l'arbre, confirmant les observations faites par Lamacque *et al.* (2020). Si Lamacque *et al.* (2020) avaient réussi à montrer sur des espèces de lavande et lavandin qu'une perte de diamètre (PLD) d'au moins 21% était systématiquement associée à la mortalité de l'individu, les résultats obtenus au cours de cette thèse n'ont pas pu être aussi convaincants sur les espèces étudiées. En effet, le PLD est apparu comme un facteur influençant la survie des arbres uniquement dans le cas *F. sylvatica* (une angiosperme) et non chez *A. concolor* (un conifère). De plus, la valeur de 21% n'a pas été retrouvée chez *F. sylvatica* où une diminution du diamètre supérieure ou égale à 3.5% conduisait dans plus d'un cas sur deux à la mort de l'arbre.

# Perspectives

## *Mourir de soif au niveau cellulaire : comment les cellules peuvent mourir et quelles implications pour la prévision de la mortalité des arbres ?*

*Identification des mécanismes physiques provoquant la mort cellulaire*

L'une des premières questions qui s'est révélée au cours de ce travail de thèse a été la compréhension des mécanismes induisant la mortalité cellulaire et comment ceux-ci pouvaient être influencés par la composition et la structure des cellules. A ce jour, deux mécanismes principaux ont été avancés pour expliquer la mortalité des cellules lors d'un manque d'eau. Premièrement, comme décrit par Sakes *et al.* (2016), les cellules pourraient mourir à cause d'un phénomène de **cavitation**, c'est-à-dire quand une pression critique est rencontrée à l'intérieur de la cellule provoquant ainsi la fracture du cytoplasme et la formation d'une bulle de gaz à l'intérieur de celle-ci. Si ce phénomène, théorique, a déjà été observé dans le mécanisme de catapulte des spores de fougère (Noblin *et al.*, 2012; Llorens *et al.*, 2016), il n'a cependant jamais été relié empiriquement à la mortalité des cellules et nécessiterait donc d'être étudié. Secondement, les cellules pourraient mourir de **cytorrhyse** (Oertli, 1986; Taiz & Zeiger, 2006). En effet, la cytorrhyse consiste en la déformation de la paroi cellulaire lorsque la cellule perd de son volume du fait de la déshydratation, conduisant donc à l'écrasement de la cellule et provoquant son rétrécissement jusqu'à des niveaux létaux. Cependant, tout comme la cavitation cellulaire, aucun résultats empiriques ne sont venus apporter de support à cette théorie.

Ainsi, les résultats issus du Chapitre 2 et plus particulièrement les observations réalisées à l'aide du microtomographe PSICHE ont amené un nouveau questionnement sur les mécanismes de mortalité des cellules mais aussi sur les facteurs influençant la mise en place de l'un ou l'autre des phénomènes. Dès lors, une étude préliminaire utilisant un cryomicroscope à balayage (Cryo-SEM) a été menée conjointement avec le laboratoire Holbrook à Harvard. En effet, le Cryo-SEM est une technique de microscopie permettant de capturer des images sans altérer le contenu en eau des échantillons et ainsi en évitant les artefacts de déshydratation qui peuvent exister lors de l'utilisation d'autres techniques de microscopie conventionnelles. Ainsi, des observations de cryofractures transversales de feuilles de *Hibiscus rosa-sinensis* et *Laurus nobilis*, deux espèces sempervirentes présentant des résistances à la cavitation contrastées, ont été réalisées à différents RWC pour tenter d'élucider l'existence de l'un ou des deux mécanismes pouvant provoquer la mort cellulaire. **Ainsi, ces cryofractures ont permis d'observer que la majorité des cellules semblaient souffrir du phénomène de cytorrhyse au cours de la déshydratation, et ce, très rapidement.** En effet, les cellules qu'elles soient du parenchyme palissadique ou du parenchyme lacuneux semblaient majoritairement s'écraser sur elles-mêmes au cours de la déshydratation dans le cas de *H. rosa-sinensis* et *L. nobilis*. Cependant, si cette étude préliminaire a confirmé qu'il existait bien des phénomènes de cytorrhyse, elle n'a pas permis de déterminer les facteurs influençant la déformation. Ainsi, la réalisation de coupes transversales de feuilles permettrait de mesurer précisément l'épaisseur des parois cellulaires ; de comparer entre les différents tissus si cette

valeur change et enfin de comparer entre espèces si cette valeur exerce une influence sur l'atteinte du $RWC_{crit}$.

De plus, les résultats préliminaires n'ont pas encore démontré si ces déformations mécaniques étaient à l'origine de la mortalité des cellules. Ainsi, en posant l'hypothèse qu'une cellule morte ne puisse pas récupérer son volume initial du fait de la perte d'intégrité de sa membrane plasmique, il serait alors nécessaire de réaliser une réhydratation forcée des feuilles pour déterminer jusqu'à quel niveau de déformation cellulaire, les cellules seraient capables de récupérer leur volume initial. Si les résultats montraient que dès qu'une cellule est déformée alors elle ne peut plus se réhydrater, il serait possible de conclure que la déformation de la cellule est un élément très important dans la détermination de sa survie, puis de celle de l'organe et finalement celle de la plante. Si des cellules extrêmement déformées pouvaient toutes récupérer leur volume initial, signifiant que la membrane plasmique n'a pas été atteinte, alors il serait possible de conclure que la déformation des cellules n'est pas à l'origine de leur mortalité ce qui signifierait que les processus biochimiques seraient plus importants dans la détermination de la mortalité des cellules.

*Et les processus biochimiques dans tout ça ?*

Une autre possibilité présentée comme étant potentiellement responsable de la mort des cellules et donc des arbres en condition de sécheresse était **la destruction de la membrane plasmique provoquée par l'accumulation de dérivés réactifs de l'oxygène (ROS).** En effet, lors des stress abiotiques, une accumulation de ROS peut se produire dans la cellule amenant alors à un stress oxydatif. Ce stress oxydatif est alors à l'origine de nombreux changements biochimiques conduisant notamment à la peroxydation des lipides et à la rupture de la membrane plasmique provoquant la mort de la cellule (Suzuki *et al.*, 2012; Petrov *et al.*, 2015; Guadagno *et al.*, 2017). Cependant, le travail de thèse ne s'est pas attardé sur les aspects biochimiques de la mortalité des cellules. Néanmoins, il semblerait nécessaire d'étudier la production des ROS tout au long de la sécheresse mais aussi d'évaluer la gestion du stress oxydatif par les plantes. En effet, il a été montré chez les plantes qui sont capables de tolérer des sécheresses extrêmes, comme les plantes de la résurrection, que l'accumulation de ROS pouvait être contrée par une augmentation de la production d'enzymes neutralisant les ROS et d'antioxydants (Ingle *et al.*, 2007; Singh *et al.*, 2015). Dès lors, il semblerait judicieux de comparer la production de ROS et d'antioxydants au travers d'espèces présentant des cellules tolérant différemment la sécheresse. De plus, il a aussi été montré chez les mousses aquatiques anhydrobiotiques que la vitesse de déshydratation imposée à la plante lors d'un événement de sécheresse était d'une grande importance dans l'induction des dommages cellulaires (Singh *et al.*, 2015). En effet, une déshydratation lente protègerait les cellules contre la production de ROS et leur permettrait de survivre en présence de très peu d'eau. **Ainsi, des expériences faisant varier la vitesse de déshydratation des plantes**, par exemple en faisant varier le déficit de pression de vapeur (VPD) de l'environnement desséchant, pourraient conduire à l'élucidation du rôle des ROS lors de la mortalité des arbres en condition de sécheresse.

*La prédiction de la mortalité cellulaire méristématique est-elle inévitable lors de la prédiction de la mortalité des arbres ?*

L'une des questions soulevées par ce travail de thèse était de savoir s'il était nécessaire de prédire la mortalité cellulaire ou si la prédiction de la défaillance hydraulique pouvait à elle seule déterminer le moment où un arbre pouvait mourir d'un épisode de sécheresse. En effet, **les résultats rapportés dans le Chapitre 3 ont démontré que le maintien de l'intégrité cambiale était l'un des éléments les plus importants pour permettre à un arbre de se remettre d'un épisode de sécheresse, de produire de nouveaux organes et de continuer à croître la saison végétative suivante.** Cependant, les résultats du Chapitre 3 ont également montré que certains arbres, bien que présentant des cellules cambiales intactes, pouvaient ne pas survivre à l'épisode de sécheresse suggérant qu'une défaillance hydraulique située en amont du continuum hydraulique et du point de mesure s'était déjà produite, condamnant ainsi l'avenir de ces arbres. Ainsi, **la défaillance hydraulique semble donc être le processus qui déclenche la mort des arbres à plus ou moins long terme, mais certainement de manière inexorable.** Dès lors, au vu des résultats obtenus, il semblerait que pour prédire avec précision la mortalité des arbres due à la sécheresse, la prise en compte de l'interaction entre la défaillance hydraulique et la vitalité cellulaire soit la seule voie possible. Cependant, **les résultats obtenus dans cette thèse suggèrent que seule la prise en compte de la PLC de l'ensemble du continuum sol-plante-atmosphère au lieu de la PLC d'un seul point permette de faire un pas en avant dans la prédiction du risque de mortalité des arbres induit par la sécheresse.** Par conséquent, une suggestion serait d'effectuer d'autres expériences telles que celles réalisées au cours du Chapitre 3 en prenant, cette fois, en compte la PLC de l'ensemble du continuum sol-plante-atmosphère afin d'essayer de relier la défaillance hydraulique avec le niveau de dégradation cellulaire dans les méristèmes. Ainsi, ce n'est qu'en réalisant une expérience de cette manière qu'il serait possible de comparer les individus entre eux et de voir si deux individus ayant la même PLC globale présenteraient des niveaux de dommages cellulaires dans leurs méristèmes identiques. Si tel était le cas, alors il ne serait plus nécessaire de modéliser la mortalité cambiale mais uniquement le niveau de défaillance hydraulique global de l'individu.

*Considérer la récurrence des sécheresses sur la survie des individus*

Un autre point qui mérite d'être pris en considération dans l'étude de la mortalité des arbres en conditions de sécheresse, et qui n'a pas été abordé dans cette thèse, est qu'un arbre dans des conditions naturelles sera, en général, confronté à plusieurs événements de sécheresse au cours de sa vie. Par conséquent, lors de la prédiction de la mortalité des arbres en conditions de sécheresse, **la résilience et l'acclimatation des individus à ces événements de sécheresse au sein d'une population apparaissent comme cruciales pour pouvoir résister à la récurrence de ces événements et donc survivre à long terme** (DeSoto *et al.*, 2020 ; Lemaire *et al.*, 2021). Si certaines études ont suggéré qu'une faible résilience à la sécheresse pourrait augmenter le risque de mortalité des arbres (DeSoto *et al.*, 2020), d'autres ont également mentionné que l'acclimatation représenterait une source majeure d'incertitudes lors de la détermination du risque de mortalité pendant une sécheresse et que ce processus n'a pas été suffisamment pris en compte dans les modèles, probablement parce qu'il existe un manque de connaissances sur les traits susceptibles de s'acclimater (McDowell *et al.*, 2022).

En termes de résilience, il a été démontré que les espèces de gymnospermes, telles que les *Pinaceae*, ont tendance à montrer des effets hérités plus forts et à plus long terme sur leur croissance radiale après une sécheresse (Anderegg *et al.*, 2015), se rétablissant ainsi plus lentement et étant donc plus vulnérables à de nouveaux épisodes de sécheresse que certaines espèces d'angiospermes telles que les *Fagaceae* qui se rétablissent plus rapidement de la sécheresse et font donc mieux face à un nouvel épisode de manque d'eau (Gazol *et al.*, 2017). Cependant, si la résilience en termes de croissance a été largement étudiée ces dernières années (Lloret *et al.*, 2011 ; Martínez-Vilalta *et al.*, 2012 ; Carnwath & Nelson, 2017), **aucune des études sur les arbres n'a évalué la résilience des cellules à un événement de sécheresse.** En effet, aucune d'entre elles n'a essayé, par exemple, de déterminer si une cellule extrêmement déshydratée et présentant un protoplaste rétréci, comme ce qui était le cas au sein des cellules cambiales observées au microscope électronique à transmission au cours du Chapitre 3, pouvait reprendre sa forme initiale si le stress hydrique était atténué.

L'acclimatation de divers traits physiologiques et morphologiques, comme le changement d'allocation des ressources aux branches au détriment des feuilles ou la plasticité du point de perte de turgescence, a déjà été bien documentée (Mencuccini & Bonosi, 2001 ; Martínez-Vilalta *et al.*, 2009 ; Rosas *et al.*, 2019). Récemment, la plasticité et l'acclimatation des caractéristiques hydrauliques, en réponse au stress hydrique, ont été évaluées en pratique par Lemaire *et al.* (2021) et une augmentation significative de la résistance du xylème à la cavitation lors de la culture d'arbres de *P. tremula x alba* sous un stress hydrique modéré a été observée. En outre, cette résistance accrue à la cavitation du xylème, a été responsable, dans les simulations effectuées avec le modèle SurEau (Cochard *et al.*, 2021), d'un temps nécessaire pour atteindre la défaillance hydraulique 200 % plus long que celui des plantes non acclimatées à la sécheresse. Ainsi, ces résultats suggèrent que la compréhension et la prise en compte de l'acclimatation des espèces à la suite d'un stress hydrique modéré est un paramètre essentiel pour améliorer les prédictions du risque de mortalité des arbres en conditions de sécheresse. Ainsi, bien que les études menées au cours de cette thèse n'aient pas cherché à étudier les effets de l'acclimatation sur la survie des arbres, il serait possible de suggérer, au vu des résultats obtenus, d'évaluer la capacité d'acclimatation des cellules après un stress hydrique modéré. En effet, considérant que, pour les conifères, un niveau élevé de mortalité cellulaire est lié à une probabilité plus faible de survivre à un épisode de sécheresse (Chapitre 1 et Chapitre 3) et que cette mortalité cellulaire se produit après un seuil de déshydratation défini ($RWC_{crit}$) (Chapitre 2 et Chapitre 3), une question qui se pose maintenant est de savoir si un individu exposé à un premier épisode de sécheresse modérée présenterait des cellules plus tolérantes à la déshydratation par la suite, c'est-à-dire que les cellules produites lors d'un épisode de sécheresse modérée présenteraient un $RWC_{crit}$ plus faible.

*Extrapolation des résultats, de la cellule à l'écosystème*

**Une conclusion unanime des dernières années de recherche concerne la nécessité de caractériser les réponses au stress hydrique à une échelle plus large en procédant à des études au champ dans différents environnement et au travers de différents niveaux de développement** (Matallana-Ramirez *et al.*, 2021). En effet, comme constaté par Choat *et al.* (2018), la plupart des études ont été menées sur des petites plantes en pots exposées à des sécheresses extrêmes et cela a aussi été le cas lors de ce travail de thèse. Dès lors, des études

qui incorporent les effets de sécheresses longues (plusieurs années) sur des arbres matures apparaissent comme essentielles pour comprendre et prédire la mortalité des arbres en condition de sécheresse. De plus, depuis quelques années, la modélisation de l'hydraulique des plantes et plus particulièrement celle de la mortalité des plantes en condition de sécheresse s'est faite à de larges échelles (Tai *et al.*, 2017). Cependant, très peu d'études ont été réalisées pour assurer la précision de ces prédictions. Ainsi, cela a conduit à un besoin croissant d'observations de grande ampleur, c'est-à-dire au niveau de la forêt ou de l'écosystème.

Cependant, bien que de nombreuses études, dont les résultats issus de cette thèse, ont montré (i) que les plantes qui survivaient à l'événement de sécheresse présentaient en général un RWC plus élevé que les arbres qui ne survivaient pas (Mantova *et al.*, 2021; Sapes & Sala, 2021) et que (ii) il existait un $RWC_{crit}$ en deçà duquel les cellules des différents organes commençaient à être endommagées par le stress hydrique (Chapitre 2), **les mesures fréquentes et généralisées de RWC sur le terrain restent un défi en pratique.** Dès lors, des outils de **télédétection** ont été utilisés pour à la fois recenser les effets de la sécheresse au niveau global à l'aide de capteurs par satellite (McDowell *et al.*, 2015) et au niveau régional *via* des capteurs posés sur des avions (Asner *et al.*, 2016) et le RWC, présenté comme extensible de l'organe à l'écosystème (Martinez-Vilalta *et al.*, 2019), a été démontré comme de grand intérêt lors de l'évaluation du stress hydrique des forêts *via* télédétection (Van Emmerik *et al.*, 2017; Konings *et al.*, 2019; Rao *et al.*, 2019; Marusig *et al.*, 2020).

Ainsi, une des perspectives à donner à ce travail serait d'utiliser une combinaison des mesures réalisées au cours de la thèse et des outils de télédétection pour à la fois suivre le risque de mortalité des arbres à grande échelle, c'est-à-dire au niveau de la forêt voire même de l'écosystème, mais aussi paramétrer plus précisément les modèles de type SurEau (Cochard *et al.*, 2021) afin de mieux prédire les risques de mortalité liés au changement climatique au cours des futures années. Ainsi, en fonction de la résolution souhaitée pour ces observations, il serait alors possible d'utiliser des techniques radar (allant jusqu'à 1 mètre de précision) (Van Emmerik *et al.*, 2017) ou de radiométrie pouvant avoir une résolution de 10km (Konings *et al.*, 2019) et d'utiliser les données issues des spectres pour confronter les résultats obtenus aux résultats prédits par les modèles. **De plus, en confrontant les données obtenues *via* les techniques de télédétection aux données mesurées *in situ*, il serait alors possible de travailler à la fois sur de jeunes individus et sur des arbres matures et d'ainsi comparer leurs vulnérabilités**. Plus généralement, une combinaison de ces mesures permettrait, *in fine*, de mieux gérer les écosystèmes tels que les forêts cultivées et les vergers, voire même de sélectionner des individus en se basant sur la meilleure interaction génotype-environnement-survie détectée à l'aide des techniques de télédétection.

*"Long story short, I survived*…"*
*- Taylor Swift, Long Story Short, Evermore, (2020) –*
**The Cochard's method*

# Résumé

Les forêts, bien qu'essentielles à la survie de l'Homme du fait de leurs nombreux services écosystémiques, font face à d'importants dépérissements causés par des sécheresses intenses depuis le début de l'Anthropocène. Comme les modèles climatiques globaux prévoient, pour un futur proche, une augmentation de la fréquence et de l'intensité de ces sécheresses qui, par conséquence, accentuera le risque de mortalité des arbres, il apparait alors crucial de mieux comprendre les bases physiologiques de la mortalité des arbres induite par sécheresse afin d'identifier des seuils physiologiques permettant de mieux prédire l'impact de ces changements climatiques sur les écosystèmes forestiers. Si la défaillance hydraulique du xylème a été reconnue comme un facteur omniprésent de la mort des arbres en conditions de sécheresse, des preuves fondamentales du lien mécaniste reliant la défaillance hydraulique, la mortalité des cellules et celle des arbres n'ont pas encore été identifiées. Ainsi, l'objectif principal de cette thèse était d'élucider ce lien tout en identifiant les seuils physiologiques clés au-delà desquels la survie de l'arbre est grandement compromise.

Dès lors, en s'intéressant, tout d'abord, à deux espèces, un conifère (*Pseudotsuga menziesii* M.) et une angiosperme (*Prunus lusitanica* L.) le travail de thèse a démontré que les niveaux de défaillance hydraulique considérés jusqu'alors comme létaux pour les plantes ($P_{50}$ pour les conifères et $P_{88}$ pour les angiospermes) n'étaient pas assez précis pour définir avec certitude le sort d'un arbre après un événement de sécheresse. Cependant, alors que le lien causal entre défaillance hydraulique du xylème et la mortalité cellulaire restait non élucidé, l'interaction entre ces deux phénomènes semblait expliquer la capacité des arbres à récupérer d'un stress hydrique. Ainsi, en combinant, à la fois, la détection des événements de cavitation à l'aide de la méthode optique, des mesures de contenu en eau relatif au niveau tissulaire, et des mesures de lyse cellulaire au niveau d'un organe facilement accessible : la feuille, nous avons mis en évidence que la défaillance hydraulique du xylème, en entrainant une baisse du contenu en eau des tissus en dessous d'un niveau critique, le $RWC_{crit}$, provoquait la mort des cellules. Finalement, en partant du postulat que toutes les cellules n'avaient pas la même importance dans la survie des arbres et que cette survie devait certainement être liée au maintien de l'intégrité des cellules responsables de la croissance de la plante, c'est-à-dire des cellules méristématiques, nous avons cherché, en travaillant sur un conifère (*Abies concolor* (Gordon & Glend) Lindl. Ex Hildebr) et une angiosperme (*Fagus sylvatica* L.), à montrer que les cellules méristématiques étaient bien des cellules clés lors de l'évaluation du lien mécaniste entre la défaillance hydraulique et la mortalité de l'arbre. Sur cette dernière partie, bien que les analyses statistiques aient à nouveau révélé l'importance du niveau de contenu en eau relatif des tissus de la tige avant réhydratation pour la survie des arbres, des résultats préliminaires obtenus en microscopie électronique à transmission ont montré qu'à niveaux de contenus en eau égaux, des plantes présentant des cellules méristématiques intègres étaient plus à même de survivre à l'événement de sécheresse que les autres et, ce, dès leur ré-arrosage.

**Mots clés :** Mortalité des arbres, Sécheresse, Cavitation, Contenu en Eau Relatif, Déshydratation Cellulaire, Fuite d'Electrolytes, Cambium, Microscopie Electronique à Transmission

# Abstract

Forests, although essential for human survival due to their numerous ecosystem services, have been facing a significant dieback caused by intense droughts since the beginning of the Anthropocene. As global climatic models predict an increment in the frequency and intensity of droughts in the near future, which will consequently increase the risk of tree mortality, it is crucial to better understand the physiological bases of drought-induced tree mortality in order to identify physiological thresholds that will allow us to better predict the impact of climate change on forest ecosystems. While xylem hydraulic failure has been recognised as a ubiquitous factor in tree death under drought conditions, fundamental evidence for the mechanistic link between hydraulic failure, cell mortality and tree mortality has not yet been identified. Therefore, the main objective of this thesis was to elucidate this link while identifying key physiological thresholds beyond which tree survival is greatly compromised.

Thus, by focusing first on two species, a conifer (*Pseudotsuga menziesii* M.) and an angiosperm (*Prunus lusitanica* L.) the thesis work demonstrated that the levels of hydraulic failure previously considered as lethal for trees ($P_{50}$ for the conifers and $P_{88}$ for the angiosperms) were not precise enough to define with certainty the fate of a tree after a drought event. However, although the causal link between xylem hydraulic failure and cell death remained unclear, the interaction between these two phenomena appeared to explain the ability of trees to recover from water stress. Thus, by combining the detection of cavitation events using the optical technique, measurements of relative water content at the tissue level, and measurements of cell lysis on an easily accessible organ: the leaf, we demonstrated that the hydraulic failure of the xylem, by causing a drop in relative water content below a critical level, the $RWC_{crit}$, caused cell death. Finally, based on the assumption that not all cells were equally important for the survival of trees and that this survival should certainly be linked to the maintenance of the integrity of cells responsible for plant growth, i.e., the meristematic cells, we sought, by working on a conifer species (*Abies concolor* (Gordon & Glend) Lindl. Ex Hildebr) and an angiosperm species (*Fagus sylvatica* L.), to show that the meristematic cells were indeed key cells when evaluating the mechanistic link between hydraulic failure and tree mortality. On the latter part, although statistical analyses revealed again the importance of the level of stem relative water content before re-watering for tree survival, preliminary results obtained by transmission electron microscopy showed that, for the same level of stem relative water content, plants with intact meristematic cells were more likely to survive the drought event than the others as soon as they were re-watered.

**Key words:** Tree Mortality, Drought, Cavitation, Relative Water Content, Cell Dehydration, Electrolytes Leakage, Cambium, Transmission Electron Microscopy